
Lasers

This is the third issue of the *RCA Engineer* devoted primarily to papers on lasers, their application, and closely related subjects. The first was in 1963, about four years after RCA initiated research on lasers. It included seven papers and two engineering notes, mostly on basic laser research and associated component development. Only one was on a practical and enduring application: that of laser rangefinding. The laser was described by some as "a cure looking for an illness."

The second laser issue was in 1966 and its papers dealt with a vastly expanded variety of lasers, new components such as detection devices, propagation measurements, and some experimental laser radar and communication systems. There were other articles on potential applications in medicine, on safety considerations, and laser machining. The subject of holograms as a potential storage medium of pictorial information, immune to physical damage, was introduced in this issue. But still science and technology outweighed the practical applications of the new technology.

While this issue shows an even broader spectrum of laser technology and related components, it is clear that laser research is still very much active and that most of the work reported here is still in the earlier phases of development. But more and more real applications are emerging. This issue includes papers on valid military uses such as gated vision, intrusion alarms, and ranging. In a future issue, RCA's approach to prerecorded video for the home will be covered. Based on lasers and holography, this may well be the first large-volume application.

It seems that, in its tenth year, the laser is coming of age.



A handwritten signature in dark ink that reads "W M Webster". The signature is fluid and cursive, written in a dark ink.

William M. Webster
Vice President
RCA Laboratories
Princeton, New Jersey

RCA Engineer Staff

W. O. Hadlock Editor
J. C. Phillips Assistant Editor
Mrs. J. Heritage Editorial Secretary
V. Bartholomew Art Director
A. Whiting Design and Layout

Consulting Editors

C. A. Meyer Technical Publications Adm.,
Electronic Components
C. W. Sall Technical Publications Adm.,
Laboratories

Editorial Advisory Board

A. D. Beard Chief Engineer,
Computer Systems Div.
E. D. Becken Executive VP, Operations
RCA Global
Communications, Inc.
J. J. Brant Staff VP, Personnel Adm.
F. L. Flemming VP, Engineering, NBC
Television Network
C. C. Foster Mgr., Technical Information
Services, RCA Laboratories
M. G. Gander Manager, Consumer Product
Adm., RCA Service Co.
Dr. A. M. Glover Div. VP, Technical Programs,
Electronic Components
W. R. Isom Chief Engineer,
Record Division
E. O. Johnson Manager, Engineering
Technical Programs,
Electronic Components
L. R. Kirkwood Chief Engineer,
Consumer Electronics Div.
A. Mason Chief Engineer,
Commercial Electronic
Systems Division
A. R. Trudel Director, Corporate
Engineering Services
G. O. Walter Chief Engineer,
Graphic Systems Division
Dr. H. J. Woll Chief Defense Engineer,
Defense Engineering

Our cover

Typical of the many advances described in this issue, the cadmium laser on our cover is an extension of laser technology into a new area of possible applications—in this case, the violet and ultraviolet range of importance in photographic work (see Dr. Hernqvist's article, p. 14).
Photo credit: Tom Cook, RCA Laboratories.

RCA Engineer

A technical journal published by
RCA Corporate Engineering Services 2-8,
Camden, N.J.

RCA Engineer articles are indexed
annually in the April-May Issue and
in the "Index to RCA Technical Papers."

• To disseminate to RCA engineers technical information of professional value • To publish in an appropriate manner important technical developments at RCA, and the role of the engineer • To serve as a medium of interchange of technical information between various groups at RCA • To create a community of engineering interest within the company by stressing the interrelated nature of all technical contributions • To help publicize engineering achieve-

ments in a manner that will promote the interests and reputation of RCA in the engineering field • To provide a convenient means by which the RCA engineer may review his professional work before associates and engineering management • To announce outstanding and unusual achievements of RCA engineers in a manner most likely to enhance their prestige and professional status.

Contents

Editorial input	Science, society, and the seventies	2
Engineer and the corporation	Why and how RCA engineers should write technical reports	W. O. Hadlock 3
Advances in laser technology	Future of the laser	Dr. H. R. Lewis E. Kornstein 7
	Advances in gas laser technology	Dr. K. G. Hernqvist 14
	Recent progress in injection lasers	Dr. H. Kressel H. Nelson 17
	Improving solid-state lasers	Dr. R. J. Pressley 20
	Electron-beam-pumped semiconductor lasers	Dr. F. H. Nicoll 24
	Sealed-off CO ₂ lasers	Dr. R. A. Crane J. I. Wood 28
Advances in laser detectors	Solid-state detectors for laser applications	Dr. R. J. McIntyre H. C. Sprigings P. P. Webb 32
	New photomultiplier detectors for lasers	D. E. Persyk 40
Laser applications	Lasers in communications	Dr. R. M. Green A. L. Waksberg 42
	Measurement of laser communication parameters	A. L. Waksberg J. C. Boag 46
	The laser in education	F. S. Philpott 49
	Machining with the carbon dioxide laser	Dr. D. Meyerhofer 52
	Gated vision techniques	D. G. Herzog 58
	Laser tracking and ranging systems	G. Ammon S. Russell 62
	Effectiveness of IR covert illuminators	F. J. Gardiner 68
	Tradeoff analysis of neodymium and ruby laser rangefinders	E. Kornstein N. Luce 72
	Gated-sensor and pulsed-laser illuminator systems for seeing through fog	Dr. H. J. Wetzstein E. Kornstein 74
	A GaAs transmissometer	Dr. E. J. Fjarlie 79
	Light scattering with laser sources	Dr. G. Harbeke Dr. E. F. Steigmeier 82
	Infrared images made visible by laser techniques	Dr. A. H. Firester 86
	Of general interest	System tests for the VideoComp 70/830
New developments in controlled solder plating of printed-wire boards		E. E. Gilbert 94
Three RCA men elected IEEE Fellows		100
Notes	Inventions and obviousness	A. Russinoff 101
	Mini-skirts, micro-skirts, and mini-microwave couplers	R. E. Bridge 101
	Method of producing a photographic type transparency with a CO ₂ laser beam by	Dr. D. L. Ross 102
Departments	Pen and Podium	103
	Patents Granted	108
	Dates and Deadlines	109
	News and Highlights	110

editorial input

science, society, and the seventies

This is not just another year; 1970 heralds a vibrant new decade in which the needs, challenges, and adjustments will be greater than ever for engineers and scientists—new and experienced alike. Each year new engineering graduates bring with them fresh knowledge, new determination, and startling concepts for the engineering profession. However, the smooth transition for the new engineer, who must preserve and extend his objectives, will depend greatly on the skills and abilities of the experienced engineer who will be called upon to provide counsel and to establish performance goals.

Engineers have always been dedicated to the satisfaction of human needs, but now their role will be greater than ever. Working with their counterparts in medicine, law, education, and other learned professions, today's engineer is uniquely suited to share in the satisfactions as well as the responsibilities for achieving progress in the interests of society. He is characterized by his desire to live by ideas, to acquire and share new knowledge, to train associates, to document for the benefit of the world body of knowledge, and to exert the patient determination to achieve even though the recognition and rewards may be delayed. His ability to innovate and to present new advances and ideas to society—and concurrently his ability to reduce the costs of the products of science to a level within the economics of the majority—are the influences that the engineer will bring to solve the problems of the seventies.

The seventies will impose demands that are advanced far beyond any that have faced scientists and engineers of prior decades.

For example, what will the scientific community contribute toward a practical solution to urban problems, to the transfer of electronic power and atomic energy, and to the design of new systems for air and land transportation? What about development of new materials for low-cost home construction? Ironically, many of the problems now begging for solution are a result of past decades of engineering achievement—the problems of noise, air, and water pollution for example. What will be the role of the engineer in devising automatic refuse and waste disposals; and in the realization of the electric car? What about the role of the computer in freeing man's time in business and in the home? Will electronics play a leading role in the maintenance and preservation of health and education and in the proper utilization of the earth's and sea's natural resources?

These are just a few of the sociological challenges for the engineer of the 70's—the engineer who will be recognized for his humanitarian contributions made possible by his technical accomplishments regardless of his age, his experience, or his prior accomplishments.

If we examine what we as professional engineers have done to lead the way to a new life for the seventies, we may be forced to admit to being somewhat inert and unimaginative. To adapt science to serve the best interests of mankind, we should now start a fresh examination of our role in society . . . reflect seriously on how we can be a major force . . . accept the changes that will be brought about in our role as engineers . . . and make responsible recommendations. The pages of the *RCA Engineer* are open to your ideas and reactions.

Future issues

The next issue of the *RCA Engineer* features RCA engineering on the West Coast. Some of the topics to be discussed are:

- Monoscope character generators**
 - Two-color alphanumeric displays**
 - Drum memory systems**
 - Random access memories**
 - Power supply protection techniques**
 - Automated design**
 - Custom monolithic circuits**
 - Communication and navigation system for aviation**
 - Airline weather radar**
 - One-tube color camera**
- Discussion of the following themes are planned for future issues:
- Linear integrated circuits**
 - Consumer electronics**
 - RCA engineering in New York**
 - Displays and optics**
 - Computers: next generation**
 - Mathematics in engineering**
 - Advanced Technology Laboratories**

Why and how engineers should write technical reports

W. O. Hadlock

Engineers and scientists who prepare RCA internal technical reports accomplish several important goals: 1) they share valuable information with other RCA engineers; 2) they help solve related problems in other activities; and 3) they alert leaders and managers to the need for sharing valuable information with other activities. This paper includes up-dated definitions and new information on distribution, approvals, and numbering of internal technical reports; it describes RCA's technical reporting programs and answers questions about the author's professional task of writing reports.

ENGINEERS AND SCIENTISTS who provide Technical Reports (TR's) and Engineering Memoranda (EM's) benefit their associates in other divisions, implement important RCA policy, and help secure for RCA a maximum return on its investment in engineering and research.

RCA's policy for TR's and EM's

Quoted here is a statement of RCA's policy¹ regarding the purpose of TR's and EM's:

"To record the significant results of engineering and research investigations and to make such information available to the major operating units and interested RCA Staff activities."

The essence of this policy is incorporated in the formal procedures of the major divisions of RCA.

Each division in RCA has a specific operating procedure (Refs. 2, 3 and 4 are examples) covering the preparation and distribution of TR's and EM's. Because such instructions vary in minor detail, the information in this paper is generally applicable to report preparation in all activities. For additional information, engineers are encouraged to seek the advice of engineering supervisors, and the Technical Publication Administrators (listed on the back cover of each RCA ENGINEER).

General information on technical reports

Reports embrace research, applied research, and engineering development investigations throughout RCA and are utilized for documenting information

of value, whether technical or non-technical. Such reports provide a convenient means for sharing results of research and development efforts, and furthering RCA's total competence.

TR's and EM's are *company private* documents; they provide information for use by technical personnel only within RCA. Such documents are one of the traditional communication media used by RCA for nearly three decades and are available for reference at major RCA engineering libraries.

Why write reports?

Engineers realize they must do much more than solve new problems. Among their professional responsibilities, the preparation of reports is important for several reasons:

- 1) To provide a permanent record (for patent, legal, engineering, and management) of valuable work completed.
- 2) To avoid duplication of engineering and research.
- 3) To inform other engineers of results accomplished to help solve their related problems.
- 4) To suggest techniques for other scientific work.
- 5) To show that certain methods of solution may be blind alleys.
- 6) To use as a basis for technical papers.

TR's and EM's capture the interest of associates, engineering management, and others who may further apply new ideas—a novel idea usually has value far beyond that envisioned originally. The two types of reports and their basic functions are as follows:

Technical Reports (TR's) are used to record research and engineering results, during the course of the investigation or at its conclusion, or any technical information within RCA, except as provided by engineering memoranda.

The Engineer and the Corporation



W. O. Hadlock, Mgr.
Technical Publications
Corporate Engineering Services
Research and Engineering
Camden, N.J.

received the BSEE from Clarkson College of Technology and joined General Electric's Radio Receiver Engineering upon graduation, where he worked in components engineering, design of AC/DC battery radios, and later in television transmitter design. During World War II he became Assistant Mgr. of Commercial Service Activities, GE Electronic Tube Division, and introduced GE's series of Electronic Tube Manuals. Mr. Hadlock joined RCA in 1947 to work on the Advertising and Promotion of RCA technical equipment for sale to TV and Broadcast Stations. In 1949, he became Mgr., Broadcast and TV Advertising and Sales Promotion and Managing Editor of *Broadcast News*. In 1955, Mr. Hadlock became Editor, RCA ENGINEER, to inaugurate and publish the present company-wide journal. In 1959, he was also named RCA Staff Technical Publications Administrator. In 1965, Mr. Hadlock was named Manager, RCA Technical Publications, Corporate Engineering Services, in which position he continues as Editor, RCA ENGINEER. In 1967, he was also made responsible for RCA's TREND, The Research and Engineering News Digest. Mr. Hadlock is a Senior Member of IEEE, Member of EWS, and a member of the American Association of Industrial Editors.

Engineering Memoranda (EM's) are used to record non-technical and certain technical information which is of limited significance within RCA. The Engineering Memorandum is not a substitute for the Technical Report, however. Examples of EM's are reports of meetings, trips and conferences; competitive product evaluations; computer programs, charts, tables and nomographs.

When to write reports?

The occasion to write a TR or an EM may arise during the course of an engineering investigation as well as upon its completion (although contract reports are usually stipulated and scheduled by the contracting agencies, such work may later form the basis for valuable TR's—subject to the approval of the contracting agency). The engineer can, with the guidance of his leader, manager or lab director, determine the proper timing; generally, preparation of TR's should be considered as follows:

- 1) Upon completion of a major engineering project.
- 2) Upon completion of any discrete portion of a project.
- 3) Whenever the information is of value to RCA engineers.
- 4) Whenever new techniques are developed.
- 5) When unclassified contract reports are of interest to other divisions, and are approved for issuance as TR's.
- 6) When classified contract reports are declassified, and are approved for conversion to TR's.
- 7) Prior to public disclosure of new information.

Who is eligible to write a report?

RCA engineers or scientists are strongly encouraged to prepare TR's and EM's as a part of their work. However, all members of the RCA technical staff, including the managers, leaders, project administrators, and technicians are eligible to write reports.

Other RCA reports, and government reports

Several other categories of "Company Private" information are used in some divisions of RCA, such as Government Contract Reports, Progress Reports, and Coded Engineering Letters. Distribution and release of such material is controlled by the Chief Engineer and/or Technical Publication Administrator.

Government Contract Reports are prepared and distributed in accordance

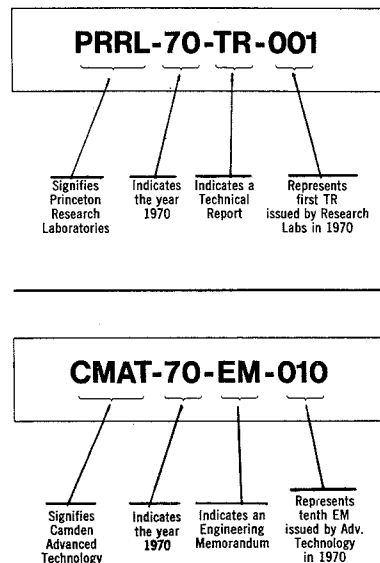
with the terms of the contracts in which RCA participates, and in conformance with Government security regulations included in the RCA Personnel Policy Manual and Procedures of each division.

RCA technical reports are **not recommended** for reporting classified work; however, certain phases of such work may be unclassified; if so, approval can be sought to report such information to engineers in other divisions. When certain Contract Reports are declassified, engineers may also wish to obtain approval to distribute pertinent information as TR's.

New system for report numbers

Every TR and EM must bear an appropriate index (file) number^{1,2,3,4} to facilitate future reference, library filing, and retrieval. Report numbers should appear in the upper left hand corner of the report cover, and be repeated on the abstract pages.

Starting in January 1970, a new numbering system was established. In this system, corporate report numbers consist of four discrete parts of significant information, as follows: 1) a location division designator; 2) a number indicating year of issuance; 3) the letters TR or EM indicating the type of report; and 4) a 3-digit sequential number:



Upon completion of reports, engineers should contact the Technical Publications Administrator (TPA), librarian, or others in their division responsible for the assignment of corporate TR and EM numbers.

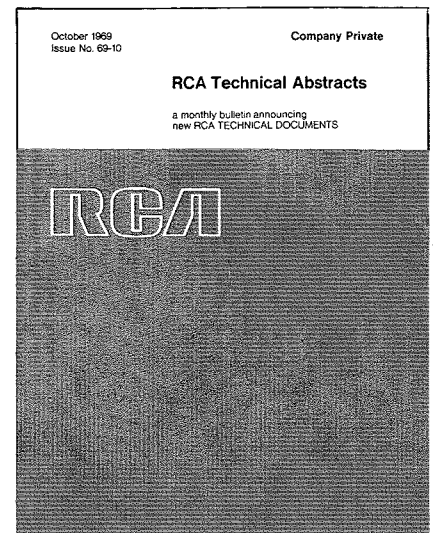


Fig. 1—RCA Technical Abstracts is distributed by the Technical Information Systems activity to key engineering and research personnel throughout RCA.

Required approvals

Each division has a definite set of approval requirements for technical reports. These nearly always include the following, in advance of distribution: 1) technical and administrative (policy) approval by the head of the engineering activity (the Chief Engineer or his designated representative), and 2) patent approval by the Director, Domestic Patents.

Distribution of TR's and EM's

Each division of RCA initiates a corporate-wide minimum standard distribution of complete reports. This minimum (and mandatory) distribution includes only the major technical libraries serving engineering and research, one copy for patent operations, and one copy for joint use by Technical Publications and by the Technical Information Systems activity for information-retrieval purposes. Additional distribution of complete reports within United States may be made by the author (after appropriate approvals) to qualified RCA personnel.

Every RCA technical report and engineering memorandum is categorized, indexed, and announced in "RCA Technical Abstracts" (Fig. 1)—circulated monthly to key research and engineering personnel in all activities of RCA. Recipients of the "Abstracts Bulletin" may borrow the reports of interest from local technical libraries.

Planning and organizing TR's

A technical report should present pertinent facts together with logical conclusions and recommendations. Thus,

the writer's goal is to accumulate, organize, and present essential information so that the report can be quickly and easily understood.

Value of an outline

Before beginning an engineering project, a preliminary outline frequently helps determine the progression of the developmental steps to be taken. To analyze a project, ask and answer the following questions:

- What will be the purpose?
- Who will need the information?
- How much background should be included?
- What steps should be followed?
- What is the final message to convey?

You can change your outline, add to it, or subtract from it, as work progresses. Major headings in the outline may become the table of contents of your report (Fig. 2).

Convey your idea

Remember that the function of the report is to convey an idea; thus, it need not be a treatise. A brief technical report can be more effective than a lengthy, involved one.

Writing effective reports

To communicate your idea, the report should favor the specialized readers to whom it is directed—and, at the same time, be understood by as wide an audience as possible. So, select the "nuggets" of the work for special at-

Fig. 2—Combination topic-sentence outline for preparing TR's and EM's.

- I. Planning and organizing
 1. Preliminary
 - a. Study available material;
 2. Early Writing Stages
 - a. Decide on audience and reader needs.
 - b. Analyze material; decide what to say.
 - c. Make rough outline as a guide.
 3. Consider Forms of Organization
 - a. Chronological account (rare)
 - b. Describe a product or technique
 - c. Emphasize methodology
 - d. Describe a project
 - e. Describe an investigation
- II. Writing the report
 1. Get it on paper promptly; rewrite and polish.
- III. A "TR" on an investigation
 1. **Front matter:** Title—summary, distribution, and content pages.
 2. **Introduction:** Importance of work, objectives, preview of contents, and gist of conclusions.
 3. **Body:** Summarize findings; describe equipment, methods, and results.
 4. **Conclusions, recommendations and bibliography.**
 5. **Appendix:** History, derivations, and detailed data.
- IV. Illustrating
 1. Complement and illuminate the text.
 2. Simplify diagrams; use in right places.
- V. Observe conventions of uniformity
 1. Spelling and punctuation.
 2. Tables, literature citations, etc.

tention instead of repeating all the stages of thought and action. However, occasionally unproductive results may be of great interest and of value to certain engineers. This is a matter of judgment for the author.

Write the abstract, report proper, and the appendix with appropriate degree of detail. The abstract provides the gist of the report. The body appeals to the reader who follows the work closely. The appendix supplies calculations and detailed analyses. Thus, an effective, easy-to-read report tells the story in barest facts, repeats it in greater detail, and supports the main thesis with related information.

Elements of TR's and EM's

Uniformity in appearance, content, and arrangement of RCA TR's and EM's is desirable. Understandably, minor variations such as the types of covers do exist. However, all reports usually require the basic elements illustrated by the sample pages (Figs. 3 through 8).

Report covers

TR's and EM's can be bound in any appropriate folder or cover. Satisfactory covers are available in the various divisions and Technical Publications Administrators will recommend the most suitable types. Only one number (the RCA designator-based number) should appear on the front cover of the report.

SMSS-70-TR-999

Company Private
July 1970

M. B. Knight
Special Product Development,
Solid State Division,
Somerville, New Jersey

Transistor High-Voltage and Scanning Circuits for Color Receivers

RCA Electronic Components

Technical Report Abstract	RCA	Company Private
#20 Title		#19 RCA Report Number
Transistor High Voltage and Scanning Circuits for Color Receivers		SMSS-70-TR-999
#21 Title Note (Type of report—informal, interim, review, final, contract)		#26 Date
Final Report		July 1970
#22 Number		#27 Number of Pages
36		36
#23 Author		#24 RCA Project Number
M. B. Knight		TRAD-67-920
#25 RCA Organization/Work Report		#28 Government Contract Number
Division: EC Solid State Division Location: Somerville, N. J. Author: M. B. Knight #29 For Submission to Other Contract or Other Customer Report		
#30 For Classified Reports Only		
When Declassified	Class	Conf
When Declassified	Limit	Conf
When Declassified	Limit	Conf
#31 Abstract—Briefly summarize objectives, methods, results, and applications—Type single spaced		
Object: To develop high-voltage and horizontal scanning circuits suitable for 6117 transistor demonstration color receivers having "off-the-line" or "transistor" power supplies so that developmental devices could be specified and evaluated for such service.		
Conclusions: Circuits meeting the objectives were built for two receivers using 61172 picture tubes and one using a 21922 tube. The circuits operate from regulated off-the-line power supplies and generate by novel means low-voltage power for other receiver functions. A novel horizontal AFC circuit is also utilized. Adequate high-voltage power and regulation is provided. Power efficiency is excellent. Device requirements are technically and economically within reach in the near future subsequent to scheduling of active development program. Protection of semiconductor devices from high-energy discharges in vacuum high-voltage receivers, however, has not been investigated in these receivers.		
Approved: Name, title and location		

Fig. 4—The technical abstract page provides the necessary information for indexing in RCA Technical Abstracts.

SMSS-70-TR-999	RCA Handbook Containing Source Data (See handbook number)	
#32 Related RCA Reports (Title, report or paper number)	Related Patent Disclosures (Title, report or paper number)	
	DIRT-51,819 DIRT-52,971 DIRT-53,128 DIRT-57,394	
#33 Table of Contents (Relevant to This Report (Other one or more below))		
Basic Theory, Phenomena, & Methodology		
101 Chemistry—organic, inorganic, physical		
102 Earth & Atmospheric Sciences—geology, geodesy, meteorology, atmospheric physics, etc.		
103 Life Sciences—biology, physiology, zoology, etc.		
104 Physics—acoustics, optics, quantum physics, etc.		
105 Mathematics—mathematical physics, statistics, etc.		
106 Space Sciences—astronomy, astrophysics, etc.		
107 Electronics—electronics, instrumentation, etc.		
108 Electrical Measurements & Calibration		
109 Manufacturing & Fabrication		
110 Management & Business		
111 Manufacturing & Fabrication		
112 Mathematics		
113 Medicine		
114 Mechanical		
115 Systems Analysis & Operations Research		
116 Miscellaneous Theory & Methodology		
Materials, Components, & Subsystems		
201 Circuits, Circuit Devices, & Microcircuits—Discrete, integrated, hybrid, & active devices (tube & solid state)		
202 Semiconductors		
203 Energy & Power Sources—batteries, cells, generators, reactors, etc.		
204 Materials—mechanical, structural, physical, chemical, electrical, etc.		
205 Mechanical Structures & Structures—Composite, structural, strength, stress, waves, etc.		
206 Optics		
207 Signal Detectors—antennas, sensors, etc.		
208 Signal Processing—modulation, demodulation, transmission, reception, etc.		
209 System Transfer & Subsystems—microphones, loudspeakers, etc.		
210 Thermal Systems—heating & cooling		
211 Transportation		
212 Instrumentation & Computers		
213 Systems, Equipment, & Applications		
301 Avionics & Space Support		
302 Communications (Phone & Telex)—radio, television, etc.		
303 Communications (Phone & Telex)—radio, television, etc.		
304 Control Systems		
305 Computing, Programming & Applications		
306 Education Systems		
307 Gas Turbine—propulsion, propulsion, etc.		
308 Medical Research & Life Sciences—life sciences, etc.		
309 Metallurgy		
310 Metallurgical & Machine Construction		
311 Metals, Steel & Other Technical Systems		
312 Transportation		
313 Structural & Support		
314 Transportation Systems & Applications		
This report has been indexed and announced in "RCA TECHNICAL ABSTRACTS". Complete reports distributed in accordance with RCA Minimum Standard Distribution List 25.0.		
City: Somerville	Princeton	Lakewood
W. E. Babcock	R. H. Pollack	W. H. DeGroot
J. C. Bann	R. C. Bann	W. A. Goring
M. S. Fisher	M. A. Santilli	J. Santilli
M. L. Turner	H. L. Turner	C. E. Kelly
M. F. Kieppinger	M. F. Wheatley	M. J. Albert
J. O. O'Brien	J. F. Wolff	G. E. Rogers
* Complete reports, others abstract page only.		

Fig. 5—Typical indexing and distribution information.

Fig. 3—Report covers should include the basic information shown above.

Technical abstract page

The title, names of the authors, report file number, date, and indexing information are required on the abstract page (RCA form 3003). Carefully select titles to be brief but comprehensive enough to be distinguished from other reports. Government contract numbers (when required) are included.

The abstract (or subject, object, and conclusion) should provide useful information and give the reader a concise preview of what he will find in the report. Such a capsule assists the reader who scans—and encourages the serious reader to study the report more thoroughly.

Index and distribution page

This page includes the following information: Company Private notation, file number, date, field of interest categories, and a statement concerning announcement and distribution. Additional author distribution is listed by name and location, indicating whether complete reports or abstract pages were sent.

Table of contents

The table of contents (when one is considered necessary) should include the main divisions and subdivisions of the report, showing page numbers where material can be found. Appendixes, tables, and figures may also be listed on the contents page.

Introduction

To help the reader, repeat the title at the top of the introduction page. A good introduction indicates what is to follow, defines the subject under discussion, and states objectives. Reference to companion projects will be helpful—assume the reader has little knowledge of the purpose or scope of the investigation. Prior research problems, associated concepts, and prevailing ideas may be briefly described.

Description of the investigation

The section following the introduction describes what was done and how it was achieved. Include enough information so the readers can reach an opinion of the accuracy, reliability, and usefulness of the work. Typical items to discuss are as follows: 1) theoretical considerations, 2) experimental procedures, 3) design of apparatus, 4) comparison of predicted and observed data, and 5) summarized results.

Conclusion and recommendations

This section enumerates significant findings, and supplies supporting information needed to understand what was achieved. Recommend steps for applying the results of the work. Describe benefits expected from such application and mention unique feature of the work. Suggest further work that seems desirable. State opinions, but distinguish those not supported by proof.

Appendixes

Supplementary information too specialized to include in the body of the report (but important to some readers) should be presented in appendixes. Examples are as follows: lengthy historical background, details of experimental equipment, procedures, analytical methods, calculation, and derivations.

References and bibliography

Referenced items are numbered sequentially to agree with the order in which superscript numbers appear in the text. Bibliographies may include any publication that the engineer-author considers helpful. Abstracts, letters, or private communication may be referenced in the absence of formal publications. A sample bibliography is included to show the style for eight types of literature citations.

Acknowledgment

The Technical Publications Administrators supplied valuable source material and made helpful suggestions for this article (see inside back cover).

Bibliography

1. *Technical Reports and Engineering Memoranda*, RCA Policy No. 16212.
2. *Preparation and Control of Technical Reports, Engineering Memoranda and Contract Reports*, DEP Procedure No. 2001.
3. *Technical Reporting Procedure*, RCA Laboratories No. 503.
4. *EC Management Policy on Engineering Reports*, MP501.7

		Page 1
GATE-COMPUTER/CONTROLLER FOR AUTOMATIC TEST EQUIPMENT		
by B. Rainstrom, I. N. Vent and C. Reate		
SECTION		
	SUMMARY	2
	INTRODUCTION	3
I.	SELECTION OF A COMPUTER/CONTROLLER FOR ATE.	4
	General	4
	Characteristics of Automatic Testing	4
	Typical UUT Requirements	6
	Operational Requirements	13
	Summary of Computer/Controller, Table I-1.	25
II.	LOGICAL DESIGN OF A COMPUTER/CONTROLLER FOR ATE	27
	General	27
	Computer Characteristics	27
	GATE System Operation	30
	Description of Major Components	44
	Description of GATE Commands	53
III.	PROGRAMMING OF GATE	72
	Introduction	72
	Characteristics of GATE and FADAC	72
	Typical Test Operations	74
	Use of Subroutines	94
	Data Conversion	96
	Sample Test Routine	97
	Programming Costs	116
	Compiler Routines	117
APPENDIX A. INTEGRATING THE COMPUTER/CONTROLLER		119

Fig. 6—A table-of-contents page (introductory and text pages follow).

Page 2

FRESNEL REGION POWER DENSITIES

I. INTRODUCTION

As aperture size and power increase for a fixed wavelength, power densities in the vicinity of the antenna must be considered for personal safety reasons. The MADRE antenna consists of two rows of 10 dipoles placed in corner reflectors with power and antenna dimensions as follows: 1) average power, 100 kilowatts; 2) antenna length, 330 feet; and 3) antenna height, 138 feet. This report is concerned with computation of Fresnel region power densities.

II. FRESNEL REGION ON-AXIS POWER DENSITY EQUATION

There has been much work done on the computation of Fresnel region field distributions¹⁻¹². The references given do not include computed results which can be used to approximate the Fresnel region fields of the fixed MADRE antenna. It is therefore necessary to derive an expression for the fields of interest. For simplicity, the results of Hu's^{2,3} investigations are used as a starting point. The derived equations are expressed as functions of range, aperture dimensions, and wavelength in the same manner as used by Bickmore and Hansen.⁸ An expression for the Fresnel region fields is:⁹

$$E(x, y, z) = \exp(-jkz) \frac{jk}{z\sqrt{z}} \int_{-b/2}^{b/2} E(n) \exp(jk) dn \quad (1)$$

Where: k = propagation constant of free space.

Fig. 7—Typical text page for "TR's"; a report title and introduction are included.

Page 33

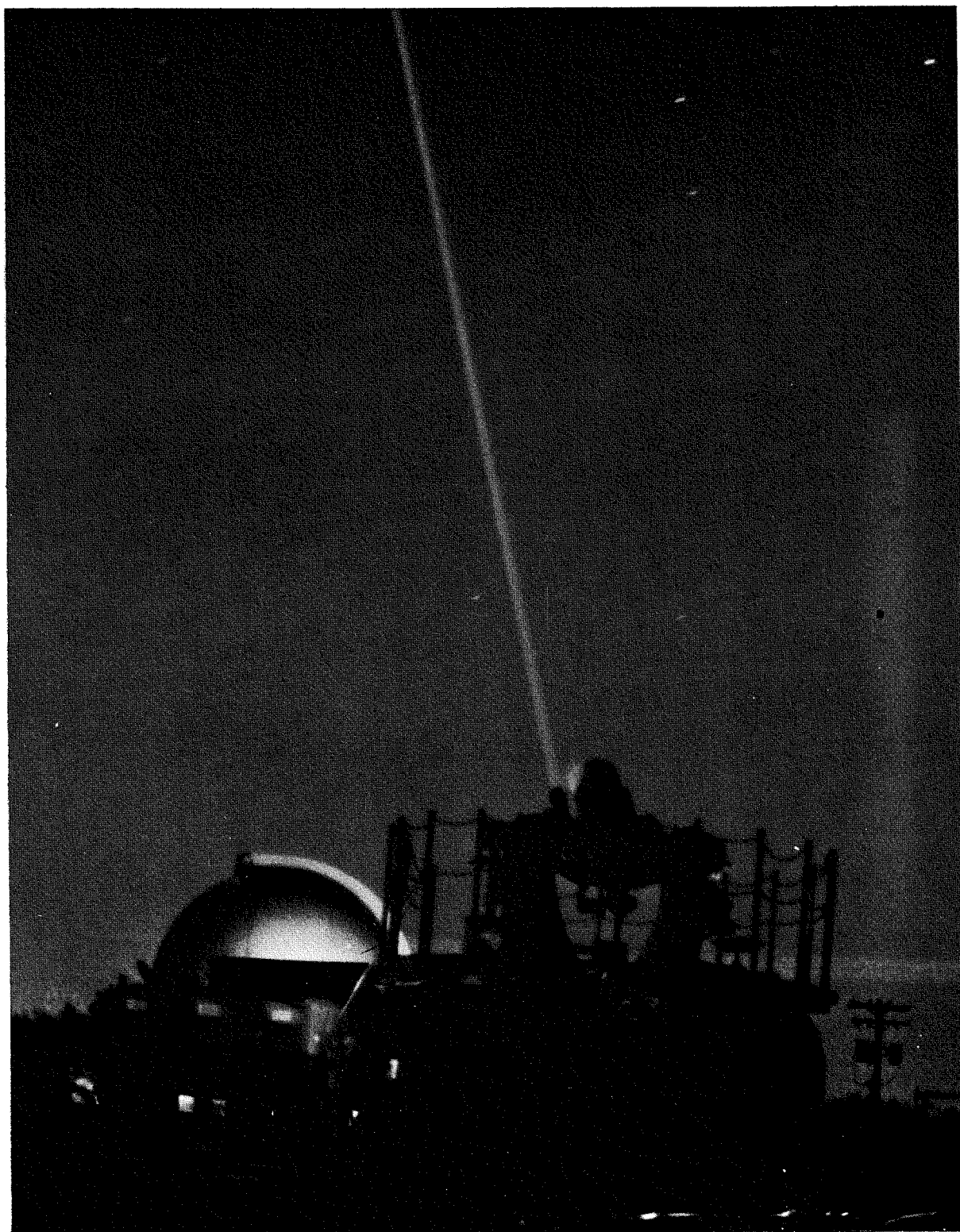
BIBLIOGRAPHY

1. K.K.N. Chang, G.H. Heilmeyer and H.J. Prager, "Low Noise Tunnel Diode Down Converter Having Conversion Gain," *Proc. IRE*, May 1960.
2. Jess J. Josephs, "A Review of Panel-Type Display Devices," *Proc. IRE*, Vol. 48, pp. 1380-1394, August 1960. (This reference contains a very extensive bibliography on display devices).
3. G.A. Swartz and L.S. Napoli, "High Density Cesium Plasma Discharge," American Physical Society Meeting, Colorado Springs, Nov. 1961.
4. R.A. Santilli and H. Thanos, "Consideration of Automobile AM-FM Receiver Design," presented at IRE/EIA Radio Fall Meeting, Syracuse, N.Y., October 1961; (to be published in *Semiconductor Products*).
5. S. Bloom and B. Vural, "Asymptotic Noise Spectra of a Drifting Maxwellian Beam," RCA Laboratories; (to be published).
6. H.S. Black; *Modulation Theory*, D. Van Nostrand Company, Inc., New York (1953), pp. 37-58.
7. K.K.N. Chang, et. al.; *Research and Development on Semiconductor Parametric and Tunnel Diode Microwave Devices*, Final Report Air Force Contract #19 (604) 4980, Oct. 31, 1961; RCA Laboratories.
8. G.A. Smith and L.S. Jones, *Data on GaAs Lasers*, TR-0000, RCA Semiconductor and Materials Division, Somerville, N.J.

Fig. 8—Typical reference list or bibliography. Eight types of citations are included.

Future of the laser

Dr. H. R. Lewis
E. Kornstein



To help engineers come abreast of recent innovations in laser technology, the authors have attempted to review the current status of lasers from two points of view. First, what is available now and what use is being made of it? Second, what other application ideas are current, but unexploited because of inadequate devices? Obviously the second question leads back to considering the direction component work should take in the near future. In addition, we have indicated some of the locations within RCA where specific kinds of laser work are underway. Other papers in this Laser Issue give additional details on specific developments within RCA.

THE SUCCESSFUL CONSTRUCTION OF LASERS in 1960 suddenly presented engineers and scientists with a new and very different tool. Even in these days of rapid technological change, the abruptness of this transition was unusual. The production of coherent electromagnetic radiation had steadily advanced in the 20th century through radio frequencies into the microwave region, and by 1950, small steps were being made toward sub-millimeter wavelengths. The ruby laser made possible a sudden leap to the visible over a portion of the spectrum 1,000 times larger than all of that used previously. As a result, some very new scientific and technological applications were immediately possible but others still seem to hover just beyond reach. To use more fully the potentialities of the laser, two or possibly three kinds of advances are required. One is improvement of lasers themselves with efficiency being perhaps the dominant problem. A second is improvement of the auxiliary components that enable one to handle light usefully. Probably new device concepts are also needed here. The third required advance must be in the thinking of the engineer who will eventually make best use of the laser. It takes time to catch up with such an innovation.

Components

The following is a condensed summary of what is now available in lasers and auxiliary components. It is not at all complete; in fact, its main value may be its selectivity within each category. For example, there are many hundreds of lasers, but we list the current status of only the few that now seem particularly interesting.

Lasers

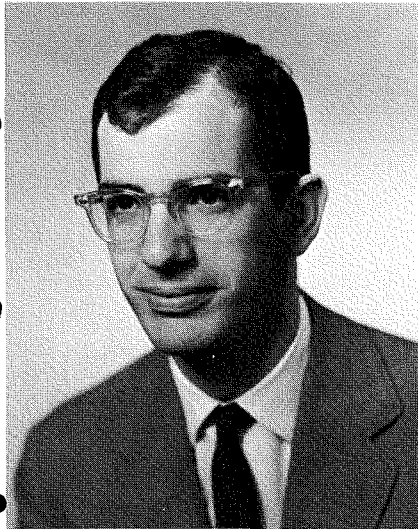
Laser	Type	Wavelength (micrometers)	Comments
He-Cd	Gas	0.4416	Performance in the violet similar to that of He-Ne laser shown below.
		0.3250	
Ionized Argon	Gas	0.4880	Produces about ten times the power/unit volume compared to a He-Ne laser. Efficiency increases with size being about 0.05% at the 1 watt output level.
		0.5145	
Ionized Krypton	Gas	0.3507	Provides a variety of lines throughout the visible range, but efficiency lower than for argon.
		0.4762	
		0.5208	
		0.5682	
		0.6471	
He-Ne	Gas	0.6328	Produces approximately 0.08 watts/meter of optical cavity at constant efficiency of about 0.05%, independent of length.
Ga _{1-x} Al _x As	Injection	0.6300	Alloys can be made to emit at any desired wavelength in this range. At the long wavelength end, efficiencies of 40% can be obtained in pulsed devices operating at room temperature with peak power of 50 W and repetition rates of kHz. Alloys range from 0 ≤ x ≤ 0.34.
		↓ 0.9000	
Cr ³⁺ :Al ₂ O ₃ (Ruby)	Optically pumped, crystal laser	0.6934	Very high-power pulses can be obtained by Q-switching at about 0.1% efficiency. In cw operation, 1 watt can be obtained at room temperature and 0.05% efficiency.
Nd ³⁺ :glass	Optically pumped, crystal laser	1.065	Size of laser limited only by material strength. Extremely high peak power (Gigawatts) and high energy (1000's of joules) per pulse. Efficiency somewhat less than YAG host.
Ho, Er, Yb, Tm YAG	Optically pumped crystal laser		In cw operation, 15 watts can be obtained at 5% efficiency at 77°K.
Nd ³⁺ :Y ₃ Al ₅ O ₁₂ (YAG)	Optically pumped crystal laser	1.065	Very high power pulses can be obtained by Q-switching. In cw operation, 200 watts can be obtained at 3% efficiency at room temperature.
Dy ²⁺ :CaF ₂	Optically pumped crystal laser	2.358	1 watt cw at 78°K and 1% efficiency.
CO ₂	Gas	10.57	Produces approximately 50 to 75 watts/meter at constant efficiency of about 10%.
H ₂ O	Gas	118.	1 milliwatt pulsed.
CN	Gas	337.	50 milliwatts pulsed.

Frequency translating devices

Mixing of microwaves and light: The output of a laser has been shifted by frequencies of several kHz by passage through an electrooptic modular driven by a microwave signal. Precise shifts over a range from 0 to 100 kmC

should be possible.

Mixing of two light signals: Very far infrared or sub-millimeter radiation may eventually be produced most efficiently by mixing two light signals. The effect has been demonstrated in GaAs.



Dr. Henry R. Lewis, Director
Materials Research Laboratory
RCA Laboratories
Princeton, N.J.

received the AB, MA, and PhD from Harvard University in 1948, 1949, and 1956 respectively. His doctoral thesis field was nuclear resonance using the molecular-beam technique. From 1951 to 1953, and for a year after receiving the doctorate, he worked with the Operations Evaluation Group of the Massachusetts Institute of Technology on various problems in naval warfare. Dr. Lewis joined the Technical Staff of RCA Laboratories in 1957 and worked on new paramagnetic materials for masers. For that work he shared an achievement award with H. J. Gerritsen for studies on a new maser material, Cr^{3+} in TiO_2 . In 1960, he became head of the Quantum Electronics Group whose projects included masers, lasers, and associated devices. He was Director of the Electronics Research Laboratory from 1966 to 1968 and is now Director of the Materials Research Laboratory.



Edward Kornstein, Mgr.
Optical Physics Techniques
Aerospace Systems Division
Burlington, Mass.

received the AB in Physics and Mathematics from New York University in 1951. He received the MS in Physics from Drexel Institute of Technology in 1954. He attended Boston University on the RCA David Sarnoff research fellowship and completed course requirements for the PhD. Mr. Kornstein joined RCA in Camden in 1951. Mr. Kornstein has been with ASD since 1960. His group has developed Q-switching techniques for laser rangefinders; CW optically pumped lasers; undersea second harmonic laser generators for the Navy; 50-MW 10-pps ruby rangefinders for missile trackers; high power lasers for atmospheric research; laser alignment equipment; lightweight, compact, ruby laser rangefinders; and a laser obstacle scanner for the Department of Transportation. He is a member of the Optical Society and was Boston regional chairman for the SMPTE.

ever, available material is presently of poor optical quantity, has residual absorption, and must be temperature controlled. Improvements in materials here could make the relatively high efficiency of the near IR lasers an important source of visible light.

Modulators

Even now, many modulation and deflection requirements can best be satisfied mechanically. However, there is

little doubt that electro-optic devices are the method of the future. Electro-optic materials are those in which a DC or relatively low-frequency applied electric field changes the index of refraction of a material for a particular polarization of the optical field. Tensors are required to describe the interaction and the electro-optic effect can be used in a large variety of device configurations. This makes simple descriptions difficult. One somewhat inadequate figure of merit is the half-wave voltage: the voltage that must be applied to a material to produce 100% modulation. In the early 1960's only *KDP* was available for modulators in the visible, and its half-wave voltage was 8000. A great deal of materials research has now produced a number of materials with half-wave voltages under 100 (e.g., $Sr_xBa_{1-x}Nb_2O_6$). In addition, small effective half-wave voltages can often be obtained by applying the field perpendicular to the direction of light propagation so that the required voltage is reduced by the ratio of the dimensions of the material. Two very promising new materials are $LiTaO_3$ and $LiNbO_3$, with half-wave voltages of 2800. With these materials, modulators with 100 MHz of bandwidth can be achieved at center frequencies from baseband to microwaves and drive powers of 1 to 10 mW per MHz.

Deflectors

Three classes of light deflection are possible by the use of electro-optic or elastic-optic effects. In the simplest device, the index of refraction of an electro-optic prism is changed to deflect a beam. Unfortunately, realizable changes of index are not as yet large enough to make effective devices in this way. A second means is to combine electro-optic control of polarization with naturally birefringent materials. Combining n pairs of such materials produces 2^n digital displacements of the beam. The digital control is desirable, but to date the complexities of fabrication have been forbidding. The third, and currently favored technique, uses the elasto-optic effect whereby an acoustic wave in a material produces a periodic index of refraction. The resulting thick diffraction grating produces Bragg diffraction of the light beam. This device is most

● **Harmonic generation:** The nonlinear polarizability of some materials produces significant amounts of second harmonic radiation when a coherent optical wave passes through it. If the velocities of the two waves are matched, the effect is greatly enhanced. A relatively new material, $Ba_2NaNb_5O_{15}$ (banana) can in principle produce almost 100% conversion to second harmonic in focused, moderately-high-power, cw lasers. How-

appropriate for sequential deflection rather than random access. Lithium niobate, with its large piezoelectric effect, provides a good generator of acoustic waves, and $PbMoO_4$ (a crystal not difficult to grow with good optical quality) can be used as the elasto-optic material. With it, 100 resolvable spots have been produced at megacycle rates. Water is the best material for use where the deflection requirements are small. A larger number of resolvable spots (perhaps 500) can be obtained by combining this device with what amounts to a travelling lens produced electro-optically. This can only be done in a sequentially scanned system.

Sensors

For applications in which laser properties other than the ability to concentrate energy into a small area are utilized, the response speed of laser detectors is important. In this case, photon effect receivers rather than thermal detectors are required. The photon effect receivers used most widely today can be subdivided into:

- 1) Photoemissive devices
- 2) Photoconductive devices
- 3) Photovoltaic devices

1) *Photo-emissive detectors*: The photoelectric effect occurs when photons fall upon a surface and cause electrons to be emitted. It is difficult to have photoemissive detectors at lower frequencies than the very near infrared (2.7×10^{14} Hz) or, equivalently, at longer wavelengths than about $1.1 \mu\text{m}$. The quantum efficiency of these devices is defined as the average yield of electrons per input photon. For photoemissive detectors, the quantum efficiency ranges from about 0.2 in the ultraviolet to 10^{-4} in the near infrared. Photoemissive devices have been widely used in the visible for both energy detectors and for imaging detectors. The use of electron multiplication has made possible low noise post-detection power gains of 120 db.

Ordinary photomultipliers have a flat frequency response out to about 100 megahertz, but with precautions, several hundred megahertz can be achieved. Special purpose phototubes and multipliers have been developed to achieve microwave bandwidth op-

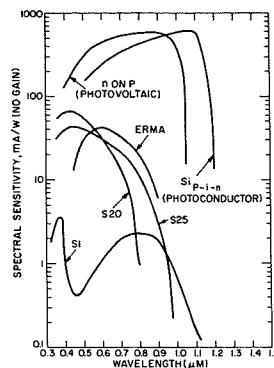


Fig. 1—Sensitivity versus wavelength for photodetectors.

tical detection largely for laser communications and heterodyning applications.

For most laser work, the S-20 surface, the S-25 surface, the ERMA surface, and the S-1 surface are the most significant. All of these can also be utilized for imaging devices such as image intensifiers (see Fig. 1). A new photoemissive material recently developed by RCA, $Ga_{0.2}In_{0.8}As$, should have at least 10 times the sensitivity of the S-1 at 1.06 micrometers, and substantially lower dark current.

2) *Photoconductive detectors*: In the photoconductive process, a change in the number of incident photons causes a fluctuation in the number of free-charge carriers in the material. The electrical conductivity of the responsive element is inversely proportional to the photon number. Photoconductors extend into the infrared region where photoemissive devices do not function. There are two classes of photoconductors:

1) *semiconductor types* (germanium, lead sulfide, indium antimonide) with relatively high dark current at room temperature and roughly microsecond response times, and

2) *insulator types* (cadmium sulfide, cadmium selenide) with low dark currents at room temperatures, but much slower response times.

Because of the relatively poor response times at room temperature and the availability of other detectors, the photoconductive devices are not typically used for visible and near-infrared laser applications. In applications involving long-wavelength lasers, such as the CO_2 laser at $10.6 \mu\text{m}$, the doped germanium devices at cryogenic temperatures have been successfully

employed. Through special design, some of these detectors have been pushed to GHz response and used for heterodyne detection at $10.6 \mu\text{m}$. Other techniques, such as inserting photoconductors in microwave cavities, have resulted in very fast, sensitive detection out to $10 \mu\text{m}$; however, the complexity of these devices have not yet permitted large scale operational use.

Photovoltaic type devices: When the junction of a semiconductor is illuminated and a connection is made to both sides of the junction, a current will be seen to flow during the period of illumination. This is the photovoltaic effect, and no external bias on the cell is required to generate an e.m.f. when illuminated.

If an external bias is applied in the reverse direction at the P-N junction, current will also flow under illumination. Operation in this mode is commonly known as the "photoconductive" mode. The primary advantages of this mode are that it offers higher sensitivity and faster response time than the photovoltaic mode.

Diodes with multiplication gain have recently become available. A typical avalanche diode consists of a deep-diffused graded P-N junction in a silicon wafer. Surface contouring allows the diode to be reverse biased in excess of 1800 volts to achieve a high internal field without surface breakdown. This bulk field is high enough to allow internal multiplication of the charge carriers (electrons) by impact ionization. Multiplication gains in excess of 100 to 200 have been reported. Quantum efficiencies of 20% at 1.06 micrometer and about 50% at 0.9 micrometer are typical.

Recording media

Holographic applications have resulted in a requirement for materials which are sensitive to laser radiation and have high resolution capabilities. Many materials such as 1) silver halide emulsion, 2) photo-polymer materials, 3) dichromated gelatin, 4) photochromatic crystals, 5) thermoplastic films, 6) ferroelectric crystals (lithium niobate), 7) silver halide single crystal colored with F centers,

8) ferromagnetic thin films (manganese bismuthide), 9) photoresist, and 10) Kalvar film have been investigated. A sample list with some of the more important properties is given in Table I.

Applications

Material processing

The growth of integrated circuit technology has resulted in a need for micro-material processing that seems to be well suited for laser systems. Commercial laser micro-welders, resistor and capacitor trimmers, and micro-hole drilling systems are presently available from several sources. These systems generally use pulsed ruby, pulsed or cw neodymium-doped YAG or glass, or pulsed or cw CO₂ lasers as the power source, although some trimming work has been done with argon gas lasers.

On a larger scale, higher power lasers have been used for macro-material processing. These include high power pulsed ruby or neodymium lasers for "on the fly" balancing of rotating machinery, and high power cw neodymium and CO₂ lasers for continuous cutting of thin metal sheets and seam welding of conventional and exotic materials. The high power cw neodymium and CO₂ lasers have also been used for drilling holes in non-rigid materials such as rubber and plastic,

and cutting cloth, paper and plastic sheets.

In addition to the actual material processing laser instruments are being developed for precision control of metal cutting machines. Rather simple He-Ne lasers can be used for this application; the bulk of the cost is in the detectors and control servomechanisms. Similarly, applications for alignment of machine tool ways and fixtures and jigs are under development.

Communications

The communication applications can be divided into four arbitrary areas:

- 1) Applications in which the range is short so that attenuation of the medium is not significant. Examples of this would be the use of lasers to replace umbilical cords for missile checkout.
- 2) Short to moderate range terrestrial communications that are limited by line-of-sight requirements and atmospheric attenuation. Examples are GaAs injection laser communication systems operating out to about 5 miles.
- 3) Long-range space communications limited only by laser and receiver performance, geometry and physical optics. Examples are space qualified He-Ne lasers already developed and CO₂ lasers presently under development.
- 4) Guided optical communications

to augment existing cable systems. Examples are hollow pipes filled with gas or optics to control the passage of a laser beam.

If one considers the optical spectrum for communication, the carrier frequency of about 10¹⁴ Hz is very attractive and even if only 0.1% is usable, this still permits a bandwidth of 10¹¹ Hz. The main problem is to develop suitable modulators and demodulators on the input and output ends so that this bandwidth can be utilized.

At present, several short-range, handheld GaAs voice communicators have been delivered to the military. Experimental TV transmission over short links has been demonstrated.

Military

Much of the funding for basic work in the laser area has been for potential military and space applications.

This has led to the development of laser illuminators as an aid for night vision systems. The use of GaAs diodes in arrays to produce tens to hundreds of watts of average power seems to be reasonable goals. The advantage of these illuminators is that they can be "covert," that is, they produce radiation in a special region that can be detected by S-20 or extended-red-response imaging detectors, but not seen by the naked eye. The ability to produce very short pulses also permits range gating of the receivers, reducing

Table I—Potential materials for holographic storage media.

Material	Phase or absorption type	Environmental considerations	Resolution (lines/mm)	Reproduction (J/cm ²)	Dimensional storage features	Comments
Kodak 649F Film	(a) absorption, normally with diffraction efficiency of <6%. (b) bleaching out the silver halide after exposure produces phase type with higher diffraction efficiency	none	1500 to 3000	wet process 0.001	(a) thin normally (b) thick if formed as a reflection hologram (which improves diffraction efficiency)	low grain noise may result from the bleaching process
Dichromated gelatin film	phase only, with diffraction efficiency of 96% for a thick hologram and 32% for a thin hologram	none	2000	0.01	thick or thin	no grain noise
Thermoplastics	phase only (formed by surface deformations)	none	200	0.001	thin surface effects	fatigue is present
Solid Crystal Lithium Niobate	phase only, with 42% diffraction efficiency	erased by heat	1600	1-100	thick	limited storage life
Silver Halide with F Center	absorption only	discolor in ambient light	1500 to 3000		thick	(a) white light readout tends to discolor crystal (b) low efficiency into first order
Photoresist	phase only (formed by surface deformation or index change, with diffraction efficiency of 34%)	none	2000	~0.01 for KOR	thin	surface noise under investigation

Note:

- (1) Diffraction efficiency = % of incident laser beam diffracted into first order.
- (2) A phased hologram has higher efficiency than an absorption type and a thick hologram has higher efficiency than a thin hologram of the same material.

the amount of backscatter and providing enhanced detection in many cases.

Another major class of device for the military is the target designator in which the narrow beam of the laser is used as a pointer. These are similar in construction to rangefinders and utilize mostly neodymium or ruby as the laser source, although some work has been done utilizing practically every laser device. The rangefinders are probably the most advanced application with many prototypes in the field and production contracts currently in progress. Offshoots of the rangefinder are laser altimeters, laser fuses, and laser radars. Among the more sophisticated applications are high-power, frequency-stabilized lasers for doppler navigation, real-time target velocity determination and moving target indication (MTI) surveillance scanners. CO_2 lasers have been stabilized to the order of 1 part in 10^9 and are used experimentally in many of these applications. Neodymium, argon, and CO_2 lasers are used in reconnaissance line scanners (similar to a flying spot scanner) in which the moving aircraft provides the scan in one direction. Laser beacons for signalling and IFF (identification friend or foe) systems have been proposed and are under evaluation.

One of the earliest military applications discussed since the discovery of the laser has been the "death ray". It is not inconceivable that as lasers get more powerful, and as more understanding of high power phenomena is developed, laser weaponry for defensive applications may ultimately be possible.

Laser intrusion alarms for securing sensitive areas have been developed for the military and can also be used as commercial burglar alarms. These are primarily $GaAs$ injection laser devices that sound an alarm or record an event when a line of sight is broken. One outgrowth of this type of device is the obstacle-detector system recently built by RCA for the Office of High Speed Ground Transportation of the Department of Transportation.

Data processing/holography

In these applications, the coherence of the laser becomes of prime impor-

tance, and gas lasers seem to be more appropriate. The optical data processing applications include the extraction of signals from noise through cross-correlation and/or autocorrelation techniques. In addition, two-dimensional Fourier transforms can be done along with bandpass filtering. In all these applications, the laser is used as a generator of coherent radiation.

Another class of application that may loosely be placed in this category of data processing is the use of lasers in holography. In this application, lasers are used for the recording and playback functions. Lasers of all types have been used, but the main emphasis is on gas lasers because of their superior coherence properties. The applications of holography would be an article in itself, and it is conceivable that the greatest number of lasers will be used in this application. A prime example is the pre-recorded video tape system recently announced by RCA. In its present form, the system utilizes a small helium-neon gas laser in each playback unit. A second major application area is the holographic credit card verification system presently in development. This system utilizes a small cold-cathode pulsed argon laser at each credit card imprintation location.

Holographic memories for computers, and the actual use of laser devices as logic components in computers have been demonstrated in the laboratory.

Medical

One of the earliest medical applications of the laser has been the development of retinal coagulators. These devices for "welding" detached retinas have become almost standard in many hospitals. Ruby pulsed lasers are the main radiation source for this function.

Recently some success in dental research on laser use has been reported. The laser was used to re-fuze pinholes in the enamel outer protective coating of teeth. This may greatly reduce the development of cavities in the enamel.

"Bloodless" surgery and wart and skin blemish removal have been performed by laser.

One application, although not strictly medical, can be put in the biological

effects category. A company has been formed to exploit the use of a laser for branding cattle. A high powered CO_2 laser is used.

Alignment and reference devices

The laser has proven to be a very useful tool for many alignment applications such as pipe laying, tunnel boring, surveying, and establishing reference lines as needed in the construction industry. These devices use primarily low-power gas-laser systems.

Laser gravitometers, based upon the doppler shift of the laser beam reflected from a falling retroreflective prism have been demonstrated and are made in limited quantities.

Laser gyros have been under development for several years and are now beginning to show signs of acceptance for specific applications.

Displays

Combining a laser with a deflection system results in a bright large-screen display. For color displays, a krypton gas laser is used and more recently a krypton/argon gas laser has been developed. These lasers emit in several spectral regions and can be designed to emit proper balances of three primary colors producing a very bright display. Laboratory systems have been built and demonstrated. The main difficulty at the present time seems to be the poor efficiency of the laser and the lack of good beam deflectors.

Laser recording

High-density recording on film has been done by use of a modulated argon laser. The capability of such a system is presently about 100 MHz. The beam deflection is done by a high-speed rotating prism assembly, electro-optical crystals such as KDP (potassium dihydrogen phosphate) controlling the modulation. The system is used for wide bandwidth recording of radar signals and high resolution video systems.

Research application

Use of the laser as a research tool in many areas is rapidly developing. Among some of the more successful applications have been:

- Atmospheric probes
- Analysis of materials using laser probes

Table II—Laser work being performed in various divisions of RCA.

	RCA Laboratories Princeton, N. J.	Electronic Components Somerville, N. J.	Electronic Components Lanester, Pa.	DEE Advanced Technology Camden, N. J.	Apoptose Systems Dorchester, Mass.	Electric Applied Materials Laboratory Research, N. J. Princeton, N. J.	Astro-Electronics Princeton, N. J.	RCA Limited Montreal, Canada	Electronic Systems Div. Van Nuys, Calif.	Electronic Systems Div. Princeton, N. J.
Lasers	Injection Gas Optically pumped	Injection	Gas (HeNe, He- Cd, Argon)	Optically pumped Injection	Optically pumped Injection	Gas			Gas (He-Ne, CO ₂)	
Deflection	Mech. Acoustic			Mech.						
Modulators				KDP			GaAs			
Sensors	Photo-emitters Arrays of photo-diodes		Photo- multipliers Vidicons		IR mosaic arrays Low light level tv		Arrays of photodetectors		Arrays of photodiodes	
Recording Media	Photo-chromics Holographic materials Bleachable materials			Holographic media	Holographic media					
Radar				Intrusion alarm Line scanners	Range finders (portable, tank, airborne) Obstacle detectors		Tracker (GaAs)		Fusing	
Recording				100-MHz recorder			100-MHz recording			
Optical Memory	Read only Read and write								Read only	
Communications				Short-range voice (GaAs)	Funded Navy study					
Target designation		Illuminator GaAs, GaAlAs		GaAs arrays	GaAs, Ruby, Nd.					

Spectroscopy (both optical emission/absorption and Raman)
Setting up of standards
Sources in Schlierin systems
Interferometry
Source in high-speed photography
Seismograph

Potential applications

Displays

An interesting possibility might be a 2x3-ft. image produced by a beam deflected at tv speeds. About 10 watts of light, properly color balanced, are required at the screen. Assuming a transmission factor of 20%, we need 50 watts at the source. A laser with 5% efficiency would require a kilowatt input. The modulators would need 6-MHz bandwidth, and the deflection systems would have to produce 500 resolvable spots. Available gas lasers have the power, but their efficiencies are a factor of 50 off from this figure and little or no improvement has been made recently. However, the CO₂ laser in the far-infrared operates at 15% efficiency and provides encouragement for further work.

Radar

Optical radar is now being used successfully for such diverse problems as to track satellites, to measure the distance to the moon, and to construct installations requiring very precise location. Lasers now available are adequate for these applications. However, if high-power Q-switched lasers could be made with 10% efficiency, a convenient, portable radar would much enlarge military use of lasers. To fully take advantage of the laser capability, matching improvements are required in the detector.

Illuminators

Presently used illuminators consisting of arrays of GaAs diodes must be cooled to obtain significant average power output. The development of diode arrays capable of producing hundreds of watts of output power at 20 to 30% efficiency without the need for cooling to liquid nitrogen temperatures would permit the development of small easily handled illuminators. The military applications for this improved night vision capability are evi-

dent. Commercial applications such as special lighting for aircraft, landing aids, and beacons, could develop into significant volume.

Work at RCA

Table II lists groups in RCA that develop, design or manufacture laser components or laser systems. It is not complete because of the rapid growth of laser work, but it will serve as a fair guide to the location of the main laser efforts at RCA.

Conclusion

The laser will probably be identified as one of the significant scientific advances of the twentieth century. Claims made in the early 1960's concerning applications and market potential minimized the difficulties of converting a laboratory device into an operational system. As laser technology matures, these proposed applications are becoming commercially feasible.

Advances in gas laser technology

Dr. K. G. Hernqvist

Some recent advances in the gas laser field are reviewed in this paper. Improvements in reliability, cost, and noise characteristics are described. Progress towards the mass-produced gas laser is reported and the latest addition to the gas laser family—the helium-cadmium laser, (see cover)—is introduced.

PROGRESS IN THE GAS LASER FIELD during the last three years has been characterized by improvements in small steps rather than by giant breakthroughs. Advances in technology have brought about greater device reliability and lower cost. The low-cost, mass-produced laser is just around the corner. One important new member—the helium-cadmium laser—has been added to the family.

It is the purpose of this paper to describe some of these advances, to which RCA has contributed. This work has primarily concerned the visible and the ultraviolet range of the spectrum, which is of great importance for information-handling applications.

Argon laser for high power

The argon laser is still unrivaled for high power in the visible range of the spectrum.¹ This performance is not as much due to its superior efficiency but primarily to its relatively high gain and power output per unit volume. Typically the argon laser yields an output power of the order of 500 mW/cm² compared to 5mW/cm² for the He-Ne laser.

Unfortunately no major improvements in the efficiency of argon lasers have been accomplished during the last few years; the laser has, however, become more reliable. One of the major life-limiting factors in the original sectioned-bore graphite construction of argon lasers² was the loss of gas due to sputtering processes. By careful selection of low-sputtering-yield materials (such as molybdenum) in the cathode construction, as well as by providing very gradual transitions to and out of the main discharge bore, considerable

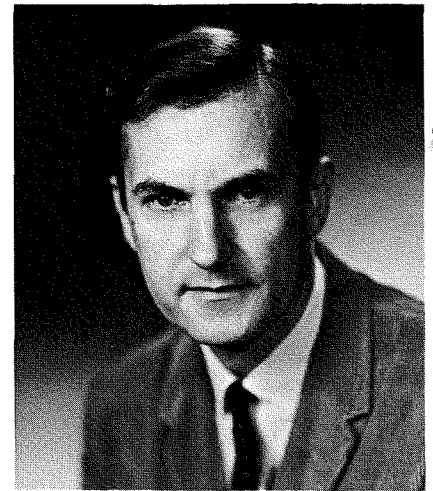
reduction in gas clean-up has been accomplished. It is now possible to construct lasers capable of thousand-hour life without the need for gas refill. Advances have also been made in the processing techniques of argon lasers. Window contamination was a major problem in the manufacture of these laser tubes; today lasers come through the production cycles with few rejects, a contributing factor to lower costs.

Argon lasers have been built with output powers ranging from a few milliwatt to tens of watts.³ Fig. 1 shows the use of a laser for satellite tracking. The laser used here was built by RCA for NASA and has a power output of 10 watts. A laser with an expected output of 100 watts is presently being built for the Army by Electronic Components in Lancaster.

Towards the mass-produced laser

In complexity of construction and processing, a gas laser is comparable to a conventional gas tube such as a thyratron. In large quantity production, such tubes sell at prices of the order of ten or tens of dollars.

The pulsed argon laser is a good candidate for an inexpensive mass-produced laser. Its relatively high gain gives it a good tolerance for imperfections in the optical components, which are part of the laser. The complexity of the continuous duty argon laser is primarily due to the heat handling problem. Most of the input power of the laser results in heating of the discharge walls at high power densities. These complexities are greatly relieved for pulse operation at low duty cycles (of the order of 1/100 or lower). For such a pulsed laser, convection-cooled glass or ceramic capillaries can be used to contain the discharge. Such laser tubes then may be simple diodes using glass envelopes onto which the



Dr. Karl G. Hernqvist
Materials Research Laboratory
RCA Laboratories
Princeton, N.J.

received the EE., Master's, and Ph.D. at the Electrical Engineering Department of the Royal Institute of Technology, Stockholm, Sweden, in 1945, 1950, and 1959 respectively. He worked on radar and microwave instrumentation in the Royal Swedish Air Force in 1945 and 1946. From 1946 to 1952 he was concerned with electron-tube research at the Research Institute of National Defense, Stockholm. He was an American-Scandinavian Trainee at RCA Laboratories in 1949. In 1952 he joined RCA Laboratories, where he has worked on microwave tubes, electron guns, gas-discharge devices, and lasers. In 1956 he independently conceived and reduced to practice the thermionic energy converter. He is presently doing research in the field of gas lasers where he recently contributed to the development of a new laser device having superior life and reliability. Dr. Hernqvist has gained an international reputation for his work. He has been the recipient of three RCA Achievement Awards for outstanding work in research and is a co-recipient of a 1967 Industrial Research (IR-100) Award for the development of a "Family of Long-Life Gas Lasers". He has authored thirty-three technical papers and holds 16 U.S. patents. He is a Fellow of IEEE and a member of the American Physical Society and Sigma Xi.

laser mirrors can be directly attached. Fig. 2 shows a pulsed argon laser being processed on mass production machinery such as used for conventional gas tubes.

Pulsed argon lasers become particularly simple when cold cathodes are used. A superior cold cathode suitable for lasers has recently been developed at RCA Laboratories. This cathode consists of a thick alumina coating which is made conductive and emissive by potassium metal. Metal atoms adhere to the alumina particles, thus penetrating the coating. When the potassium-activated alumina cathode is operated in the pulsed argon laser, small emission centers are developed on the coating, a new center forming for each pulse. Potassium is evaporated from these centers, but because

Reprint RE-15-5-8

Final manuscript received October 10, 1969.

the potassium is continuously transportable within the coating, self-healing takes place within a short time restoring the surface to its original status. Thus, the cathode is almost indestructible. Pulse currents up to 500 amperes and pulse lengths ranging to a few microseconds up to 1/2 millisecond have been obtained from this cathode. Fig. 3 shows an argon laser using such a cold cathode and delivering up to 50 watts peak output power.

Thus, it is seen that gas lasers need not be complicated or costly.

The quiet laser

One of the main problems with gas lasers is the power output fluctuation in the high-kilocycle frequency range. These fluctuations are caused by discharge instabilities and are of particular concern when the laser is used in information-handling applications. An improved *He-Ne* laser has been constructed for such applications.⁴ It yields a power output of about 1 mW and exhibits power output fluctuations less than 0.2% peak-to-peak. Several new constructional details were employed in this tube to minimize the discharge noise. The laser uses a 1-mm-diameter, 10-cm-long bore which is coaxially arranged in the laser tube to assure a symmetrical discharge path from the cathode to the anode. The tube uses the potassium-activated alumina cold cathode described in the previous section. Fig. 4 illustrates the performance characteristics of such a laser. The radiation noise has a very low value at nearly the optimum discharge current for maximum power output.

Enter cadmium

One of the first gas laser transitions discovered was that of ionized mercury. This laser, and numerous other metal-vapor lasers subsequently discovered, could only be made to lase for short-pulse ($\sim 1\text{-}\mu\text{s}$) operation. Recently it was discovered,⁵ however, that cadmium vapor seeded into a helium discharge could be made to lase under continuous duty. The operation of the *He-Cd* laser is quite similar to that of the *He-Ne* laser. In both cases, the atoms of the lasing gas (*Ne* or *Cd*) move about in a sea of *He* atoms excited by the discharge. During collisions, *He* atoms transfer their

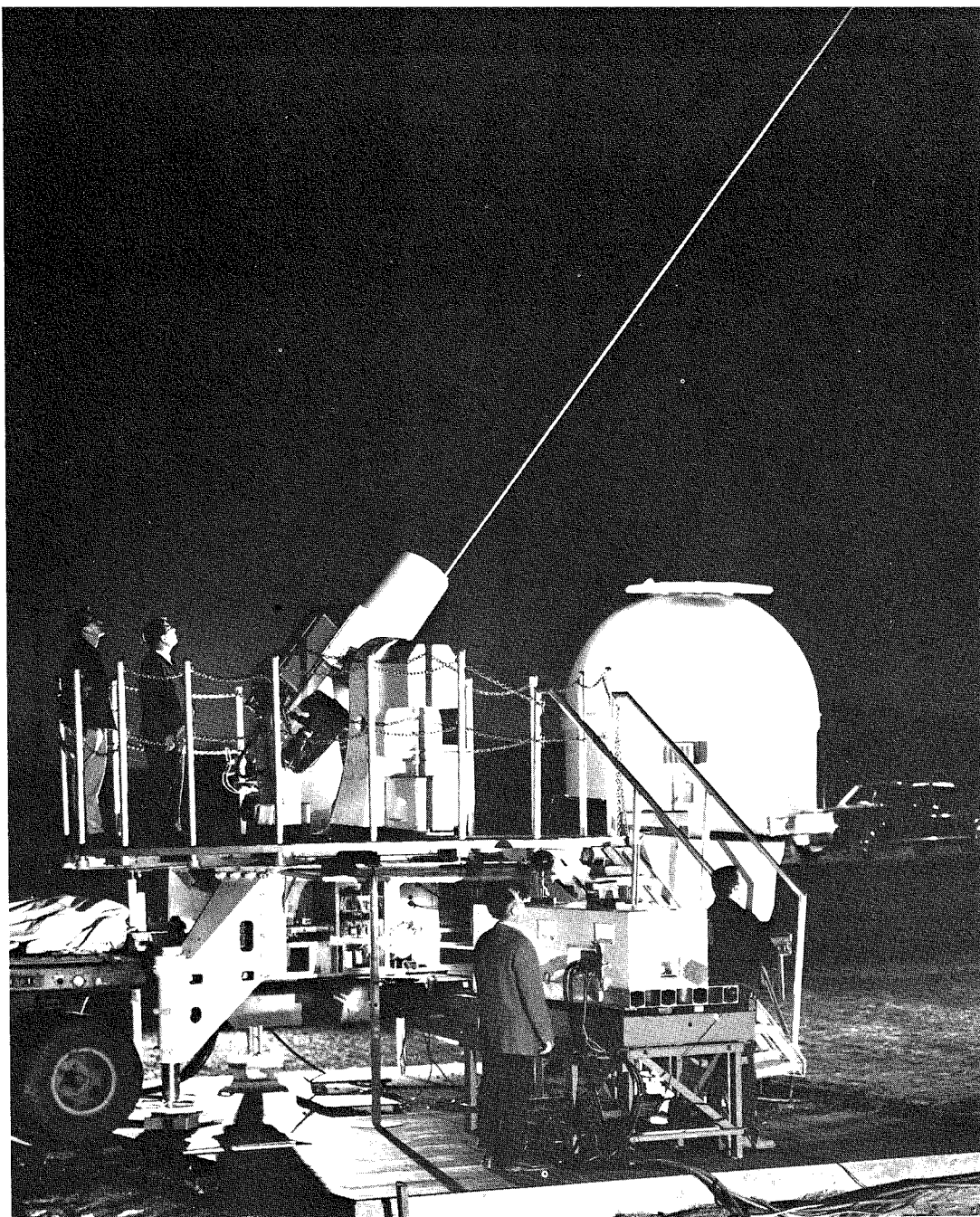


Fig. 1—Satellite tracking using RCA 10-watt Argon laser.

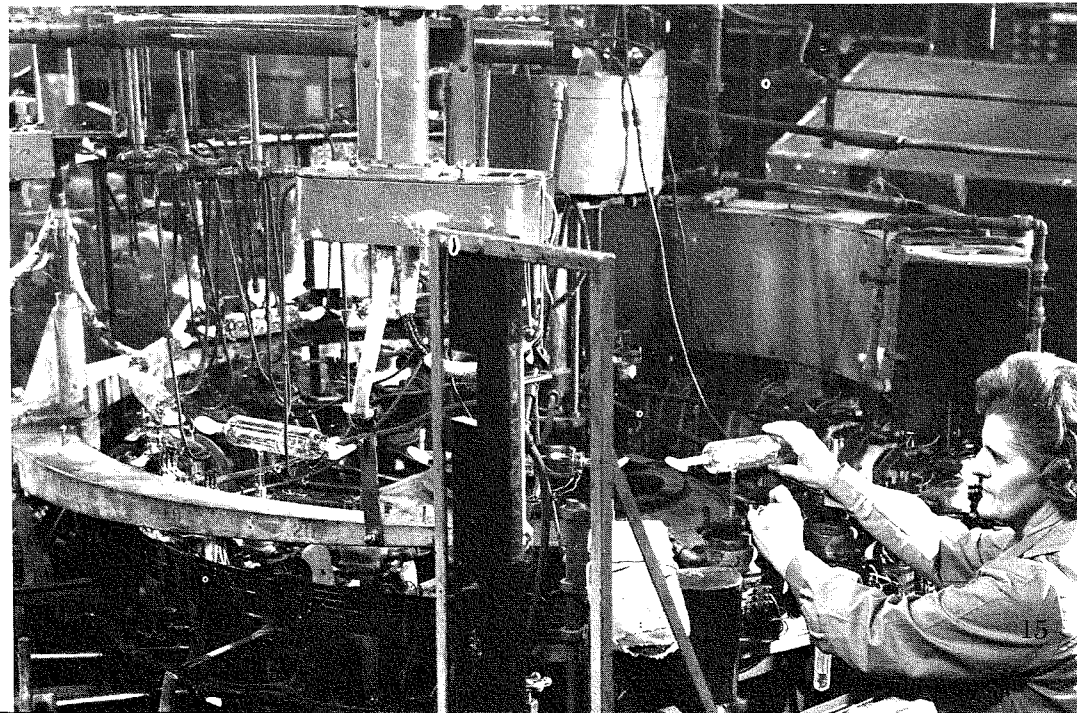


Fig. 2—Gas lasers processed in mass production machinery at RCA plant in Lancaster.

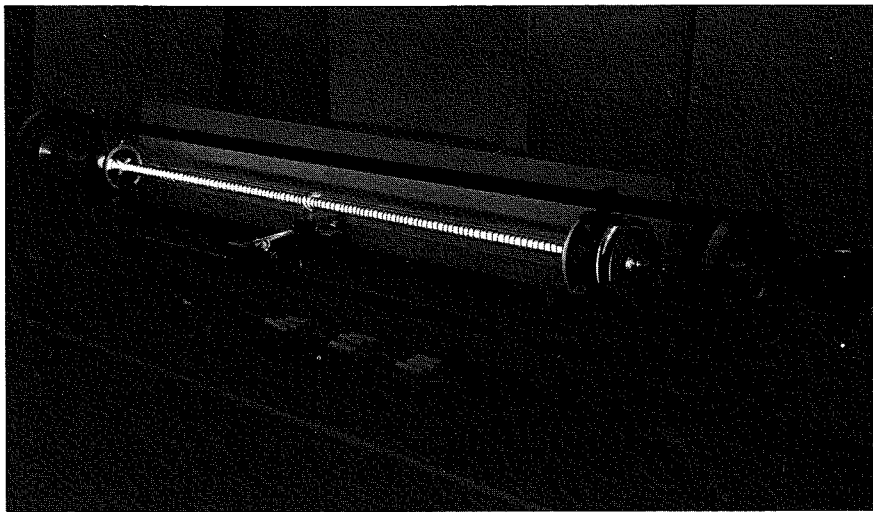


Fig. 3—50-watt pulsed Argon laser.

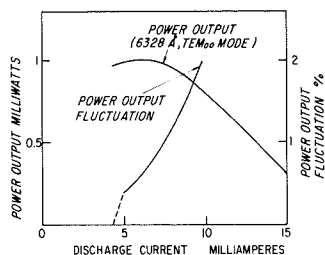


Fig. 4—Performance of low-radiation-noise He-Ne laser.

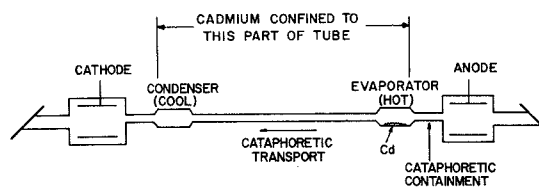


Fig. 5—Schematic drawing showing cataphoretic effects in sealed-off He-Cd laser.



Fig. 6—Commercial 10-mW He-Cd laser.

excitation energy to the neon which becomes excited to the upper laser level of the *neutral* atoms or to the cadmium which becomes excited *and ionized*.

The appropriate vapor density for the cadmium laser corresponds to a temperature of the cadmium of nearly 300°C. Such a hot cadmium vapor would be incompatible with optical components such as windows and mirrors. A technique has been developed⁶ where the hot metal vapor is confined to a restricted region of the laser tube,

separated from the optical components. This technique is making use of the cataphoresis effect, that is the rapid transport of the highly ionized cadmium vapor towards the negative electrode (the cathode). Fig. 5 shows schematically how cataphoretic containment and transport may be applied to a He-Cd laser. Assume that cadmium is introduced at the point marked EVAPORATOR in Fig. 5. Cataphoresis prevents the cadmium vapor from drifting toward the ANODE. Cadmium is, however, transported towards the CATHODE. If the CONDENSER

region is kept cool, cadmium will condense there and be prevented from reaching the cathode region. In this way, the cadmium vapor is confined to the main discharge region without reaching the cathode or the anode regions or the Brewster windows at the ends of the laser tube. To minimize the amount of cadmium needed (a matter of importance if the expensive enriched isotope of cadmium is used), the tube may be made symmetrical with the roles of the CATHODE and ANODE and the EVAPORATOR and CONDENSER being reversed after a certain amount of time, which is determined by the initial supply of cadmium and the transport rate.

The cadmium laser brings the simplicity of construction and operation of the He-Ne laser into the violet and near ultraviolet range of the spectrum, where photochemical processes are of great importance. The principal line is at 4416 Å. About 1/4 of the power at this wavelength is available in the 3250 Å line. Fig. 6 is a photograph of the first publicly shown He-Cd laser; a He-Cd laser tube in operation is shown on the front cover. It is made by RCA and yields 10 mW at 4416 Å and about 2 mW at 3250 Å.

Conclusions

Progress in the gas laser field has resulted in reliability and lower cost. The gas laser can be simple and inexpensive. Applications need not be limited to the industrial and educational markets but may encompass the mass markets such as the home entertainment field.

References

- Hernqvist, K. G., "Argon Lasers", RCA reprints PE-327, PE-328, PE-329; *RCA Engineer*, Vol. 12, No. 3 (Oct.-Nov. 1966).
- Hernqvist, K. G. and Fendley, J. R., "Construction of Long-life argon lasers" *IEEE J. Quantum Electronics*, Vol. QE-3, No. 2 (Feb. 1967).
- Buzzard, R. J., Powell, J. A., Mark, J. T. and Medsger, H. E. "Noble-Gas-Ion Lasers" RCA reprint PE-430, *RCA Engineer*, Vol. 14, No. 4 (Dec.-Jan. 1968).
- Hernqvist, K. G., "Low-Radiation-Noise He-Ne Laser" *RCA Review*, Vol. 30, No. 3 (Sept. 1969).
- Silfvast, W. T., "Efficient CW Laser Oscillation at 4416 Å in Cd II" *Applied Physics Letters* No. 13, 169 (1968).
- Fendley, J. R., Gorog, I., Hernqvist, K. G., and Sun, C., "Characteristics of a Sealed-Off He³-Cd¹¹⁴ Laser" *RCA Review*, Vol. 30, No. 3 (Sept. 1969).



Dr. Henry Kressel, Head
Semiconductor Optical Devices
Semiconductor Device Research Laboratory
RCA Laboratories
Princeton, N.J.

received the BA in Physics from Yeshiva College in 1955, the MS in Applied Physics from Harvard in 1956, and the MBA in 1959 from the University of Pennsylvania. In 1965 he received the PhD in Metallurgy also from the University of Pennsylvania. He joined the RCA Semiconductor Division in 1959, engaged in the development of high frequency switching transistors. In 1961 he was named Engineering Leader responsible for research and development of silicon and GaAs microwave diodes. He was co-recipient in 1963 of an Engineering Achievement Award for his work in this field. He was awarded a David Sarnoff Fellowship for the period 1963 to 1965 under which he pursued his doctoral studies. Upon his return to RCA in 1965, he became Head of the Device Physics Groups in the Technical Programs Laboratory (Somerville), and engaged in the investigation of avalanche effects in semiconductors with particular emphasis on the role of lattice defects and optical properties of P-N junctions. He joined the Technical Staff of the RCA Laboratories in October 1966. In 1969, he was appointed Head of the Semiconductor Optical Devices Group. His research interests since that time have included avalanche microwave devices and, primarily, radiative recombination processes and electroluminescence in III-V compounds. He was co-recipient of an RCA Laboratories Achievement Team Award (1967) for development of high power, high efficiency Si avalanche oscillators, and in 1968 (with H. Nelson) received a second award for the invention of the close-confinement laser. Dr. Kressel is author or co-author of numerous publications dealing with a wide variety of solid-state topics. He is a member of Sigma Xi, the American Physical Society, and the IEEE.



Recent progress in injection lasers

Dr. H. Kressel | H. Nelson

A great deal of progress has been made recently in improving the efficiency and reliability of injection lasers, as well as in extending their practical room temperature operation into the visible portion of the spectrum. These improvements are due to increased theoretical understanding of the device operation and of the role of metallurgical flaws. As a consequence, a heterojunction is now incorporated in the new "close-confinement" (CC) injection lasers¹ which results in a sharp reduction in their internal optical loss and an increase in their operational efficiency and reliability. Furthermore, successful technological developments in the growth of (GaAl)As from a Ga solution have greatly facilitated the fabrication of heterojunction GaAs diodes and have made possible the fabrication of visible-light-emitting (GaAl)As lasers.

THE NEW BASIC LASER STRUCTURE (Fig. 1) consists of three regions. Region 1 is P⁺ with bandgap energy E_{g1} . Region 2 (in which lasing occurs) is compensated p-type with bandgap energy E_{g2} , and region 3 is N-type also with bandgap energy E_{g2} . It is of primary importance that $E_{g1} > E_{g2}$. As explained in detail in Ref. 1, this results in an improved optical waveguide which sharply reduces internal optical loss, particularly at elevated temperature, because of the decrease in the refractive index at the lasing wavelength in region 1. Furthermore, the absorption of the junction radiation is reduced in region 1 since the energy of the junction emission is less than the bandgap energy of region 1.

H. Nelson
Semiconductor Device Research Laboratory
RCA Laboratories
Princeton, N.J.

received the BS from Hamline University in 1927 and the MS in physics from the University of Minnesota in 1929. From 1929 to 1930, he was an engineer with the Westinghouse Lamp Company. He transferred to RCA in 1930 and was engaged in R&D at the Tube Plant in Harrison, New Jersey, until 1953, when he joined the Semiconductor Research Group at the RCA Laboratories. Mr. Nelson's work has covered almost every important phase of vacuum-tube and semiconductor-device technology and research. His many original contributions include novel space-charge amplifiers, vacuum gauges, and new types of transistor structures. Mr. Nelson has been one of the pioneers responsible for the development of epitaxial technology. His recent investigations have contributed greatly to the successful fabrication of GaAs injection lasers. He has received three "RCA Laboratories Achievement Awards," and shared in the "1962 David Sarnoff Outstanding Achievement Team Award in Science." In 1968, he received the David Sarnoff Outstanding Achievement Award in Science "for conception and application of the solution regrowth technique for making semiconductor devices." He has published many technical papers and has been issued numerous patents. He is a member of Sigma Xi and of the APS.

Fig. 2 illustrates the improvement in laser performance directly due to the use of this new structure; the room temperature power output vs. current of a conventional epitaxial GaAs laser is compared with a state-of-the-art close-confinement (cc) laser emitting at the same wavelength ($\sim 9000 \text{ \AA}$). Both devices have the same dimensions. Note that the threshold current density is reduced from $40,000 \text{ A/cm}^2$ to 8000 A/cm^2 , while the differential quantum efficiency is increased from 20% to 38%. As a consequence, the cc laser operating at 25 A emits as much power as the conventional laser operating at 70 A. This has important consequences for laser reliability as will be discussed below. Furthermore, the power-conversion efficiency is substantially higher for the cc than for the conventional laser. Values as high as 11% have been obtained with cc lasers, as compared to about 2 to 3% for conventional devices. Close-confinement devices are commercially available from Electronic Components as TA 7606, TA 7608 and TA 7610.

Fabrication of CC injection laser diodes

In the fabrication of the new cc GaAs laser diode, region 1 is generated by the solution growth (liquid phase epitaxy)² of a P⁺-type (GaAl)As epitaxial layer onto an N-type GaAs substrate; region 2 is formed by the diffusion of zinc from this layer into the N-type substrate. In the fabrication of the cc visible laser diode, regions

Reprint RE-15-5-9
Final manuscript received October 10, 1969

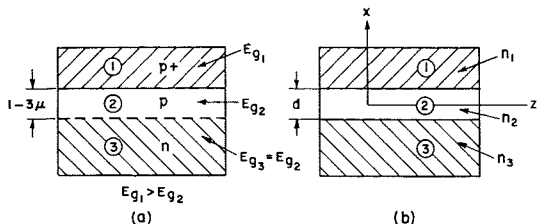


Fig. 1—(a) Injection laser structure. (b) Schematic of the junction region showing index of refraction (n_1 , n_2 , n_3) in the 3 regions to indicate the optical waveguide effect.¹

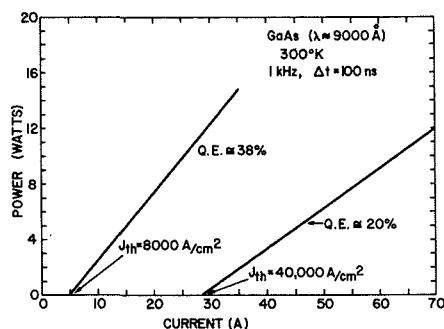


Fig. 2—Comparison of power output vs. current of conventional epitaxial GaAs laser with state of the art cc laser. Both devices have equal dimensions (6 x 12 mils) with reflective film on one facet.

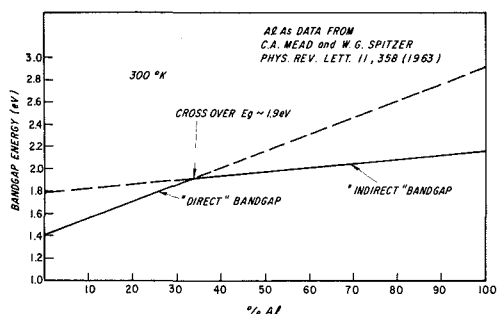


Fig. 3—Estimated variation of the bandgap energy in the $Al_xGa_{1-x}As$ system as a function of x at 300°K. The plots are based on the known band structure of GaAs and AlAs.⁶

1 and 3 are formed by the solution growth of $(GaAl)As$ layers onto a N-type GaAs substrate; region 2 is formed by diffusion. The dependence of the bandgap energy of the $Ga_{1-x}Al_xAs$ alloy system on Al content is shown in Fig. 3 as estimated from the band structures of GaAs and AlAs. The transition from direct to indirect energy gap occurs at about $x=0.34$ with $E_g \approx 1.9 \text{ eV}$ at 300°K. It follows therefore that room-temperature $(GaAl)As$ lasers can be fabricated that emit at any wavelength between that corresponding to an $E_g \approx 1.43$ (9000 Å) and that corresponding to an $E_g \approx 1.9$ (6600 Å) depending upon the Al content of the alloy. At this time, however, lasing has been observed only at wavelengths $>7150 \text{ \AA}$ at 300°K.

The band structure of $Ga(AsP)$ is nearly identical to that of $(GaAl)As$. For this reason and because it is a better known alloy system, it has been used more often for the fabrication of visible-light-emitting diodes.³ However, $(GaAl)As$ possesses a great advantage

over $Ga(AsP)$ in that the lattice mismatch of $(GaAl)As$ with GaAs is far less. Thus, the lattice constants of GaP, GaAs and AlAs are 5.4506, 5.6533 and $5.6605 \pm 0.0010 \text{ \AA}$ respectively. Since GaAs substrates are used for the epitaxial deposition, the lattice mismatch is substantially larger for $Ga(AsP)$ films than for equal bandgap $(GaAl)As$ films. The lattice mismatch between the epitaxial film and the substrate gives rise to dense arrays of misfit dislocations which, in turn, may cause non-planar junctions and provide sites for impurity precipitation.⁴ These and other untoward effects due to lattice mismatch can seriously impair laser diode operations.

A double epitaxial process is used to fabricate $(GaAl)As$ lasers with emission wavelengths shifted toward the visible portion of the spectrum.⁵ This process consists of the sequential growth of first N and then p+ $(GaAl)As$ layers on [100] oriented GaAs substrates by liquid phase epitaxy from Ga solutions. Zinc is the acceptor ($2 \times 10^{19} \text{ cm}^{-3}$) and Te the donor (2 to $3 \times 10^{18} \text{ cm}^{-3}$). The melt compositions are adjusted in such a manner that the Al content (and hence bandgap energy) is higher in the p+ region than in the N-layer.⁶ Following the epitaxial growth, the diodes are heat treated to displace, by Zn diffusion, the p-n junction a distance of $1-3\mu$ into the N-layer thus forming the optical waveguide (region 2) in which the recombination occurs. As in GaAs lasers, the lasing peak energy is 0.03 to 0.05 eV below the bandgap energy. The minimum lasing wavelength is $\sim 6600 \text{ \AA}$ (at 300°K) and $\sim 6200 \text{ \AA}$ (at 77°K), as limited by the direct to indirect bandgap transition.

Laser characteristics of CC $(GaAl)As$ diodes

Optical power measurements were made using the ITT F-4000 phototube and the calibration supplied by the manufacturer. The threshold current density was determined by extrapolation of the linear curve of power output vs. diode current to the intersection with the current axis, which checked with the usual criterion of the onset of spectral narrowing. The current pulses were about 100-ns wide at a repetition rate of 500 Hz. Both the threshold current density J_{th} and the external differential quantum efficiency

η_{ext} were determined as a function of the lasing wavelength λ_L of the diodes. Fig. 4 shows plots of the variation of J_{th} with λ_L at 300°K and 77°K. The values of J_{th} are the lowest which we have observed in uncoated lasers having cavity lengths of 10 to 11 mils. Lower threshold current density values are observed with longer diodes and those provided with a reflective film on one facet. Shown for comparison are data for the best previously reported $Ga(AsP)$ ³ and $(GaAl)As$ ^{5,7} lasers of comparable length.

The dependence of the differential quantum efficiency η_{ext} on λ_L is shown in Fig. 4 at 77°K and 300°K for uncoated lasers 10 to 11 mils long. The efficiency was calculated from the sum of the power emitted during lasing from both facets. Fig. 5 shows that η_{ext} at 300°K gradually decreases with decreasing wavelength, from a maximum of 43% at 8550 Å to 16% at 7340 Å. Similarly, at 77°K, the efficiency decreases from a maximum of 70% at 8100 Å to 20% at 6450 Å.

As discussed below, the relatively low efficiency values at short wavelengths are due to the small separation between the direct and indirect conduction band minima as well as to metallurgical factors which impair laser performance at high Al contents. cw operation has been obtained at wavelengths as short as 6900 Å at 77°K with the emission of 0.4 W from a single laser at that wavelength.

Fig. 4 shows that the lasers described here have values of J_{th} which are substantially lower than those of previous $(GaAl)As$ devices at 300°K, but which are comparable to them at 77°K. This observation is consistent with results previously obtained with GaAs lasers having the same type of close-confinement structure.¹ There, it was found that the internal optical loss was reduced by a factor of 5 at 300°K from the value observed in conventional liquid-phase epitaxy lasers, but that the difference became smaller at low temperature. This is because the 77°K internal absorption is low in any case (10 cm^{-1} or less) with much of the contribution coming from free carrier absorption in the active region which is not affected by the incorporation of a heterojunction.

Turning to a comparison with the vapor-phase grown $Ga(AsP)$ lasers in

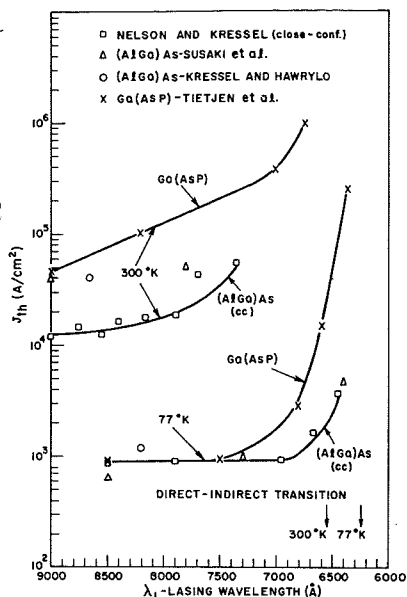


Fig. 4, we note that the 77°K values of J_{th} diverge below $\lambda_L \cong 7500 \text{ \AA}$. Since in both alloy systems the direct-indirect transition occurs at very nearly the same bandgap energy,⁸ the improved performance of the $(GaAl)As$ is attributed to the superior metallurgical properties of its junctions.

The impairment of performance by poor metallurgical quality may become a factor at the high Al content. Fig. 5 shows a gradual decrease in the external quantum efficiency with increasing Al content at both 77°K and 300°K which is not easily explained as arising only from the thermal depopulation of the electrons in the "direct" conduction band minimum. It is possible that with increasing Al content, the junction quality deteriorates to some extent. Refinements in the fabrication process should further improve the efficiency over a significant range of Al composition below the direct-indirect transition composition.

Reliability

Questionable reliability has plagued numerous semiconductor devices, lasers included. It is clear that in the case of injection lasers, many of the problems encountered in their use were due to ignorance of the phenomena responsible for their failure.

Research conducted at the RCA Laboratories has helped to elucidate a number of the key factors affecting laser reliability. Two basic failure mechanisms were isolated. The first, denoted *catastrophic*,⁹ is due to mechanical damage of the facets caused by excessive optical flux density in the junction region. This failure point de-

Fig. 4—Threshold current density J_{th} as a function of the lasing wavelength λ_L at 300°K and 77°K. All of the diodes have roughly comparable cavity lengths (about 10 mils). Present laser data are compared to previous data by Kressel and Hawrylo,⁸ Susaki et al.,⁹ and Tietjen et al.⁸

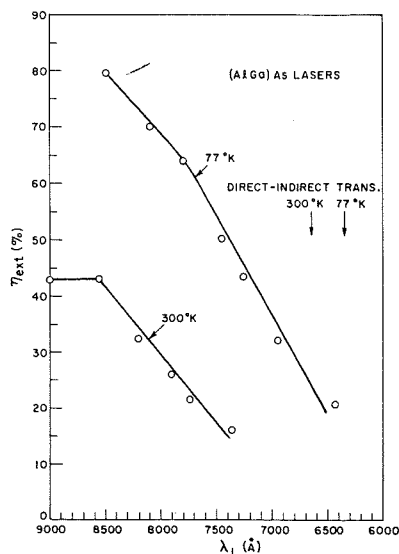
pends on the laser fabrication process, the laser length, the temperature of operation, and the pulse width. At 300°K with a pulse of about 200 ns, catastrophic failure will occur at about 1.2 to 2 Watts/mil of facet for a laser about 10 mils long. This failure is not a function of the current density.

A more gradual failure is possible (at power levels below those where catastrophic failure can occur) which depends on the *current density of operation*.¹⁰ There is evidence that the degradation rate is a superlinear function of the current density and that it is increased if the imperfection density in the junction region is high. It is therefore important to operate lasers at current density as low as possible consistent with a required power output. The close-confinement process described above has resulted in a very important increase in laser life because the current density required to obtain a given power level is now greatly reduced (see Fig. 2).

Data accumulated by RCA Electronic Components (Optical Products Department) have indeed shown that long-term room-temperature operation is possible under conditions of typical laser utilization. Close-confinement GaAs lasers have so far operated with virtually no degradation for a period of 600 hours at a duty cycle of 0.02% emitting about 1 Watt/mil of facet (current density $\sim 50,000 \text{ A/cm}^2$).

The future

Continued progress will be made in controlling the impurity distribution as well as the imperfection density in the laser recombination region. As a result, further reductions will be made in the threshold current density at room temperature, bringing us closer



to cw operation. One of the major areas of future improvements is in the reduction of the beam spread in the emitted light from injection lasers. This would considerably simplify the optical systems used. Improved theoretical understanding as well as changes in the laser structure may bring us closer to single-mode laser operation and consequent reduced beam spread. Finally, as $(GaAl)As$ devices become commercially available, we expect to see applications such as high-speed film recording and optical pumps for Nd:YAG lasers.

Acknowledgements

We are grateful to H. S. Sommers, Jr. for discussion, to D. Marinelli and J. Alexander for the material preparation, and to P. LeFur for technical assistance with the measurements. F. Z. Hawrylo collaborated in many aspects of the research program. We are also indebted to V. Cannuli and M. Falk for the device assembly. The work reported here was partly supported by the U.S. Air Force, WPAF, Dayton, Ohio, and the U.S. Army Electronics Command, Ft. Monmouth, N.J. and Ft. Belvoir, Va.

References

1. Kressel, H., and Nelson, H., "Close Confinement Gallium Arsenide p-n Junction Lasers with Reduced Optical Loss at Room Temperature", *RCA Review*, Vol. 30, No. 1 (1969) p. 106.
2. Nelson, H., "Epitaxial Growth from the Liquid State and Its Application to the Fabrication of Tunnel and Laser Diodes", *RCA Review*, Vol. 24, No. 4 (1963) p. 603.
3. Tietjen, J. J., Pankove, J. I., Hegyi, I. J., Nelson, H., "Vapor Phase Growth of $GaAs_{1-x}P_x$ Room Temperature Injection Laser" *Trans. AIME*, No. 239 (1967) p. 385.
4. Abrahams, M. S., Weisberg, L. R., Buioocchi, C. J., and Blanc, J., "Dislocation Morphology in Grated Heterojunctions: $GaAs_{1-x}P_x$ " *J. of Materials Science*.
5. Kressel, H., Hawrylo, F. Z., Nelson, H., "Stimulated Emission at 300°K and Simultaneous Lasing at Two Wavelengths in Epitaxial $Al_xGa_{1-x}As$ Injection Lasers" *Proc. IEEE (Corr.)* No. 56 (1968) p. 1598; IEEE Device Conference, Washington (Oct. 1968).
6. Nelson, H., Kressel, H., "Improved Red and Infrared Light-Emitting $Al_xGa_{1-x}As$ Laser Diodes Using the Close-Confinement Structure" *Appl. Phys. Letters*, No. 15 (1969) p. 7.
7. Susaki, W., Sago, T., and Oku, T., "Laser Action in $(Ga_{1-x}Al_x)As$ Diodes" *J. of Quantum Electronics*, QE-4 (1968) p. 422.
8. Cusano, D. A., Fenner, J., and Carlson, R. O., "Recombination Scheme and Intrinsic Gap Variation in $GaAs_{1-x}P_x$ Semiconductors from Electron Beam and p-n Diode Excitation" *Appl. Phys. Lett.*, No. 5 (1964) p. 144.
9. Dobson, C. D., and Keeble, F. S., "GaAs", *Proc. International Symp. (Reading 1966)*; and Kessel, H., and Mierop, H., *J. of Appl. Phys.* No. 38 (1967) p. 5419.
10. Kressel, H., and Byer, N. E., "Role of Optical Flux and of Current Density in Gradual Degradation of GaAs Injection Lasers" *Proc. IEEE*, No. 57 (1969) p. 25; and Byer, N. E., *IEEE of Quantum Electronics*, QE-5 (1969) p. 242.

Fig. 5—Variation of the external differential quantum efficiency n_{ext} with lasing wavelength λ_L at 300° and 77°K of $(AlGa)As$ lasers with the cc structure. Extensive comparative data for previous lasers are lacking, but 300°K values of 15% and 18% were reported in Ref. 3 at 8630 Å and 8827 Å, respectively.

Improving solid-state lasers

Dr. R. J. Pressley

After tracing the many recent developments in solid-state lasers, this paper discusses the advantages and disadvantages of various laser materials—including Yttrium Aluminum Garnet (YAG) and Yttrium Vanadate (YVO₄)—used as hosts in Neodymium (Nd³⁺) lasers. Also covered are recent advances in operating techniques that have led to more-efficient, higher-power solid-state lasers.



Dr. Robert J. Pressley
Materials Research Laboratory
RCA Laboratories
Princeton, N.J.

received the BS in 1954 from Michigan State University, majoring in physics. He joined RCA Laboratories in 1954 as a member of the research training program. Following this he engaged in research on infrared sensitive photoconductive surfaces for imaging systems. Upon receipt of a David Sarnoff Fellowship in 1956, he took a leave of absence and entered Princeton University Graduate School. He received the MA in 1958 and the PhD in 1962, both in physics. During this time he also returned to RCA on projects involving ammonia gas masers; communications systems studies, and optical beating experiments in sodium vapor. His thesis research was an investigation of the interaction of electron spins and nuclear magnetic moments in very pure lithium metal, an experimental investigation using simultaneous ESR and NMR monitoring of the same sample in thousand-gauss fields. During the 1961-62 academic year, Dr. Pressley served as an instructor at Princeton University setting up laboratory courses in optics and electromagnetic theory. He returned to RCA Laboratories in 1962 and has been associated with the Quantum Electronics Group. He has worked in optical masers with the emphasis upon laser operation and characteristics, in particular, the optimization of the CaF₂:Dy and the Nd:Cr:YAG systems. At present, he is continuing spectroscopic analysis of potential laser systems with emphasis on interfacing the spectrometers with a time-sharing computer. He is also constructing apparatus for sub-nanosecond spectroscopy using a mode-locked and frequency-doubled Nd³⁺:YAG laser as the active probe. He has served two years on the New Jersey Department of Health Laser-Safety Subcommittee and is a member of the American Physical Society, the Optical Society of America, and Sigma Xi.

Reprint RE-15-5-11

Final manuscript received November 14, 1969.

THE CONDITIONS FOR MASER ACTION at optical frequencies were first described by Schawlow and Townes in 1958.¹ The first demonstration of laser action by Maiman two years later was achieved using ruby (Al₂O₃:Cr³⁺)—a crystalline solid system.² In the following year, much effort was expended on the search for new laser transitions in various media: crystalline solids, gases, liquids, glasses, plastics, and semiconductors. The progress was indeed rapid, and today we have thousands of laser frequencies covering the spectrum from the far IR to near UV.

The next step in the development of solid-state lasers after the pulsed three-level ruby system was the operation of a pulsed four-level system, CaF₂:Sm²⁺ by Sorokin and Stevenson.³ The first continuously operating crystal laser was constructed by Johnson, et al,⁴ using CaWO₄:Nd³⁺. In the following years, a systematic search was begun for new laser systems, using trivalent rare earths, divalent rare earths, and transition metals as the impurities in a great variety of host crystals.⁵ An all-important spur to the development of crystalline lasers was the generation of giant laser pulses by Q-spoiling techniques.⁶ Laser transitions were soon found covering the spectrum from 0.55μ (CaF₂:Ho³⁺)⁷ to 2.6μ (CaF₂:U³⁺).⁷ The effort then shifted towards increasing the total efficiency of crystalline lasers, finding cw systems in the visible region of the spectrum, and optimizing the parameters and techniques for Q-switching laser pulses.

Advantages of solid lasers

At the present state-of-the-art of laser technology, solid crystalline lasers have certain advantages over other laser media. Since the longest-lived, excited, metastable energy levels exist in these impurity-doped solids (~10⁻³ seconds compared to ~10⁻⁶ seconds in

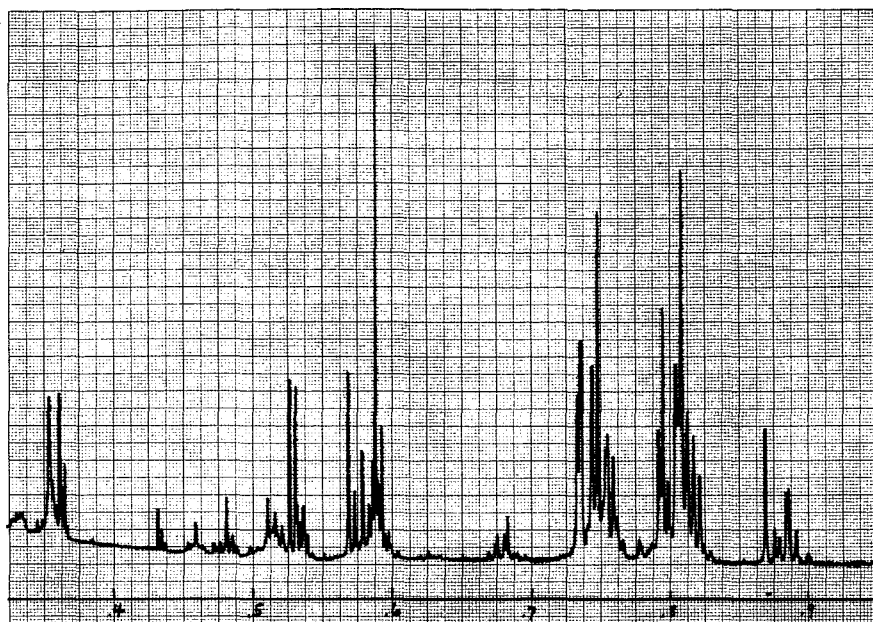


Fig. 1—Absorption spectrum of yttrium aluminum garnet doped with neodymium over the range from 3250A to 9500A taken to 300°K.

Material active system	Sensitizer	Optical pump	λ (μ)	Eff. (%)	Power (watts)	Operating temp. (°K)
Dy ²⁺ CaF ₂	—	W	2.36	0.06	1.2	77
Cr ³⁺ Al ₂ O ₃	—	Hg	0.69	0.1	1.0	300
Nd ³⁺ Y ₃ Al ₅ O ₁₂	—	W	1.06	0.2	2	300
			1.06	0.6	15	300
Nd ³⁺ Y ₃ Al ₅ O ₁₂	—	Plasma arc	1.06	0.2	200	300
Nd ³⁺ Y ₃ Al ₅ O ₁₂	—	Na doped Hg	1.06	0.2	0.5	300
Nd ³⁺ Y ₃ Al ₅ O ₁₂	Cr ³⁺	Hg	1.06	0.4	10	300
Ho ³⁺ Y ₃ Al ₅ O ₁₂	(Er ³⁺ , Yb ³⁺ , Tm ³⁺)	W	2.12	5.0	15	77

Table I—Continuous solid-state laser powers and efficiencies.

gases and $\sim 10^{-9}$ seconds in injection lasers) these lasers can be best utilized for energy storage and hence for Q switching and for generating high peak powers. The density of active impurity ions in crystal lasers is $\sim 10^{17}$ to 10^{20} ions/cm³ as compared to 10^{15} to 10^{17} atoms/cm³ in gases and 10^{22} electron-hole pairs/cm³ in injection lasers. Thus, the active ion density of the crystalline-solid-laser medium is a good compromise for high cw powers: on one hand, it is dilute enough so that the power is not limited by cooling problems as in the case of injection lasers; yet for a given power, smaller active volumes are needed than for gas lasers. Table I, from a survey article in 1966⁹, indicates the experimental state-of-the-art at that time.

Several generalizations can be made concerning Table I:

- 1) Longer wavelength systems only operate at cryogenic temperatures;
- 2) There are no efficient visible lasers; and
- 3) The performance of a laser is highly dependent upon the particular optical source used to excite it.

This last point is particularly true if the absorption of the laser is in a series of sharp lines as it is for the Nd³⁺:YAG (Y₃Al₅O₁₂) laser. The absorption spec-

trum for this laser is shown in Fig. 1. This would not in general appear to be a good laser system, but the optical quality of the YAG host is so high that the necessary gain coefficient for laser action is extremely low even with black-body pumps. This reduces threshold to such an extent that this laser can be operated at 300°K with greater efficiency and higher average power than any other.

Trivalent neodymium is in fact unique among the rare earths in that it has many absorbing levels which rapidly decay to a metastable level at about 11,000 cm⁻¹. This level decays radiatively, mainly to normally depopulated levels about 2000 cm⁻¹ above the ground state. This allows laser action near 1.06 μ in many hosts. A great deal of effort has gone into looking for other ions in various site symmetries to find comparable laser operation at shorter wavelengths, but as yet the results are orders of magnitude inferior to those obtained with trivalent neodymium.

Recent improvements

The most profitable line of work over the past few years has been, in fact,

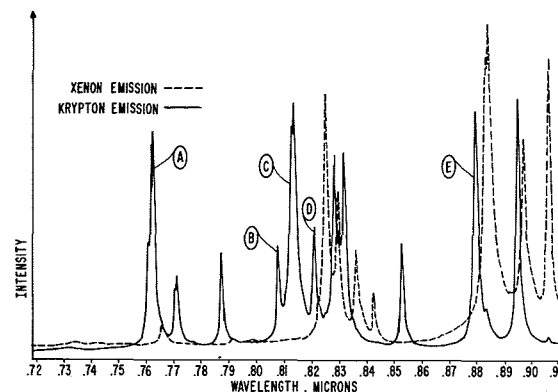


Fig. 2—Emission spectra of Xenon and Krypton arc lamps in the spectral range from 7200A to 9200A.

the engineering of the entire laser system using trivalent neodymium to obtain rather impressive advances over the 1966 state-of-the-art. This engineering has been on all aspects of the system, but the most important ones were the laser rod itself and the optical pump source.

A first improvement in the laser material was the increased broad-band absorption obtained by incorporating trivalent chromium in the rod as a sensitizer.¹⁰ This increased the laser output to 25 watts, but at the expense of the optical quality of the host.

A second improvement was in the use of a non-blackbody pump source with emission matching the Nd³⁺ absorption bands.¹¹ This was an improvement both in the spectral match and in the energy per unit area that could be imaged on the laser rod. This combination gave almost an order of magnitude increase in both efficiency and total power output.

Limitations of YAG

Powers in the 200-watt range are now obtained using 7- to 8-kW krypton lamp pumping instead of the 100-kW plasma arc previously required.¹²⁻¹⁴ The corresponding efficiencies have risen to almost 3% and beam divergences are approaching the diffraction limit. In view of these advances in Nd lasers using YAG as a host, it might appear that there is no need for improvement. This is not, however, the case as YAG has several limitations. First, it is very expensive; it is grown by high temperature pulling from a melt contained in an iridium crucible. Secondly, the absorption lines are, as mentioned before, narrow and do not effectively couple to optical pump sources. A third difficulty, which



Fig. 3—Absorption spectrum of yttrium vanadate doped with neodymium over the range from 3250 Å to 9500 Å taken at 300°K.

Host	YAG*	FAP**	YVO ₄
Density	4.55	3.2	4.2
Melting point (°C)	1950	1705	1750-1900
Hardness (Moh)	8.0	5.0	5.5
Refractive Index	1.82	1.63	1.86
Thermal conductivity (w/°C cm)	0.13	0.02	0.053
Linewidth 300°K (Å)	3.0	6.0	9.0
Fractional emission into laser line	0.18	0.33	0.5
Relative threshold for blackbody pump	1.0	?	0.8
Relative efficiency above threshold for blackbody pumping	1.0	?	1.25

*Yttrium Aluminum Garnet Y₃Al₅O₁₂

**Calcium Fluorophosphate Ca₅(PO₄)₃F

Table II—Properties on Nd³⁺ lasers.

would be important in any large scale use, is that it is very difficult to scale up existing growth facilities.

The problem of matching the emission lines of an optical pump lamp is demonstrated in Figs. 1—4. Fig. 2 shows the emission spectrum of xenon and krypton arc lamps over the range from 0.7 to 0.9 microns—the most important pump region for a trivalent neodymium laser. While there is a weak continuum over the entire range, the majority of the emission intensity is in the lines. Comparison of these lines with the absorption of Fig. 1 demonstrates the difficulty of matching the absorption and emission lines. The absorption is a much better match for krypton than for xenon. The improvement is so much that it more than compensates for the lower overall efficiency of the krypton lamp, and Nd:YAG laser operation with krypton pumps is over two times better than operation pumped with xenon.

Advantages of Yttrium Vanadate

Trivalent neodymium in YAG is still not an optimum match to krypton, however, mainly due to the narrowness of the absorption lines. A laser host with broader lines would be bet-

ter for trivalent neodymium. One such host is yttrium vanadate. The absorption spectrum of this is shown in Fig. 3. The match of this absorber to the krypton lamp is dramatized in Fig. 4, which is the spectrum of light from a krypton lamp after it has passed through 2 cm of Nd:YVO₄. Notice that the lines in Fig. 2 (labelled A through E) are completely absorbed in this path length. This is the kind of strong absorption that is needed for utilization of a simple optical-pumping cavity.

Nd³⁺:YVO₄ also has satisfactory fluorescent emission characteristics as listed in Table II. It should have almost identical threshold to Nd:YAG and higher efficiency above threshold. Beyond these spectroscopic considerations, there are the practical ones of material quality of the host. Many beautiful potential laser hosts exist that are hygroscopic, brittle, and/or poisonous—any one of these features may severely limit their usefulness.

One important consideration is the thermal property of the material; if the proposed host material has too low a thermal conductivity, continuous laser action will be possible only in very thin filaments, as in the glasses.

Another important consideration is the surface characteristics; if it cannot be polished or is attached by water or other solvents, use outside of controlled laboratory conditions will be limited. The pertinent parameters for YAG and YVO₄ are also listed in Table II. From this it can be seen that while YVO₄ is not quite as good as YAG, it is adequate for all but the most extreme power applications. An example of a material that also has good spectral characteristics but very limiting materials characteristics is Fluoroapatite, Ca₅(PO₄)₃F, or FAP. It is very brittle, has low thermal conductivity, and tends to develop color centers when illuminated with ultraviolet radiation.

Having determined that YVO₄ satisfies most of the spectroscopic and material demands of a laser host, the last requirement is inexpensive growth of large single crystals of high optical quality. While this crystal can be grown from the melt and in flux, neither of these methods provide sufficient optical quality due to particular idiosyncracies of the material. Hydrothermal growth, on the other hand, both provides material of high optical quality and holds the promise of enabling growth of laser rods at very low cost. This is due to the fundamental steady-state properties of the hydrothermal process. This type of growth takes place inside a pressure vessel at an elevated temperature in a suitable solvent. A temperature gradient is maintained with the cooler region at the top, and saturated liquid rises from the bottom where the polycrystalline nutrient is placed to the top where crystalline growth takes place. The growth rate is very slow, being of the order of 0.010 inches/day. However, a large number of crystals can be grown at the same time, and the system requires no supervision or changes once the proper conditions have been achieved.

Indications are that the cost of Nd:YVO₄ can be less than Nd:YAG by a factor of from five to ten if the quality of the hydrothermal material is satisfactory in large-scale growth. This is very important as the laser rod is now the most expensive component of the entire laser head.

Summarizing the present state of the art, YAG is the best host for Nd³⁺. It

is also continuing to improve in optical quality and resultant performance. YVO_4 , should be better, cheaper, and available in volume if present growth indications hold true.

Advances in operating techniques

Simultaneous with these advances in laser hosts and pump lamps have come innovations in the techniques of operating solid lasers. Perhaps the most important of these is mode-locking. A typical crystalline solid laser has a fluorescent linewidth of several angstroms within which there will be many Fabry-Perot modes of the cavity. Laser action typically occurs in an unrelated way at each of these. There is no phase coherence between them. If they can, however, be locked in phase by some means, the laser output will be changed into a series of pulses spaced in time by the period of the Fabry-Perot mode spacing. The minimum pulse duration is given by $T = 3/\pi\Delta\nu$ where $\Delta\nu$ is the frequency range over which the Fabry-Perot modes are locked. A Nd^{3+} laser—locked over 1 Å (33 GHz)—would have 25-psec pulses. Correspondingly, if phase locking could be achieved over the 200 Å emission observed of Nd^{3+} in glasses, pulses as narrow as 0.1 psec would be expected.

Fig. 5 shows the experimental arrangement used to continuously generate 20-psec pulses at a 75-MHz rate. This system also incorporates a nonlinear optical element to convert some of the 1.06 μ radiation to 0.532 μ , giving simultaneous green and infrared pulses. These can be used as short-time probes to examine such phenomena as phototube response to a delta function light input, relaxation phenomenon in materials in the sub-nanosecond range, and experiments where the phenomenon to be measured is proportional to the peak power of the incident beam. This system typically gives peak powers of 20 watts in the green portion of the spectrum and 1kW at 1.06 μ .

Pulsed and Q-switched lasers can also be mode locked giving rise to the highest powers and shortest pulses yet observed. Q-switched lasers can, when operating in a normal mode, emit typically 20 joules in 5 nanoseconds. The peak power is thus 4×10^9 watts. If the same laser is mode locked, the peak

power of the individual 5-psec pulses may be 10^3 higher. The effects on material of these extremely high powers have not yet been examined to any extent, but one attractive proposal is to use them to initiate thermonuclear reaction in a 10- μ -diameter sphere of lithium deuteride. The energy is dumped into the material so fast that the temperature is raised to the millions of degrees necessary for fusion before the sample can explode thermally.

At the opposite extreme from coupling a large number of laser modes together is single-frequency operation. This was first achieved in lasers having extremely narrow fluorescent lines by using short cavities to spread the Fabry-Perot modes apart. With the exception of these limiting cases, however, single-frequency operation has not been reliably achieved until recently. By inserting a thin-metal film—typically 50 Å thick nichrome—inside the optical cavity, a degree of mode selection is achieved that allows single-frequency single-mode operation at as much as 25% of the normal output power. This now is laser operation in the naive original sense of a continuous, coherent, collimated output at a single optical frequency.

New optical materials

In view of the degree of sophistication now accompanying the existing lasers, in particular the 1.06- μ neodymium systems, research on new laser materials is not being emphasized as much at this time as is research on electro-optic and nonlinear optical materials to modify the coherent output of the existing lasers. Techniques now exist for further shortening picosecond pulses to subpicosecond by optical "chirping" techniques similar to the RF chirping used in radar in the past. The frequency of the coherent signal can also be modified by harmonic generation, parametric upconversion, downconversion and oscillation, as well as by stimulated Raman scattering. The time dependence can be further modified by internal acoustical, or electro-optic modulation of either phase or loss, and the spatial properties of the output can also be varied by intracavity loss modulation.

These advances are rapidly increasing the versatility of lasers, although at

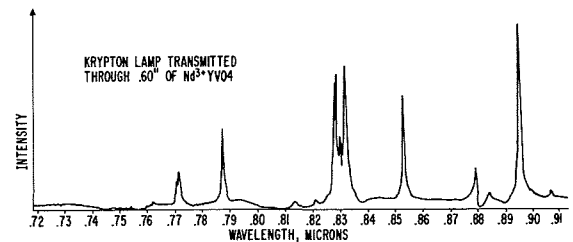


Fig. 4—Spectrum of Krypton lamp emission after passing through 0.60" of Nd doped yttrium vanadate.

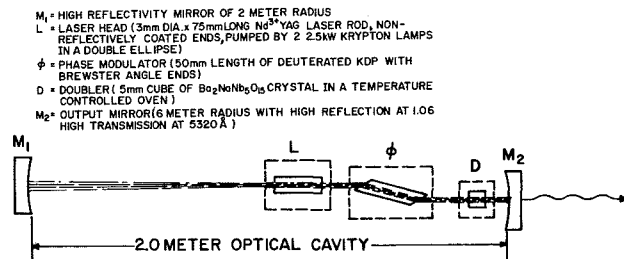


Fig. 5—Optical system for generating laser pulses at both 1.064 and 0.532 μ of about 30-ps duration at a rate of 75 MHz.

this time the largest volume use predicted for any laser is as a simple continuous coherent light source to read out phase holograms.

References

- Schawlow, A. L. and Townes, C. J., "Infrared and Optical Masers," *Phys. Rev.*, Vol. 112, (Dec. 1958), p. 1940.
- Maiman, T. H., "Stimulated Optical Radiation in Ruby Masers," *Nature*, Vol. 187 (Aug. 1960), pp. 493-494.
- Sorokin, P. P. and Stevenson, M. J., "Stimulated Infrared Emission from Trivalent Uranium," *Phys. Rev. Lett.*, Vol. 5 (Dec. 1960), pp. 557-559.
- Johnson, L. F., Boyd, G. D., Nassau, K., and Soden, R. R., "Continuous Operation of the $CaWO_4:Nd^{3+}$ Optical Maser," *Proc. IRE (correspondence)* Vol. 50 (Feb. 1962), p. 215.
- A summary of the materials work up to 1963 can be found in *Proceedings of the Third International Congress of Quantum Electronics*, Grivet, P., and Bloembergen, N., Eds. (New York: Columbia University Press, 1964).
- McClung, F. J. and Hellwarth, R. W., "Giant Optical Pulsations from Ruby," *J. Appl. Phys.*, Vol. 33 (1962), p. 828.
- Voronko, U. K., Kamynsky, A. A., Osiko, V. V., and Prokhorov, A. N., *Jour. of Exp. and Theor. Phys. USSR (letters to the Editor)*, Vol. 1, No. 1 (1965), p. 5.
- Kiss, Z. J., see e.g., "Zeeman Tuning of the $CaF_2:Tm^{2+}$ Optical Maser," *Appl. Phys. Lett.*, Vol. 2 (Feb., 1963), pp. 61-62.
- Kiss, Z. J. and Pressley, R. J., "Crystalline Solid Lasers," *Appl. Opt.*, Vol. 5 (1966), p. 1474.
- Pressley, R. J., "Nd:Cr:YAG High-Efficiency High-Power Solid-State Laser Systems, RCA Reprint PE-327, 328, 329, 323 (1966).
- Read, T. B., "The CW pumping of Nd:YAG by Water Cooling Krypton Arcs," *Appl. Phys. Lett.*, Vol. 342 (1966).
- Osterink, L. M. and Foster, J. D., "Efficient High Power Nd:YAG Laser Characteristics," *Proc. CLEA*, Washington, D.C. (May 1969), p. 38.
- Lieberman, J., "A High Power Nd:YAG Continuous Laser" *Proc. CLEA*, Washington, D.C. (May 1969), p. 39.
- Koehnner, W., "YAG Challenges Carbon Dioxide in High CW Power," *Laser*, Vol. 29 (Sept. 1969).

Electron-beam-pumped semiconductor lasers

Dr. F. H. Nicoll

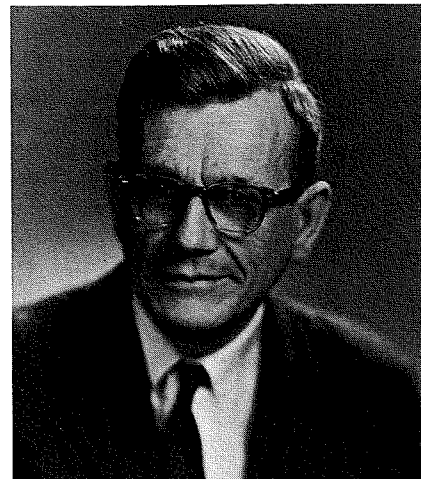
Phosphors have been a part of RCA research since the earliest beginnings of television, and they have continued to play a part in this and many other display techniques. Cathodoluminescence in certain phosphors has all the properties necessary for lasing except an optical cavity. This cavity however can be provided if the phosphor is available in single-crystal form. Some of RCA's accomplishments in pumping such crystals with an electron beam are described in this paper. These include the first observation in zinc oxide, of ultraviolet lasing in a solid state material, and the first observation of lasing in cadmium sulfide at room temperature. New far-field patterns associated with total internal reflection cavities have also been observed and described. The directionality of the light of electron-beam-pumped lasers makes their eventual use in cathode ray tubes very attractive. To this end a sealed-off laser cathode ray tube has been made which can be operated under pulse conditions at room temperature.

THE HISTORY OF ELECTRON-BEAM-PUMPED semiconductor lasers is rather closely linked to the development of the *GaAs* injection laser. Although the ruby laser and the gas laser were the first lasers to be realized in practice, it was the small size and high-current-density excitation of the injection laser which indicated the possibilities for semiconductor lasing in a very small optical cavity. It was easy to calculate that conventional well-focused electron beams in the 20 to 100 kV range could reach the necessary excitation density for possible laser action. A number of laboratories both here and abroad started experimental work on electron-beam-pumped lasers at the time that the injection laser was being developed. The chronological sequence of materials made to lase under electron-beam pumping is covered in the literature.¹ RCA, with a large amount of experience in cathodoluminescence, had done experimental work on *ZnO* and *CdS* powder phosphors which had a considerable bearing on later laser work. In both these phosphors, it was discovered that at high current density the ratio of short-wavelength-light emission to long-wavelength-light emission was considerably greater than at low current density.² Thus, under increasing current density, the *CdS* emission color changed from red to green, and the *ZnO* emis-

sion color changed from greenish to violet. Furthermore, the shortwave emission consisted of a rather narrow spectral line which continued to increase in output up to the highest current densities readily attainable at that time. These results with *ZnO* encouraged RCA to work on electron-beam-pumping of *ZnO* single crystals, and this led to the realization of the first solid-state ultraviolet laser.³

Demountable cathode ray tube

It was clear from the beginning of the work with electron-beam-pumped semiconductors that something rather better than the usual beam focus on a conventional cathode-ray tube (CRT) would be necessary to achieve the high density of excitation required for laser action. While other workers in the field chose to examine the 50 to 250 kV range, our activity was confined to voltages under 30 kV which we believed to be adequate and which had a more practical appeal. With this lower voltage requirement, it was possible to use the RCA standard 5TP4 television projection tube gun and in addition eliminate a number of the usual high-voltage breakdown problems and reduce X-ray shielding to a minimum. While some of the early work was done on sealed off CRT's, a demountable tube was preferred with its greater flexibility of operation. The salient features of such a continuously pumped system are shown in Fig. 1. The 5TP4 gun, which is not visible



Dr. F. H. Nicoll
Semiconductor Device Research
RCA Laboratories
Princeton, N.J.

received the BSc in 1929 and the MSc in 1931 from the University of Saskatchewan, Canada, followed by the Ph.D. in Physics in 1934 from the University of Cambridge, England. From 1934 to 1939 he was a research physicist with Electric and Musical Industries, Ltd., England, working on television, cathode ray tubes, and theatre TV projection. In 1939 he joined RCA Manufacturing Company, Camden, working mainly in the field of optics and television. In 1943, Dr. Nicoll transferred to RCA Laboratories, Princeton, New Jersey. Dr. Nicoll, a Fellow of the Technical Staff, RCA Laboratories, has had experience in optics, electron optics and the making of various vacuum devices. He has worked with cathodoluminescent phosphors and electroluminescent materials and also photoconductors, and in particular with the application of these materials to light amplifier display panels. He has continued to work in the solid-state and semiconductor field and more recently in the field of lasers. Dr. Nicoll is a Fellow of the IEEE, a member of Sigma Xi, the Optical Society of America, and the American Physical Society. He has received a number of RCA Achievement Awards for his work and in 1963 was awarded an RCA Fellowship for a year of study abroad which was spent at the Cavendish Laboratory, Cambridge University, England.

in the horizontal tube neck, has a special thorium cathode and uses conventional electrostatic focusing plus magnetic focusing from a concentric iron-clad coil. The sample, on a liquid-nitrogen-cooled cold finger, is located as near as possible to the focusing lens. This is done to increase current density over that normally obtained in a 5TP4 projection tube. The proximity of the sample to the focusing coil makes it very difficult to use magnetic deflection for positioning the electron beam on the sample. For this reason, a spherical ground joint was used in combination with a micro-control which provided the x-y deflection of the whole gun assembly. This arrangement had both high precision and excellent reproducibility. The demountable CRT is used in conjunction with a microscope so that the sample can be observed at various angles. At the same time, a beam splitter in the microscope allows the observed light

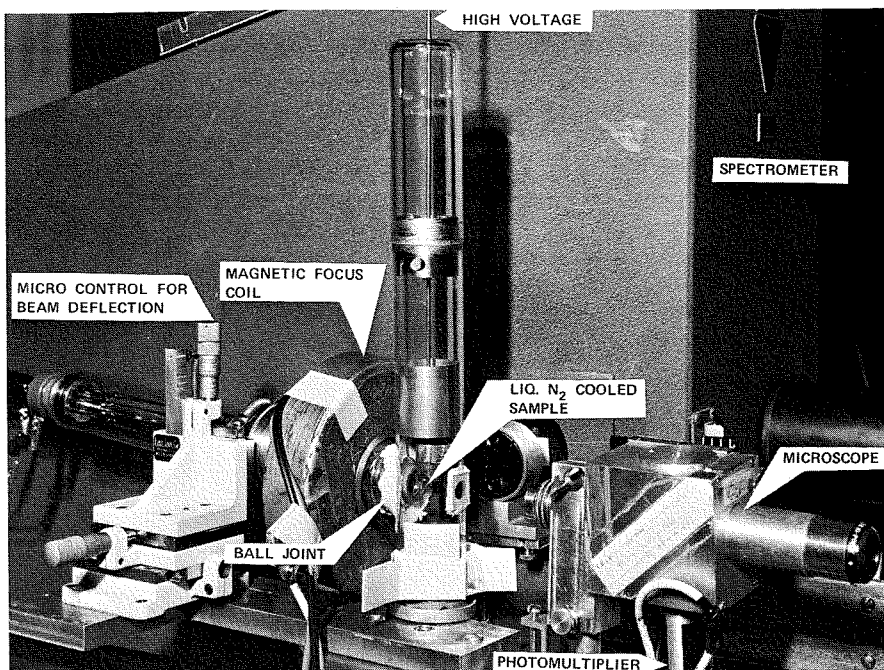


Fig. 1—Demountable CRT for investigating electron-beam-pumped lasing in semiconductors.

to be monitored by a photomultiplier whose output is displayed on an oscilloscope synchronized with the pulsed electron beam. The near-field emission pattern of a lasing crystal can be observed by focusing the microscope on the crystal face. The far-field emission pattern can be observed by allowing the emitted light to strike a diffusing piece of paper wrapped around the vertical tube containing the cold finger. Light emitted by the sample can also be passed through the Bausch and Lomb spectrometer to record its spectral properties.

Semiconductor samples are prepared from thin grown platelets a few microns thick which are cleaved to a width of about 100 microns. These are mounted on a transparent sapphire piece with a small amount of silicon grease and the sapphire is cooled by a copper cold finger.

Cathodoluminescence

A high-voltage electron beam impinging on a semiconductor sample produces a chain of events not all of which are helpful in producing population inversion and laser output. Some of the incident beam is lost upon striking the sample and appears as reflected or back scattered electrons. Loss to the crystal lattice produces phonons, and causes undesirable heating of the sample to such an extent that, for high excitation densities, only pulsed low-duty-cycle operation is possible. Some of the energy of the beam is also converted to X-rays which, however, may be partially reconverted

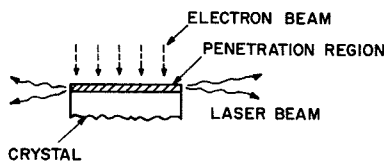


Fig. 2—Fabry-Perot laser cavity with laser beams perpendicular to the exciting electron beam.

to light. Estimates have been given that it requires 2 to 4 times the energy gap of the semiconductor material to create a hole-electron pair, so that about 10^4 electron-hole pairs are created by a 20 kV electron.

The penetration of the electron beam into the laser crystal is an important consideration in determining the most suitable operating voltage. Above 5 kV, the experimentally observed penetration of an electron into a material of density ρ is given by $\rho d = 2.3 \times 10^{-12} V^2$ where d is the penetration in centimeters and V is the accelerating voltage on the electron.⁴ For 20 kV electrons, the penetration is only a few microns, and the excitation is confined to a region very near the surface. This was used as an argument for operation at very high voltages to give deeper penetration and thus reduce surface effects. It turns out, however, that these surface effects are not serious in many materials; therefore low-voltage excitation is possible.

Laser cavity

In the case of gas lasers, the Fabry-Perot cavity is produced between two plane mirrors separated by a distance of many centimeters. A Fabry-Perot cavity in a semiconductor injection laser is produced between two cleaved

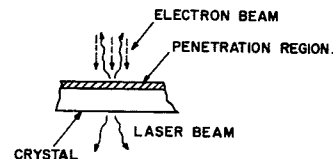


Fig. 3—Fabry-Perot laser cavity with laser beams emitted parallel to the exciting electron beam.

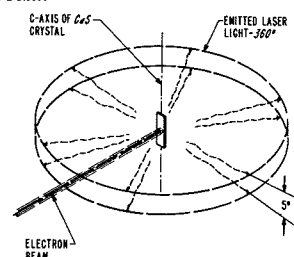


Fig. 4—Total internal-reflection cavity producing 360° laser beam in one plane with 5° divergence in orthogonal plane.

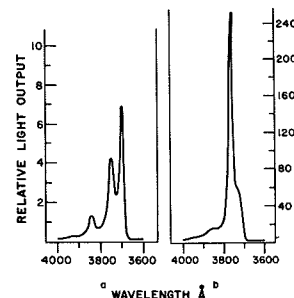


Fig. 5—Emission spectrum of a ZnO single crystal excited by electrons a) below laser threshold (current density 1.5 Amps/cm²), and b) above laser threshold (current density 6 Amps/cm²). Temperature 77°K.



Fig. 6—Far-field pattern of ZnO laser showing 180° horizontal spread and 5° vertical spread of laser beam striking a paper cylinder surrounding the vacuum envelope.



Fig. 7—Intense laser emission a) from corners of 150-μ wide crystal viewed towards the electron-beam source and b) from corners of 30-μ edge of same crystal.

facets of the material which are parallel by virtue of the cleavage property of the crystal and may be only a fraction of a millimeter apart. For many semiconductors, the refractive index is sufficiently high that the Fresnel reflection is adequate for the mirrors of the Fabry-Perot cavity without resort to evaporated reflectors as required for other lasers. The sample size for electron-beam pumped lasers must be comparable in size to the focused electron beam which is usually under 1 millimeter. Electron beam pumping allows more freedom in the choice of optical cavity than is possible with injection lasers because no electrodes are necessary on the sample. Three possible cavities are illustrated in Figs. 2, 3, and 4.

Fig. 2 shows the usual Fabry-Perot cavity between cleaved facets with the electron beam exciting the shaded portion, and the two narrow laser beams being emitted perpendicular to the cleaved ends.

Fig. 3 is also a Fabry-Perot cavity between parallel cleaved or grown faces but with one face excited by electrons so that the laser beam is emitted perpendicular to these faces and parallel to the electron beam. In this case, part of the material in the cavity is unexcited and therefore contributes loss.

A third type of cavity can be produced in a crystal of rectangular cross section by total internal reflection⁵ as in Fig. 4. This produces a large number of modes and the coherent light is emitted as a 360° disc-like beam centered on the crystal with a divergence of about 5° perpendicular to the disc. In a material such as *CdS*, which shows little absorption for its emitted light, operation in the internal reflection modes of Fig. 4 gives the lowest threshold.

A higher threshold is observed for the cavity of Fig. 2 where the whole optical path between the facets is excited but the reflection coefficient is only a fraction of the 100% provided by total internal reflection in the cavity of Fig. 4. The highest laser threshold occurs in the Fabry-Perot configuration of Fig. 3 in which only a portion of the optical path between the facets is excited and the reflection coefficient is the same in Fig. 2. The threshold for this so-called end pumping may be excessively high unless efficient reflection

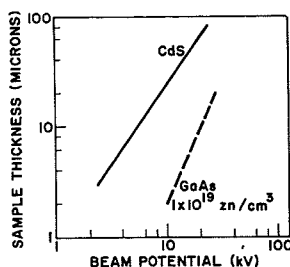


Fig. 8—Voltage threshold for lasing vs. thickness of crystal cavity (current density constant).

mirrors are applied to both Fabry-Perot cavity faces.

Results

The strongest experimental evidence of lasing in electron-beam-pumped semiconductors is the observation of marked threshold in the simultaneous occurrence of a number of phenomena. These include a narrowing of the spectral emission as observed in a spectrometer, a strong directionality of the emitted light as seen in the far-field pattern, and a sudden increase in light output measured in the direction of the laser beam. In addition, one or more brilliant spots are seen in the near-field pattern if the microscope is focused on the sample.

The ZnO single crystal

A *ZnO* single crystal was the first solid-state material to show laser emission in the ultraviolet region of the spectrum,³ a result which was obtained in the demountable tube of Fig. 1. The *ZnO* sample was maintained at 77°K and was bombarded with a 100-ns pulsed beam of electrons at a rate of 100 to 3000 Hz. In Fig. 5a, the spectral emission of the *ZnO* crystal is shown just below threshold. In Fig. 5b, above threshold, the narrow laser line at 3750 Å is quite evident. The disc-like emission of the laser beam from the total internal reflection cavity produces a line of light where it strikes a fluorescent paper cylinder surrounding the sample. This is shown in the photograph of Fig. 6, where the laser beam spread in the vertical direction is about 5° consistent with the width of the line. The flattened circle of light in the center is due to light from the cathode falling on the paper.

The near-field pattern of one of these lasing crystals shows an intense emitting spot at each of the four corners of the total-internal-reflection cavity. Fig. 7a is a photomicrograph of the wide face of the emitting crystal looking towards the electron-beam source. The spontaneous luminescence is shown in the center area with the laser beam

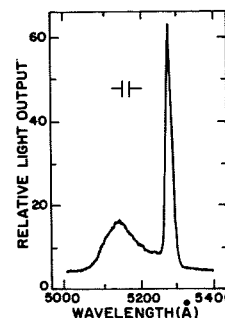


Fig. 9—*CdS* spectral emission above laser threshold at room temperature (current density 4 Amps/cm²). Note the narrow laser line.

being emitted from the spots at the corners. Fig. 7b shows the 30-micron edge of the same crystal with its two intense spots. These far-field and near-field patterns are also characteristic of other semiconductors lasing in the internal reflection mode under electron bombardment.

The *CdS* single crystal

Platelets of *CdS* single crystals lase very readily on a substrate at 77°K. The voltage threshold for lasing in a total-internal-reflection cavity (Fig. 4) is a function of the crystal thickness. If the crystal is too thick, the unexcited portion of the crystal may introduce sufficient loss to prevent lasing in the internal-reflection mode. In Fig. 8, the threshold voltage is plotted as a function of the crystal cavity thickness. The full line shows results for *CdS* while the dotted line shows results for *GaAs*—both at 77°K. These curves clearly show that the crystal thickness is directly proportional to the threshold voltage. However, in the case of *GaAs* which is known to have higher absorption for its laser emission than *CdS* has for its emission, the voltage threshold is higher for the same thickness. The relationship shown in Fig. 8 has now been extended to lower voltage for *CdS*, and lasing has been observed at 77°K down to 1.7 kV for the internal-reflection mode. At this voltage, penetration is only about 200 Å which indicates that even for this extremely shallow beam penetration the losses introduced by possible surface states are very small. Using very thin *CdS* crystals, it is possible to obtain laser action on a room temperature substrate.⁶ In Fig. 9 the laser emission line is shown appearing on the long wavelength side of the cathodoluminescent peak. Room temperature lasing of *CdS* made possible the construction of an experimental sealed-off cathode ray tube.⁷ This was not scannable but did contain a number of aluminized crystals on the faceplate

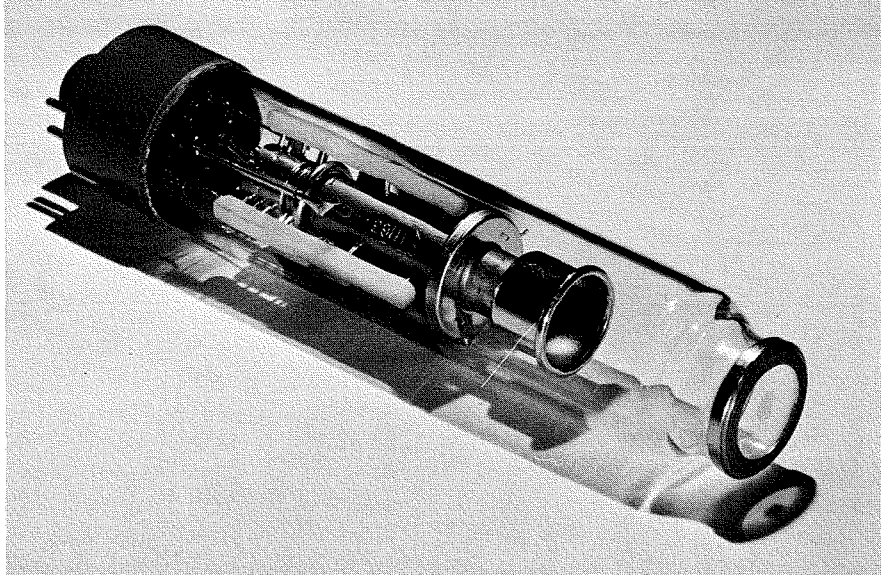


Fig. 10—Experimental laser cathode ray tube with 1-inch-diameter faceplate.

of the tube as shown in Fig. 10. Any portion of any one of these could be excited by the low-duty-cycle, pulsed, electron beam to give a 180°, horizontal, fan-shaped laser beam in a plane perpendicular to the faceplate, with a divergence of about 5° in the direction orthogonal to the fan. The near field pattern consisted of emission from two very brilliant spots separated by the width of the crystal, about 100 microns. At large distances, greater than 5 cm, these two beams interfere to produce the line pattern of Fig. 11 in which a portion of the fan beam was recorded directly on photographic film without the use of a lens. The vertical height of these lines corresponds to an emission angle of 5%. This laser cathode-ray tube can be used as a source of pulsed green laser light. The input power is converted to laser light with about 0.5% efficiency giving a peak output of 120 mW. The intense bombardment with the 15-kV electron beam reduces the laser output to one half after about 10^5 pulses. The reason for this deterioration is not understood, but it is connected with an increase in losses caused by absorption in the bombarded region. The operating voltage range of the sealed-off laser cathode-ray tube is 15 to 25 kV. However, demountable tests have shown that room temperature lasing of CdS can be observed down to 5 kV. It has also been shown that at 25 kV the same crystals will lase at temperatures up to 120°C, where the laser wavelength is 5420 Å.

The first laser results with ZnO and CdS were obtained with crystals specially grown as very thin platelets (10 microns or less) and prepared with

cleaved sides. Attempts to obtain lasing in mechanically polished crystals of similar dimensions were unsuccessful at voltages below 25 kV. This was found to be due to high optical absorptions introduced by damage at the surface of the crystal caused by the grinding and polishing operation. The use of chemical polishing eliminated this work damage thus making platelets cut from bulk material comparable in performance to as-grown platelets.⁸ This observation is of considerable interest since it was previously believed that thin platelets lased readily because they were of particularly high quality due to special growth characteristics of platelets. The ability to use bulk material when properly polished and cleaved is a considerable practical advantage since suitable platelets are not always readily available or easily grown.

Conclusion

A large number of semiconductor lasers pumped by an electron beam have now been described in the literature.¹ Some of these have been operated only at high voltage (>50kV), but they are of great interest because of the wide range of observed emission wavelengths at 77°K. At the long-wavelength end of the spectrum, materials such as PbSe have given laser emission at 8 μ. At the short wavelengths, ZnS, with laser emission at 3200 Å, is the shortest ultraviolet wavelength reported so far. Of special interest is the wide range of wavelengths obtainable by alloys such as Zn_xCd_{1-x}S and Cd(S_xSe_{1-x}). The first of these covers wavelengths from ZnS at 3200 Å to CdS at 4960 Å; the sec-



Fig. 11—Far-field interference of laser beams from two corners of CdS crystal at room temperature.

ond extends the range to CdSe at 6800 Å. Thus together they cover the range from deep red to ultraviolet. Not all of these materials have been examined below 25 kV, but our own results on ZnO, CdS, ZnSe, and CdSe indicate that many of the materials, especially the alloys, certainly operate in this range at 77°K. The desirable color characteristics, the low voltage operation, and the fact that ZnO and CdS have been operated as lasers at room temperature combine to make electron-beam-pumped lasers attractive for possible future application in cathode ray tubes. Of even more interest is the possibility of making cathode ray tubes having directional light emission patterns. This directionality can lead to considerably increased brightness to the viewer (or the device located within the directional pattern). Conservation of emitted light by putting it where it is wanted gives a greatly increased effective efficiency which will become especially desirable as present phosphors approach their maximum theoretical efficiency.

Acknowledgments

The author thanks H. Lewis and H. S. Sommers, Jr. for their support during this work. Competent technical assistance was provided by R. L. Quinn and J. Valachovic in many of the experiments.

References

1. Nathan, M. I., "Semiconductor Lasers" *App. Optics* Vol. 5 (1966) p. 1514. Reynolds, D. C., "Coherent and Noncoherent Light Emission in II-VI Compounds" *Trans. Met. Soc. of AIME*, Vol. 239 (1967) p. 300.
2. Shrader, R. E. and Leverenz, H. W., "Cathodoluminescence Emission Spectra of Zinc Oxide Phosphors," *J. Opt. Soc. Am.* Vol. 37 (1947) p. 959.
3. Nicoll, F. H., "Ultraviolet ZnO Laser Pumped by an Electron Beam," *App. Phys. Letts.* Vol. 9 (1966) p. 13.
4. Ramberg, E. G., *private communication*.
5. Nicoll, F. H., "Far-Field Patterns of Electron-Bombarded Semiconductor Lasers," *Proc. IEEE*, Vol. 55 (1967) p. 114.
6. Nicoll, F. H., "Room-Temperature Lasing of CdS Under Pulsed Electron Bombardment," *App. Phys. Letts.*, Vol. 10 (1967) p. 69.
7. Nicoll, F. H., "An Experimental Pulsed CdS Laser Cathode-Ray Tube," *RCA Review*, Vol. 29 (1968) p. 379.
8. Nicoll, F. H., "Zinc Oxide Crystals for Electron-Beam Pumped Lasers," *J. App. Phys.*, Vol. 39 (1968) p. 4469.

Sealed-off CO₂ lasers

Dr. R. A. Crane | J. I. Wood

An extensive research program has been in progress at the Research Laboratories of RCA Limited towards the development of the CO₂ laser in communication systems. A description is given of two parallel phases of this program: the development of long sealed-off tube life, and the parameter measurements necessary to test and predict performance.

DURING THE PAST FEW YEARS, interest has been increasing in the use of the CO₂ laser in its most sophisticated form, namely, as a carrier for high-grade communication systems. This interest is based primarily on three factors:

- 1) Laser radiation conversion efficiencies obtainable (about 20%);^{1,2}
- 2) Low atmospheric attenuation of 10.6-micrometer radiation (0.1 dB/km); and
- 3) The wide bandwidths inherently possible at optical frequencies.

Although the full potential of the CO₂ laser has yet to be realized, highly efficient communication systems using this laser are now feasible for field use.

Laser research has been an important feature of the program at the Research Laboratories of RCA Limited for several years. However, during the past year, effort has been concentrated on the CO₂ laser for communications purposes. Specifically, the CO₂ laser has been developed for uses in earth-based links and for applications in outer space. This has involved two related parallel programs:

- 1) To attain reliable sealed-off operational life of the laser, and
- 2) A parameter study to predict and test performance for specified applications.

The latter effort also includes optimization studies to reduce size, weight, and power requirements.

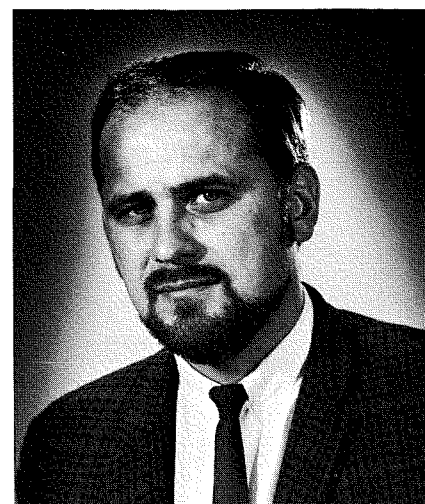
Basic considerations

The most important requirement in communication systems is a laser with a sufficiently long sealed-off operational life and as high an efficiency as possible. However, each particular application must be carefully considered in the design, as the environmental

conditions can place severe restrictions on the tube and window materials, fabrication techniques, cooling mechanism, etc. which in turn can prove detrimental to the primary requirements. Fortunately, there is a wide selection of tube materials available that can be used for long sealed-off life. These materials are listed in Table I with some of their relevant properties. Materials with low absorption at 10.6 micrometers that can be used for the optical components are shown in Table II. Power requirements vary from about 0.1 to 5 watts so that these lasers are small devices varying from 5 to 30 cm in length.

The design requirements can be divided broadly into two classes: ground-based and space-qualified systems. For ground-based systems, tube life of about 1000 hours is usually adequate since tube replacement is in most cases neither difficult nor disruptive. Consequently, less costly tube material and optical components can be used in these cases. Glass laser tubes guaranteed for 1000 hours of operational life are currently on the market but in most cases, tube life is gained at the expense of efficiency, and the warrantee replacement rate is not known.

On the other hand, a space-qualified CO₂ laser represents an ultimate in achievement, as these lasers must be designed for minimum weight, minimum total input power, ruggedness to withstand the vibrational shock of the launch, and the thermal shock of outer space, and yet operate reliably for at least two years. As a result, designers are turning more to the use of the alumina and beryllia ceramics as these materials have the highest shock resistance and in addition offer high bake-out temperatures which would be necessary to obtain the ultra-clean systems required for long tube life. To take advantage of these materials, rug-



Dr. R. Anthony Crane
Research Laboratories
RCA Limited
Montreal, Canada

received the BA Sc. in Engineering Physics with honours in 1957 from the University of Toronto. At the same university he also obtained the MA in 1961 and the PhD. in 1965 for his work on the induced absorption of solid hydrogens. During the period 1958 to 1960, he was a lecturer in the Department of Mathematics at the University of Waterloo. In June 1965, Dr. Crane joined the staff of the Research Laboratories of RCA Limited, where he is engaged in the study of the properties and applications of gaseous lasers. In particular, this has involved emission and impedance studies of CO₂ laser plasmas and currently, the development of sealed-off CO₂ laser systems for communications applications. During 1968, Dr. Crane developed the software in the data processing for the millimeter PCM Test Link Study Phase of the Project Mallard. Dr. Crane is a member of the Canadian Association of Physicists and of the IEEE.

ged leak-free seals must be used. An ideal seal between components would be between optically flat surfaces with a braze or a high temperature epoxy on the outside serving to hold the parts together. This would apply not only to the tube sections but also to the attachment of Brewster windows and mirrors.

Since the power budget for a space-craft is very restrictive, it is desirable to operate the laser at that discharge current which gives maximum efficiency. This point is less than that corresponding to the peak output power and can represent a saving of several watts of input power in the case of a CO₂ laser. Consequently, the usual definition of tube life—3-dB down on the output power—should be replaced by a tighter and more realistic 10% down on the efficiency.

To maintain efficiency, the tube wall must be kept below about 40°C, and in a space environment, fluid-flow

Reprint RE-15-5-7

Final manuscript received November 14, 1969.



John I. Wood
Research Laboratories
RCA Limited
Montreal, Canada

joined RCA Limited (Defense Engineering) in 1960, where he worked on high frequency transmitting equipment and servo-systems. He later transferred to the Satellite Division where he was responsible for the design of the solid-state high-frequency generators and power amplifiers for the Relay satellite. He then worked on design of logic circuitry for a solid-state digital video generator. Mr. Wood was transferred to the Research Laboratories in 1964 and has been working on plasma diagnostics and Q switching of high power CO_2 lasers. More recently he has been involved in laser propagation studies and the development of laser communication systems. In 1965, he graduated extra-murally from Sir George Williams University with a B.Sc (Mathematics and Physics).

cooling would require undesirable ancillary equipment and power. This represents an ideal situation for the use of heat pipes but for the present further development would be required. Fortunately, with use of high thermally conductive ceramic tube material, heat removal can be adequately handled via metal or ceramic conduction blocks—such a system has already been designed in our laboratories.

The CO_2 laser operates with a gas mixture of CO_2 , He , and N_2 , with Xe and/or H_2O added in small amounts to further enhance tube life and efficiency.^{1,2} Tube life is limited by loss of the primary gas component CO_2 through decomposition and reversible reactions in the discharge and at the electrodes, as well as gas clean up due to sputtering and absorption. These deleterious effects can be largely eliminated by the use of suitable electrode materials and electrode design and by suitable tube-treatment procedures—

the details of these materials and techniques are presently company-proprietary information. Xe is one of our basic gas additives since it also dominates the discharge leading to lower operating tube voltages.

Reliability is necessarily a crucial factor in space-qualified systems. For the sealed-off CO_2 laser, this factor will only be known when a very large number of life tests have been made and the statistics compiled. For example, to obtain reliability of 98% at the 2000-hour level, a total of about 100,000 hours of successful life testing is required in the same laser configuration. In addition, test-point parameters will have to be determined and evaluated so that tube life can confidently be predicted.

Sealed-off CO_2 laser development

The development of a sealed-off CO_2 laser was initiated at the Research Laboratories in July, 1968. The progress, since then, is graphically illustrated in Fig. 1 where, at each stage, tube life was approximately doubled by using the knowledge obtained from previous tests. This program was primarily concerned with maintaining a favorable gas balance over long periods of time by suitable tube processing and electrode design. The optimization of the configuration for efficiency is a parallel development.

A number of glass laser tubes were tested ranging from 20 to 50 cm in length with output powers from 1 to 10 watts. A photograph of a typical laser configuration for life testing is shown in Fig. 2. The optical configuration is simply a gold-coated glass mirror and a polished Ge etalon attached directly to the tube ends with torr-seal. The Ge plate provides about 20% output coupling which in all cases was excessive but adequate. To minimize gas clean up by electrode sputtering, the electrodes were designed in the form of hollow cylinders with guard rings at the open end. In this way, the discharge was confined to the inside region of the electrode. Materials used for the electrodes in these experiments were Ni (#270) and Pt . For a tube ID of 10 mm, the gas mixture used was 14% CO_2 , 22% N_2 and 64% He with 1.0 torre Xe for a total pressure of 20 torr.

Fig. 5—Output power and efficiency vs discharge current. Mixture: CO_2 , 14%; N_2 , 22%; He , 64%.

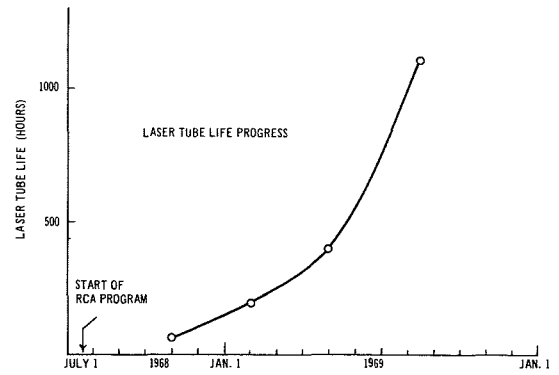


Fig. 1—Progress in sealed-off CO_2 laser development program.

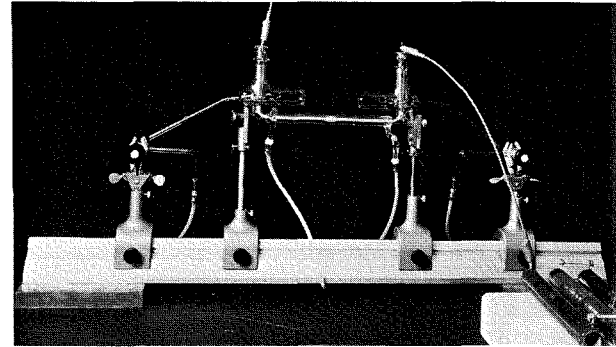


Fig. 2—Laser configuration for tube life test.

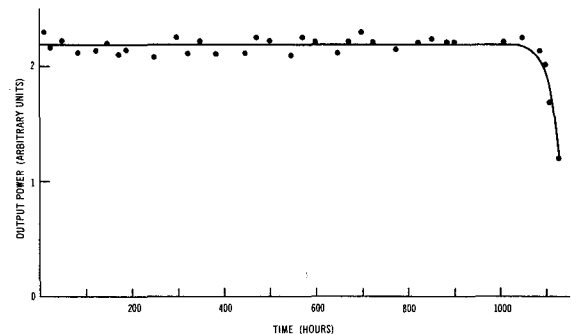


Fig. 3—Life characteristic of a sealed-off CO_2 laser.

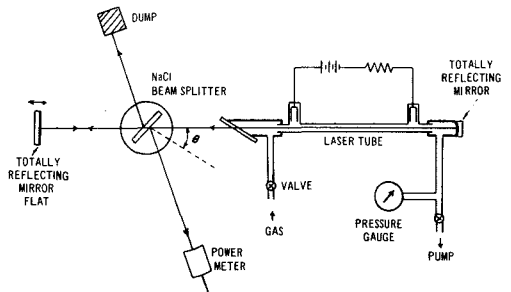
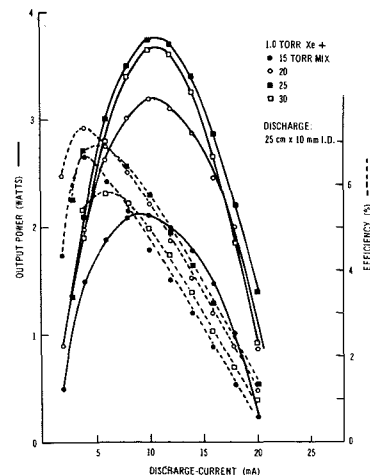


Fig. 4—Apparatus for parameter measurements.



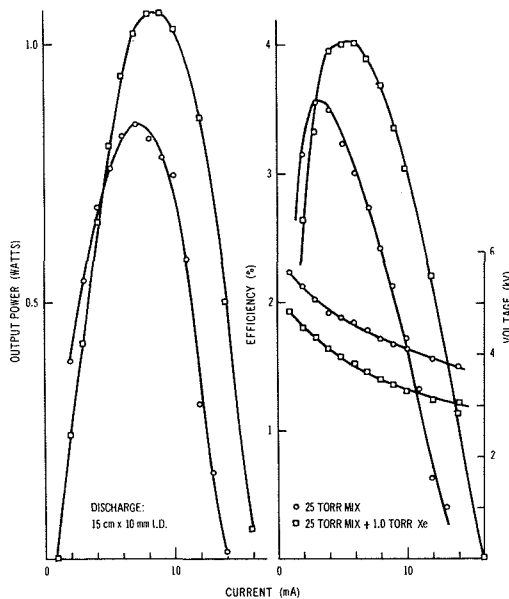


Fig. 6—Increase in output and efficiency as a result of adding Xe to the gas mixture of Fig. 5.

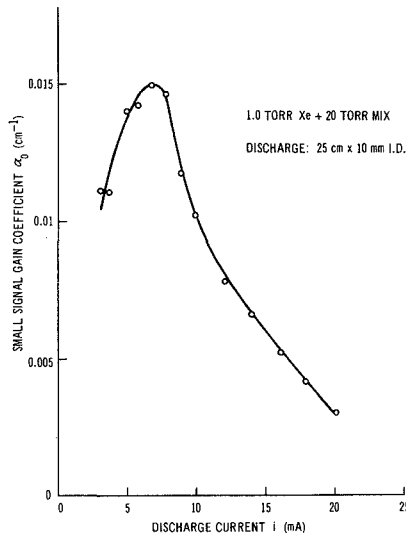


Fig. 7—Variation of gain coefficient with discharge current gain is integrated over mean-mode cross-section. Mixture: CO₂, 14%; N₂, 22%; He, 64%.

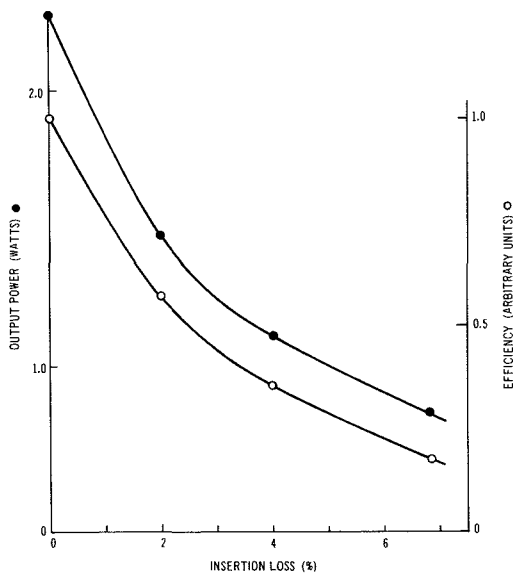


Fig. 8—Variation of output and efficiency with in-cavity loss.

Table I—Properties of some laser tube materials

Material	Thermal conductivity (cal/cm cm sec°C)	Thermal expansion °C (0-100°C)	Melting point (°C)	Young's modulus (psi)	Approximate cost factor for an assembled tube
Glass	0.0026	4.8×10^{-6}	~800	9×10^6	1
Silica	0.0032	5.5×10^{-7}	1670	10×10^6	2
Cervit	0.004	0.2×10^{-7}	~800	13×10^6	~4
Alumina	0.09	8.0×10^{-6}	2040	51×10^6	10
Beryllia	0.525	5.4×10^{-6}	2573	50×10^6	30

The life characteristic for one of our most recent tests is shown in Fig. 3 where tube life in excess of 1000 hours was obtained. Degradation to the half-power level occurs over approximately 10% of the life of the laser—this was also typical of our less successful runs. With the data on hand and the resulting improvement in the laser design, tube life significantly greater than this is expected in the near future.

Parameter measurements

Parameter studies are in progress to accumulate data which will enable accurate prediction of tube performance for specified output powers. Measurements have been made on a wide range of tube dimensions varying from 5 to 30 cm in length and 5 to 10 mm in bore diameter.³ To facilitate the study a versatile parameter test facility was constructed—this is shown schematically in Fig. 4. The mirrors, Brewster window, output coupling plate (NaCl), and gas inlet ports form an integral part of the laser cavity. The laser tube, including electrodes, is a separate item which is easily inserted into the cavity. Torr-seal provides the

vacuum seals and this scheme allows rapid tube replacement. With this facility measurements can be made over a wide range of variation in parameters, such as gas mixture, excitation current, optical cavity configuration, output coupling, tube temperature, tube geometry and material. In all cases, the results are quoted for sealed-off operation, laser action on a single transition and for the lowest transverse, TEM₀₀, mode.

Fig. 5 displays typical curves of output and efficiency vs. tube current for a number of gas pressures. As remarked above, the peak in the efficiency profile occurs at a lower current value than the peak in the output power. The effects of the addition of Xe to the usual triple gas mixture of CO₂, N₂, and He is illustrated in Fig. 6 where an increase of 25 and 15% in the output and efficiency, respectively, has been obtained with the inclusion of Xe. A further desirable feature is the lowering of the operating tube voltage by about 1 kV for this particular case. As a result of our studies, Xe is a basic additive in all our laser designs requiring high efficiency and efficiency and also for long tube life.

Table II—Properties of some optical materials for 10.6 micrometers

Material	Index of refraction	Absorption coefficient (cm ⁻¹)	Melting temperature (°C)	Remarks
NaCl	1.49	0.0019	801	Hygroscopic and fractures easily
KCl	1.46	0.0005	776	" "
AgCl	1.98	0.01	455	Bends and flows. Reacts to UV Radiation
AgBr	~2	~0.01	432	Better than AgCl
Ge	4.00	0.03 to 0.06	936	Thermal absorption runaway above 40°C
GaAs	3.09	0.006 to 0.02	400*	The best all round material, can be brazed to metal seals.

* Sublimation temperature

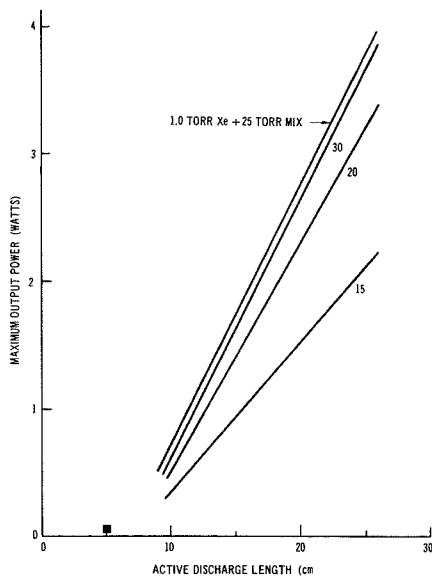


Fig. 9—Output power vs discharge length. Mixture: CO₂, 14%; N₂, 22%; He, 64%.

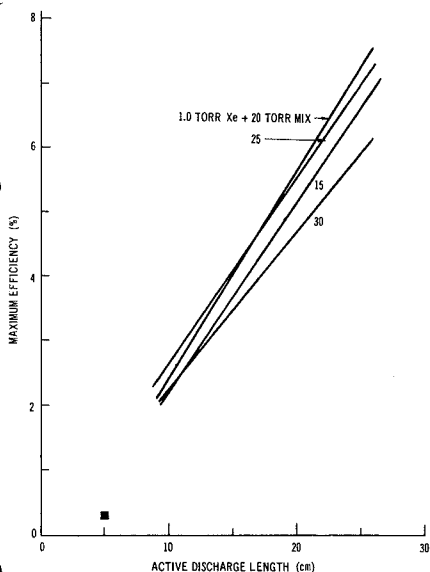


Fig. 10—Efficiency vs discharge length. Mixture: CO₂, 14%; N₂, 22%; He, 64%.

The design equation relating output power, P , to the losses can be expressed as⁴

$$P = \frac{\Gamma T}{(1 - \Gamma R)} \frac{A}{2\beta} (2\alpha_0 L + \ln \Gamma R) \quad (1)$$

where $(1 - \Gamma)$ is the lumped in-cavity losses excluding the output coupling $T = (1 - R)$; A is the mean mode cross-section; β is the saturation parameter and α_0 is the small-signal gain. By varying the output coupling and measuring P , all the factors in Eq. 1 can be determined for a particular laser configuration. A typical profile of the gain

(integrated over the mode diameter), determined in this way, is shown as a function of tube current in Fig. 7. For each case, the facility allows (in principle) all the vital parameters to be determined so that the effects of insertion losses on the efficiency and output power can be accurately predicted. Fig. 8 shows the effect of increasing cavity losses on the efficiency (with optimum output coupling at each point). Data of this form are required when in-cavity elements such as modulator crystals are to be included in the final design.

Correlations of tube length vs. output and efficiency are shown in Figs. 9 and 10 respectively. These represent our actual experimental results and do not include corrections for the losses within the window and internal mirror mounts of the test facility. This dead-space loss, for the small laser tubes studied, is excessive and would be minimized in complete laser units. Consequently, designs based on this data will be underestimated but on the safe-side. Upgrading of these correlation curves will result when a number of these final versions are constructed and tested. The data point for a discharge length of 5 cm represents the smallest, known CO₂ laser to be operated in the sealed-off mode. In Fig. 11 are some additional correlations related to the tube bore diameter.

Concluding remarks

The above results represent examples of the type of measurements made during our studies. Not all the data has been presented here nor has the versatility of the experimental facility been fully realized. Data obtained with glass tubes can be applied to other tube materials provided certain basic requirements of the material are met. Fig. 12 shows a photograph of an alumina laser tube currently undergoing study to test this assertion.

These parameter studies will continue in a constant effort to update existing data and to test new materials as they become available. It is anticipated that a handbook technology will have been acquired in the near future so that, for each specific application, the most efficient sealed-off CO₂ laser can be designed. Ultimately, of course, the optimization of these communication

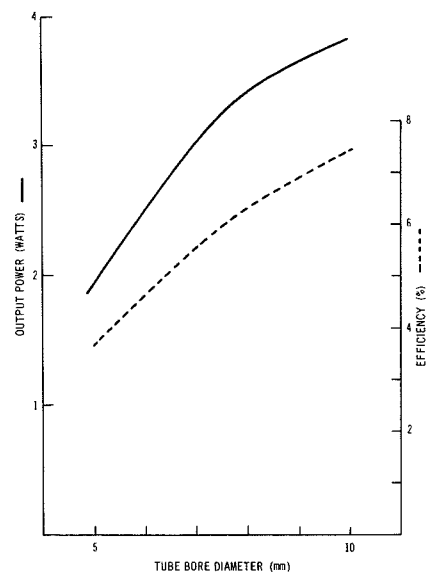


Fig. 11—Output power and efficiency related to tube-bore diameter.

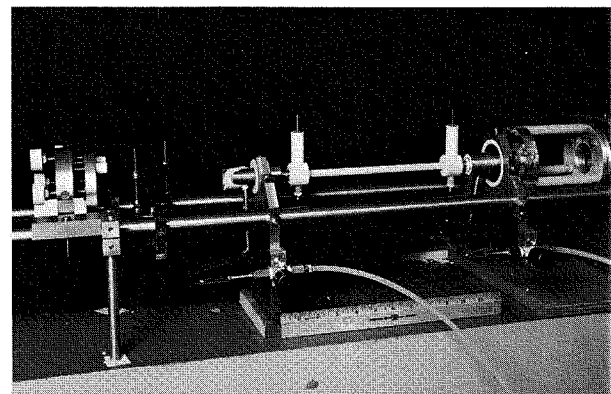


Fig. 12—Ceramic laser tube in test facility.

systems will include modulation techniques so that the final parameter would relate the information bit rate/pound weight/watt of input power/dollar cost of the system.

Acknowledgment

The authors acknowledge the support of the Canadian Directorate of Industrial Research for part of the work described. The assistance of Dr. R. M. Green and Mr. R. Bilodeau is gratefully acknowledged.

References

1. Clark, P. O. and Wada, J. Y., "The Influence of Xenon on Field-Off CO₂ Lasers" *J. of Quant. Elect.*, Vol. QE4, 263 (1968).
2. Wittman, W. J. "High-Power Single-Mode CO₂ Laser" *J. Quant. Elect.*, Vol. QE4, 786 (1968).
3. Crane, R. A. "Parameter Measurements on Small CO₂ Lasers", RCA Research Report 96123-9 (May 1969); "Parameter Measurements Small CO₂ Lasers II", RCA Research Report 96123-16 (Aug. 1969).
4. la Tourette, J. "An Oscillator Study" TRG Report, RAD-TR-67-407 (1968).

Solid-State detectors for laser applications

Dr. R. J. McIntyre | H. C. Sprigings | P. P. Webb

Solid-state photosensors are fast convenient detectors for many laser applications. In this paper some of the factors affecting the design and optimization of solid-state photosensors are discussed. The performance of two types of silicon photodiode, designed especially to meet the requirements of laser-pulse detection in the near-infrared out to and including 1.06 μm , is described. These types are 1) a large-area multi-element photodiode for wide-field-of-view applications and 2) an avalanche photodiode for narrow-field-of-view applications.

THE GROWTH OF LASER TECHNOLOGY within the last decade has provided many new requirements for fast, sensitive, rugged photodetectors, particularly in the near-infrared. In this article, some of these requirements are discussed, and some of the special photodiodes which have been developed in the Research Laboratories of RCA Limited to satisfy these requirements are described.

Since lasers can be used in a myriad of ways, a completely general discussion of the techniques of detection is impractical. We shall confine our discussion to the problem of detecting short pulses of light, i.e., the detection of light from lasers which are Q-switched, phase- or mode-locked, or otherwise modulated so that most of the energy is delivered in a series of short pulses. Most of these applications fall into one of two classes:

- 1) Narrow-field-of-view systems;
- 2) Wide-field-of-view systems.

The first class comprises all systems in which the point of origin of the laser energy is known, be it from the laser itself, or reflected from a "target" in a known direction. This includes point-to-point communications systems, laser ranging systems, some intrusion alarms, and some fuse systems. For this class, since the detector system need only have a narrow field of view, a relatively small detector, with dimensions of the order of a millimeter or less, is all that is required. For the second class of systems, in which the source of energy is spread over a wide

range of angles, or of unknown direction, the detection system must have a wide field of view and will therefore require a detector with dimensions of the order of centimeters or more. Examples are laser search systems, target designation systems, and collision avoidance systems. Because the criteria for optimizing detectors for these two classes of systems are different, they will be discussed separately.

Small-area detectors

Quantum efficiency

Quantum efficiency is that fraction of the incident photon flux from the laser which interacts positively in the active part of the detector. A positive interaction, in the case of a photodiode or an intrinsic photoconductor, would be the generation of an electron-hole pair. For an extrinsic photoconductor, it would be the ionization of an electron or hole to or from an impurity. The active part of the detector is that region from which the carriers generated will be collected and detected in a time of the order of the laser pulse length. Thus for this discussion, the quantum efficiency does not include those photons which are absorbed in a base layer sufficiently far from the active region of the detector so that the generated carriers must diffuse to the active region before being detected in a time of the order of microseconds or longer. Such carriers will contribute to any quantum efficiency measurement made at low frequencies, but not to the height of the signal from a short laser pulse in a wideband system.

It is usually possible to make a photodiode in which—apart from two thin, diffused, contact layers—the total

thickness of the device is active. Under such conditions, the quantum efficiency, η , is given by:

$$\eta = \frac{[1 - r_1][1 - \exp(-\alpha w)]}{[1 + r_2 \exp(-\alpha w)] \exp(-\alpha d)} \quad (1)$$
$$1 - r_1 r_2 \exp[-2\alpha(w + d)]$$

where r_1 is the reflectivity of the front surface; r_2 is the reflectivity of the back layer; d is the effective thickness of the front contact layer; w is the effective thickness of the active layer; and α is the absorption coefficient of the detector material for light of the wavelength being detected.

Thus, to maximize η , r_1 should be made as small as possible (by using an anti-reflection coating), αw should be greater than unity if possible, αd should be much less than unity, and r_2 should be as large as possible (i.e., the back layer should be thin and have a highly reflective coating). Typical values achieved to date, with silicon diodes, are $r_1 \approx 0.05$, $r_2 \approx 0.95$, $d < 1 \mu\text{m}$, w up to $700 \mu\text{m}$ for a non-multiplying diode, and w up to $300 \mu\text{m}$ for an avalanche diode. In the visible and ultraviolet, where α is in the range 10^4 to 10^5 cm^{-1} , the contact layer thickness d must be kept well under $1 \mu\text{m}$ (10^{-4} cm) so that the absorption loss in this "dead" layer is not too high. For the ultraviolet particularly, a sufficiently thin dead layer is difficult to achieve with a diffused layer, so that quantum efficiencies of only 10 to 20% are typical. For this range, better results can be obtained with Schottky barrier devices. For wavelengths greater than $0.6 \mu\text{m}$, however, $\alpha d \ll 1$, and quantum efficiencies in the range of 80 to 90% can be obtained for wavelengths out to about $1.06 \mu\text{m}$, beyond which point it becomes difficult to keep αw greater than unity. At $1.06 \mu\text{m}$, the wavelength of the Neodymium laser, a quantum efficiency of 80% has been obtained in large-area detectors, and about 35% in avalanche detectors. These two devices are described more fully later in this paper. Long narrow silicon diodes, with the light entering in a direction parallel to the depletion layer, have also been used at $1.15 \mu\text{m}$, one of the wavelengths of the He-Ne laser, with a measured quantum efficiency of about 40%.

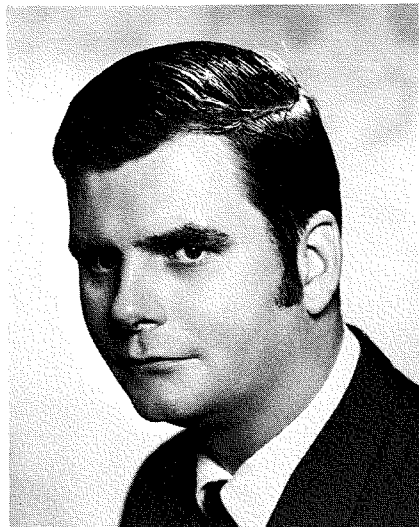
With uncoated germanium photodiodes, quantum efficiencies of about 50 to 60% have been obtained in the

This work was partially supported by the Defense Research Board of Canada under Contract DRB5501-55, DIR Project E114.
Reprint RE-15-5-3.
Final manuscript received November 17, 1969.



Dr. Robert J. McIntyre, Director
Semiconductor Research Laboratories
Research Laboratories
RCA Limited
Montreal, Canada

graduated *summa cum laude* in Physics from St. Francis Xavier University in 1950. He remained there the following year as Instructor in Physics. In 1951 he commenced graduate studies at Dalhousie University where he worked in the field of beta-ray spectroscopy, receiving the M.Sc. in 1953. He then moved to the University of Virginia where in 1956 he obtained the Ph.D. with a theoretical thesis on the surface energies of monovalent metals. Dr. McIntyre joined the Research Laboratories of RCA Limited in 1956 where he has been engaged in solid state and semiconductor physics, in particular in studies of infrared photoconductivity, transistor physics, avalanche effects in semiconductor diodes, variable capacitance diodes, photodiodes, radiation detectors, transport properties of semiconductors at low temperatures and ion pairing on semiconductors. He was for one year (1958) on loan to the Electronics Wing of the Canadian Armament Research and Development Establishment at Valcartier, Quebec. In 1967 he became Director of the Semiconductor Electronics Laboratory, where he is directing research programs in advanced semiconductor sensors and microwave integrated circuits. He is a member of the Canadian Association of Physicists, the American Physical Society, and a Senior Member of the IEEE.



Howard C. Springs
Semiconductor Research Laboratories
Research Laboratories
RCA Limited
Montreal, Canada

received the B.Sc. from Sir George William University in 1962. In 1956 he joined the Northern Electric Company's Materials Inspection Laboratory where he carried out chemical and metallurgical analysis on metals. He was transferred to the Research and Development Laboratories in 1959 and assisted in development work on the NPN planar transistor. Mr. Springs joined the Research Laboratories of RCA Limited in April 1960. Initially he was engaged in doing research and development on various types of silicon nuclear particle detectors using oxide passivation techniques. He has since been involved in the development of a high power frequency transistor and more recently has been doing research and development on multi-element photodiodes for detection of 1.06-micron radiation. He has also examined various methods for passivating devices fabricated from ultra-high resistivity silicon. He is a member of the IEEE and the Canadian Association of Physicists.



Paul P. Webb
Semiconductor Research Laboratories
Research Laboratories
RCA Limited
Montreal, Canada

received the B.Eng. in Engineering Physics from McGill University in 1955 and was awarded an Athlone Fellowship to study in the United Kingdom from 1955 to 1957. He received the M.Sc. in Engineering from the University of London, and the Diploma of Imperial College in 1957. At the University of London he was engaged in research in semiconductors, with particular interest in the vapour diffusion process for the introduction of impurity layers into germanium. An outcome of the research was the construction of a very high frequency transistors. Mr. Webb joined the Research Laboratories of RCA Limited in February 1958, upon his return to Canada from England. Since then he has been engaged in research on semiconductor devices including the study of voltage breakdown phenomena in diffused silicon P-N junctions and the development of silicon-junction nuclear particle detectors. He was also responsible for the development of Lithium-drifted Germanium diodes for high-resolution gamma spectroscopy, and was involved in a study of material problems related to their manufacture. He is presently engaged in a program to develop large area silicon avalanche photodiodes. He is a member of the IEEE.

1.0 to 1.65 μm range. With coating, a 20 to 30% improvement can be expected. Such a device should be most suitable for use with the Erbium laser, at 1.6 μm .

Speed of response

For most applications, it would be desirable to have the speed of response of the detector comparable with, or somewhat less than, the duration of the laser pulse to be detected. In some cases, however, to maximize the signal-to-noise ratio, it may be desirable to use electronic time constants considerably longer than the laser pulse length. In such cases it would not be a disadvantage to use a slower detector, and it might be a distinct advantage

if in so doing the quantum efficiency could be increased and in the detector capacitance decreased.

In a non-multiplying photodiode, the speed of response is essentially the transit time of an electron across the depletion layer. This is covered more fully in the discussion of "large-area multi-element photodiodes for use at 1.06 μm ." In a multiplying photodiode, this is lengthened somewhat by the time required for multiplication, although the lengthening is only appreciable for ultra-fast (sub-nanosecond) diodes, and depends on the device design and material.¹

Dark current

Generally speaking, the dark current

I_d , (i.e., the detector current flowing under normal bias conditions when no light is incident on the device) should be as low as possible. Leakage current is normally of two types: 1) a surface-leakage current, which enters the device at the junction periphery, and 2) a bulk-generated current. In small devices, the former usually is the larger of the two. It can be controlled by careful adjustment of the surface states under the masking oxide. The latter usually predominates in larger devices. Typical values are in the range 10^{-9} to 10^{-8} amperes per cubic millimeter of active volume, depending considerably on the processing techniques.

Perhaps a more important quantity

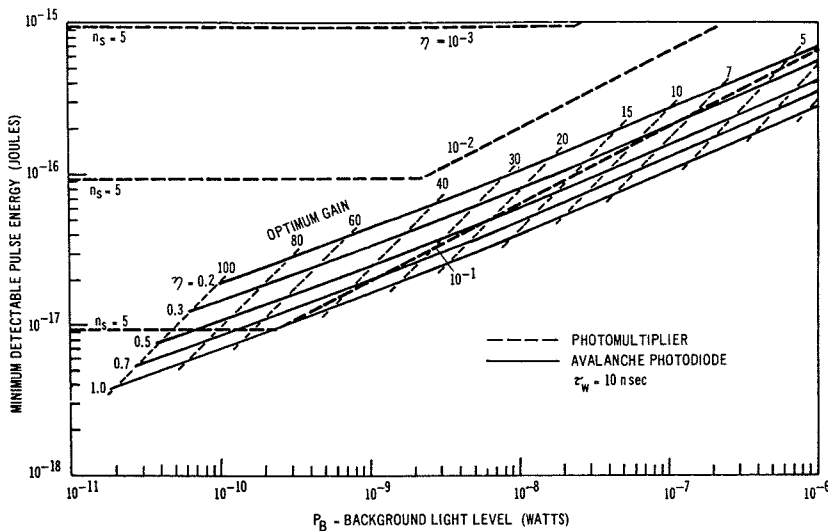


Fig. 1—Calculated values of the minimum detectable laser pulse energy for a 10-ns laser pulse at 1.06 μ m for photomultipliers and avalanche photodiodes of various quantum efficiencies as a function of background light incident on the detector. At low light levels, the photomultiplier is limited by the requirement that a minimum average number n_s of photoelectrons is required so that the probability of getting a pulse large enough to distinguish from a noise pulse is high. In other regions, a power signal-to-noise ratio of 10 has been assumed. For the avalanche photodiode, the indicated optimum gain is the calculated value assuming that $k=0.1$.

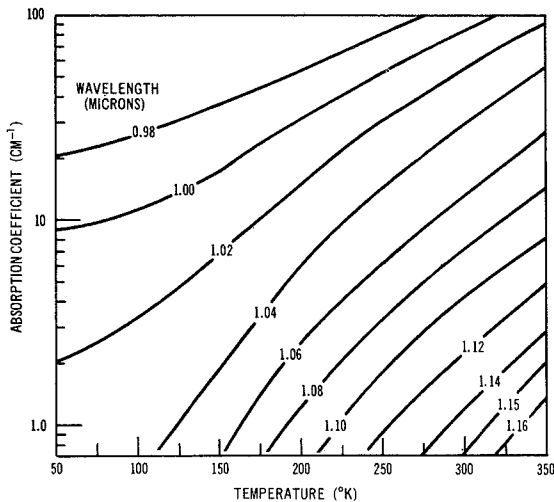


Fig. 2—Absorption coefficient of silicon near its absorption edge as a function of temperature.⁴

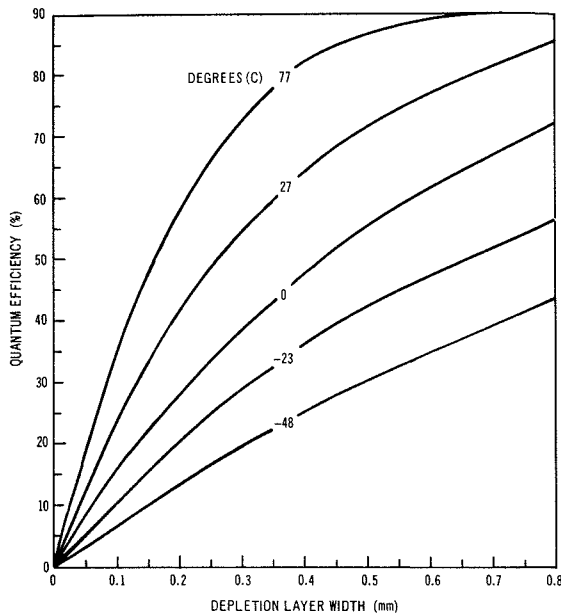


Fig. 3—Achievable quantum efficiencies in silicon P-I-N photodiodes as a function of temperature and depletion layer width.

orders of magnitude less than I_{a_1} . Note that in our notation, I_{a_2} and R are the un-multiplied current and responsivity respectively.

The expressions above only hold at frequencies such that contributions from the so-called $1/f$ noise can be ignored. This will usually be the case in wideband systems designed for laser pulse detection.

Detector capacitance

The capacitance of a P-N junction is given by:

$$C = \frac{\epsilon A}{w} \quad (4)$$

where ϵ is the product of the dielectric constant of the detector material and the permittivity of free space; A is the detector area; and w is the depletion layer width.

Generally speaking, small-area detectors designed for high quantum efficiencies in the near-infrared will have depletion layers wide enough so that the detector capacitance will be small compared to the input capacitance of the following amplifier. Thus capacitance is not a major consideration, except for detectors designed for ultra-high speed (sub-nanosecond response).

Gain

The choice between an avalanche and non-avalanche photodiode is not always an easy one to make. The former will usually give better performance for a system where the signal-to-noise ratio for a non-multiplying device would be limited by amplifier noise. For background limited conditions, the latter is usually a better and cheaper choice. In some systems the choice is likely to be one of economics: avalanche photodiodes are difficult to fabricate and likely to be expensive, at least for the foreseeable future. For systems requiring the ultimate in performance, however, particularly those such as laser ranging systems where it is desirable to use very wide bandwidths to recover the shape of the laser pulse for timing reasons, the avalanche device is clearly superior. Later in this paper, the design of avalanche diodes suitable for use at 1.06 μ m is described. These have given noise equivalent powers (NEP)—measured with a wide-

than I_a is the dark equivalent power, abbreviated P_a , which would give a RMS noise current equal to the actual RMS noise current in the detector under dark conditions. For normal non-multiplying photodiodes, in which the noise spectral density is given by the shot noise in the dark current, P_a and I_a are related by:

$$I_a = \frac{q\eta\lambda}{hc} P_a = R P_a \quad (2)$$

where q is the electronic charge; η is the quantum efficiency; h is Planck's constant; λ is the wavelength of the light being detected; c is the velocity of light; and R is the detector responsivity (amps/watt).

If, however, the detector has within it a gain mechanism,

$$P_a = \frac{1}{R'} (I_{a_1} + I_{a_2} G) \quad (3)$$

where $R' = q\eta\lambda G/hc$ is the measured responsivity; G is the detector gain; I_{a_1} is that portion of I_a which is not multiplied; and $I_{a_2} G$ is that portion of I_a which has undergone gain. For large gain, Eq. 3 reduces to $P_a = I_{a_2}/R$.

For example, in an avalanche photodiode much of the dark current occurs at the junction periphery and is not multiplied. Only the space-charge current I_{a_2} , generated in that part of the depletion layer such that the carriers are swept into the multiplying region, undergoes gain. Often I_{a_2} is one or two

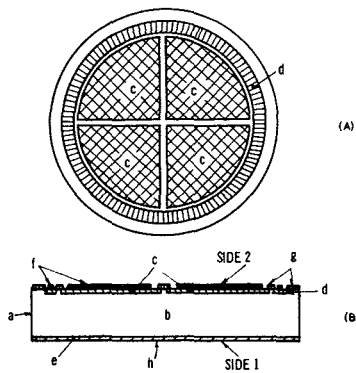


Fig. 4—Typical quadrant photodiode structure: (A) quadrant and guard-ring geometry, (B) cross-section of oxide passivated device. Legend: a) silicon slice, b) intrinsic region, c) diffused N-type quadrant electrodes, d) diffused N-type guard-ring, e) diffused P-type anode electrode, f) metallized contacts and reflecting layer, g) silicon dioxide, h) antireflection coating. Light enters through side 1.

band amplifier—of 3×10^{-34} watts/cycle^{1/2} at a gain of 25. Similar devices designed for use at $0.9 \mu\text{m}$ should have still lower NEP.

For avalanche diodes, the noise performance depends rather critically on the ratio of the ionization coefficient of the holes to that of electrons.² A small ratio is desirable for low noise. For this reason, silicon—having a ratio in the range of 0.03 to 0.1 (depending on the maximum field)—is a much more suitable material than germanium—which has a ratio close to unity. Moreover, since silicon diodes have much lower dark currents than germanium devices, they will be much superior, provided a respectable quantum efficiency can be achieved. Fig. 1 shows the calculated minimum detectable laser pulse energy at $1.06 \mu\text{m}$ for avalanche photodiodes of various quantum efficiencies assuming a power signal-to-noise ratio of 10, a laser pulse length of 10 ns, $k=0.1$, and a matched amplifier having an equivalent noise resistance of 200 ohms.³ For the avalanche diodes discussed later in this paper in more detail, an effective value of $k \leq 0.03$ has been measured. This would reduce the minimum detectable energy by almost a factor of two. For this device, which has a dark-equivalent background light level of 5×10^{-30} watts, the minimum detectable laser pulse should be about 10^{-37} joules.

Also plotted in Fig. 1 for comparison are the minimum detectable energies for photomultipliers of various quantum efficiencies. It is seen that an

avalanche photodiode with a quantum efficiency of 30% compares favorably with a photomultiplier having a quantum efficiency of 10%.

The use of a power signal-to-noise ratio of 10 in the comparison above is questionable for pulse detection applications. For a photomultiplier, a threshold-voltage-to-RMS-noise-voltage ratio of about 7 or 8 is usually required to reduce the false count rate to an acceptable level. For the avalanche photodiode, recent calculations by one of the authors (R.J.M.) have shown that the amplitude distribution of noise pulses is not Gaussian, so that the same ratio cannot be used. The proper ratio is a function of the diode gain, and is quite large for large gains. These calculations are now being completed and will be published in the near future.

Large-area photodiodes

The factors affecting the design and choice of a large area photodiode are similar to those for small area photodiodes with the exceptions noted in the following paragraphs.

Diode capacitance

Whereas junction capacitance is not a major consideration for small area photodiodes, it certainly is for large area devices. For example, a depletion layer width of $100 \mu\text{m}$ is perfectly adequate to give a good quantum efficiency at $0.9 \mu\text{m}$ (the wavelength of the GaAs laser) and the detector will have a relatively fast response time of about 1 ns. Thus $100 \mu\text{m}$ would be a good choice for a small-area detector for use at this wavelength. However, such a device will have a capacitance of about 106 pF/cm^2 . By widening the depletion layer to $500 \mu\text{m}$, the response time is only lengthened to about 12 to 15 ns and the capacitance is reduced to about 21 pF/cm^2 . For the detection of laser pulses in the 10- to 20-ns range, the wider device would be the better choice for large detectors, since it allows the use of a larger load resistor, thereby giving a better signal-to-noise ratio.

Gain

Whereas with small devices one must decide between an avalanche and non-avalanche device, with large detectors the choice is simplified, since at the present time large-area avalanche pho-

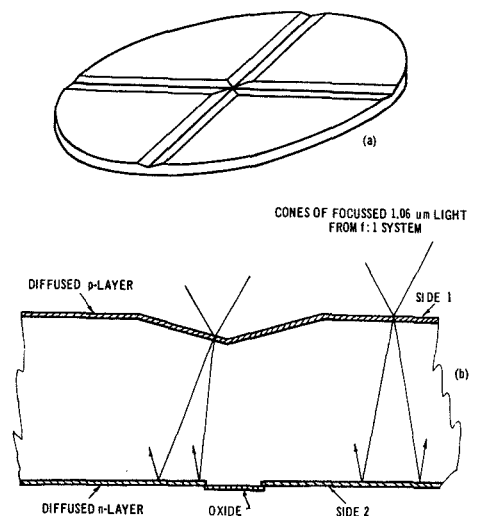


Fig. 5—Quadrant photodiode with grooves to reduce effective quadrant separation. (A)—showing crossed beveled grooves in silicon diode chip, (B)—exploded view showing paths of extreme rays of the cone of radiation from an f:7 optical system.

todiodes are practically impossible to fabricate. Moreover, since large-area devices tend to be used in applications in which a fair amount of background light is encountered, they tend to be background limited, or nearly so, so that little or no gain could be used advantageously even if the devices existed.

Multi-element arrays

Often a large area detector will be broken up into an array of smaller devices, each with its own preamplifier. This could be done either to improve the signal-to-noise ratio, or to provide positional information, as in a laser tracking or a target designation system. Methods of forming arrays with little or no dead space between the elements are discussed in detail later.

Area

The area of a photodiode is limited physically by the dimensions of the material from which it is made. Silicon diodes, made from hyperpure silicon, are available with a diameter (or longest diagonal) up to about one inch.

Summary comparison of small- and large-area photodiodes

Small-area photodiodes are sensitive, reliable, and relatively cheap sensors suitable for many laser applications. For low-light-level applications requiring only small sensitive areas, avalanche photodiodes compare favorably with photomultipliers in signal-to-noise ratio in the visible spectrum

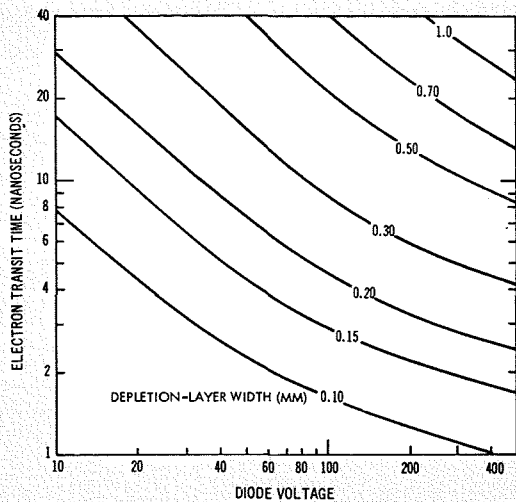


Fig. 6—Electron transit time in a P-I-N photodiode as a function of depletion layer width and diode voltage at room temperature. Diode response time (70% of charge collected) is about 70% of the electron transit time. Drift velocity data taken from Ref. 5 and other references quoted therein.

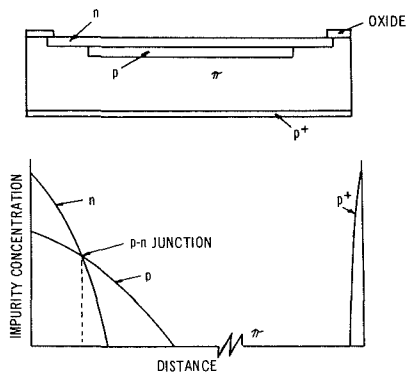


Fig. 7—Reach-through avalanche diode structure and impurity concentration profile. The starting material is P-type silicon of about 5000 ohm-cm resistivity. The P and N diffusions are, respectively, Boron and Phosphorous.

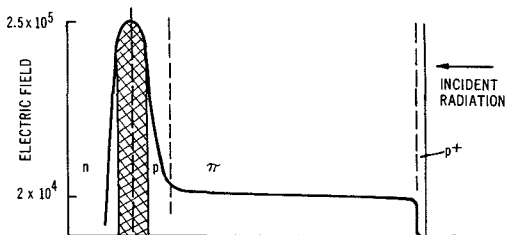


Fig. 8—Electrical field profile for a reach-through avalanche diode.

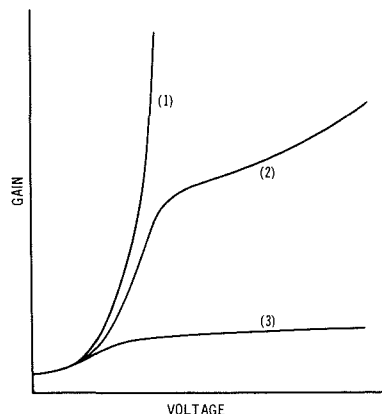


Fig. 9—Three general gain-voltage characteristics which may be obtained during the final Phosphorous diffusion: 1) not enough diffusion, no-reach through; 2) desired characteristics; and 3) Diffusion too far, the gain is very low.

and surpass them in the near-infrared. Large-area single- and multi-element photodiodes, having quantum efficiencies close to unity and speeds adequate for most laser applications, have detectivities close to the theoretical maximum, particularly under background-limited conditions.

Large-area multi-element photodiodes for use at 1.06 μm

The Neodymium-doped laser has been creating considerable interest during the past few years, and at present is being considered for several commercial and military systems. The advent of this laser has generated a demand for multi-element detection devices optimized to operate at 1.06 μm .

Quantum efficiency considerations

Fig. 2 shows how the absorption coefficient of silicon varies with wavelength and temperature in the near infrared.⁴ At 1.06 μm , the absorption coefficient is about 15 cm^{-1} at room temperature, and the mean path length is about 0.7 mm. The absorption coefficient drops off fairly quickly as the wavelength increases and as the temperature is lowered. Fig. 3 shows the attainable values of quantum efficiency at 1.06 μm as a function of temperature and depletion layer width. These curves were calculated from the data of Fig. 2 and Eq. 1. They also correspond very closely with experimentally measured values. It is interesting to note that under background-limited conditions, improved performance could be obtained by heating the detector.

It is possible to fabricate diodes with depletion layers up to 1 mm, but a more practical limit is about 0.7 mm. Typical reverse voltages required to deplete such devices are in the 150-to-200-volt range, although normal operating voltages are somewhat higher. To optimize quantum efficiency, the front of the detector is coated with an anti-reflective coating to minimize reflective losses. Similarly, the back is coated with an evaporated layer of aluminum to reflect that part of the 1.06 μm radiation which is not absorbed on the first pass through the wafer.

Multi-element array

Fig. 4 shows a typical multi-element

structure for use at 1.06 μm . In this structure, ultra-high resistivity P-type silicon is used as the substrate material. The initial resistivity of the silicon before processing is in the 20,000-to-50,000-ohm-cm range, but has been found to increase by a factor of two or three during processing. Light enters through a shallow P⁺ contact diffused into one side of the device. On the other side, an array of N⁺ electrodes is diffused (a quadrant array in the case illustrated). In some cases, this array is surrounded with an N⁺ guard-ring to reduce surface leakage currents.

In most applications, it is desirable that the dead space between adjacent elements be kept to a minimum. At the present time, an oxide mask is used to define the quadrant regions, the width of the oxide strip between elements being about 0.010 inch. The effective separation between quadrants is much less than the actual width of the oxide strip and a dead space is practically non-existent, since carriers which are generated optically in the region between the quadrants are collected by the closest electrode. The important parameter of this type of device is the distance in which one quadrant cuts-off as a point of light moves across it into the adjacent quadrant. The distance in which the signal drops from 90% to 10% has been found to be in the 0.004- to 0.005-inch range for a point source of light at normal incidence. For the more practical case of a focussed cone of light, say 0.004 inch in diameter, a typical value is 0.008 inch to 0.010 inch, due to the spreading of the light inside the wafer. However, this can be reduced to about 0.005 inch for a 0.004-inch light spot if the front surface of the detector is "grooved" as shown in Fig. 5. The "groove" serves to refract all the light into one quadrant when the light spot approaches the transition zone. A second advantage of the groove is that an increase in signal is observed when the light spot is on the grooved surface, due to the light being refracted at an angle greater than the critical angle for internal reflection, so that it gets "trapped" in the diode until it is absorbed.

Speed of response

A major requirement for devices used in laser detection applications is that

they have fast response-times. For a photodiode, current starts to flow the instant the light is absorbed. For most cases, about 70% of the charge is collected in a time equal to the electron transit time:

$$\tau_e = \frac{w}{v_e} \quad (5)$$

where w is the depletion layer width and v_e the average velocity of electrons.

If the field is low,

$$v_e = \mu_e E = \mu_e V/w \quad (6)$$

where μ_e is the electron mobility, and E is the electric field. This gives

$$\tau_e = w^2/\mu_e V \quad (7)$$

However, at higher fields the drift velocity is no longer proportional to the field but tends to saturate.⁵

Fig. 6 shows the electron transit time as a function of bias and depletion-layer width. From this figure it can be seen that for a P-I-N diode 0.7-mm thick, with an applied reverse bias of 200 V, an electron transit time of about 25 ns can be expected. Actual measurements using a 1.06- μ m laser have confirmed these expectations.

Leakage current

Leakage current is one of the most critical parameters in determining device and system performance. Provided care is taken to prevent surface inversion layers, the dark current is largely determined by volume-generated current in the depletion layer. With careful annealing, this can be reduced to less than 10^{-8} A/mm², giving a leakage current less than 1 μ A/cm² for a 0.7-mm thick diode. This is usually less than the current generated by background light under normal operating conditions.

Summary of tradeoffs

For any application, there is a trade-off between quantum efficiency, response-time, and capacitance. To have a fast response-time, some quantum efficiency must be sacrificed and some increase in capacitance accepted; if it is possible to relax the response-time requirement, the converse is true.

It is now possible to fabricate very good large-area silicon devices in which an optimum balance between

quantum efficiency and response-time can be achieved for any wavelength out to 1.06 μ m. New packaging methods to improve long-term reliability, and integrated preamplifiers to be encapsulated with the detector are now being investigated.

Avalanche Photodiodes

The device to be described in this section is a double-diffused 'reach-through' structure, a working model of which, designed for use at shorter wavelengths, has previously been discussed by Ruegg.⁸ Fig. 7 illustrates the diode configuration and impurity profiles. The two diffusions—P-type first (boron) and N-type later (phosphorus)—are so adjusted that, when a reverse-bias voltage is applied, the depletion layer of the diode just 'reaches-through' to the low concentration π region when the peak electric field at the junction is just slightly less than that required to cause avalanche breakdown. Additional applied voltage then causes the depletion layer to increase rapidly out to the P⁺ contact while the field throughout the device increases relatively slowly.

The π region of the device, which is the substrate crystal, is typically about 5000 ohm-cm resistivity. Thus, widths up to about 300 μ m can easily be de-

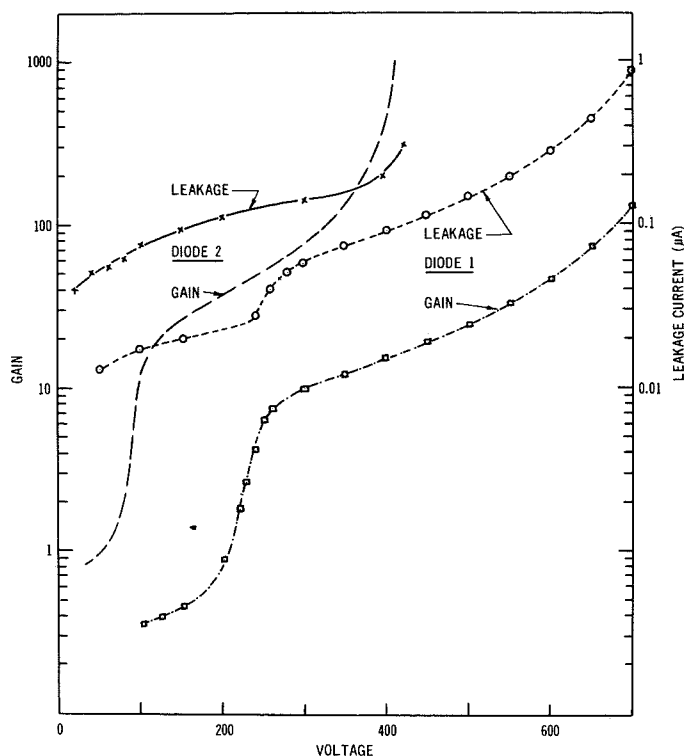


Fig. 10—Gain and leakage current characteristics for two diodes.

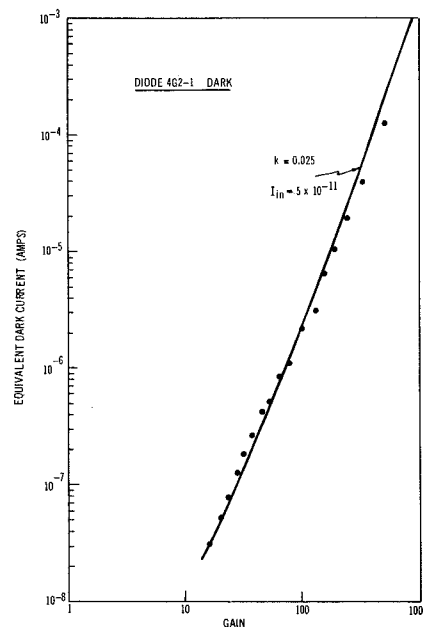


Fig. 11—Equivalent dark current for diode 4G2-1 as a function of gain. The calculated curve has been fitted assuming $k=0.025$ and $I_{in}=5 \times 10^{-11}$ A. The amplifier contribution of 2×10^{-8} A has been subtracted.

pleted with application of relatively little additional voltage over and above that required for reach-through. Since electrons are more strongly ionizing than holes in silicon, optimum conditions are obtained when the incident radiation is absorbed in the π region. Thus the device is used with radiation entering the P⁺ contact. Elec-

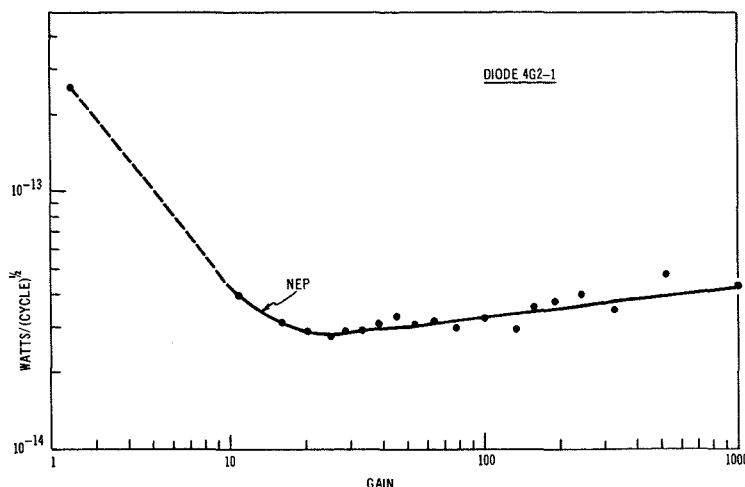


Fig. 12—Noise equivalent power of diode 4G2-1 for 1.06 μm radiation. The amplifier had a bandwidth of about 20 MHz and an equivalent dark current of approximately 2×10^{-8} A. A broad minimum of about 3×10^{-14} W/Hz $^{1/2}$ is observed at a gain of about 25.

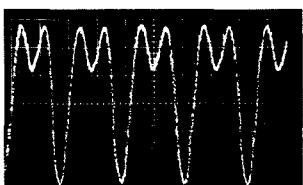


Fig. 13—Speed of response measured for one diode using fast pulses of phase-locked HeNe laser. Horizontal time scale 5 ns/cm.

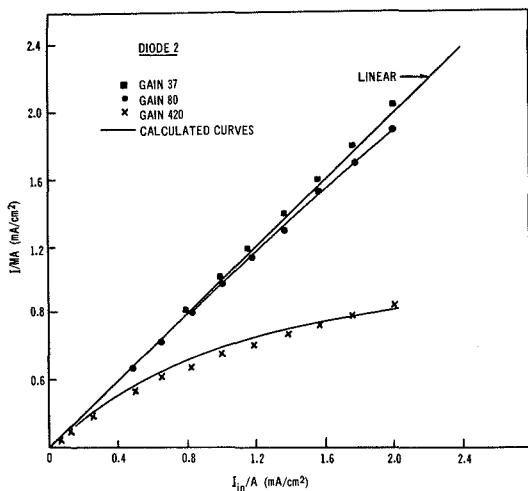


Fig. 14—Experimental and calculated curves of linearity as a function of injected current for diode 2.

trons are swept to the high-field region where multiplication occurs. The resulting holes which are produced there traverse the π region to the p^+ contact, and constitute the multiplied signal.

The field profile, and several possible gain-voltage characteristics are shown in Fig. 8 and 9. From Fig. 9, we observe the three general conditions which may occur during the diffusion:

- 1) N-type impurity not adequately diffused so that avalanche occurs before reach-through is achieved;
- 2) The desired condition where reach-through occurs just as the gain has

risen to some intermediate value, typically 10 or 20, beyond which point additional applied voltage gradually increases the field and hence gain; or

- 3) Phosphorus diffused too far, so that useful gain would be achieved in the device only at excessively high voltages.

The salient features of this device, some of which are a very distinct advantage over conventional P-N junction avalanche diodes, are as follows:

- 1) Relatively low slope to the gain-voltage characteristic in the operating region;
- 2) Relatively low operating voltage;
- 3) Wide active layer, up to about 300 μm in thickness and hence useful quantum efficiency at 1.06 μm ;
- 4) Fast response time;
- 5) Gain insensitive to position of absorption of the radiation; and
- 6) Thin window, (thickness of the p^+ layer).

Gain and leakage current

Fig. 10 shows gain-voltage and leakage-current characteristics for two typical diodes. (The apparent values of gain below 1 at low voltages are due to lower quantum efficiencies at these voltages than when the device is fully depleted). For one device, we note that the leakage current apparently follows the shape of the gain characteristic at high gain, thus indicating that the increase in leakage current is almost entirely due to multiplication. In the other device, the background leakage, undoubtedly due to leakage under the oxide, is high enough that a significant increase due to multiplication is apparent only at very high multiplication (greater than 1,000). The quantum efficiency of the #2 diode (sensitive thickness 225

μm) was measured to be approximately 30% at 1.06 μm , by comparison to a calibrated P-I-N photodiode.

Noise

The theoretical noise characteristics of avalanche diodes have been discussed previously by McIntyre.² For this case, where electrons are the predominant ionizing carrier, the noise spectral density, ϕ , is given by:

$$\phi = 2qI_{in}M^3 \left[1 - (1-k) \left(\frac{M-1}{M} \right)^2 \right] \quad (8)$$

where I_{in} is the injected current; M is the multiplication; and k is the ratio of hole to electron ionization coefficients.

From this we see that minimum noise is obtained for small k . For silicon, in the electric field range of interest (2 to 4×10^5 V/cm) k is expected to be approximately in range 0.05 to 0.1.⁷ However, measurements on illuminated diodes suggest that the effective value of k may be as low as 0.025. From Eq. 8 we can define an equivalent dark current as follows:

$$I_{eq} = I_{in}M^3 \left[1 - (1-k) \left(\frac{M-1}{M} \right)^2 \right] \quad (9)$$

thus:

$$\phi = 2qI_{eq} \quad (10)$$

Fig. 11 shows the equivalent dark current for a typical diode. The calculated curve has been fitted, selecting $k=0.025$ and $I_{in}=5 \times 10^{-11}$ Amps. Since the sensitive volume of this particular detector was 0.12 mm^2 , the thermally generated current in the π region was about 0.4 nA/ mm^2 .

Of interest to a potential user of such a device is the noise equivalent power (NEP). We have:

$$\text{NEP} = \frac{(2qI_{eq})^{1/2}}{MR} \quad (11)$$

where R is defined in Eq. 2.

For this diode $R \approx 0.26$ amps/watt, the equivalent dark current of the amplifier (bandwidth=20 MHz) was approximately 2×10^{-8} Amps. Thus the curve of Fig. 12 can be calculated. We note a minimum value of NEP for the system to be about 3×10^{-14} watts/cycle $^{1/2}$ at a gain of 25. Somewhat better results could probably be obtained using an amplifier of narrower bandwidth. It is interesting to note that the optimum gain is not

at all critical: any gain in the range 25 to 100 gives practically the same NEP. The same device should have a responsivity about 2½ times higher, and therefore an NEP about 2½ times lower at 0.9 μm. However, for this wavelength, a device with a narrower depletion layer should suffice, which should lower I_{in} still further.

Speed of response

The operation of 'reach-through' avalanche diodes has already been indicated above. Once the photogenerated electrons reach the high-field region, they are multiplied very rapidly. The multiplied photocurrent results primarily from holes created in the high field region, which drift across the π region to the p⁺ contact. Thus the speed of response for the multiplied signal is essentially the transit time for holes in the π region:

$$\tau_h = w/v_h \quad (12)$$

where w is the width of the π region, and v_h is the average hole velocity.

The average hole velocity is, of course, dependent on the field in the drift region. Typically, this will be about 1 to 3 × 10⁴ V/cm, so that the hole velocity⁵ would be about 3 to 5 × 10⁶ cm/s, and the speed of response, therefore, will be about 1.5 to 3 ns/100 μm of depletion layer width.

Fig. 13 shows the result obtained for one diode of about 140 μm depletion-layer width, illuminated with pulses from a phase-locked He-Ne laser (pulse width ~ 0.3 ns). In this device, the field in the drift region was about 1.6 × 10⁴ V/cm, so that $v_h \approx 4 \times 10^6$ cm/s. The horizontal time scale in the photograph is 5 ns/cm, so that the pulse widths are approximately 3 ns—in general agreement with the calculated response time of 3.5 ns.

Linearity

Avalanche photodiodes are linear with incident light intensity over 6 or 7 decades of signal intensity. At high injection levels, some gain saturation occurs due to the fact that the holes traversing the depletion layer affect the magnitude of the electric field in the multiplying region. The effect is to lower the field, thereby reducing the gain. The magnitude of the effect can be easily calculated: the result can be

expressed in terms of an effective resistance of magnitude

$$R_{eff} = w^2/2e\nu A \quad (13)$$

where ν is the average drift velocity in the "drift" region, and A is the illuminated area. Thus if the multiplied current is I , the effective voltage on the diode, from which the gain is determined, is not the applied voltage V , but $V - R_{eff}I$. In diode 2, for example, $w = 225 \mu\text{m}$, $\nu \approx 3.5 \times 10^6$ cm/s, $A = 0.5 \times 10^{-2}$ cm², so that $R_{eff} = 1.4 \times 10^4$ ohms for a uniformly illuminated diode. The injection level at which saturation effects begin to occur depends on the gain. From Fig. 10 it can be seen that for diode 2 at a gain of 100, a 10% drop in gain would occur when $R_{eff}I \approx 10$ volts. This would require that $I = 700 \mu\text{A}$, corresponding to an injected current of about 7 μA, or to an incident light level of 27 μW at 1.06 μm. At a gain of 1,000, however, a 10% loss in gain occurs when $R_{eff}I \approx 2$ volts. This would occur when $I = 140 \mu\text{A}$, corresponding to an injected current of 0.14 μA, or an incident light level of only 0.54 μW at 1.06 μm. Saturation will occur at lower light levels if the incident energy is not uniformly distributed over the sensitive area.

Fig. 14 shows actual measurements of the departure from linearity at high injection levels for various levels of gain on diode 2. It is seen that the experimental points agree closely with the calculated curves, obtained using Eq. 13.

The saturation effect, combined with the fall-off of gain with heating (discussed below), means that avalanche photodiodes are self-protecting and are not very subject to damage from exposure to very high flux levels.

Temperature effects

Ionization coefficients for electrons and holes decrease with increasing temperature.⁸ Thus, for any fixed voltage of operation, we expect decreasing gain with increasing temperature. The results for one device are shown in Fig. 15, and are seen to be in agreement with the above comments. At room temperature, for this particular device we can calculate a value for $G^{-1}dG/dT$ of approximately $-0.025/^\circ\text{C}$.

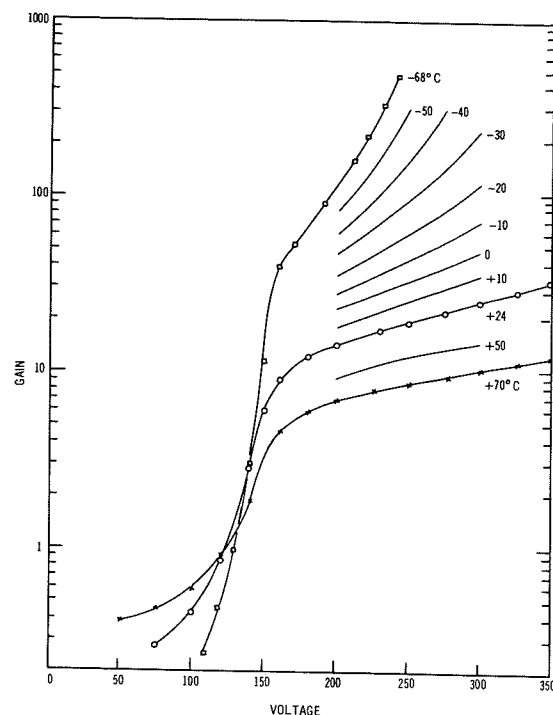


Fig. 15—Temperature dependence of the gain-voltage characteristics measured for one diode.

Summary of avalanche photodiode characteristics

Avalanche photodiodes have been designed and fabricated which have excellent quantum efficiencies in the near-infrared spectrum out to and including 1.06 μm. These devices have low noise, good gain-vs-voltage stability, and sufficient speed for most pulsed laser applications.

Further work on these devices will include a study of long-term stability, the design of suitable packages, and the inclusion of integrated optimized amplifiers.

References

- Emmons, R. B., "Avalanche-Photodiode Frequency Response", *J. Appl. Phys.*, Vol. 38 (1967) pp. 3705-3714.
- McIntyre, R. J., "Multiplication Noise in Uniform Avalanche Junctions", *IEEE Trans. Electron Devices*, ED-13 (1966) pp. 164-168.
- McIntyre, R. J., "Comparison of Photomultipliers and Avalanche Photodiodes for Laser Applications", RCA Limited Research Report 5.004, (May 1968); to be published in *IEEE Trans. Electron Devices*.
- McLean, T. P., *Progress in Semiconductors*, Vol. 5 (Wiley and Sons, 1967).
- McCombs, A. E., Jr., and Milnes, A. G., "Calculation of Drift Velocity in Silicon at High Electric Fields", *Int. J. Electronics*, Vol. 24, (1968) pp. 573-578.
- Ruegg, H. W., "An Optimized Avalanche Photodiode", *IEEE Trans. on Electron Devices*, Vol. ED-14 (1967) pp. 239-251.
- Lee, C. A., et al, "Ionization Rates of Holes and Electrons in Silicon", *Phys. Rev.*, Vol. 134, (1964) p. A761.
- Nuttall, K. I. and Nield, M. W., "Temperature Dependence of the Ionization Rate in Silicon", *Int. J. Electronics*, Vol. 24 (1968) pp. 543-551.

New photomultiplier detectors for lasers

D. E. Persyk

This paper reviews recent innovations in photomultiplier detectors for laser applications. New photocathode materials for both opaque and semitransparent-type photocathodes are discussed. Opaque-type photocathodes which utilize the negative electron affinity of certain III-IV compounds to obtain high quantum efficiencies are described. A newly developed red-sensitive, semi-transparent photocathode is described and contrasted to the traditional S-20 photosurface. Electron-multiplier dynodes utilizing GaP as a secondary emitter are discussed, and data are presented on the small-signal resolution afforded by GaP-dynode electron multipliers. Pulse-height discrimination techniques are described which take advantage of the inherently high electron resolution of GaP electron multipliers. A summary of new photomultiplier detectors for laser applications is included.*

THE TECHNOLOGY OF III-V COMPOUNDS has produced opaque photocathode surfaces that provide response from the ultraviolet to the near-infrared. [Opaque (or reflection-type) photocathodes may be considered as integral elements of the electron-multiplier section; the photocathode area is thus limited by the physical size of the electron-multiplier dynodes.] With appropriate doping and surface cesiation, these materials exhibit high quantum efficiency.^{1,2} The long-wavelength thresholds for photoemission occur at photon energies corresponding to the band gap energies of the materials. Photomultiplier tubes using GaAs photocathodes have provided a quantum efficiency of 5% at a wavelength of 694 nm. Photomultiplier tubes incorporating GaAs-P alloy photocathodes have provided quantum efficiencies of 9% at 633 nm.³ Higher quantum efficiencies are likely to be obtained when processing technology becomes optimized.

The useful detection range for these materials is limited at the short-wavelength scale by the transmission of the window material. The long-wavelength threshold is determined by the band-gap energy of the material, and is of the order of 960 nm for GaAs and 750 nm for GaAs-P alloy. Fig. 1 illustrates the spectral-response characteristics of photomultiplier-tube photocathodes of GaAs and GaAs-P.

Experimental work indicates that InGaAs will provide useful detection

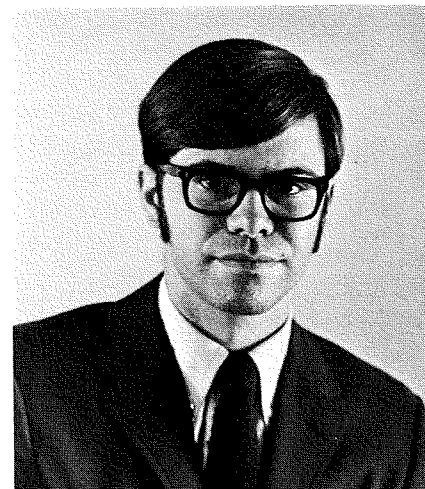
to 1.3 μm .⁴ Photomultiplier tubes for applications at wavelengths out to 1.8 μm may be available in the future.

Semi-transparent photocathodes are deposited on the window of a photomultiplier tube. Such photocathodes can be used in large-area detectors, in contrast to opaque photocathodes which are usually small-area detectors. A red-sensitive semi-transparent photocathode designated the Extended-Red Multi-Alkali (ERMA) photocathode has been developed. Its quantum efficiency is typically 6% at 633 nm, and its useful photo-sensitivity extends to approximately 960 nm. [Quantum efficiencies of 15% at 633 nm. have been measured.] The ERMA photocathode exhibits higher quantum efficiency than either the S-20 or S-25 types, as shown in Fig. 1.

GaP secondary emitter

The signal-to-noise ratio of the electron-multiplier section of a photomultiplier tube is determined primarily by the secondary-emission ratio of the first stage of multiplication. The gain of the first stage should be as large as possible to provide the best signal-to-noise ratio and the best small-signal resolution. Conventional BeO electron-multiplier dynodes usually have a secondary-emission ratio no greater than seven, while GaP dynodes exhibit secondary-emission ratios of thirty or more, as indicated in Fig. 2.^{5,6}

The secondary-emission process gives rise to a distribution in the number of emitted secondary electrons that is approximately Poissonian. Thus, an



electron-multiplier section that uses a BeO first dynode having a secondary-emission ratio of seven cannot resolve a signal consisting of one photoelectron from a signal consisting of two photoelectrons. However, an electron multiplier utilizing a GaP first dynode with a secondary-emission ratio of thirty can distinguish between signals consisting of 1, 2, ..., 5 photoelectrons.

A typical pulse-height spectrum obtained with a multi-channel analyzer is shown in Fig. 3. The pulse-height spectrum was obtained by applying pulses of varying amplitude to a GaP light-emitting diode so that the photocathode liberated one to five photoelectrons, which were in turn focused upon the GaP first dynode and amplified in the electron multiplier to a level that could be easily detected by the multichannel analyzer. The importance of electron resolution is discussed in the following section.

Single-electron resolution and pulse-height discrimination

It has been demonstrated that photomultiplier tubes utilizing a GaP dynode at the first stage of multiplication can differentiate between input signals consisting of 1, 2, ..., 5 photoelectrons.⁷ Such photomultiplier detectors are ideally suited to detection of weak pulsed signals of short duration. By use of pulse-height discrimination techniques, it is possible to detect very weak signals (of the order of a few photons) in the presence of high noise. A brief review of the nature of photocathode dark current will aid in understanding these techniques.

The dark current of a photomultiplier tube is known to consist chiefly of single electrons emitted one at a time at the photocathode. A photomultiplier (such as the C31000 F two-inch-

Reprint RE-15-5-5

Final manuscript received October 14, 1969.

received the MA in Physics in 1964 from the University of Wisconsin. His current projects include design of a fast photomultiplier tube and a study of III-V compound photocathodes. His fields of interest include computer-aided photomultiplier tube design and laser applications for photomultiplier tubes. He is a member of the American Association of Physics Teachers and the American Vacuum Society.

diameter ERMA-photocathode type) with a GaP first dynode may be operated with a multichannel analyzer to demonstrate this phenomenon. Fig. 4 illustrates a typical dark-current pulse-height spectrum. It should be noted that incoherent background illumination has an identical distribution.

In evaluating a photomultiplier tube for the detection of weak pulsed-light signals, the distribution of the dark noise (determined by the electron multiplier) as well as the magnitude of the dark noise (determined by the photocathode) must be considered.

If the pulsed signal of interest gives rise to two or more photoelectrons released simultaneously at the photocathode, pulse-height discrimination circuitry may be employed to eliminate dark-current noise (and single-electron noise due to background illumination). A pulse-height discriminator set of 1.5 photoelectron equivalents in the distribution of Fig. 4 would block nearly all of the dark-current noise, while allowing signals of two or more photoelectron-equivalent pulse-heights to be recorded. This example assumes that the dark-noise single-electron emission rate does not exceed the count-rate capability of the combined detector-and-pulse-height-discriminator system.

New devices

By exploiting the high-gain characteristics of GaP multiplier dynodes, it is possible to design a photomultiplier

tube with only five GaP dynodes that will provide the gain of a conventional ten-or-twelve-dynode photomultiplier tube. Physical size can thus be reduced and time response can be improved by use of fewer stages of multiplication. Several developmental-type photomultiplier detectors have been built incorporating five stages of GaP dynodes. The C31025 series of detectors (C31025, C31025A, . . . , C31025E) are small-size photomultiplier tubes that are suited to spectrographic and photometric applications. Opaque photocathodes of GaAs or GaAs-P have been combined with electron multipliers consisting of five GaP dynodes or nine BeO dynodes. The useful range of detection varies from 150 to 940 nm, depending on photocathode material and window type.

Semi-transparent ERMA photocathodes have been used in photomultiplier tubes utilizing GaP first dynodes (C31000E, C31000F). Such detectors are well suited to detecting weak pulsed-light signals, as well as steady-state light signals. Signals modulated at frequencies up to approximately 200 MHz may also be detected because the anode-pulse rise time is of the order of two or three nanoseconds.

A developmental-type photomultiplier tube (C31024) using a semi-transparent photocathode and five GaP dynodes can be used to detect sub-nano-second signals. The anode-pulse risetime of this tube is less than 1 ns.

Conclusions

New materials for photo- and secondary-emission have been discovered and breakthroughs in photocathode processing technology have been made. Detectors which distinguish between signals of one to five photoelectrons liberated at the photocathode have been built. It has been shown that detection of weak pulsed-light signals can be improved through the use of pulse-height discrimination techniques. More than a dozen new photomultiplier detectors have been designed for various applications in the detection of laser light.

Acknowledgment

The author thanks H. R. Krall for his encouragement and assistance in writing this paper.

Fig. 1—The S-20, S-25, and ERMA are semi-transparent photocathodes; the GaAs-P and GaAs photocathodes are opaque. The GaAs curve represents initial efforts; higher sensitivity is expected as processing techniques optimized.

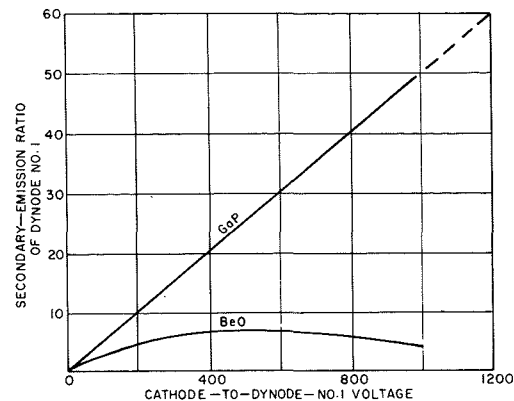
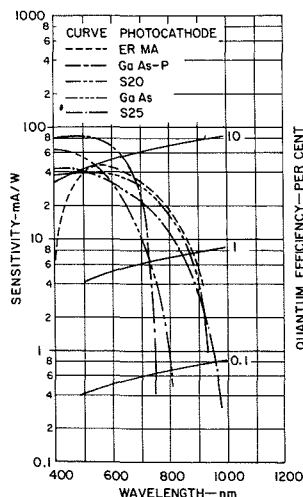


Fig. 2—Secondary-emission ratio as a function of primary-electron energy for GaP and conventional BeO electron-multiplier dynodes.

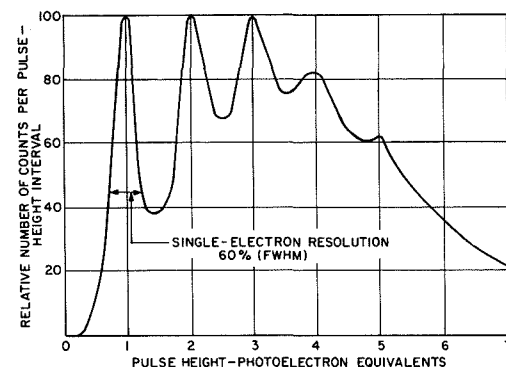


Fig. 3—Pulse-height spectrum illustrating the resolution of weak light signals that liberate 1 to 5 photoelectrons at the photocathode.

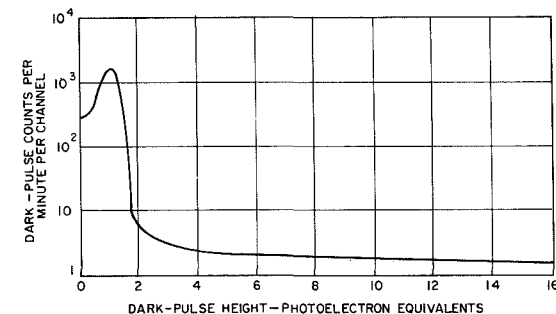


Fig. 4—Dark-current pulse-height spectrum of a C31000F photomultiplier tube. Note that the dark noise is contained primarily in the well resolved single-electron peak.

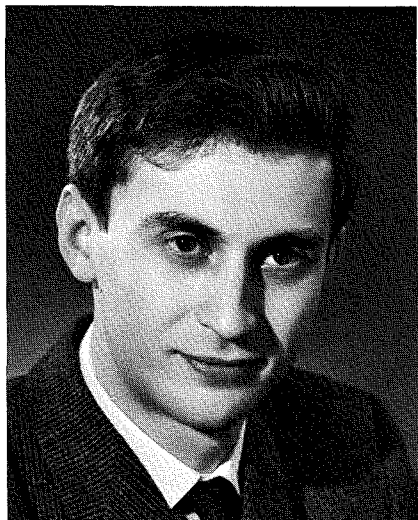
References

- Sommer, A. H. *Photoemissive Materials* (John Wiley & Sons, Inc., New York, 1968).
- Van Laar, J. and Scheer, J. J., "Photoemission of Semiconductors," *Philips Technical Review*, Vol. 29 (1968).
- Simon, R. E., Sommer, A. H., and Williams, B. F., "GaAs_{1-x}P_x as a New High-Quantum-Yield Photoemissive Material for the Visible Spectrum" *Appl. Phys. Ltrs.*, Vol. 15 (Jul. 15, 1969) p. 43.
- Williams, B. F., "InGaAs-CsO, A Low Work Function (less than 1.0 eV) Photoemitter" *Appl. Phys. Ltrs.*, Vol. 15 (May 1969).
- McIntyre, R. J., Sprigings, H. C., and Webb, P. P., "Solid-State Detectors for Laser Applications" *this issue*, Reprint RE-15-5-3.
- Simon, R. E., Sommer, A. H., Tietjen, J. J., and Williams, B. F., "New High-Gain Dynode for Photomultipliers" *Appl. Phys. Ltrs.* Vol. 13, No. 10 (Nov. 15, 1968).
- Morton, G. A., Smith, H. M., and Krall, H. R., "Pulse-Height Resolution of High-Gain First Dynode Photomultipliers" *Appl. Phys. Ltrs.* Vol. 16 (1969) p. 92.

Lasers in communications

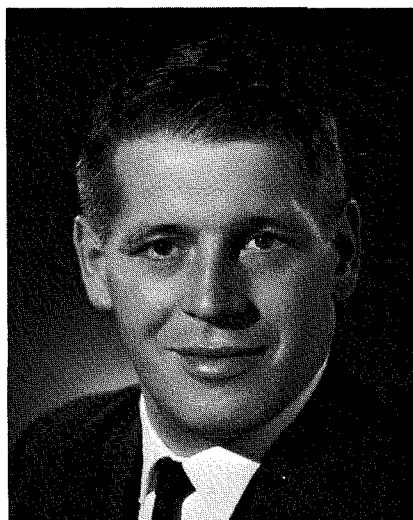
Dr. R. M. Green | A. L. Waksberg

Among the many applications for lasers, one of the most exciting, both technically and economically, is in the field of communications. Dr. A. I. Carswell summarized those laser properties of particular significance to communications applications in an article just two years ago.¹ This article describes the developments that have occurred in the interim; progress has been rapid, and will continue to be so if one can use the current level of effort as any yardstick. A substantial fraction of this effort is in defense applications, encompassing both communications and radar, and it should be realized that information on these programs is restricted. One attraction of such a system lies in the security it provides; it is extremely difficult to intercept or otherwise tamper with the system.



Armand Waksberg
Optics and Microwave Laboratory
Research Laboratories
RCA Limited
Montreal, Canada

graduated in 1956 from McGill University where he received the BSc in Honours Mathematics and Physics and the MSc in Physics (1960). For his thesis he designed, built, and operated an S-band parametric amplifier. He was awarded a "University Scholarship" in 1952 and 1953. He joined Canadair in 1956 where he worked on aerodynamic and dynamic problems of aircraft, and later in the system group of the special weapon system, he prepared test vehicle requirements for the Sparrow II missile flight evaluation program. After receiving the MSc, he joined Canadian Aviation Electronics (R&D Department) where he worked on an L-band parametric amplifier, an S-band beacon, and an optical scanner; he also made feasibility studies on ferrite magnetometers, lasers for ASW, special magnetic compensators, and a magnetometer detection system. Mr. Waksberg joined the Research Laboratories of RCA Limited in 1963. Since that time, he has played a major role in laser research programs. He has made theoretical studies of the He-Ne laser system, noise in lasers, detection of weak laser signals, and the feasibility of laser pumping with mono-energetic electrons. Experimental studies have included work on off-axis laser modes, measurement of high speed detectors, and side-light properties of lasers. This last work led to the development of the stimulated transition spectroscopy (STS) technique. More recently, he has developed techniques to stabilize CO₂ lasers and is currently working on communication experiments both with pulse-code modulation and FM systems. He is a member of the IEEE and the Canadian Association of Physicists.



Dr. Roy M. Green, Director
Research Program Development
Research Laboratories
RCA Limited
Montreal, Canada

received the BSc in Physics from Liverpool University in 1956. He then joined Canadian Westinghouse for one year before continuing his studies at the University of Toronto. He received the MA in 1958 and the PhD in 1961. Dr. Green worked with the nuclear physics research group at Toronto and was engaged principally in the measurement of radioactive sources with low specific activity, with particular application to assessment of fallout levels in the body and foodstuffs, and development of tracer techniques. After obtaining his Doctorate, Dr. Green went to Australia to set up a gamma-ray spectrometry group in the Health Physics section of the Australian Atomic Energy Commission. He returned to Canada in April 1964 to join the Research Laboratories of RCA Limited, becoming engaged in the development of semiconductor detectors and their application to problems in the nuclear and biophysics field. He was appointed senior member and head of the semiconductor group in 1965. In 1968 he became Director of Research Program Development and also Acting Director of the Optics and Microwave Laboratory, in which capacity he directs the work in infrared and optical phenomena, lasers and electro-optical systems. Dr. Green is an associate member of the Institute of Physics and the Australian Institute of Physics, a member of the Canadian Association of Physicists and a senior member of the IEEE. He has served on several committees of the IEEE Nuclear Science Group. Dr. Green has published 16 papers in the fields of health physics, gamma-ray spectrometry and semi-conductor radiation detectors.

THE ENORMOUS POTENTIAL of the laser for communications arises from the very large bandwidth available; lasers have basic frequencies in the region of 10^{14} Hz (compared with 10^7 Hz for short-wave radio). If full utilization of this bandwidth was realized, a single laser beam could carry a million TV channels, for example. Current technology falls well short of this zenith, but remarkable strides have been made since the discovery of the laser in 1960. Laser communications systems are now being used in some specific cases, and considerable R&D is being performed by many groups which undoubtedly will lead to improvements and innovations and result in a diversity of systems in the coming years.

Lasers and laser properties

While laser action is evidenced by a large number of materials, a few of these have significant advantages, and emphasis has been placed on this relatively small number of laser materials. These are listed in Table I, together with their characteristic properties. The power levels quoted in the Table do not represent the upper limit, since continual progress is being achieved in the technologies associated with lasers.

Each type of laser has individual properties which lend themselves to particular applications. For example, the GaAs injection laser is extremely small; the diode itself is about 0.005 inch on a side, and a 20 element array is only match-box size, including the mounting blocks. This permits very compact, light, rugged systems to be fabricated. On the other hand, the CO₂ gas laser is relatively bulky, but enormous power densities can be achieved. The CO₂ and Neodymium lasers are of greatest interest for communications, in part because of the high power capability, but also because the optical wavelength of their respective radiations occurs in atmospheric window regions, where absorption effects are reduced. The erbium lasers have been receiving attention recently primarily because the radiation they emit does not penetrate to the retina, which substantially reduces the risk of eye damage. The carbon monoxide laser shown in the table has just been reported at

Reprint RE-15-5-2
Final manuscript received June 11, 1969.

Table I—Characteristics of lasers.

Gas	Emission wavelength	Efficiency	Typical power levels	Operating cycle
He-Ne	0.6328 μ	~0.01%	to 100 mW	continuous
Argon	0.4880 μ	~0.1%	to 25 W	continuous
CO ₂ -N ₂ -He	10.6 μ	~20%	to 8 kW	continuous
CO	5 μ	~20% (estimated)	~75 W	continuous
Solid state				
Ruby	0.6943 μ	>1.0%	to 10 ¹⁰ W	pulsed
Neodymium	1.06 μ	>1.0%	to 10 ¹⁰ W	pulsed
Erbium	~1.6 μ	>1.0%	100 W	continuous
			to 10 W	continuous
Semiconductor				
GaAs	0.9 μ	~10%	to ~800 W (array)	pulsed

the Conference on "Laser Engineering and Applications" in Washington. One can anticipate intensive studies of this laser and it may well prove to be the most promising for communications applications.

In addition to the bandwidth capability discussed above, the other laser properties of importance to communications are the coherence and the collimation of the beams. Thus, one is able to transmit over large distances, recover a major fraction of the energy with a small "antenna" and using simple optics, focus this received energy to a spot size of a few wavelengths.

What are the problems? One is the single frequency operation, since it means that the output frequency cannot be tuned, as is possible with radio waves. Recent work³ provides hope that this problem may eventually be overcome. The other major disadvantage lies in the absorption and scattering effects of the atmosphere in the wavelength region in which lasers operate. This is a serious problem, particularly when allowance must be made for dense fog or snowstorms. Recent studies⁴ indicate a loss in signal of 1.9 dB/km for fog, using a carbon dioxide laser. Several of the studies in progress today are obtaining quantitative results for these effects and are refining techniques to determine just what ranges can be achieved. Others circumvent this problem by transmitting through light pipes⁵; this provides the level of performance required in commercial applications, and the cost may eventually be justified by the bandwidth capability.

Modulation techniques

Utilization of the extremely high carrier frequency of the laser is currently limited by modulation and de-

modulation techniques. [Performance of laser systems is determined just as much by the receiver characteristics as by the laser transmitter. Hence considerable effort is being devoted to detection also. A companion article in this issue "Solid-state detectors for laser applications" discusses work being performed on laser detectors at RCA Limited.] Improvement in system performance is therefore determined primarily by improvements in the modulator. It is worth noting that all normal RF communications methods have been demonstrated with laser systems: AM, FM, PCM superheterodyne, single sideband, time and frequency multiplexing, etc.

Amplitude modulation

While a variety of methods has been used to amplitude modulate laser beams, the most promising makes use of the electro-optic effect exhibited by some crystals. A polarized laser beam is projected through the electro-optic crystal; the plane of polarization is rotated by the crystal, the angle of rotation being determined by the voltage applied across the crystal. By using another polarizer (the analyzer) after the crystal, the amplitude transmitted through the analyzer can be varied by varying the crystal voltage.

Different crystals are used for different wavelengths. In the visible region, KDP crystals (potassium dihydrogen phosphate) and more recently lithium niobate and tantalate crystals are most common; for the 10.6 μ wavelength from CO₂ lasers, gallium arsenide crystals are used. It is relatively easy to amplitude modulate a laser to transmit a TV picture. By inserting a crystal in a microwave cavity, Kaminow⁶ has achieved modulation at frequencies up to 10 GHz.

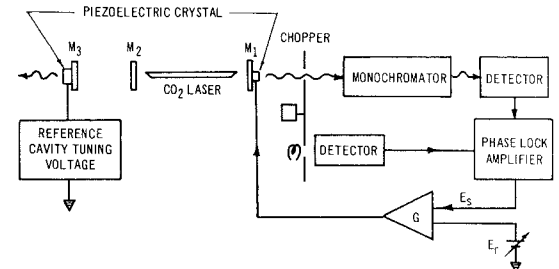
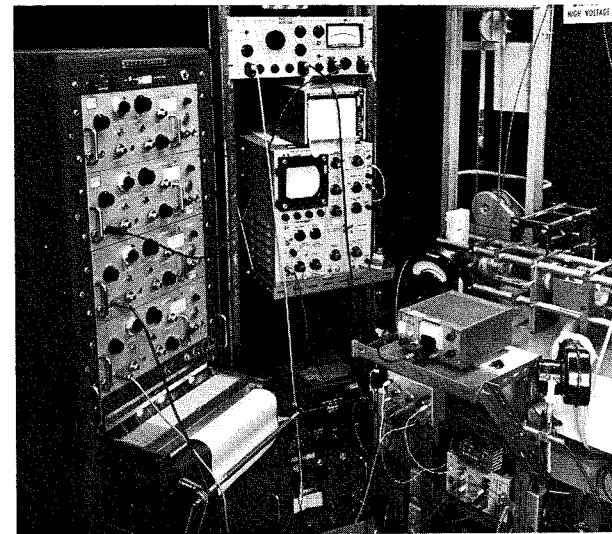


Fig. 1—a) Experimental set-up and b) block diagram of system used for frequency stabilization of a carbon-dioxide laser to within 30 kHz (better than one part in 10⁹). Mirrors M₂ and M₃ constitute the reference cavity used to stabilize the laser cavity (M₁—M₂).

Recent work⁷ with gas cells as amplitude modulators looks most promising. The technique utilizes the Stark Effect. A gas is selected which has a resonance absorption line very close in frequency to that of the laser line. By applying an electric field the absorption line can be moved in frequency to coincide with the laser line. This method has a number of advantages; low power, relative independence on thermal effects, no critical alignment problems and no mechanical resonances. Large bandwidths are also anticipated. Results at this date are preliminary, but evaluation of the technique is proceeding rapidly.

Frequency modulation

If the electro-optic modulator crystal is placed inside the laser cavity, changes in its optical length induced by the applied voltage effectively change the length of the laser cavity, and hence change the output frequency. This then permits frequency modulation of the laser beam.⁸ Just as in other FM

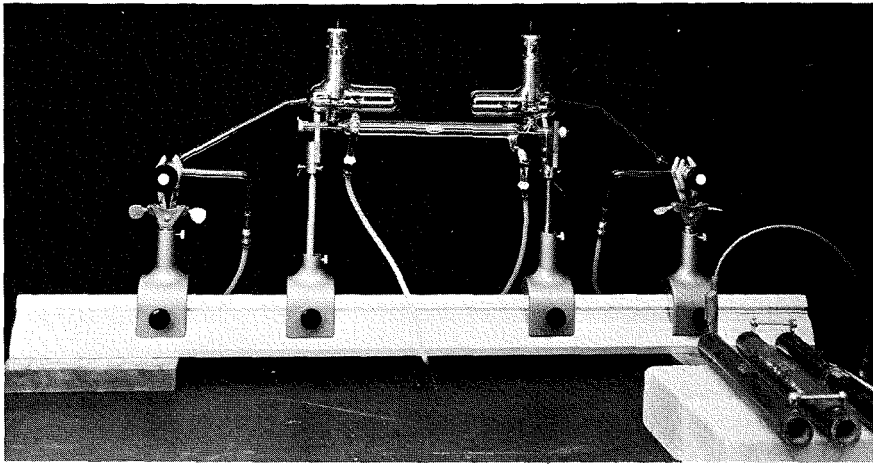


Fig. 2—A small sealed carbon-dioxide laser developed for communications applications. This laser is approximately 35 cm in length and has a maximum power output of 2 watts. It is shown mounted in a test jig undergoing lifetest.

systems, the receiver uses a local oscillator, which is another laser, and a mixer. The IF frequency will depend on how much the laser can be "tuned", which relates to the doppler width of the laser output. For a CO_2 laser the IF frequency cannot exceed 50 MHz. A $He-Ne$ laser, on the other hand, can use IF frequencies up to about 1500 MHz.

Pulse-code modulation

The advantages of pulse digital communications systems are being vigorously espoused by many groups. The requirement merely to determine the presence or absence of a pulse means that much lower signal-to-noise ratios can be tolerated, and regeneration stations can easily be introduced in the transmission links to recover the original pulse waveform. In addition, the system lends itself readily to time-

division multiplexing, and it is compatible with computer language. Error control coding can be used to correct random errors produced by noise. (It is also extremely easy to code such a transmission for secure communication.)

A recent breakthrough in mode of operation of lasers has opened the door to utilizing more of the bandwidth capability of the laser by employing PCM. The breakthrough was the discovery of the "phase-locked mode" of operation.⁹ In this mode of operation, the Q of the laser cavity is perturbed at a frequency equal to $c/2L$. This is the frequency of separation between longitudinal modes of the optical cavity. Here c is the velocity of light and L is the distance of separation between the mirrors. For a laser 1 meter long, this frequency is approximately 150 MHz. When the

laser operates in the phase-locked mode, the output of the laser consists of a regular sequence of optical pulses separated by a time $T=2L/c$, with a pulse width between half-power points of about $1/f$, where f , is the line width of the laser transition. For the $Ne-He$ laser, this width is about 0.7 ns. Pulse rates of 224 megabits/sec have been achieved in operating systems. Besides having regular intervals, these pulses have a peak intensity which is considerably higher than the power under cw operation.

A recent paper¹⁰ drew comparisons between AM, FM, and PCM as applied to transmission of real-time TV pictures using a laser system. The conclusion reached was that analog-FM subcarrier modulation is the best practical choice for TV pictures.

Recent studies

A variety of laser communication systems are being studied in many countries; only a few examples can be mentioned here. A FM link using a CO_2 laser over a 30-km path length is being studied in California.⁴ They use an IF of 30 MHz, and an operational bandwidth of 8 MHz. A modulation index of 0.3 is used for a peak-to-peak deviation of 3 MHz. The results are very promising, with good signals even in poor weather conditions. A group at Bell Laboratories has published results on a PCM system, using a $He-Ne$ laser.¹¹ They had a pulse rate of 224 MHz with pulse widths of 0.9 ns. The peak amplitude was about 6 mw. They were able to transmit information quite successfully at these rates in laboratory tests.

Transportable systems have been assembled and proven in field tests, using ruby and neodymium YAG crystals and $GaAs$ laser diodes. Information on ruby and neodymium laser systems is primarily for range-finding applications, where ranges of the order of 12 miles can be measured with accuracies of a few yards. Gallium-arsenide laser communications systems have been developed with ranges exceeding 5 miles.

At the RCA Laboratories in Montreal, studies related to the use of lasers in communications have been in progress for several years with the support of the Defense Research Board.^{12,13} Emphasis has been on cw gas lasers. A

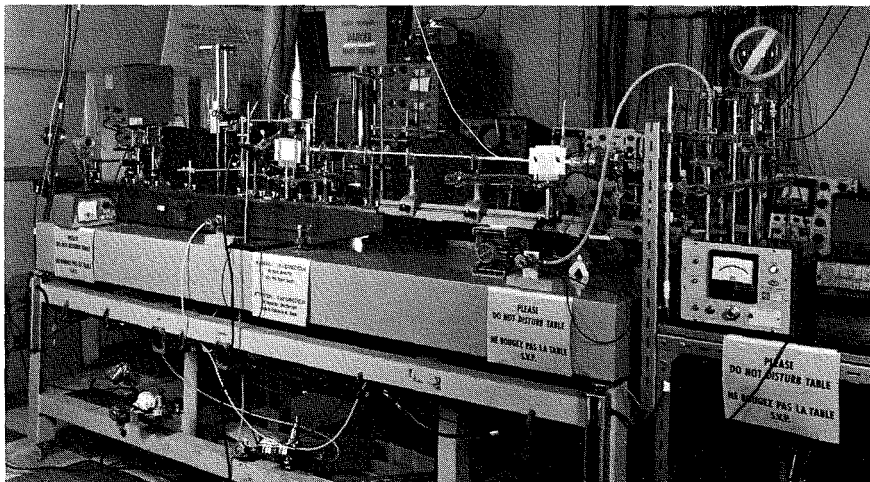


Fig. 3—The PCM laser communications system at the RCA Laboratories in Montreal. The helium-neon laser can be seen in the foreground mounted on the optical bench. The laser and associated optics are mounted on a stable platform weighing 4,000 lbs. The electronics gear shown is used in the propagation experiments for signal monitoring.

most important parameter insofar as communications applications are concerned is that of transmitter noise. Detailed measurements have been made of the noise emanating from a *He-Ne* laser and how it is affected by changes in pressure, temperature, and geometrical configuration.¹⁴ The results are quite startling, showing order of magnitude changes in the noise level for small variations in parameters. Noise studies of the CO_2 laser are in progress, these are described in more detail in Ref. 15 and in the article "Measurement of Laser Communications Parameters" in this issue. For a FM system, frequency stability is extremely important. Techniques have been developed in these Laboratories to frequency stabilize the CO_2 laser to about 1 part of 10^9 (see Fig. 1).¹⁶

Use of the CO_2 laser in practical systems is inhibited by the fact that the lifetimes and reliability of sealed laser tubes (as opposed to flowing gas systems which require reservoir tanks of gas and hence are most cumbersome) have been poor. Many laboratories including RCA are expending considerable efforts to improve this situation. However, in general the work is aimed at high powers, whereas at RCA smaller lasers are being studied for compact systems. One sealed laser (shown in Fig. 2) is only 15 cm long, producing over 1 watt of cw power.¹⁷ A 10-cm-long tube gave 650 mW.

An experimental laser link (Figs. 3, 4, and 5) is also operating in Montreal. This is a PCM link using a phase-locked *He-Ne* laser producing pulses less than 1-ns wide at a rate of 80 megabits/sec. The beam is transmitted approximately 1/4 mile to a retroreflector and back to the receiver, giving a total path length of a 1/2 mile. In the time during which this link has been operating studies of phase jitter and absorption effects due to atmospheric conditions have been performed, with most encouraging results. The facility has now been completed with A-to-D and D-to-A converters and electro-optic modulator to enable the performance as a communications link to be determined.

Future prospects

It is always difficult to predict what the future holds for an application such as this, where there is intensive activity, and a new breakthrough or

even continuing rapid development can alter the picture drastically. However, it is clear even now that the application of lasers to communications systems will increase substantially in the next few years. In addition to military applications, NASA has been promoting studies in this field for many years. NASA intends to fly a laser communications experiment in an Advanced Technology Satellite to be launched in 1972. This will be a FM system using a CO_2 laser, with a 5-MHz bandwidth; they are already considering a second generation experiment with a 100-MHz bandwidth.

But looking further than these somewhat exotic applications, there appears to be considerable scope for the use of lasers in more mundane areas. For example, remote terminals could be linked to a master computer by a rooftop laser link using simple optics, and the excellent collimation would permit many such links without interference problems. It might also prove a very useful system to link mobile units with a main TV station, such as is required at sports telecasts, etc. Many similar possibilities will spring to mind.

In summary then, the potential is obvious and immense, the practicality is rapidly being ascertained and improved, and the future appears most promising.

References

1. Carswell, A. I., "Applications for Lasers in Communications—Canadian Research Demonstrates Vast Potential", *Electronics and Communications* (July 1967).
2. Eppers, W. C. Osgood, R. M., and Greason, P. R., "A 75 Watt CW Carbon Monoxide Laser", IEEE Conference on Laser Engineering and Applications, Washington, (May 1969).
3. Dowley, M. W., "Efficient CW Second Harmonic Generation to 2573A", *Appl. Phys. Letters*, Vol. 13, No. 11 (Dec 1968) p. 395.
4. Goodwin, F. E., and Nussmeier, T. A., "Optical Heterodyne Communications Experiments at $10.6 \mu m$ ", *IEEE J Quantum Electronics* QE4, 612 (1968).
5. Miller, S. E., "Communications by Laser" *Scientific American*, Vol. 214, 18 (1966).
6. Kaminow, I. P., "Microwave Modulation of the Electro-optic Effect in $KH_2 PO_4$ ", *Phys. Rev. Letters* 6, (May 1961).
7. Pao, Y., Case Western Reserve Institute, *private communications*.
8. Harris, S. E., and Tary, R., "FM Oscillation of the He-Ne Laser", *Appl. Phys. Letters*, Vol. 5, 202 (1966).
9. DiDomenico, M., "Small Signal Analysis of Internal Modulation of Lasers", *J. Appl. Phys.*, Vol. 35, 2870 (1964).
10. Hannan, W. J., and Bordogna, J., "Comparison of Electro-Optic Modulation Methods", *IEEE Trans. Aerospace and Electronics Systems* AES-4, No. 6, 874 (1968).
11. Derton, R. T., and Kinsel, T. S., "Terminals for a High-speed Optical Pulse Code Modula-

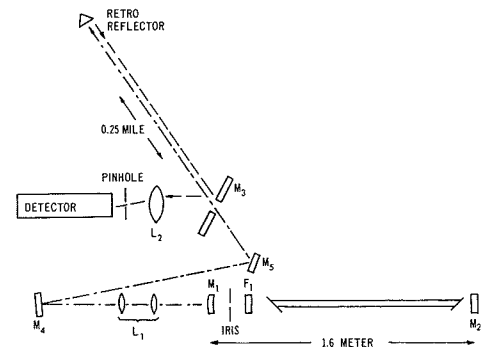


Fig. 4—Block diagram of the PCM system. Mirrors M_1 and M_2 form the hemispherical cavity, with F_1 a filter to eliminate the unwanted 3.9μ radiation. The iris is utilized to induce self mode locking and to vary the power level for the propagation experiments. L_1 consists of two high quality lenses that form the collimating telescope, the beam being steered by M_4 and M_5 through a hole in the center of M_3 to the retro reflector. Collection optics are formed by M_3 , L_2 and a pinhole.

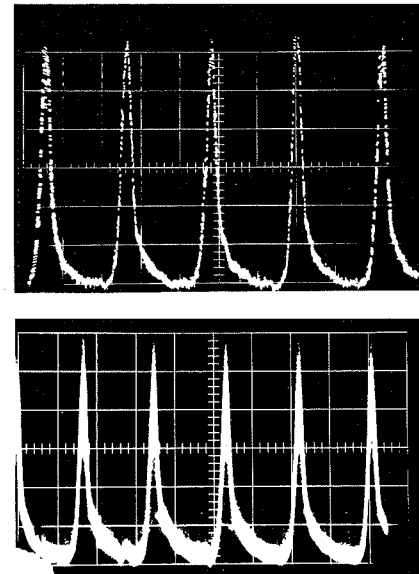


Fig. 5—Pulses obtained from the phase locked laser: (top) before propagation, (bottom) after propagation. The pulse width at half intensity points is 1.4 ns. While the amplitude varies appreciably after transmission over the 1/2 mile path, there is no detectable pulse broadening.

- tion Communication System", *Proc. IEEE* Vol. 56, No. 2, 140 (Feb 1968).
12. Buizert, H., Moody, H. J., Waksberg, A. L., and Crane, R. A., *Laser Communications Considerations*, RCA Limited Research Report 3-950-1 (Oct 1968).
13. Waksberg, A., and Shkarofsky, I. P., *Noise Considerations for the Detection of Weak Laser Signals*, US Research Report AD646744 (Sept 1966).
14. Waksberg, A., and Wood, J. I., "Noise Power Spectrum Characteristics for a He-Ne Laser Operating Under Various Discharge Conditions", *Rev. of Scientific Instruments*, Vol. 40 1306 (1969).
15. Waksberg, A., *Low Frequency Noise Measurements of a Passively Stabilized CO₂ Laser*, RCA Limited Research Report 3.900.13 (Jun 1968).
16. Waksberg, A., "Stabilization of a CO₂ Laser using a 3 Mirror Laser System", *IEEE J. of Quantum Electronics* QE-4, 532 (Sept 1968).
17. Arams, F. R., "Components to 10.6μ Laser Systems", IEEE Conference on Laser Engineering and Applications, Washington (May 1969).

Measurement of laser communication parameters

A. L. Waksberg | J. C. Boag

The Research Laboratories of RCA Limited in Canada are deeply involved in the research and development of CO₂ laser communication systems in space. Some preliminary parameter measurements are particularly important in defining the communication systems. These include laser-output-profile measurements, AM and FM laser noise, and laser stabilization. These measurements which are undertaken in the labs, are described here briefly.

THE RESEARCH LABORATORIES of RCA Limited are involved at present in studying the many aspects of CO₂ laser communication systems. In particular, the emphasis is given to a FM system which could be used in a two-way laser communication link between synchronous satellites or satellite and ground. The bandwidth requirement is 5 MHz, and the power output of the transmitter should be half a watt. A companion article¹ describes the development of the laser tube at RCA. This article is concerned mainly with the type of measurements we are embarking on in our labs to measure the laser parameters affecting communication. These include laser profile measurements, stabilization, and AM and FM noise measurements.

Laser profile measurements

A true frequency-modulated signal is obtained by changing the center frequency of a carrier in proportion to the amplitude of the signal being sent. If the carrier is emitted by a laser, the frequency can be changed by varying the optical length of the laser cavity. The fundamental relation is

$$\Delta\nu = \nu \Delta L / L$$

where $\Delta\nu$ is the change in frequency required; ν is the carrier frequency; L is the optical length between the two mirrors; and ΔL is the change in the optical length required.

For the laser we are using, L is about 40 cm and ν is 3×10^{13} Hz (the wavelength is 10.6μ). A change in frequency of 1 MHz will require an optical change in length of 0.013μ .

This can be obtained at low frequency by changing the physical length of the cavity by mounting one of the mirrors on a piezoelectric mount. For higher modulation frequency, use is made of the electro-optic effect of some crystals such as *GaAs*. When this material is placed inside the laser cavity and a voltage is applied in the proper direction, the effective optical length of the crystal is changed—thus producing the required frequency shift of the laser. Since the change in length required to produce appreciable shift in frequency is minute, it might be thought that the frequency excursion to be chosen for high FM improvement is limited only by the voltage requirement of the electro-optic crystal. A more serious limitation occurs because of the linewidth limitation of the CO₂ laser. The linewidth is the frequency range over which the laser can be made to oscillate. Typically, for a CO₂ laser it is about 50-MHz wide while for the *He-Ne* laser, the width is 1500 MHz. For the CO₂ laser, if an excursion of more than 15 MHz is produced about the center of the line, more than half the power is lost. A 25-MHz excursion will stop the laser oscillating. [The laser can be made to oscillate on other "lines" but these are many GHz away and are therefore of little use for a given communication channel.] Similarly the choice of an intermediate frequency is determined, in part, by how far from center the LO frequency can be while still producing enough power for the mixing operation. Fig. 1 shows a typical "laser output profile"² and a possible "fitting" of a transmitter and LO frequency within this profile. By laser output profile we mean the laser output as it is varied in frequency around the center of the laser line.



Armand Waksberg
Optics and Microwave Laboratory
Research Laboratories
RCA Limited
Montreal, Canada

graduated in 1956 from McGill University where he received the BSc in Honours Mathematics and Physics and the MSc in Physics (1960). For his thesis he designed, built, and operated an S-band parametric amplifier. He was awarded a "University Scholarship" in 1952 and 1953. He joined Canadair in 1956 where he worked on aerodynamic and dynamic problems of aircraft, and later in the system group of the special weapon system, he prepared test vehicle requirements for the Sparrow II missile flight evaluation program. After receiving the MSc, he joined Canadian Aviation Electronics (R&D Department) where he worked on an L-band parametric amplifier, an S-band beacon, and an optical scanner; he also made feasibility studies on ferrite magnetometers, lasers for ASW, special magnetic compensators, and a magnetometer detection system. Mr. Waksberg joined the Research Laboratories of RCA Limited in 1963. Since that time, he has played a major role in laser research programs. He has made theoretical studies of the *He-Ne* laser system, noise in lasers, detection of weak laser signals, and the feasibility of laser pumping with mono-energetic electrons. Experimental studies have included work on off-axis laser modes, measurement of high speed detectors, and side-light properties of lasers. This last work led to the development of the stimulated transition spectroscopy (STS) technique. More recently, he has developed techniques to stabilize CO₂ lasers and is currently working on communication experiments both with pulse-code modulation and FM systems. He is a member of the IEEE and the Canadian Association of Physicists.

It is evident that the laser output profile is of extreme importance in selecting the communication parameters. Since some methods of stabilization of the frequency are also dependent on the exact shape of the profile,^{2,3} measurements of these shapes must be performed before design of the system is possible.

Other workers have measured laser output profiles.⁴ However, the measurements were done for one set of

Reprint RE-15-5-4
Final manuscript received November 14, 1969.



John C. Boag
Research Laboratories
RCA Limited
Montreal, Canada

Joined the Atomic Energy Establishment, Harwell, in 1949 as a Scientific Assistant, later being promoted to Experimental Officer, and started studies at the Oxford School of Technology for a degree in Physics. During this time he gained experience in the design of Mass Spectrometers and associated instrumentation, later branching to the development of different types of automatic nuclear instrumentation systems. He obtained the London Intermediate B.Sc., in 1954. He emigrated to Canada in September 1959 and joined the Research Laboratories of RCA Limited, where he was engaged on the examination of the characteristics and operating mechanisms of thyristor transistor devices, the design of transistor circuitry, and measurements of transistor storage times. On leave of absence from the Company between 1965 and 1968, he attended Queen's University, and received the B.A. specializing in Physics and Mathematics. He has now rejoined the Research Laboratories and is engaged on the development of Spectral Photometers for space use.

discharge conditions. To optimize the width of the profile, we have embarked on a series of measurements to determine the width as a function of discharge parameters such as current and pressure. Fig. 2 shows the experimental apparatus used to measure the laser output profile. A sawtooth driver forces a piezo crystal mount to change the distance between the two laser mirrors. The resulting output is then passed through a monochromator to select the laser line required, and is monitored by an IR detector. This could be a thermopile when slow changes are required, or a *Cu:Ge* detector for fast response times. The output of the detector is then used to drive the Y-coordinate of a scope or that of an X-Y recorder, while the piezo driver actuates the x axis. Fig. 3

shows a typical set of curves for a CO_2 -gas-mixture pressure of 20 torr and currents ranging from 5 mA to 12.5 mA. It is seen then that the laser profile varies widely with discharge conditions. The result of this investigation will therefore help in optimizing the system.

Stabilization

Many methods are in use for stabilizing lasers.³ These consist usually of deriving a discriminating curve out of the laser output profile to detect a change in frequency of the laser and of using a feedback mechanism to readjust the absolute distance between the mirrors to reestablish the required frequency. Under certain conditions, more complicated methods using effects such as the Zeeman splitting or absorption cells can be employed. For a space laser, simplicity is of paramount importance. We are therefore analyzing, for our system, a stabilizing scheme for the transmitter which uses a temperature-compensated, stable, Fabry-Perot cavity as a reference. This cavity should be stable to the required accuracy (about ± 1 MHz) for the full length of an experiment.

Acquisition of one satellite by another brings out some special problem particular to this mode of operation. This arises because a certain amount of uncertainty exists as to the exact location of each satellite. For acquisition then, the transmitter beam has to be expanded to illuminate the whole region of uncertainty of the other satellite. As a result, the power received may be reduced by as much as 40 dB. This problem is compounded by the fact that the sensitivity of the superheterodyne system is lower during acquisition because a certain amount of uncertainty exists in absolute frequencies between transmitter and LO. The bandwidth of the receiver must therefore be widened to accommodate this uncertainty with a resulting loss in sensitivity. This problem was studied at our labs and a solution proposed.⁵ As part of the solution, the LO has to be stabilized to only a moderate degree of accuracy (of around ± 1 MHz). This can be accomplished by using the slope of the laser profile as a discriminating curve.² Once the receiver "acquires" the transmitter, the LO fre-

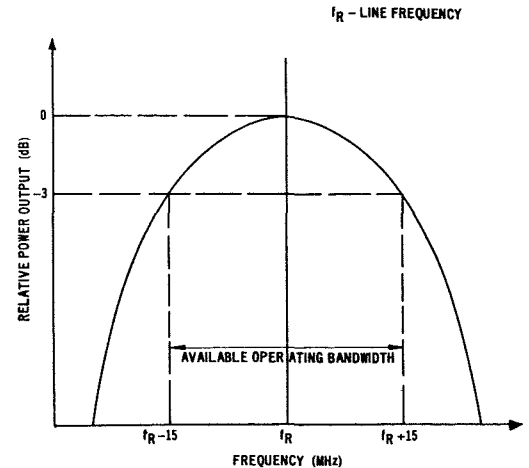


Fig. 1—Laser output profile.

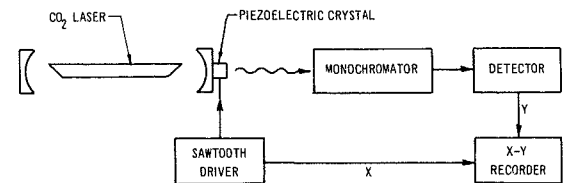


Fig. 2—Apparatus used to measure the output profile of a CO_2 laser.

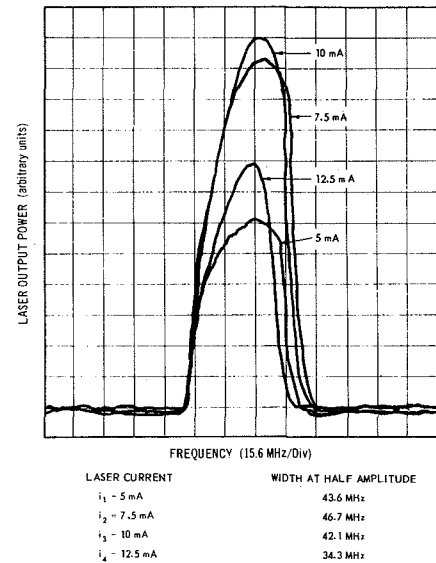


Fig. 3—Typical CO_2 laser profiles as a function of laser current at 20 torr pressure.

quency will be slaved to the transmitter via a conventional AFC loop.

Noise measurement

Although lasers are usually described as "noiseless" generators, they are nevertheless a source of noise by themselves. The amount of noise can vary widely from laser to laser, as it depends on many parameters such as pressure, current of the discharge, type of electrode used, geometry, etc. It is obvious that a noisy source will limit

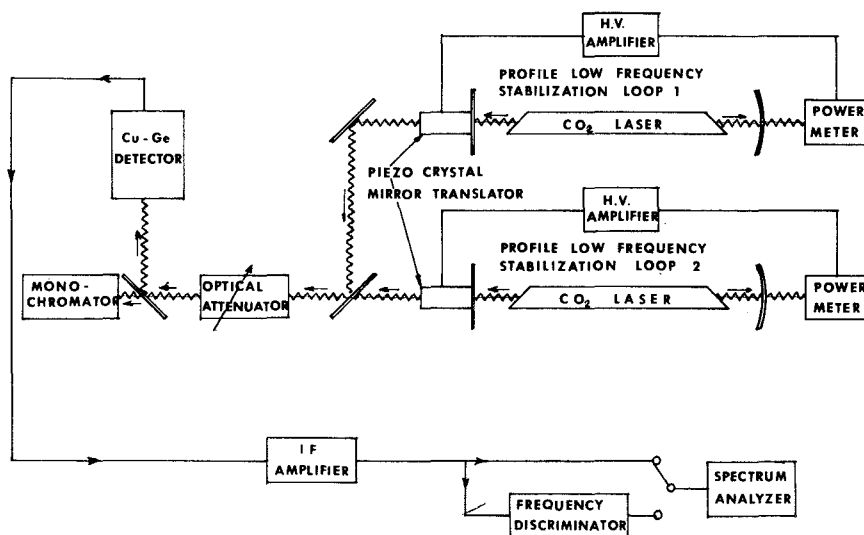
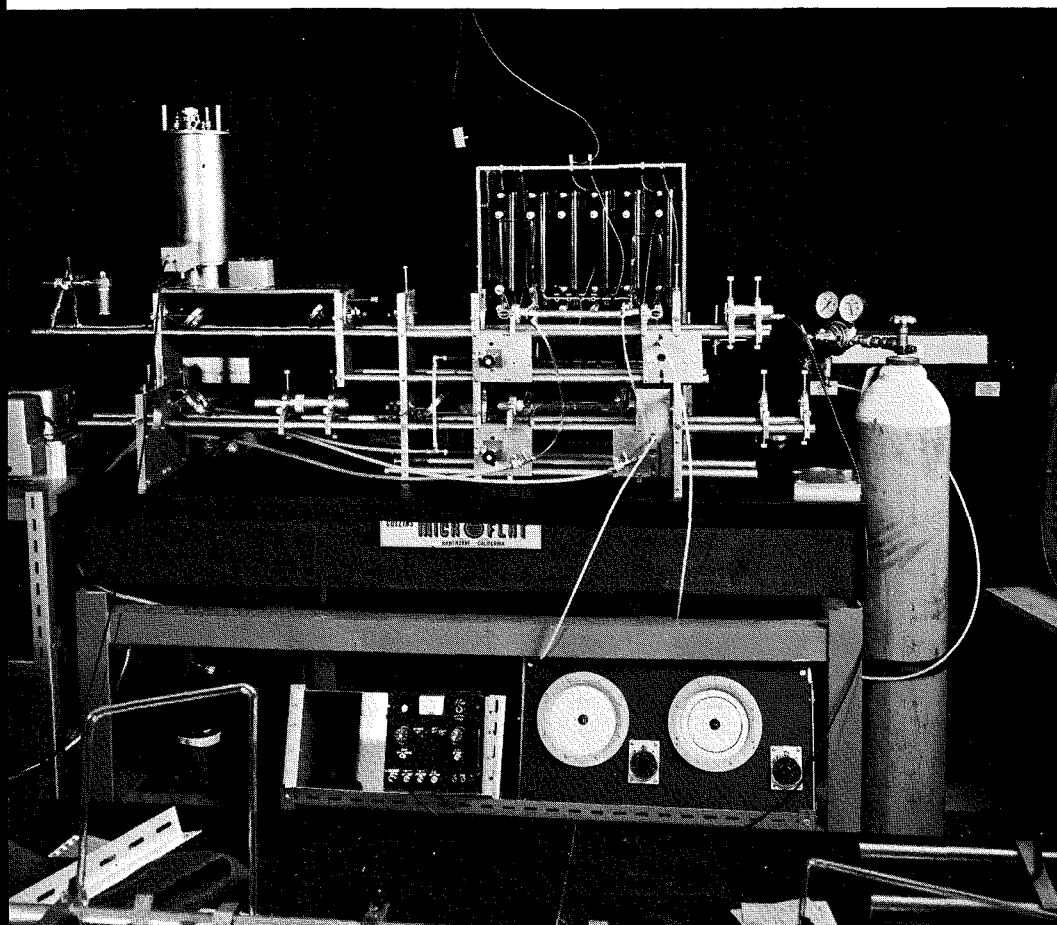


Fig. 4—Apparatus used for FM-noise measurements. In the photograph (top) note the two lasers in the center of the setup. The Dewar is the cylindrical shape on the left.

the s/N of a message. Similarly, a noisy LO will degrade the sensitivity of a receiver. It is therefore very important to determine the exact noise content of the various lasers to be used in a communication experiment to evaluate the potential performance of the system. Also, finding the cause of noise will in many cases allow the applica-

tion of corrective measures that will reduce, if not eliminate, this troublesome noise.

RCA Limited has been involved with laser noise measurements since 1966.^{6,7,8} We are now directing our attention to the noise in the frequency band of interest in the laser communi-

cation system. This includes both AM noise measurement (which can be troublesome even in a FM system if it is too large) and (of greater importance) FM noise inside the 5-MHz bandwidth of interest. The noise measurement setup is shown in Fig. 4. Two laser beams are mixed in by a $Cu:Ge$ detector which is in a Dewar. The resulting IF is analyzed through a discriminator, and then both AM and FM noise can be measured. Each of these lasers is stabilized on the laser profile curve.² By beating their output frequencies together, absolute frequency stability measurements can also be obtained.

Conclusion

Although the principle of laser communication is now well established, the implementation of a system required a large number of parameter measurements. The program under way in our laboratories will determine many of the required parameters and assist substantially in designing and fabricating practical laser communications systems.

Acknowledgment

The project was supported in part by the Defense Research Board of Canada's Industrial Research Program, Grant No. 5501-55. The author writes to thank Dr. R. Green for his helpful comments.

References

1. Crane, R. and Wood, J., "Sealed CO_2 Laser Development", *this issue*.
2. Waksberg, A., "Stabilization of a CO_2 Laser using a 3-Mirror Laser System", *IEEE J. Quantum Electronics*, Vol. QE-4, No. 532 (1968).
3. White, A., "Gas-Laser Frequency Stabilization", *Microwave* (1967) p. 51.
4. Mocker, H. W., "A 10.6 μ Heterodyne Communication System", *App. Optics*, Vol. 8, No. 677 (1969).
5. Waksberg, A., "A Dual-Scan Acquisition Technique for a Laser Communication System", RCA Research Report No. 3-900-19, Sept. 1969.
6. Waksberg, A. and Shkarofsky, I. P., "Noise Consideration for the Detection of Weak Laser Signals", U.S. Research Report AD646744, Sept. 1966.
7. Waksberg, A., "Low Frequency Noise Measurements of a Passively Stabilized CO_2 Laser", RCA Research Report 3-900-13 (June 1968).
8. Waksberg, A. and Wood, J., "Noise Power Spectrum Characteristics for a He-Ne Laser Operating under Various Discharge Conditions", *Rev. of Scientific Inst.* Oct. 1969.

The laser in education

F. S. Philpott

A laser kit has been developed to assist in teaching communications at the technical school and university levels. The method of operation of the kit is discussed and the features of using visible light for teaching are outlined. The appendix contains a basic description of the laser that is used with the laser kit; it may be of interest to those not familiar with the operation of lasers.

THE CHINESE, in the earliest recorded civilization of man, used light in the form of signal beacons to communicate with distant neighbors.¹ In recent times, it was only with the development of the laser,² in 1960, that sufficiently bright visible sources have been made available to compete with systems which man has developed using lower frequency electromagnetic waves. At the present time, communications users demand more information carrying capacity, so it seems inevitable that communications systems will be forced into the infra-red and visible regions of the spectrum.

While sophisticated systems are now being developed at RCA and elsewhere to realize the full information carrying possibilities of the laser,³ we have developed and are now producing the simple, low cost educational kit shown in Fig. 1. This kit utilizes the oldest feature of light—visibility—in point-to-point communications.

Visible electromagnetic waves are useful in educational demonstrations, and experiments, particularly for students in first-year electrical engineering and technical schools, who have not had the opportunity of becoming familiar with lower frequency electromagnetic radiation. Besides assisting in the visual demonstration of the basic properties of electromagnetic waves, i.e. reflection, refraction, diffraction, and interference, it is possible to examine the individual or cumulative effects of these on communications systems. Progressing further into communications theory, effects due to atmospheric absorption, turbulence, and scattering may be demonstrated or examined experimentally.

Method of modulation

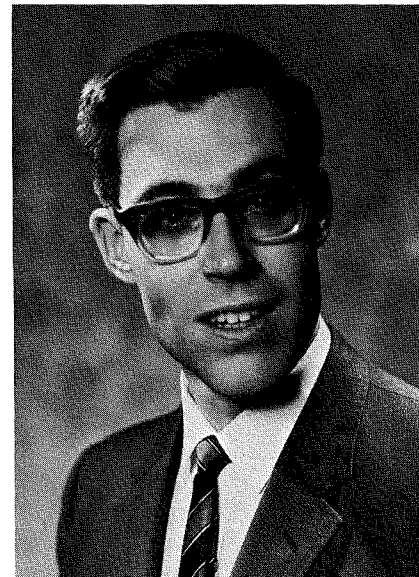
To amplitude modulate the light output from the *HeNe* laser with an audio

frequency signal, it is merely necessary to place a transformer in series with the DC power supply, feed in the amplified signal, and so cause the laser discharge current to vary according to the information signal. The arrangement is shown in Fig. 2.

The laser light output for various currents is shown in Fig. 3. While most lasers would operate in the portion of the curve corresponding to 5 mA in order to get maximum output, for modulation by variation of the discharge current, the quiescent operating point has been selected as 3.3mA. It should be noted that the curve at this point, while relatively straight, is not linear, and it is to be expected that distortion will be introduced. Considering the nature of the equipment and the necessity of minimizing costs, it was not judged necessary to compensate for this non-linearity. The distortion introduced at this point is typically less than 3%.

This intra-cavity method of amplitude modulating the laser is useful in educational equipment because of its simplicity and low cost. In practical systems, however, its information carrying ability is extremely limited when compared with established methods using lower frequency carrier waves. This is because the relevant decay time of the helium gas is of the order of $5\mu\text{s}$, preventing the laser from being modulated at frequencies higher than about 50 kHz.⁴ To make fuller use of the laser's information-carrying capability, it is necessary to use more sophisticated modulation techniques, such as using the laser as a stable oscillator to supply the carrier wave and applying high frequency modulation using one or more electro-optic crystals.⁵

As an alternative for institutions already possessing a suitable low-noise laser, electro-acoustical methods of modulating the laser beam are being developed.



Frank S. Philpott
EC Product Development
RCA Limited
Montreal, Canada

received the B.Eng. in electronics from McGill University in 1961 and the M.Sc. in physics from the University of London in 1968. After developing nuclear instrumentation for two years in Canada, he went to England in 1963. At G. & E. Bradley Ltd., London, he worked on the development of ruby and neodymium lasers as well as the application of lasers to machining and welding, the subject of his thesis. In 1966 he worked on exchange at the National Physical Laboratory, Teddington, developing cyanide lasers, and after returning to Bradley's was promoted to gas laser section leader in 1967 where he was mainly concerned with cyanide, argon, and carbon dioxide lasers. He joined RCA in 1968 and since then has been working on the development of the educational laser communications kit, new methods of modulation, and HeNe tube design.

Use in education

The complete communications kit is shown in Fig. 1. It consists of the laser, a modulator unit, and a receiver

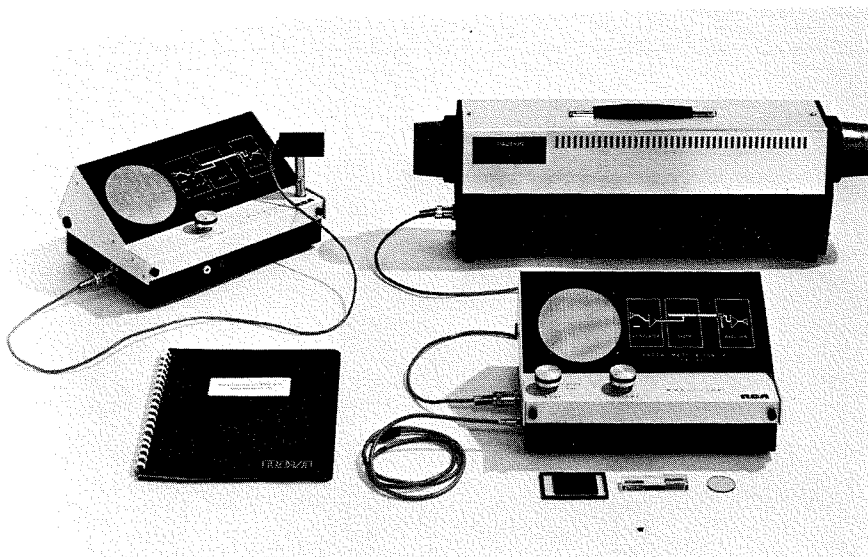


Fig. 1—Complete Laser Communications Kit, LK71.

unit. The modulator is simply a power amplifier supplying the signal at a suitable power level to the modulation transformer of Fig. 2. The detector for the laser light is a silicon photodiode mounted on a standard optical bench pin. The receiver unit consists of an amplifier feeding a loudspeaker output and an oscilloscope monitoring output.

To demonstrate the basic properties of light, a laser is particularly useful because of the nature of the light which it can be designed to emit. The laser used in the communications kit emits a single beam of red light, 2.5mm in diameter, which has been collimated to the diffraction limit so that its angle of divergence is 0.8 milli-

radian or $2\frac{1}{2}$ minutes of arc. To an observer at any one location, the beam appears to be not diverging at all, and for this reason it is suited for use as a single ray in geometric optics to demonstrate the action of various optical elements. Because the light is both bright and monochromatic, it is also possible to demonstrate the diffraction patterns of wave optics to an entire class.

Turning now to basic communications theory, the necessity of modulation for transmitting information may be demonstrated as well as the obvious method of modulating—by simply chopping the beam with a hand to send a coded message. With the basic idea hopefully absorbed by the

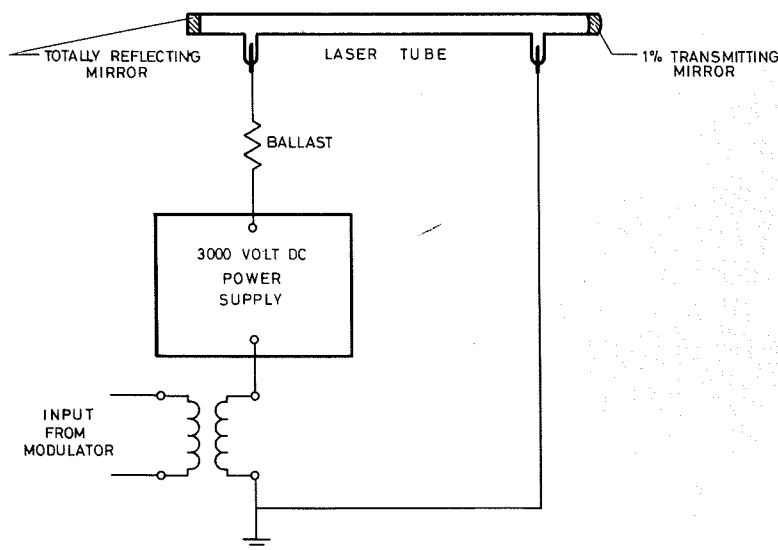


Fig. 2—Circuit for amplitude modulating laser by variation of discharge current.

students, electronic modulation may be demonstrated with the demodulated signal heard at the receiver loudspeaker. The effects on signal transmission of the basic properties of electromagnetic waves, i.e., reflection, refraction, diffraction, and interference, may be demonstrated using the laser modulated with an appropriate signal. These phenomena are of importance in many communication systems. For example, refraction and interference must be carefully considered in the design of high frequency communications systems utilizing sky-wave propagation. Progressing still further into communications theory, laser beams transmitted through ink-in-water and soap-in-water simulate absorption and scattering in the atmosphere.

The radar anti-clutter technique using polarization discrimination to eliminate unwanted back-scattered radiation may also be demonstrated. This is shown by passing the plane polarized laser light through soapy water and observing back-scattered radiation through a Polaroid sheet. As the sheet is rotated, the back-scattered signal can be eliminated.

Significance of antenna patterns may be demonstrated using a neon lamp to simulate an omnidirectional pattern and the laser to simulate a pattern of high directivity. Modulation of the neon source allows measurements to be taken under conditions of normal room lighting.

Finally, in studying optical communications, the effects of air turbulence on a system may be examined experimentally. Typical results of noise measurements are shown in Fig. 4a and 4b.

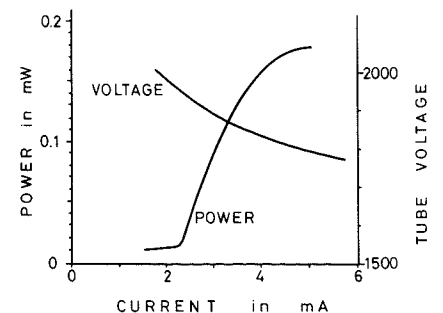


Fig. 3—Variation of tube voltage and laser light output with tube current.

Development objectives

Low-noise laser tube

To create a kit with an acceptable quality of reproduction, it was necessary to develop a new low-noise, low-cost HeNe laser tube. This was a major obstacle in the development program. While HeNe tubes are used in other educational kits, such as the Classroom Optics Demonstration Kit, it was found that the light output from these was already modulated with noise, giving a photodiode signal which was from 5 to 30% noise. Tubes of other manufacturers were similarly noisy and thus entirely unsuitable for use in a communications kit. The noise, however, dropped to a level which is tolerable, less than 1%, at a definite threshold depending both on current and pressure, as shown in Fig. 5. The fact that a noise threshold exists depending on current has been observed by others.⁵ Although reduction of pressure to allow low-noise operation is a simple matter, an excess of gas, or over-pressuring, is necessary to offset gas cleanup and thus enhance tube life. After considerable investigation into the possible causes of the noise, and by process of elimination, discharge turbulence appeared to be responsible.⁶ As considerable experimental work seemed inevitable in quieting the instabilities, the obvious solution of lowering the pressure was adopted. To solve the life problem, an obsolete tube design was rejuvenated

Appendix: a brief introduction to the laser

The laser used in the communications kit may be considered as a discharge tube containing helium and neon gases with highly reflecting mirrors placed at each end of the tube. This is illustrated in Fig. 2. The tube is manufactured with the mirrors aligned parallel to each other and these form the ends of a resonant cavity for the light frequency radiation which is characteristic of the gas mixture used. The mirror spacing is not critical because the tube is able to supply useful gain over sufficient bandwidth for the frequency of oscillation to shift according to any change in mirror spacing. It should be noted that the cavity is nearly one million wavelengths long; therefore only a change in wavelength of one in two million need be accommodated.

having a concentric reservoir, larger in volume by a factor of 3.5.

Simulation of Ionosphere

In the demonstration of sky wave propagation, it would be useful to simulate the conditions present as a wave rises through the ionosphere, experiencing a gradually decreasing refractive index. Although critical angle reflection is presently used to simulate the phenomenon, it is not strictly correct. To the present time, we have been unable to develop a simple simulator for the upper atmosphere.

Acknowledgements

The author is indebted to members of the Research Laboratories in Montreal, who contributed valuable ideas and useful discussion in the development of this kit. Mr. B. Griffin has provided diligent technical assistance.

References

1. Belloc, Alexis, "La télégraphie historique depuis les temps les plus reculés jusqu'à nos jours" (Firmin-Didot, Paris, 1888).
2. Maiman, T. H., "Stimulated Optical Radiation in Ruby", *Nature*, Vol. 187, No. 4736 (Aug 6, 1960) pp. 493-494.
3. Green, R. M. and Waksberg, A., "Lasers in Communications", in this issue.
4. Bennett, W. R. Jr.: "Gaseous Optical Masers", *Appl. Opt. Suppl.* (Sept 1962) pp. 24-61.
5. Bolwijn, P. T.: "Further Measurements on the Noise of a D.C. Excited HeNe Laser Oscillator", *Phys. Lett.*, Vol. 13, No. 4 (Dec 15, 1964) pp. 311-312.
6. Crawford, F. W. and Kino, G. S.: "Oscillations and Noise in Low-Pressure DC Discharges". *Proc. IEEE*, Vol. 49, No. 12 (Dec 1961) pp. 1767-1788.

When the gas is excited by the passage of a DC electric current, some of the excess energy appears as light. Light travelling between the two mirrors increases in intensity by extracting more light energy from the excited gas, a process called Light Amplification by Stimulated Emission of Radiation, hence the acronym: laser. When the gain in light energy derived from stimulated emission exceeds the losses in the system, oscillation is achieved, and the light intensity within the laser cavity may rise by many orders of magnitude.

The mirror at one end of the tube is designed to transmit 1% of the light incident upon it, and this is useful output from the laser. After changing the

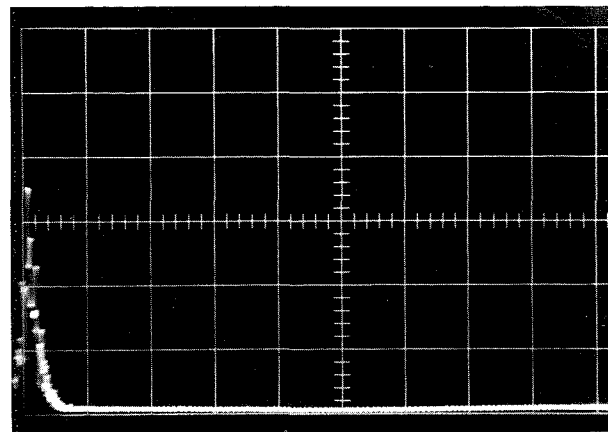


Fig. 4a—Noise spectrum of the laser operating in quiet air: vertical sensitivity=0.05 VRMS/div; horizontal=1kHz/div; center frequency=5kHz; resolution=100Hz.

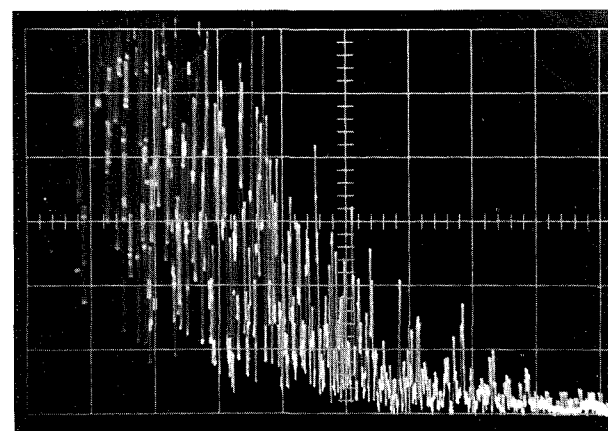


Fig. 4b—Noise spectrum of the laser operating through turbulent air stimulated by hot air blower (recording conditions are as in Fig. 4a).

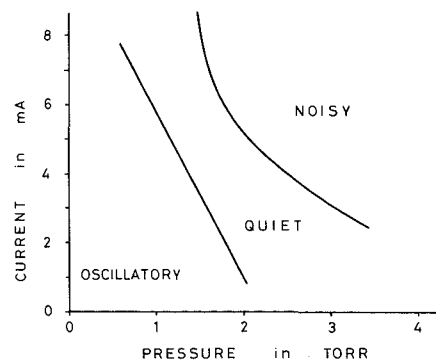


Fig. 5—Three regions of operation of a typical 50-cm-long HeNe laser.

shape of the wavefronts using a built-in lens, the light emerges from the laser as a narrow beam (in this case red in color).

Lasers of this type operate in the normal glow region of discharge and hence exhibit a negative dynamic impedance as illustrated in Fig. 3. To operate a tube of this type from a voltage source, it is necessary to place a series ballast resistor in the circuit for stable operation, as shown in Fig. 2.

Machining with the carbon dioxide laser

Dr. D. Meyerhofer

Machining with laser beams has become a practical reality in recent years. It has been used for difficult precision micro-machining jobs, particularly in cases where it is necessary to disturb the machined element as little as possible. The carbon dioxide laser is particularly attractive for such work because of its high average power and efficiency and because it can produce pulses at high repetition rates. We have studied the drilling of holes with the carbon dioxide laser in metals and insulators theoretically and experimentally. The measured drilling efficiency is in good agreement with the calculated one for metals. The fabrication of rotogravure cylinders with this type of laser was investigated and found to be a promising process if metal-plated plastic cylinders (or sleeves) can be employed. Some other specialized applications are also described.



Dr. Dietrich Meyerhofer
Electronic Printing Group
RCA Laboratories
Princeton, N.J.

studied Engineering Physics at Cornell and received his PhD degree in physics from MIT in 1957. While at MIT, he was awarded a Fellowship. His thesis was a study of the ferroelectric transitions in barium titanate. In March, 1958, he joined RCA Laboratories where he has studied various physical properties of semiconductors and insulators. In particular, he has measured galvanomagnetic effects in III-V compounds; investigated the band structure of degenerate germanium as deduced from the electrical properties of tunnel diode; and explored the transport of carriers through insulating layers by quantum mechanical tunnelling and the properties of evaporated thin films of silicon. Subsequently, he has been concerned with quantum electronic phenomena, specifically with the nature of the light emission from semiconductor diodes and lasers and its modification by piezoelectric tuning; with mixing of coherent light beams by electric field induced absorption; and with high power, high repetition rate Q-switched operation of the CO_2 laser. For two years, Dr. Meyerhofer was associated with the Graphic Systems Applied Research Laboratory and investigated electronic applications in the printing industry. This included the use of lasers for exposure of photosensitive printing plates and for direct machining of gravure cylinders; electronic halftone screening and holographic font storage. Dr. Meyerhofer is a member of Tau Beta Pi, Sigma Xi, the American Physical Society, the Optical Society of America, the American Association for the Advancement of Science, and the IEEE.

Reprint RE 15-1-22

Final manuscript received February 14, 1969.

ONE OF THE MAJOR INDUSTRIAL APPLICATIONS of lasers is the area of machining. By this we mean the removal of material from a solid by concentrated high power optical energy.¹ The solid may be a metal or an insulator, amorphous or crystalline. A related field is laser welding which will not be discussed here.

Lasers generally remove solid material by heating it to the boiling point and evaporating it. With regards to the energy used, this process is very inefficient compared to conventional machining. The situation is even less favorable for certain insulating materials that may be transparent to low power light of the laser wavelength. In that case, the absorption takes place due to nonlinear higher order processes that are always present at sufficiently large power densities. Laser machining will therefore be restricted to specialized applications where it provides compensating advantages. Examples are micro-machining where conventional techniques become very difficult and time consuming; intricate machining operations, that have to be very precise and computer controlled; or very high speed applications, which are ordinarily restricted by mechanical limitations. In this way, lasers have been used for drilling of diamond dies, wheel balancing, and resistor trimming. A somewhat different machining job was performed in the drilling of holes in plastic tape at very high rates to produce an optical memory. Lasers have also been used in the related areas of vapor deposition where

evaporation of a solid has to take place in a protective atmosphere, or a vacuum, with a minimum amount of contamination.

The lasers used in the machining operations described have generally been high powered crystal lasers operating in the visible (ruby) or near infrared (neodymium) spectral regions. They are capable of high power and energy pulses that can be focused to produce extremely large power densities. They suffer from low efficiency and limited repetition rate of the pulses. In contrast to this, the CO_2-N_2-He gas laser (carbon dioxide laser) operates at a high efficiency (to 20%) and can be pulsed at very high repetition rates.² Because the low gas density limits the number of active molecules, the maximum pulse energy and power are not as high as for the crystal lasers. The CO_2 laser will therefore complement the crystal lasers in machining applications and will be used in situations where the drilling of small holes at very high rates is required. The laser operates in the far infrared ($10.6\mu m$) and the interaction of the radiation with solid surfaces will therefore be somewhat different from that of the visible and near infrared lasers.

In this paper, we will discuss machining with a CO_2 laser. First, we consider the general problem of forming a cavity in a metal surface with a laser pulse. The size of the cavity will be calculated from theoretical considerations and compared with the measurements. This will be followed by consideration of nonmetallic solids. Fi-

nally, we discuss application of the CO_2 laser to actual drilling problems. During the period in which the experimental work of this report was being undertaken, considerable improvements in the performance of one of the near infrared lasers have taken place. Consequently, the $Nd-YAG$ laser could now perform some of the continuous or quasi-continuous drilling operations of the CO_2 laser at lower efficiency but with more compact equipment.

The CO_2 laser used in this work is a flowing gas laser with $NaCl$ Brewster-angle windows and external cavity mirrors. Maximum output was 120 W cw at 15% efficiency and about half that in a fundamental-mode Gaussian beam. The discharge was always operated continuously, but the output could be Q -switched by a mechanical chopper located at a focal point in the cavity (Fig. 1). This produced pulses of up to 6-mJ energy (multimode) and 0.2- to 1.0- μs length at low repetition rates and pulses of smaller energies at higher repetition rates (up to 100 kHz). To produce shorter pulses with higher power, a rotating-mirror Q -switch could be used. The pulse rate was then restricted to less than 300 Hz. Using a $f/1$ germanium lens, the laser beam could be focused into a spot of about 100- μm diameter for the multimode case and of 40- μm diameter for the single-mode case.

Effect of laser pulses on metal surfaces

This section describes what happens when a pulse of radiation impinges on a metallic surface. Metals are a good starting point for the discussion of laser machining because the events taking place on their surfaces can be described by a simpler model than is the case for insulators. The description follows some of the considerations of Ready³ who first discussed and investigated this problem.

Due to the generally high reflectivity of metals, only part of the incident

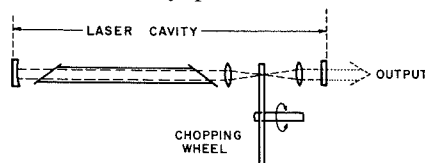


Fig. 1—Schematic diagram of CO_2 laser with chopper Q -switch for high-repetition-rate pulses.

Table I—Reflection and absorption coefficients of selected metals.

	Measured ^a values			Calculated values				
	20°C			20°C			Boiling point	
	1-R	α (μm^{-1})	σ $10^6(\Omega m)^{-1}$	1-R	α (μm^{-1})	σ $10^6(\Omega m)^{-1}$	1-R	α (μm^{-1})
Al	0.020	110	38	0.018	130	3.9	0.057	42
Cu	0.012	60	58	0.015	160	2.7	0.069	34
Ni	0.044	60	15	0.029	82	0.57	0.15	16
Fe/Steel	0.060	50	10	0.036	66	0.23	0.23	10

light flux will penetrate into the solid. That energy will be absorbed very near the surface so that a simple model can be used to describe the thermal history. For the high-power pulses being considered, most of the energy will go into vaporizing solid material so that the size of the cavity and the drilling efficiency can be calculated. For other kinds of irradiations, this simple model must be extended leading to either lower or higher efficiencies.

The light energy falling on the metal surface will be partly reflected and partly absorbed. This process is determined by the two material parameter values: R , the reflectance, and α , the absorption coefficient. Room temperature⁴ values for the four kinds of metals being considered in detail are tabulated in Table I. Use has been made of the relationship between α and the extinction coefficient k : $\alpha = 4\pi k/\lambda_0$; λ_0 is the wavelength in vacuum. While the absorption coefficients have not been measured at 10.6 μm , that they are approximately wavelength independent in the near infrared and the values measured in that region can be used.

Measured values of these parameters are not available at elevated temperatures. However, in the far infrared region, at least, they may be derived from the electrical conductivity⁵:

$$k = \left[\frac{1}{4\pi \epsilon_0} \right]^{1/2} \left[\frac{\sigma \lambda_0}{c} \right]^{1/2} \quad (1)$$

$$\alpha = \left[\frac{4\pi}{\epsilon_0} \right]^{1/2} \left[\frac{\sigma}{c \lambda_0} \right]^{1/2} \quad (2)$$

$$1 - R = \frac{2}{k} = \frac{8\pi}{\lambda_0 \alpha} = 2 (4\pi \epsilon_0)^{1/2} \left[\frac{c}{\alpha \lambda_0} \right]^{1/2} \quad (3)$$

Here, c is the wavelength of light, and ϵ_0 is the permittivity of vacuum. From measured values of high temperature

conductivity, σ , some of which were taken in the liquid phase, we extrapolate to the values at the boiling point using the simple relationship that σ^{-1} is proportional to the absolute temperature.⁶ These extrapolated values are recorded in Table I, along with the calculated values of the α and $1-R$ from Eqs 2 and 3. For comparison with the measurements, the quantities were also calculated for room temperature. Table I shows that the agreement is reasonable, thus confirming the applicability of the equations. It is apparent that, even at the boiling point, $(1-R)$ is still much smaller than 1, and only a small fraction of the incoming light is absorbed. This is in contrast to the effect of light in the visible region of the spectrum. While we cannot calculate $(1-R)$ from Eq. 3 in that region, we know from the results of Ready³ that almost all light is absorbed.

The temperature rise in the metal due to the surface irradiation may now be calculated. We assume that at time $t=0$, the entire surface starts absorbing energy at a rate of Q per unit area. Q is related to the incoming power density Q_0 by $Q=Q_0(1-R)$. This simplifies the problem to a one-dimensional heat-flow calculation. Also, it is assumed that the thickness of the absorbing region (α^{-1}) is small compared to the region over which heat flow is taking place so that all the energy can be considered to be absorbed on the surface. These assumptions will be justified below. As a further simplification for the calculation, we first take Q to be constant during the light pulse. The solution to the heat-flow equations is then straightforward and leads to the following relationship for the temperature of the surface⁷:

For $x=0$

$$(T - T_0) = \frac{2Q}{K} \left(\frac{\kappa t}{\pi} \right)^{1/2} \quad (4)$$

where

$$\kappa = \frac{K}{\rho C} \quad (5)$$

Here, κ is the thermal diffusivity, K the thermal conductivity, C the specific heat, and ρ the density. Parameter values are listed in Table II. The distribution of temperature with x is given by a combination of Gaussian exponential and error functions in the parameter $x/2\sqrt{\kappa t}$ so that the depth to which the heat has flowed substantially at time t is $x_D = 2\sqrt{\kappa t}$. After 1 μ s, this value ranges from 24 μ m for Al to 6 μ m for steel, and less at higher temperatures. The CO₂ laser used in these experiments could be focused to a minimum diameter of about 40 μ m. This means that for laser pulse lengths shorter than 1 μ s, the thermal penetration is smaller than its lateral extent so that the one-dimensional model is justified. Also, one sees that α^{-1} is always much less than the penetration distance x_D thus justifying the above assumption.

The values of thermal conductivity listed in Table II are the bulk, room-temperature values. The temperature dependence is not expected to be significant. However, Harrington⁸ found that the apparent thermal conductivity at the surface was anomalously low during high power irradiation. Values 10 to 1000 times smaller than the bulk values must be assumed to apply under our experimental conditions.

We now calculate the temperature of the metal surfaces in our experiments. The CO₂-N₂-He laser with the chopper Q-switch was usually operated to produce pulses of 5-mJ energy and 500-ns length resulting in average power of 10⁴ W during the pulse. When this power is focused into the smallest (40 μ m) spot, a power density of $Q_0 = 5 \times 10^8$ W/cm² results. The time required to heat the surface to the boiling point (t_B) is [refer to Eq. (4)]:

$$t_B = \frac{\pi}{4} \frac{K \rho C}{Q_0^2 (1-R)^2} (T_B - T_0)^2 \quad (6)$$

Values of t_B are listed in Table II. When the change of $(1-R)$ with temperature ($\propto T^{-1/2}$) is taken into account, the heat flow equations become more complicated but it can be shown that the values of t_B are reduced by approximately a factor of 2 from those

given in Table II. If the anomalous values of thermal conductivity are used in Eq. 6, t_B is even less. It is seen that, even for these long pulse lengths, the surfaces of Ni, Fe, and Al heat up in a much shorter time than the duration of the pulse. For Cu ($t_B < 600$ ns), this is not the case unless the anomalous thermal conductivity applies. Since the experimental results for copper given later in this paper are consistent with those of the other metals, the latter does appear to be the case.

It is now safe to assume that the surface reaches the boiling temperature at the very beginning of the incident light pulse. If all the absorbed power goes into vaporization of material, the rate of material removal is

$$\frac{ds}{dt} = \frac{Q}{H_v} \quad (7)$$

where H_v is the heat of evaporation plus smaller contributions from the heat capacity and the heat of fusion.

The depth of the cavity x_c formed under these conditions during the pulse length t_p is

$$x_c = \frac{Q_0 (1-R)_{B.P.}}{H_v} t_p \quad (8)$$

Because the energy density at the focused beam is difficult to determine, it is more convenient to express the efficiency of drilling (η_d) in terms of the volume of material (V_c) removed by the total pulse energy incident (E_0)

$$\eta_d = \frac{V_c}{E_0} = \frac{x_c A}{Q_0 t_p A} = \frac{(1-R)_{B.P.}}{H_v} \quad (9)$$

As long as x_c is larger than x_D , most of the pulse energy will go into evaporation of material and only a small amount into heating of the surrounding solid, and Eq. 9 will apply. As the pulse of a constant energy (constant x_c) becomes longer, this relationship will reverse, and the efficiency of removing material will decrease. The same is true as the pulse energy is decreased which explains why there is a threshold for cavity formation. For the measurements reported here, x_c is generally much larger than x_D when the true anomalous thermal conductivity value is used.

Experimental results of drilling in metals

With the CO₂ laser described in the introduction, we have drilled holes in

polished metal samples. As the laser is operated at a high pulse repetition rate, the sample was moved mechanically in the focal plane of the focusing lens. The resulting individual holes were well separated. An example of a hole formed is shown in Fig. 2. The pulse energy was 6 mJ, and the dimensions of the cavity were 93 μ m diameter and 15 μ m deep. It can be seen that the cavity is of uniform depth but that a rim has been formed around it, 5 μ m high. This must be due to some molten metal splashing out.

The drilling efficiency η_d derived from these measurements is shown in Table III for various metals. Also listed are the calculated values from Table II. The agreement is seen to be quite reasonable, except for Al where it appears that a higher fraction of the incoming energy is absorbed, i.e., the extrapolated value for $1-R$ at the boiling point is too low. In general, we find no differences in drilling efficiency for different kinds of surface preparation. Certainly, blackening the surface, for example, increases $1-R$ greatly at low temperature but by the time the sample has melted and the boiling point is reached, the surface preparation no longer has any effect.

Among the metals tested, Zn and Cd have lower heats of vaporization which accounts for the higher efficiencies observed. No cavities could be formed in Cr layers and in Ta sheets with the largest pulses used, suggesting that the boiling point cannot be reached. In contrast to this, it appears from the measured efficiency that the copper surface reaches the boiling point in $t_p < 100$ ns which confirms the anomalous value of the thermal conductivity.

For comparison, Table III also shows the drilling efficiency for visible laser light. The calculated value assumes that R goes to zero at the boiling point and the entire pulse energy vaporizes material. The experimental results are those of Ready⁹ which have been confirmed by other workers.⁹ While Ready⁹ assumes a different drilling mechanism for the non-Q-switched ruby pulses ($t_p = 600$ μ s) and the Q-switched pulse ($t_p = 44$ ns), the results are similar enough so that the simple model used here appears to be just as valid for both cases. They also imply that $(1-R)$ is at least $1/2$ and probably close to 1.

Table II—Thermal parameters and calculated drilling efficiency of metals.

	K ($J/cm\ s^{\circ}C$)	ρ (gr/cm^3)	C ($J/gr^{\circ}C$)	κ (cm^2/s)	Boiling point T_B ($^{\circ}C$)	t_B (μsec)	H_v (kJ/cm^2)	η_d ($10^{-6}cm^3/J$)
Al	3	2.7	0.8	1.4	2000	0.2	35	1.6
Cu	3	9	0.4	0.83	2300	1.2	54	1.3
Ni	0.3	9	0.5	0.07	3000	0.02	70	2.1
Fe/Steel	0.4	8	0.5	0.10	3000	0.013	~70	3.3

Drilling in nonmetallic materials

The effect of a laser beam on non-metallic solids is more complicated and more varied than in the case of metals. The absorption at 10.6 μm can vary from zero for alkali halide crystals to very high values for such crystals as quartz or for most glasses. In the latter cases, the energy is all absorbed at the surface. For intermediate values of absorption coefficient, say 1 to 100 cm^{-1} , the energy is absorbed throughout a large volume and drilling becomes difficult. All insulators have lower reflection coefficients than metals so that larger fractions of the incoming radiation are available for absorption. The thermal conductivities are generally much smaller than for the metals. This means that the absorbed energy will move much more slowly from the place of absorption and long pulses of light can be used. The high purity semiconductor crystals are exceptions. It is clear that each glassy, crystalline, and ceramic material must be considered separately.

We studied another class of materials, the organic plastics, because of their applications to gravure cylinders. They do not melt and vaporize when heated but rather decompose and react chemically. This makes the drilling process difficult to predict.

Among the materials we investigated with Q-switched pulses, polyethylene, lucite, and polystyrene had low absorption coefficients at 10.6 μm . This caused heating throughout the volume and the formation of bubbles.

Materials which formed good cavities were Bakelite, Nylon, Teflon and Celcon. In all cases, there was a threshold energy below which there was no evidence of cavity formation. Above that energy, the efficiency increased steadily up to the maximum energy the laser could supply. This is shown for Bakelite in Table IV. The peak efficiency is one to two orders of magnitude higher than for metals. Apparently, with increasing energy, more and more of the material is removed explosively without melting and decomposing.

Table III—Measured and calculated drilling efficiencies (η_d —units are $10^{-6} cm^3/J$).

Metal	CO_2 laser		Calc. ($1-R$) = 1	Visible laser	
	Calc.	Measurement		Measurements ^a	
				Long pulse	Q-switched
Al	1.6	3.25 to 4.0	30	16	35
Cu	1.3	1.5 to 2.0	18.5	18	15 to 20
Ni	2.1		14	12	10
Fe/Steel	3.3	2.5	~14	12	
Al-Mg		7.5			
Zn		6.5			
Cd		12			

Table IV—Variation of drilling efficiency in bakelite with laser pulse energy.

Pulse energy (mJ)	Cavity volume ($10^{-6} cm^3$)	Efficiency ($10^{-6} cm^3/J$)
7.4	1.9	260
4.6	0.50	110
1.95	0.18	90
0.54	0.013	24

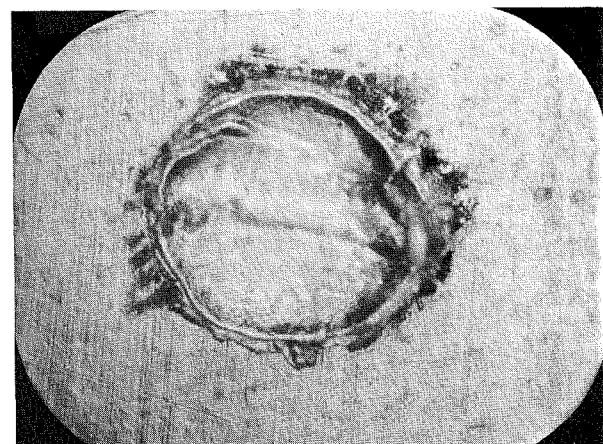


Fig. 2—Cavity produced in Al-Mg alloy by focused 6-mJ pulse of 10.6- μm radiation (400X magnification). The maximum depth of the cavity is 15 μm and the lip is 5 μm high.

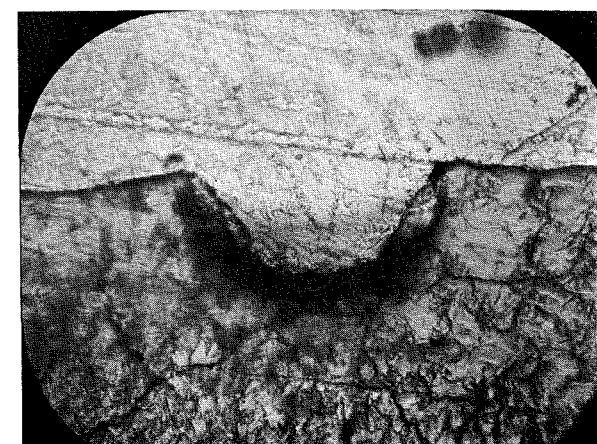
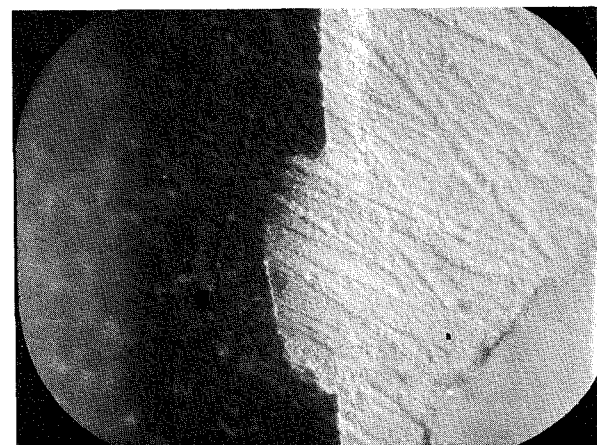


Fig. 3—Cross-sections of cavities drilled in plastics (400X magnification); (top) Bakelite (bottom) Nylon.

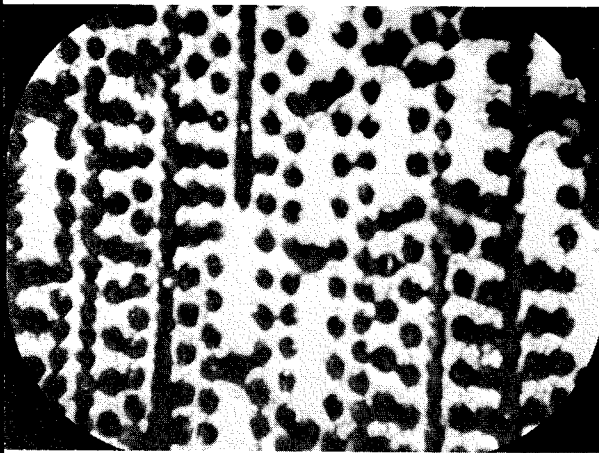


Fig. 4—Photomicrograph of a sheet of paper printed on a small gravure press from a bakelite-laser-engraved cylinder (30X magnification). Both the size and spacing of the cavities are varying.

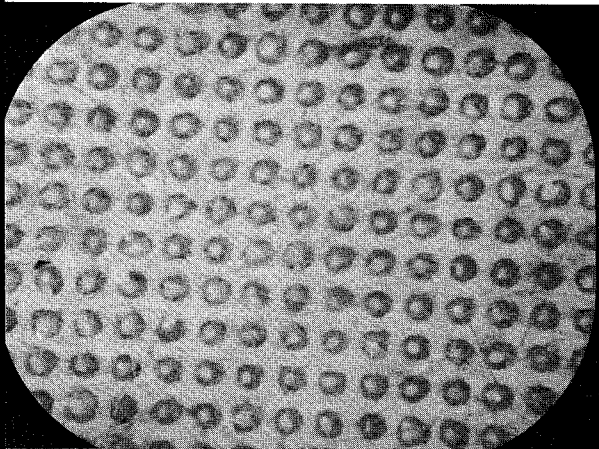


Fig. 5—A conventional sheet printed by gravure. Same magnification as Fig. 4. The cavities were of uniform size and evenly spaced.

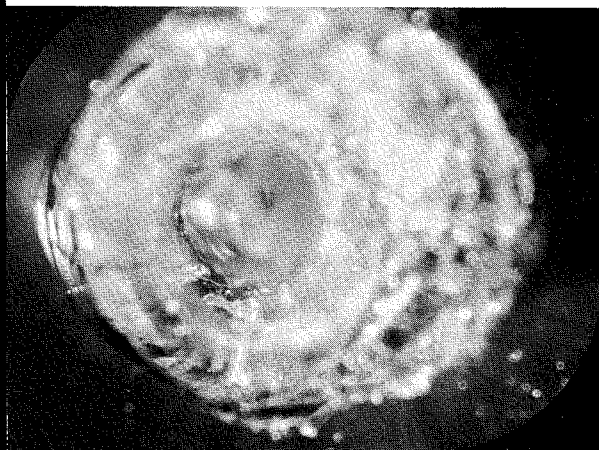


Fig. 6—Hole drilled through 2.5-mm-thick glass wall with long pulses.

Bakelite formed the best cavities of any material studied, as can be seen from a cross-section (Fig. 3a). Nylon has about the same efficiency and threshold values but shows some cratering (Fig. 3b). The latter effect is larger for Teflon. On the other hand, Celcon, which decomposes at a low temperature, produced relatively good

cavities with twice the efficiency of the other materials and a threshold of less than 0.1 mJ.

Machining of gravure cylinders

The work described in this paper received its impetus from the question whether it would be possible to machine a conventional rotogravure cylinder with a laser beam.¹⁰ The problem arises because the electronic photocomposition equipment produced by the Graphic Systems Division produces a composed page as a serial string of dots or lines. Presently, these are converted to a picture of a page by writing them on a CRT. However, it would be much more efficient if the same information could be used in machining a printing plate or cylinder in point-by-point fashion. Here, we are interested in the gravure printing plate where the cavities in the printing cylinder are filled with ink which is subsequently transferred to the paper. The largest cavities required are approximately 120- μ m square and 60- μ m deep, and they must vary in size and depth in the lighter areas to produce the best results. To form a cylinder in a practical time, say 5 minutes per page, it is necessary to form about 5 to 10,000 cavities per second. From Table III, CO_2 laser energy required per large cavity varies from 700 mJ for copper to 110 mJ for Al/Mg so that an average power of 500 to 7,000 W must be supplied. Clearly, our present CO_2 laser is much too small. Higher power lasers can be produced by lengthening the discharge region and a 1 to 2-kW laser is certainly possible. However, the problems of the other optical elements, windows, mirrors, and lenses become very severe at these high power levels. Electro-optic modulators are not yet very good at 10.6 μ m and reduce the available power.

While the efficiency is 5 to 10 times higher at the ruby wavelength, the average power available is much less.

As an alternative, the possibility of using plastic gravure cylinders or cylinders with plastic sleeves for printing was considered. In that case, the power required for machining would become a more practical quantity. The main difficulty is the softness and poor abrasion resistance of plastics allowing scratches to form by the doctor

blade (which wipes the printing plate during the printing process). However, it is well-known that many plastic materials can be plated with metallic layers which should produce surfaces equivalent to those of solid metal cylinders (copper, or chrome on copper). We therefore experimented with some of the plastics that formed nice cavities and found that Bakelite, ABS, and Nylon could be plated by conventional techniques, after drilling of the holes.

As an example, we engraved a random pattern of cavities in a small bakelite cylinder. Pulses varying from 1 to 3 mJ were used so that the cavity size varied. This cylinder was plated with Ni and Cr and then demonstrated good abrasion resistance when run on a small press. An enlarged photograph of a printed sheet is shown in Fig. 4. For comparison, a conventional gravure printed sheet is shown in Fig. 5 at the same magnification. In the latter case, the cavities are uniform size and evenly spaced.

Another approach also was found to work and may have some additional advantages. The fresh cylinder is coated first with a thin layer of Ni (about 1 μ m). The CO_2 laser readily penetrates the Ni creating a cavity in the plastic almost as big as without the Ni. After drilling, further electroplating is performed but only on the untouched surface. The interior of the cavities is not plated so that they do not change size. In addition, it may be possible to take advantage of the different wetting properties of the plastic and the metal to improve the ink transfer.

Other machining experiments

We have investigated a number of other drilling problems where the CO_2 laser might have certain advantages because of its high average power and freedom from mechanical contact with the machined surface. We will briefly describe and discuss some of the results.

Cutting of semiconductor and insulator substrates

For various semiconductor device applications, it is necessary to cut thin semiconductor wafers or glass, cer-

amic, or crystalline substrates. These cuts should be precise and small and should not disturb the surrounding areas. Laser drilling can fulfill these requirements, but because of the large amount of cutting required, a high power CO_2 laser would be necessary. For insulating substrates that have relatively low thermal conductivities, Q -switching is no advantage because the short spacing of pulses produces the same result as cw applications of the same power. At the lower levels needed for drilling, this tends to cause excess heating so that the duty cycle must be reduced by pulsing in long pulses of the order of milliseconds. As we could not pulse the discharge, we used a slow mechanical chopper to interrupt the cw beam.

Experiments with glass, ceramic, and sapphire wafers showed that smooth cuts were difficult to obtain because of regions of molten material. However, it was found that below the threshold for drilling, these materials could be scored just by heating the surface. Because of the brittleness of the samples and the differential expansion, they would break cleanly upon completion of the cut. For example, a 0.25 mm thick wafer of sapphire (with an epitaxial Si layer on the surface) was cut at a speed of 3 mm/sec. The threshold for visible drilling was 14 W into a 100- μ m-diameter beam while the threshold for scoring without damaging the surface was 10 W cw. The cutting speed could be increased by using higher powers. The scoring technique works in the entire region between the thresholds and gives clean reproducible cuts.

In contrast to these insulating materials, Si wafers are much more difficult to cut. They are poorly absorbing at 10.6 μ m so that the energy is absorbed throughout a large region. In addition, they have a much higher thermal conductivity so that continuous irradiation and long pulses lead to heating of too large a region. We were able to cut silicon wafers with the laser operating in the Q -switched mode, but only at relatively low speeds. For example, with a 100- μ m-diameter beam, 2-mJ pulses, and 10-W average power, complete cutting of a 0.25-mm-thick Si

wafer could only be performed at 0.1 mm/sec. At twice that speed, the cut was deep enough so that the wafer could be broken reliably. Considerable improvement can be obtained by high energy pulses (10 to 100 μ s long) produced by pulsing the discharge rather than by Q -switching.¹¹

Drilling of holes in evacuated kinescopes

For certain repairs, it is necessary to break open sealed picture tubes. This must be done without letting any glass dust or particles reach the delicate aperture mask. By slowly drilling a hole with a Q -switched laser, the vacuum can be broken with minimal damage. A 2.5-mm-thick glass wall was drilled through with 15 long pulses of 3 J energy (produced by interrupting the cw laser operating at 80 W). A picture of the hole is shown in Fig. 6. The diameter is 0.7 mm on the upper surface and 0.1 mm on the lower surface.

Holes in printed circuit boards

Producing holes in multiple-layer integrated-circuit boards is one of the more difficult drilling jobs because of the alternating layers of copper and fiberglass which cause rapid wear of mechanical drills. Lasers can readily punch holes through such combinations; however, because of the size and number of holes required, high average powers are required. Consequently, we attempted to use the CO_2 laser for this purpose. Because of the copper layers, Q -switching must be employed. Drilling could then be performed at a reasonable rate, but because of the quasi-cw operation, the fiberglass surrounding the hole got much too hot and swelled up. A higher powered long pulse operation would probably be more promising.

Conclusions

The CO_2 laser is already being used in some industrial machining applications such as wafer cutting, resistor trimming, microwelding and bonding. More recently, the very high power versions with oxygen assist are being used to make large cuts in exotic metals that are difficult to machine with conventional techniques. We

have studied the applications of the Q -switched CO_2 laser with its high repetition rate of short pulses. In all these applications, the high power available and its efficiency make it superior to other lasers. The far-infrared wavelength is generally a disadvantage but can also be an advantage such as in the case of glass and sapphire. It does, however, restrict the minimum size that can be drilled to 20 to 40 μ m. Where modulation is required, this becomes difficult at this wavelength. Also, the powerful versions of the laser have a very large physical size.

During the time that these investigations were performed, the performance of the Nd -YAG crystal laser (1.06 μ m) has been greatly improved. Continuous power outputs of up to 200 W are now commercially available, and Q -switching at high repetition rates has also been demonstrated. The small physical size makes it more attractive for industrial use than the CO_2 laser, however, the overall efficiency is an order of magnitude lower. It should therefore be considered for applications such as described in this paper.

Acknowledgment

I am very grateful to E. J. Gavalchin who performed most of the experiments reported on in this paper.

References

- Adams, Jr., C. M. and Hardway, G. A., "Fundamentals of Laser Beam Machining and Drilling" *IEEE Trans. Industr. General Applications*, Vol. IGA-1 (March/April 1965) p. 90.
- Clay, B. R., "Drilling of Microscopic Holes in Metals by Laser Beam;" *RCA ENGINEER*, Vol. 12, No. 3 (Oct.-Nov. 1966).
- Meyerhofer, D., " Q -switching of the CO_2 Laser;" *IEEE J. Quantum Electronics*, Vol. QE-4 (Nov. 1968) p. 762.
- Ready, J. F., "Effects Due to Absorption of Laser Radiation;" *J. Appl. Phys.*, Vol. 36 (Feb. 1965) p. 462.
- American Institute of Physics Handbook, (McGraw-Hill Book Co., Inc., New York, 1963) 2nd ed.
- Born, M. and Wolf, E., *Principles of Optics* (Pergamon Press, Oxford, 1964), 2nd ed., Chapt. 13.
- Mott, N. F. and Jones, H., *The Theory of the Properties of Metals and Alloys* (Oxford University Press, London, 1940).
- Carlsaw, H. S. and Jaeger, J. C., *Conduction of Heat in Solids*, (Clarendon Press, Oxford, 1959), 2nd ed. Chapt. 2.
- Harrington, R. E., *J. Appl. Phys.*, Vol. 37 (April 1966) p. 2028.
- Hocker, G. B., RCA Laboratories, Princeton, N.J., *private communication* (1966).
- Stephens, A. W., "Lasers and Printing Plates;" *RCA ENGINEER*, Vol. 13, No. 6 (April/May 1968).
- Schein, T. R., Aerospace Systems Division, Burlington, Mass. *private communication*.

Gated vision techniques

D. G. Herzog

Backscatter reduces the effectiveness of optical imaging systems by masking target returns. Without physically separating the transmitter and receiver, backscatter effects can be negated by pulsing the transmitter and "gating" the receiver—selectively turning the receiver on in time to receive the target returns and turning it off to block all other returns. This technique enables detection through obstacles with even less than 10% transmission without a significant loss of operating range. This paper describes the gating concept and implementation, and discusses the requirements of gated systems in terms of rise and fall times, covertness, contrast, power, and resolution. It presents examples illustrating typical requirements and tradeoffs and the power savings with gated systems.

ANYONE WHO HAS driven in a foggy or hazy night knows that objects often can be seen better when they are lighted from a streetlight than from his headlights. This is because fog causes backscatter and masks the light reflected from more distant objects. This effect is shown in Fig. 1 which shows the fog giving a strong light return, superimposed over the light return from the bike. In Fig. 2, the bike is illuminated by the streetlight—the light is from a different direction than the field-of-view. Here the primary return due to backscatter is displaced from the field-of-view, thus making the object easier to see than in Fig. 1.

To generalize the effectiveness of the light in the previous example, relative distances are assigned in Fig. 3. The backscatter due to the fog will be considered on a fog particle. The headlights and streetlight are assumed to be of equal intensity. The light intensity from a light source varies as the inverse square of the distance from it. Therefore, the fog particle will be 100 times brighter than the bike considering only illumination by the headlight. The contrast of the bike to the fog may be said to be $\frac{1}{100}$. Illumination by the streetlight produces the inverse condition where the bike appears 100 times brighter than the fog particle. A figure of merit for the ability to see the bike better with streetlight illumination rather than with headlights would be the ratios of the contrasts ($\frac{100}{1/100}$) which is 10,000. Although many liberties were taken in this analysis, it does point out the deleterious effect of scattering.

Reprint RE-15-5-23

Final manuscript received November 25, 1969.

There is a similar problem in radar, referred to as ground or sea clutter. The problem is negated by pulsing the radar transmitter and gating the receiver. This same corrective approach can be taken in visual systems with the aid of electronic devices.

Gating concept

With continuous transmission of energy—be it radar or light—energy will be continuously received at the same time from all ranges. Without physical separation between the transmitter and the receiver, it is difficult to discriminate between the energy returned from the target and that from other objects or due to backscatter. However, if the energy is transmitted in pulses, the return energy from different ranges will be received at different times. In this case, it is possible selectively to turn on the receiver to receive the target signal and to turn off the receiver to block all other signals. This technique is known as "gating" and requires an approximate knowledge of the target range in order to set the on and off times of the receiver. The length of time the receiver is activated is known as the gate width of the receiver and is at least as wide (time interval) as the transmitter pulse in order to receive the full power of the reflected transmitted pulse; power received when the receiver is gated off is wasted.

Since the speed of light is constant, a pulse width can be thought of as a distance. The elapsed time—from pulse transmission, to the time the receiver is turned on, to receive the return—is the delay time, which can also be thought of as a distance. No returns



Donald G. Herzog, Ldr.

Laser Group
Advanced Technology Laboratories
Defense Electronic Products
Camden, N.J.

attended Drexel Institute of Technology from 1953 to 1959 under the cooperative program. His cooperative periods were spent at Fort Monmouth Research Laboratories. He received the BSEE in 1959. In 1963 he received the MSEE from Drexel. Mr. Herzog joined RCA in 1959 in the Receiver Group of the Missile and Surface Radar Division at Moorestown. He performed major design work on the BMEWS system, the FPS-16 radar, and MIPEP radar receivers. He also performed many study programs in the radar receiver area. In 1963 Mr. Herzog transferred to Advanced Technology Laboratories where he was promoted to Leader of the Laser Group in 1966. Under his direction, injection laser intrusion alarm systems were developed. Rapid advances in this area stemmed from developing unique self-check and timing approaches with highly efficient laser drivers and ultrasensitive optical detectors. In parallel with this effort was the development of advanced full-duplex voice communication systems using lasers. These units were very small and portable with operating ranges of 8 miles. A laser tracker and ranging unit designed under Mr. Herzog's direction for NASA for moon operation can scan dynamically, track with 0.06° accuracy, and range with $\frac{1}{2}$ meter accuracy to beyond 1000 meters. Many different types of laser gated viewing systems were also developed. These units vary from handheld, battery powered to large wide-angle airborne equipment. Another airborne system developed is a laser line scan unit using an Nd laser source. This system can perform imaging and ranging functions. Mr. Herzog is now developing passive detector systems, near and far IR active reconnaissance systems, optical IFF techniques using liquid crystals, and advanced laser modulation techniques. Mr. Herzog is a member of IEEE and Eta Kappa Nu.

can be seen until the delay distance is reached and then only for as long as the pulse-width distance. Taking this one step further, the active pulse-width region is then actually a section of a cone or tube (a section of the beam) which is moved back and forth in range as the delay distance is changed (see Fig. 4). The minimum active pulse-width volume is determined by the gate width of the receiver.

With gating, nothing is seen unless it is within the active pulse region. If the entire energy has been blocked short of the active pulse region, no return will be seen. But if the slightest energy gets through or around the obstacle, this will be returned and seen without being obscured by the signal from the obstacle.

Most smoke, fog banks, and trees will pass a considerable amount of light. If a target were in back of such obstructions, the target could not be seen because ordinary vision cannot dismiss the primary image to concentrate on the target image behind. But with gating, the receiver can be made to see only the target. Considering a transmission through trees of approximately 10%, only ten times the power would be required to achieve the same unobstructed maximum range. Stated in more significant terms, the range performance for the same power would be reduced by a factor of only 1.8 for small targets.

The shadow cast by a target can also be detected. In fact, the shadow cast on a background (such as smoke, fog or trees) often has greater contrast than the target itself viewed directly against the background. When such is the case, gating on the background will produce a higher contrast image of the target (see Fig. 5).

Gating implementation

Fig. 6 illustrates the gating implementation in a gated image intensifier. Incoming light is focused to form an optical image on the photoemissive surface. The light is converted to electrons which pass through the grid as they are accelerated to the phosphor by the high B+ voltage (15,000 V), and are reimaged by electron-optics. The electrons, now at a higher energy because of the acceleration, strike the phosphor producing light which is brighter than the incoming light. With the grid open, image intensification takes place as described; the intensifier is in the gated-on condition. With the grid at a negative potential, the initially emitted electrons would be repelled back to the photoemissive surface, and the intensifier would be in the gated-off condition.

Requirements of gated systems

Rise and fall times

Since most of the backscatter effect is strongest in the immediate range of

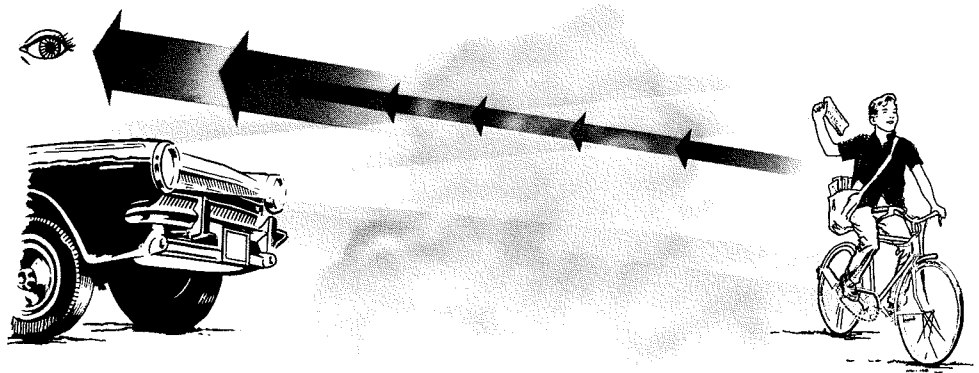


Fig. 1—In fog, a strong backscatter light return will mask light return from object.

100 feet or less, rise and fall times of both the receiver detector and the transmitter must be very fast. The gated intensifier with rise and fall times in the order of $\frac{1}{2}$ to 1 microsecond meets the requirements for a gated receiver. The only light sources available with the required fall times are lasers and spontaneous light-emitting diodes.

Covertness

The military requires that illuminating sources be covert (invisible, undetectable) in order to avoid detection by the enemy in reconnaissance, search, or observation missions. The point above which wavelengths are covert is not exactly defined. The visual bandwidth is generally considered from 4000 Å to 7000 Å with the peak sensitivity at 5500 Å. However, the eye is still sensitive at the higher wavelengths; its sensitivity decreases about 20 dB for each 500 Å increase from 5500 Å. The absolute visual cut-off is generally taken to be 8500 Å; at higher wavelengths, the brightness must be so high to be detected that eye damage may take place.

The light sources to date have used Nd-doped lasers, ruby lasers, GaAs lasers and spontaneous diodes. Ruby (6900 Å) is not covert. Nd-doped and GaAs lasers are both covert, lightweight, efficient sources.

Contrast

Radar and optical imaging differ in the attainable image contrast. Radar is

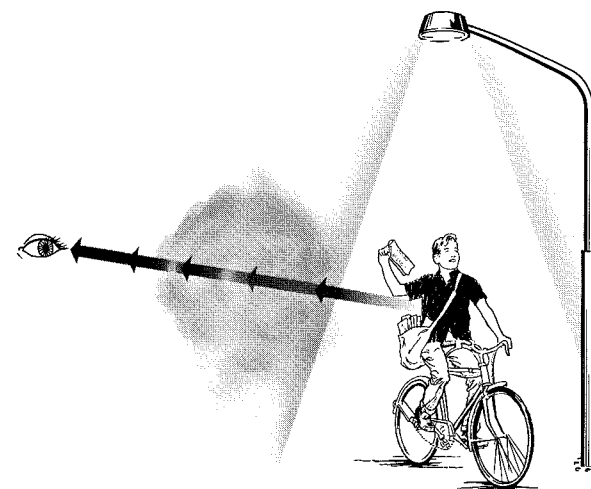


Fig. 2—When light source is removed from line of view and near the viewed object, the deleterious masking effects of backscatter are eliminated.

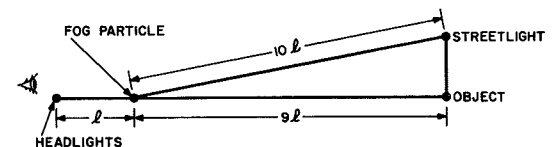


Fig. 3—Geometry of example to illustrate the effects of backscatter.

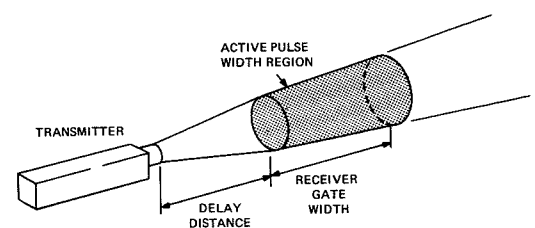


Fig. 4—Active pulse width region concept of gating.

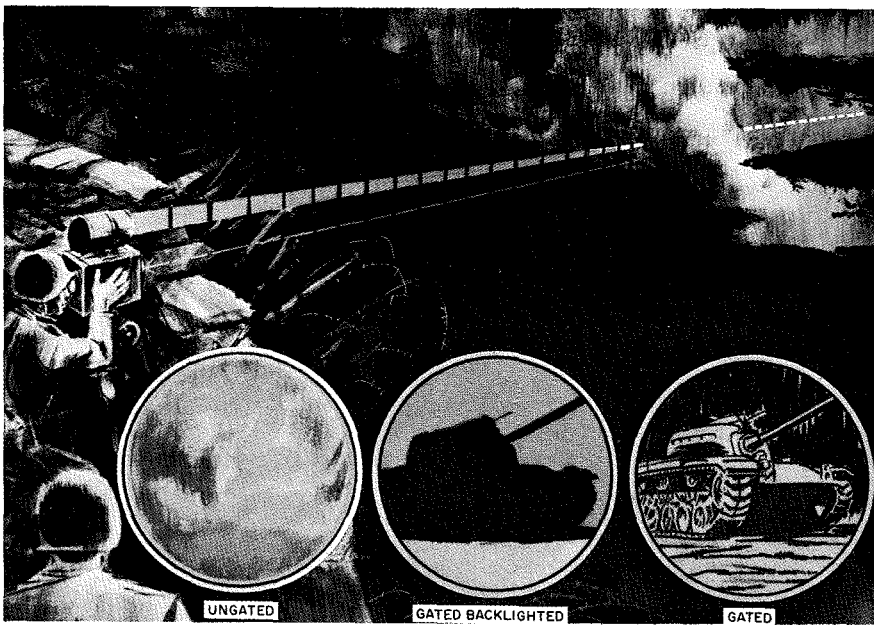


Fig. 5—Gating on shadow of low contrast target.

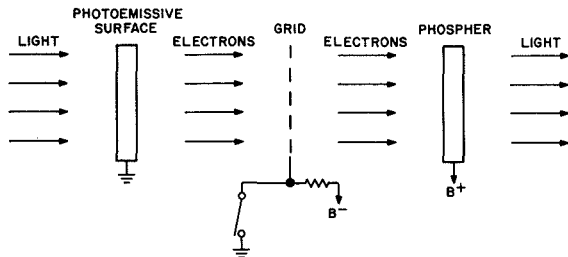


Fig. 6—Schematic representation of gating image intensifier.

usually high contrast imaging due to high reflectivities to microwave energy and imperviousness to weather conditions. At optical wavelengths, the contrasts are not as high and are further degraded by weather conditions. For example, in haze or fog, a distant building or tower, although visible, will appear as an outline image of low contrast.

Power

The following equation approximately defines the parameters that affect transmitted power:

$$P_t = \frac{4hcN_t^2 k^2 (2-C) R^4 \tan^2 \theta / 2}{K_o K_a^2 D^2 Q \tau C^2 T^2 \rho \lambda} \left(1 + \frac{100 T^2}{\pi R^2 \tan^2 \theta / 2} \right)$$

where P_t is the transmitted power (w); h is Planck's constant ($J \cdot s$); c is the speed of light (m/s); N_t is the number of effective TV lines on target; k is the Morton (k) factor (SNR requirement); C is a contrast factor; R is the range (m); θ is the illumination beamwidth (assumed conical) degrees); K_o is the transmission of the optics; K_a is the transmission of the at-

mosphere; λ is the operating wavelength (m); D is the diameter of receiving optics (m); Q is the quantum efficiency of the detector; τ is the integration time of the observations (s); p is the reflectivity of the target; and T is the linear dimension of the target (assumed square) (m).

The factors affecting the power transmitted are better seen in Fig. 7. The density and magnitudes are indicated at significant steps up to projection on the image intensifier. At that point, the factors to convert the power into photons and then electrons are introduced. Finally, the relationship of the number of electrons, resolution, and visual discrimination is shown. This illustrates the significance of the various factors (tradeoffs) in achieving operation at specific discrimination and range.

Keeping all terms in the equation constant except for target area T^2 and transmitted power P_t , linear relationship results between T^2 and P_t . This is true only for targets that are very small compared to the entire field-of-view. A target will be easier to detect as its size increases with respect to the field-of-view. However, there is a critical size relationship, beyond which very little improvement in detection results—this is arbitrarily defined and inserted in the equation as 1% of the field-of-view.

N_t is the number of resolution lines discernible across the target, and not the number of resolution lines that the image system is capable of providing across the target. Noise effectively de-

grades the resolution of the device. This effect can be noted on a very snowy TV picture—the number of scan lines and the beam size are the same, but the amount of discernible picture content is drastically reduced. The military generally defines the following functions in terms of N_t values:

Target detection	2 to 4
Target recognition	4 to 6
Target identification	8 to 12

However, the range of definition varies with different military organizations.

Detection denotes that which warrants additional investigation, is different from normal; recognition denotes a target (truck, jeep, tank, etc.); and identification denotes the specific type of target (such as truck).

System example

Consider a system using an S-25 photocathode, a *GaAs* laser illuminating source, and the reflectivities in Fig. 8. The reflectivity of foliage is very high in the infrared due to the chlorophyll content. Man-made objects generally have uniformly low reflectivity through the visible and infrared. The high contrast due to the differences in reflectivities enable better detection of man-made objects against a foliage background in the infrared, than in the visible. Fig. 8 also indicates that a good tradeoff between target contrast and S-25 sensitivity exists at the covert *GaAs* wavelength.

Assume the following parameters for the example:

$$\begin{aligned} K_a &= 0.7 \\ K_o &= 0.5 \\ \lambda &= 8500 \text{ \AA} = 0.85 \times 10^{-6} \text{ m} \\ D &= 1/8 \text{ m} \\ \theta &= 3.5^\circ \\ Q &= 1\% \\ k &= 3 \\ \tau &= 0.1 \text{ s} \end{aligned}$$

The remaining parameters in the equation are varied and the results are shown in Fig. 9.

Fig. 9 demonstrates the very wide variation in transmitter power that may be required for targets of similar nature. For example, curve A might represent the "detection" of a small vehicle, whereas curve D might be the "identification" of a man-size target with lower reflectivity and contrast. For these two cases at a range of 1.5 km, 100,000 times more transmitter

power is required by curve D than by curve A.

Too often, systems of this type are specified on the basis of the most stringent target and detection criteria. Such a worst-case design will result in equipment over-design for the usual range of performance criteria and targets. Instead, the transmitter should be designed to provide sufficient power for most of the problems encountered.

Power savings with gating

Gating enables a reduction in required transmitter power. Consider a target to be detected at a range of 3 km with a standard atmospheric visibility of 3 km. The contrast of the target to its background is 2% of that of clear air. If the contrast in clear air (C_0) is 0.4, the contrast for the 2% case (C_1) is 0.008 (0.02×0.4). The ungated trans-

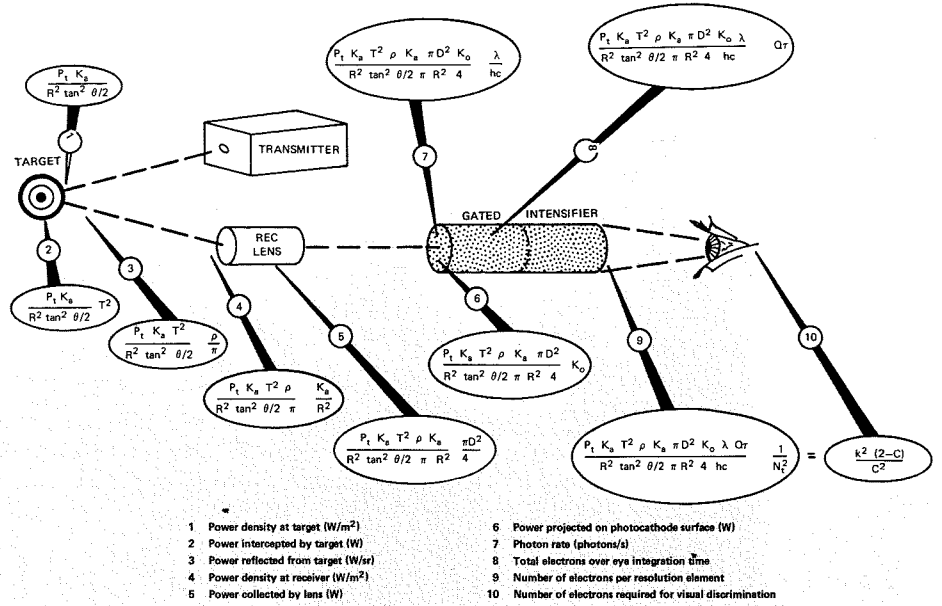


Fig. 7—Round trip of light showing relationships from transmitted power P_t at laser to number of electrons required for visual discrimination at display.

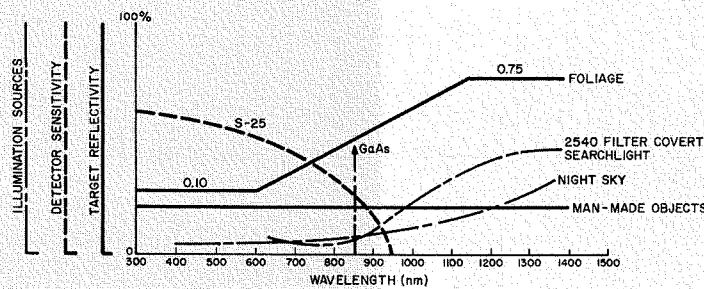


Fig. 8—Detector sensitivity, reflectivities, and illumination sources plotted against wavelength in the near visible spectrum. (Reference: *Electronic Design*, vol. 19, p. 139, Sep. 13, 1969.)

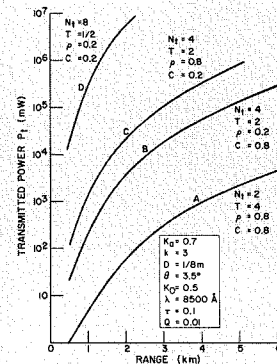


Fig. 9—Power and range relationships for four different target/detection criteria.

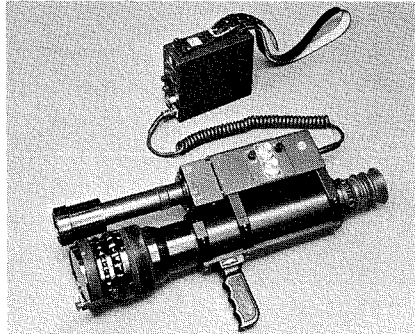


Fig. 10—Laser illumination imaging viewer.

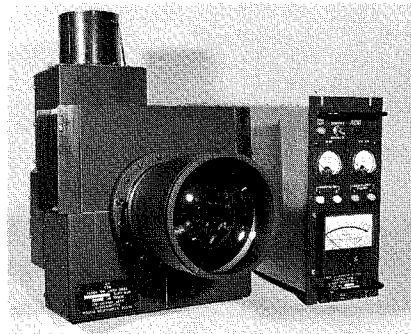


Fig. 11—GaAs illuminator for use with wide angle gated viewing.

mitted power required for the 2% case, not considering absorption and scattering losses, is then

$$P_t (\text{ungated}) = P_o \left(\frac{2 - C_1}{C_1^2} \right) \left(\frac{C_o^2}{2 - C_o} \right) = 3000 P_o$$

where P_o is the transmitted power required in clear air.

For the gated system, the transmitter

power required for the 2% case, not including absorption and scattering losses, is P_o . This shows that even though the conventionally thought of backscatter is not significant, the loss in effective contrast has required an enormous amount of additional power for the ungated case. The visibility (3 km) used in the example is sometimes obtained in the Camden area during the day; night visibilities can be lower.

RCA Gated systems

RCA has constructed many types of gated vision systems and transmitters. Fig. 10 shows a small hand-held unit. The top section is the transmitter; the bottom section with the handle attached is the receiver. The transmitter pulse width is fixed at 100 ns, and the receiver gate width and delay are adjusted with calibrated 10-turn potentiometers. Fig. 11 shows a GaAs illuminator developed for use with wide angle gated viewing. It is capable of high peak and average powers as well as adjustable transmitted pulse width for optimum range gating performance of the system.

Acknowledgment

The author wishes to thank Mr. William Rose of Plans and Systems Development, RCA, for help on the basic equations.

Laser tracking and ranging system

G. Ammon | S. Russell

An engineering model of a pulsed optical radar was developed for NASA to monitor continually the position of an astronaut on the lunar surface. The system tracks and measures range to a cooperative target (retroreflector) up to a distance of 700 m with a range accuracy of ± 1 m and an angular accuracy of ± 1 mrad. The system also directs a TV camera at the astronaut. An optical radar was used because it does not require the large complex antenna system and target reflector of conventional RF radars. The system design, which features GaAs injection laser, small retroreflector target, and silicon photodiode receiver, was directed toward providing a compact, rugged, lightweight system with high accuracy and low power consumption.



G. J. Ammon

Advanced Technology Laboratories
Defense Electronic Products
Camden, N.J.

received the BSEE from Newark College of Engineering in 1961 and the MSEE from the University of Pennsylvania in 1963. He joined the Computer Advanced Development Engineering Department at RCA in 1961 where he worked on the design of ultra-high-speed tunnel-diode memory circuits. He was co-author of a paper entitled "Tunnel-Diode Memory" which was presented at the 1964 IEEE International Convention. In 1963, he joined the logic design group of Computer Advanced Development where he worked on the logical design and checkout of a thin film memory exerciser. Since joining the Advanced Technology Laboratories in 1964, he has worked on the design and test of a sense amplifier and the logic circuits of a 65-ns thin-magnetic-film scratch-pad memory and has developed and evaluated high speed circuits for a plated-wire memory. He has also worked on a low-power monolithic ferrite memory and majority logic circuits and has designed the digital section of the head compensation circuit for a color video recorder. He was also engaged in the development of a 100-megabit analog-to-digital converter. In 1967, Mr. Ammon joined the Applied Physics group of Advanced Technology Laboratories as Project Engineer on a Laser Tracking and Ranging System developed for NASA. Most recently, he has been involved in the development of an Optical IFF system and a GaAlAs Laser Illuminator System. Mr. Ammon is a member of Eta Kappa Nu.



Samuel Russell

Astro-Electronics Division
Defense Electronic Products
Hightstown, N.J.

received the BSEE from Rensselaer Polytechnic Institute in 1956. From 1956 to 1962, he was with the Airborne Instruments Laboratory where he was involved in design, development and system integration work on two aerospace projects. From 1960 to 1962 he was manager of a project to design, develop, and manufacture all hardware for the NASA S-48 fixed-frequency topside-sounder satellite program. This project culminated in the successful Explorer XX satellite. From 1962 to 1964, Mr. Russell was with the Space Systems Division of the Fairchild Hiller Corporation as Manager of Electronic Systems. He was responsible for all electrical design on the Pegasus Meteoroid Detection Satellite. Prior to joining RCA, Mr. Russell was with the Grumman Aircraft Engineering Corporation on the LEM Project. For the past three years at AED, Mr. Russell has been the project manager of the Laser Tracking and Ranging System development and has been responsible for studies of a Lunar Surveying System. He also engaged in the Earth Resources program at AED and is presently manager of Earth Resources project systems engineering. Mr. Russell is a member of the IEEE, AIAA, and American Society for Oceanography. He is a registered professional engineer in New Jersey.

THE LASER TRACKING AND RANGING SYSTEM (LTRS) is an optical tracking radar that continuously provides the range, azimuth, and elevation of a cooperative target relative to the tracking unit. The transmitting source is a GaAs injection laser; the cooperative target is a small retrodirective corner-reflector array, called a retro-reflector.

The development effort was directed toward providing small, compact, and relatively lightweight instrument mainly as a part of the Lunar Surveying System for tracking the movement of an astronaut on the lunar surface. In this application, the astronaut carries a staff to which the retroreflective target is attached. Other possible applications include the LTRS as a navigation instrument for a Lunar Flying Vehicle and as an emergency communications device while monitoring an astronaut during any extra-vehicular activity.

Since demonstration of system feasibility and minimum cost were equally important in developing the engineering model, the design made use of many commercial and readily available components. As a result, equipment size and weight are not representative of a flight-weight configuration. For example, the tracking pedestal weighs 45 lb; in its flight configuration, it may weigh only 20 lb.

The components of the LTRS are shown in Fig. 1. The tracking pedestal contains the laser transmitter, receiver, and servo-driven azimuth and elevation drives. The pedestal also contains a dummy camera substituted for the government-furnished TV camera used

Reprint RE-15-5-15

Final manuscript received October 1, 1969.

in the Lunar Surveying System application. Supplementary servo amplifiers, logic circuits, power supplies, and operating controls are separately rack-mounted. A miniature range computer and the retroreflector complete the system.

Functional description

Functionally, the LTRS consists of two major subsystems—the laser/ranging subsystem and the tracking and acquisition subsystem (see Fig. 2). The laser/ranging subsystem includes the transmitting and receiving sections, ranging computer and electronics, tracking circuitry, and retroreflector. The tracking and acquisition subsystem includes the pedestal structure, the optical encoders, the servo drives, and the acquisition and data buffering logic.

Laser/ranging subsystem

A 300-amp, 75-ns pulse is passed through a large area *GaAs* laser diode to generate the transmitter output light pulse of about 30 W peak. The laser transmitter is operated at a PRF of 360. The narrow, high-current drive pulse is obtained by discharging a bank of capacitors with three SCR's operating in parallel; the capacitor bank is charged to an AGC voltage. Fig. 3 shows the variation of the power output of the laser transmitter with this AGC voltage. Fig. 4 shows the laser output pulse for an AGC voltage of approximately 500 V.

The power was measured at the output of the transmitter with a calibrated photodiode detector. The curve in Fig. 3 shows that the transmitter output can be controlled from a practical upper limit of 31 W to a minimum of less than 1 W. Operation at AGC voltages exceeding 560 V (31-W output) could cause the laser diode to fail. At output levels below 3 W, the junction of the laser diode is partially shut off and the laser beam intensity is not uniform. However, system operation under this condition will still be good.

The laser transmitter radiates in a narrow, rectangular beam. A convex objective lens, slightly defocused, provides the basic $1^\circ \times 3^\circ$ output pattern (see Fig. 5). The beam is wider in elevation than in azimuth to assist in acquiring targets in elevation (in azi-

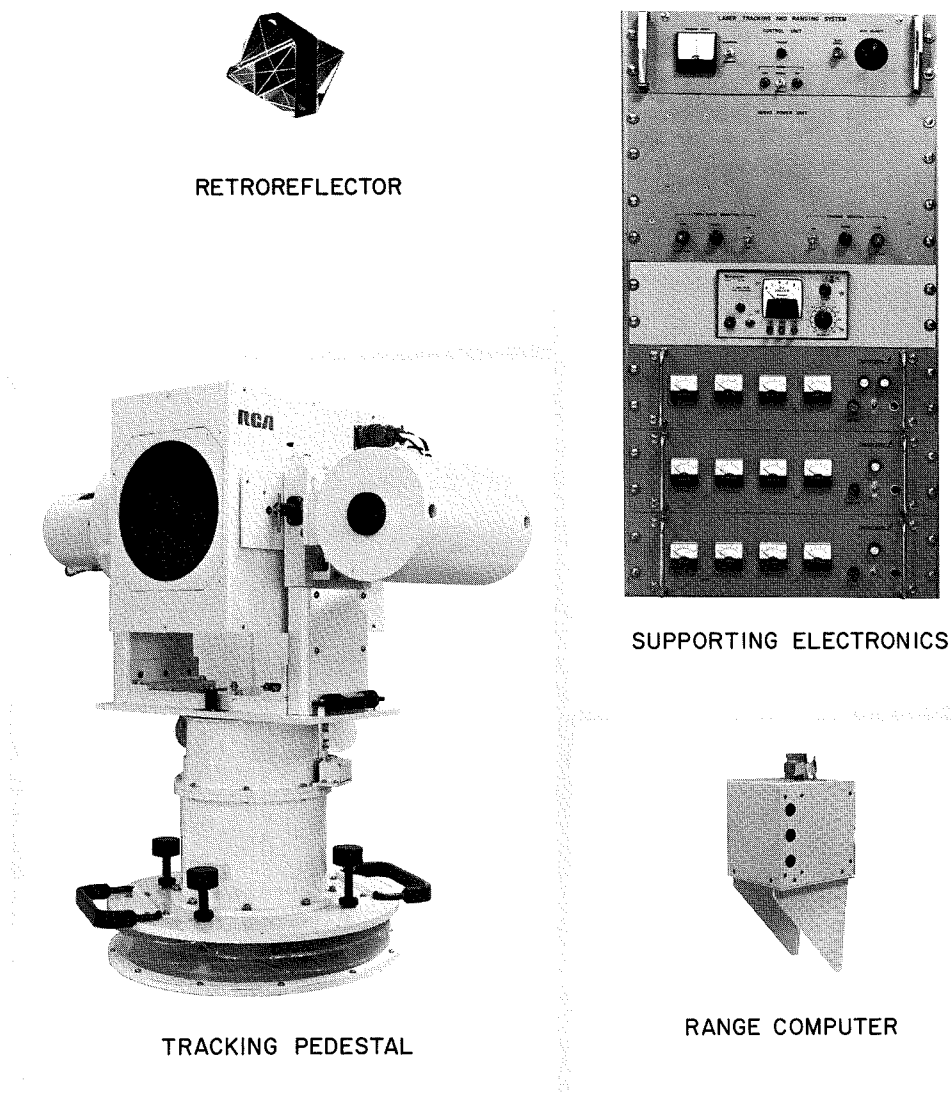


Fig. 1—Components of laser tracking and ranging system (LTRS).

imuth, the narrow 1-degree beam is scanned to acquire targets). A supplementary cylindrical lens in a removable assembly can be slipped over the basic lens to spread the vertical angle to 5 degrees. This provides better coverage in elevation but reduces the maximum range because it spreads the radiated power over a wider angle.

The transmitter mirror directs the laser beam toward the retroreflector target (see Fig. 2). A very small portion of the laser energy passes through this mirror and strikes the start-pulse photodiode detector. The detector output pulse is used as a trigger for indicating the time of transmission of the laser pulse. When the laser beam strikes the retroreflector, a portion of

the light energy will be reflected toward the source. The intensity of the light reflected back to the source is proportional to the beam intensity at the point of interception and the effective retrodirective cross-section of the reflector array. The retroreflector has a relatively constant (within 10%) retrodirective cross-section for any array orientation. Fig. 6 shows the retrodirective cross-section for three different viewing angles.

Most of the return from the retroreflector will pass around the transmitter mirror and be collected by a 5.5-inch mirror located at the rear of the laser telescope. This light energy will be focused onto the face of the quadrant photodiode detector. If the retroreflec-

tor target is located on the optical axis of the receiver mirror, the four sections of the quad detector will be equally illuminated, and the electrical output pulse from each section will have the same amplitude. When the target is located slightly off-axis, the outputs from the detector quadrants will be unequal; the amplitudes will be determined by the direction and amount the target is off-axis.

The electrical outputs from the receiver quad detector and the start-pulse detector are processed to yield angular position and range of the retroreflector relative to the laser unit. The outputs from the quad detector are amplified by four matched pre-amplifiers (A, B, C, and D). Over the operating range of 12 to 700 m, the

are summed and fed into the AGC circuitry. This circuitry adjusts the gain of the four-amplifier peak-detector channels to keep the sum of the peak-detector outputs constant. This makes the tracking error signals relatively independent of target range, thus maintaining system accuracy over a wide range of signal amplitudes.

The AGC is also applied to the laser transmitter to vary the power output inversely as a function of return signal strength from the retroreflector. This action reduces the variation in signal strength that the receiver must handle to the 66-dB range (as previously discussed) at the outputs of matched pre-amplifiers A to D.

Ranging is accomplished by measuring

signals are passed through limiting amplifiers which clip the peaks of the signals but do not disturb the zero crossing. Schmitt triggers then sense the zero crossings and trigger two high-speed monostable multivibrators which generate the very sharp START and STOP pulses to the range counter. This pulse-processing technique has produced excellent results even though the level of the signals into the summing amplifier and start-pulse detector varies over a very wide range. The transmit and receive ranging electronics were designed to be identical to cancel time-shift errors due to temperature and other effects.

The range computer measures the time delay between the START and STOP pulses (pulse transit time) to an accuracy of ± 3.33 ns ($\pm \frac{1}{2}$ m of range). The range computer consists of an interpolating time-interval counter (purchased from Nanofast, Inc.) and control circuitry that permits averaging of measurements. This unit can average the results of 32 measurements to reduce quantizing errors and random errors. The range computer generates a range "read" signal only if all of the averaged measurements are less than 1536 meters, permitting transfer of the range data to the data buffering logic. (The limit of 1536 m was selected to allow for possible system operation out to approximately twice the required range of 700 m.)

A range function generator is activated by the START pulse to establish the minimum return signal amplitude necessary to enable the counter STOP pulse for ranges up to 100 m (667 ns). The threshold level was determined by comparing the return from the retroreflector with that from background objects at the same range. Returns from the retroreflector target at various ranges will exceed the range function generator output and enable the counter STOP pulse. Returns detected from background objects will be smaller than the range function generator output, and the counter STOP pulse will not be generated. The STOP pulse is used to set a flip-flop in the range computer. The output from this flip-flop is the track command which indicates to the acquisition logic in the tracking and acquisition subsystem that a valid target is within the field of view.

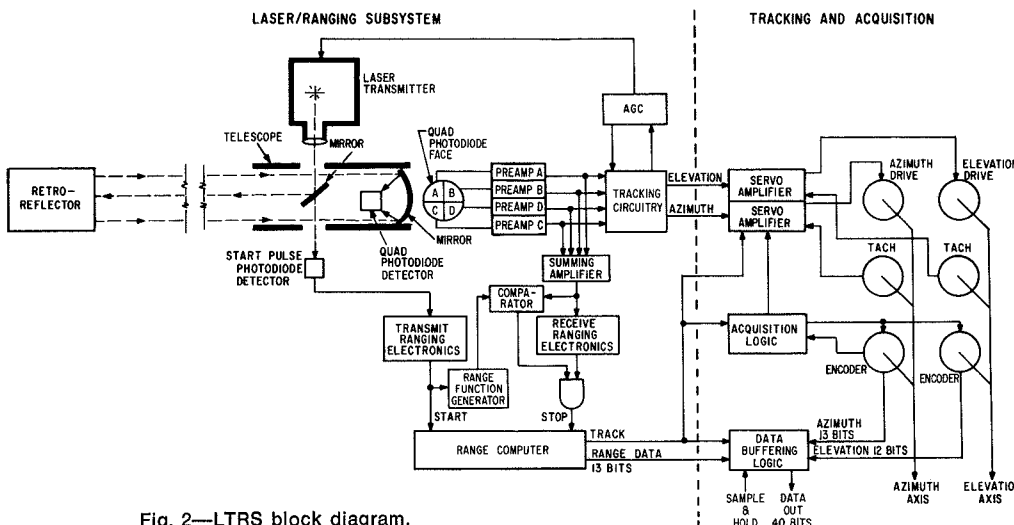


Fig. 2—LTRS block diagram.

output level from these amplifiers will vary approximately 66 dB.

The tracking circuitry contains four matched voltage-controlled pulse amplifiers whose gain can be varied approximately 66 dB. The gain of these amplifiers as a function of AGC voltage is matched to within 20%. The pulse outputs from these amplifiers are peak detected to yield DC levels proportional to the amplitude of the pulses. The elevation and azimuth error signals are then given by:

$$\begin{aligned} \text{elevation error} &= (A+B) - (C+D) \\ \text{azimuth error} &= (A+C) - (B+D) \end{aligned}$$

where A, B, C and D represent the DC outputs from the four-amplifier peak detector channels in the tracking circuitry.

Peak detector outputs A, B, C, and D

the transit time required for the laser pulse to reach the retroreflector and return. Every 6.6712 ns of round-trip transit time corresponds to 1 m of range. The signals from the start-pulse detector and summing amplifier are used to generate the START and STOP trigger pulses to the counter in the range computer. An overall system range accuracy of ± 1 m is attained by measuring the transit time of the laser pulse to within 3.33 ns and processing in the pulse circuitry to within an additional 3.33 ns. A unique pulse-processing technique was employed in the ranging electronics to achieve this accuracy. The signals out of the start-pulse detector and summing amplifier are differentiated to obtain a bipolar signal with a zero crossing corresponding to the peak of transmitted and received laser pulses. These bipolar

Tracking and acquisition subsystem

The tracking pedestal structure shown in Fig. 7 is designed to mount and aim the laser transmitter and receiver and the boresighted tv camera. A dummy tv camera and sighting scope are shown mounted in the structural location designed for the government-furnished operational tv camera. The tracking pedestal is connected to the mounting base through a ball joint and is held in position by four leveling screws. The ball joint and interconnecting cables are maintained dust-free by enclosure in a plastic bellows.

The azimuth-drive and azimuth encoder are contained within the cylindrical assembly above the leveling plate. This assembly has an annular construction, with all electrical cabling in the open center. This construction provides the required azimuth freedom without the need for slip rings.

The azimuth axis has a mechanical travel of $\pm 185^\circ$, with urethane-faced shock isolators at the limits. Electrical drive limit switches are actuated at $\pm 180^\circ$ of travel. The electrical and mechanical limiting devices are located externally just under the azimuth turntable. The azimuth axis uses a single, four-point-contact ball bearing, which is permanently lubricated and sealed with a teflon ring and a garter spring. A lock pin is provided to fix the azimuth axis during handling and setup of the tracking pedestal. Two bubble-levels are provided for accurate leveling of the instrument.

The elevation axis has a mechanical travel of $+90^\circ$ to -50° , also limited by shock isolators. The $+90^\circ$ position allows access to the tracking receiver, which is located on the underside of the laser transmitter and receiver unit. Electrical limit switches are actuated at $\pm 45^\circ$, which inhibit electrical drive beyond these points. Freedom in elevation is provided by two bearings supported by a yoke assembly, which is mounted to the azimuth axis. Four-point-contact bearings are used and are sealed in the same manner as in the azimuth axis. The elevation drive and encoder are located on one side of the yoke. A lock is provided on the elevation axis to hold the assembly in position during setup.

Servo Design

Azimuth and elevation servos were designed for 1) a dynamic target-

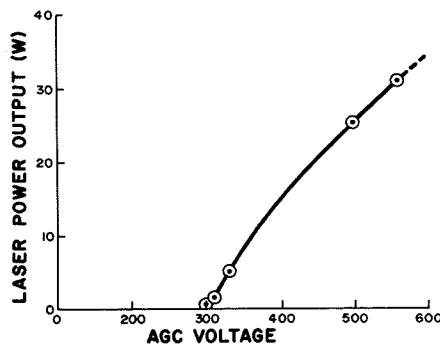


Fig. 3—Effect of AGC voltage on laser transmitter output.

following error of less than 0.5° when tracking a target at $20^\circ/\text{sec.}$, and 2) a capability to acquire and lock-on to a stationary target from a $10^\circ/\text{sec.}$ scanning velocity. This latter requirement established the servo motor sizing and power consumption. The azimuth axis will be described here since it has greater inertia and a smaller beam-width and, thus, provided the more difficult design.

Lock-on

The size of the azimuth motor was established on the basis of the torque needed to stop the azimuth axis inertia within 0.5° upon receipt of a lock-on signal. The track signal is obtained from the ranging circuitry in the range computer and has a time constant of less than 20 ms. The angular stopping distance is determined by the pedestal angular momentum and the motor and friction torques available for stopping the pedestal.

Inertia

Since azimuth inertia affects stopping distance directly, the pedestal was designed for minimum inertia. In the original configuration investigated, the azimuth axis was a column which supported the elevation drive unit directly above, with the tv camera and laser transmitter and receiver unit mounted outboard to either side of the drive unit. The azimuth inertia for this configuration was at least 5 in-lb/s². It was reduced to 3 in-lb/s² by changing to the current yoke design in elevation

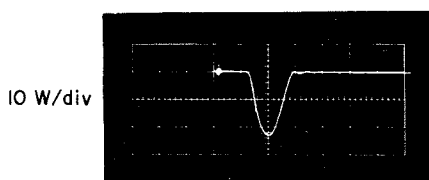


Fig. 4—Laser output at 500-V AGC.

in which the greatest inertia member (the laser transmitter and receiver unit) is mounted directly over the azimuth axis.

Motor selection

An Inland Motors T4424 torque motor was chosen for its high torque, good torque-to-weight ratio, and favorable diameter. Before friction and inertia levels were well established, it was decided that one motor should be used in elevation and one in azimuth, but with provision for an additional motor in azimuth if required. (On a weight basis, two T4424's in azimuth are better than a single motor with equivalent torque output.) The azimuth power amplifier was chosen to provide the power reserve. Subsequent estimates of inertia and friction indicated that only one motor was required in azimuth.

Tachometer loop

High gain is desirable in the tachometer loop for saturation of the power amplifier resulting in maximum torque for lock-on, and for high torque sensitivity to minimize static error due to friction and wind torques. Tachometer loop gain is limited by

- 1) The effect of the pedestal resonant frequencies,
- 2) The tachometer ripple voltage at maximum tracking rate, and
- 3) The laser receiver noise level.

Inland Motors TG-4401-B tachometer is dimensionally compatible with the torque motor and has the highest gain of any standard winding. The spatial ripple frequency is 71 cycles/revolution. At $20^\circ/\text{sec.}$, this frequency is 4 Hz; at lower tracking rates, it is proportionally lower. A significant reduction in ripple by filtering was not feasible. The design value for the tachometer loop gain was established at 427, which is just below the value that would cause saturation of the servo amplifier from the ripple.

Tracking loop

The azimuth tracking loop employs typical lag-lead compensation for stabilization. The bandwidth of the system is low (slow servo response) consistent with the target dynamics because:

- 1) Fast servo response might adversely affect tv image quality when tracking

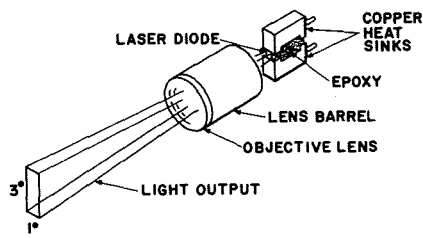


Fig. 5—Laser diode assembly and basic optics.

an astronaut moving erratically or in short jerky motions.

2) Wide bandwidth would cause greater noise perturbation of the axis with the target stationary at maximum range.

3) Low bandwidth aids in maintaining lock-on near maximum range where noise is most significant.

The operational reasons for using a low bandwidth are supplemented by power and weight considerations. If the structural resonant frequency in either axis is to be a decade above the loop cross-over frequency, it is clear that increasing the crossover frequency results in increasing the minimum structural resonance by the same ratio. For a given structural configuration, this is reflected in greater weight. For an increased weight, increased power is also required to maintain the same lock-on performance. Therefore, to arrive at a lightweight, smooth-tracking pedestal design for flight use, the bandwidth is designed as low as possible, consistent with the maximum target dynamics.

Servo operation

The azimuth and elevation servos differ only in that the azimuth axis has a scan velocity input for acquisition scanning and the azimuth servo amplifier has a higher drive capability than the elevation servo amplifier.

For each axis, the tracking servo signal is amplified in a compensation amplifier and then supplied to the servo amplifier. The compensation amplifier gain establishes the dynamic following error of 0.5° for a scan rate of $20^\circ/\text{sec.}$ and provides balance and gain controls.

The output of the compensation amplifier is gated by the track command and the slew control relay to the servo amplifier which drives the torque motor for that axis. Velocity feedback is provided to the input of the servo amplifier by a dc tachometer.

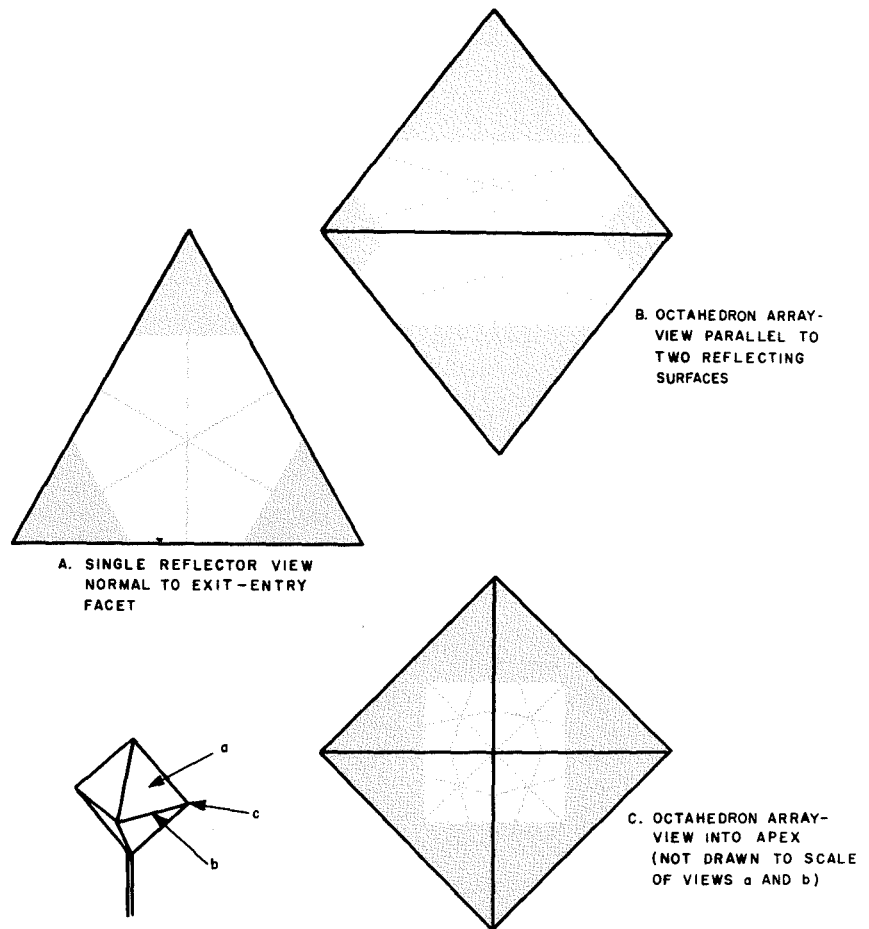


Fig. 6—Retrodirective cross-section of retroreflector for three viewing angles.

When the track command or slew control relay opens the tracking loop, the velocity loop acts as a speed-control servo for acquisition scanning or slew control. When the tracking loop is closed, the system acts as a position servo stabilized by velocity feedback.

Operating modes and logic

Operating modes

The azimuth and elevation servos and acquisition logic are designed to provide 1) target tracking and 2) acquisition scanning when the target track is lost. The tracking and acquisition subsystem functions in four basic modes of operation:

1) *Tracking and acquisition scanning mode.* This is the primary mode used for tracking and reacquiring a lost target. The target is tracked within azimuth and elevation limits if the received signal is above the threshold. If the target is lost, the azimuth and elevation axes are stopped at the point of target loss. After a 10-second interval, if the target has not been reacquired, an azimuth search is begun which scans an ever-increasing angle until the target is reacquired or the

electrical limit is reached. When the target is reacquired, normal tracking resumes.

2) *Limit scan mode.* When an azimuth electrical limit is reached during acquisition scanning, the scanning mode changes to one where the pedestal scans between the electrical limits until the target is reacquired. This limit scan mode is also entered if an electrical limit is reached during tracking and the target is subsequently lost. This allows the system to follow a target through the azimuth limits. There is no time delay before this scan begins.

3) *Acquisition scan disable.* A control is provided that disables the acquisition scanning mode. With the scan disabled, if the target is lost, the tracker remains indefinitely at the position it had when the target was lost. However, if track is lost beyond an electrical limit, the limit scan mode, which is not disabled, is entered, allowing the LTRS to "track through" the azimuth limit.

4) *Manual remote positioning.* The pedestal may be manually positioned by the actuation of a slew control and operation of a two-axis joy stick, which is used to insert small, variable velocities into the azimuth and elevation axes. The slew control overrides all other operating modes (tracking, acquisition scanning, and limit scanning). When the slew control is

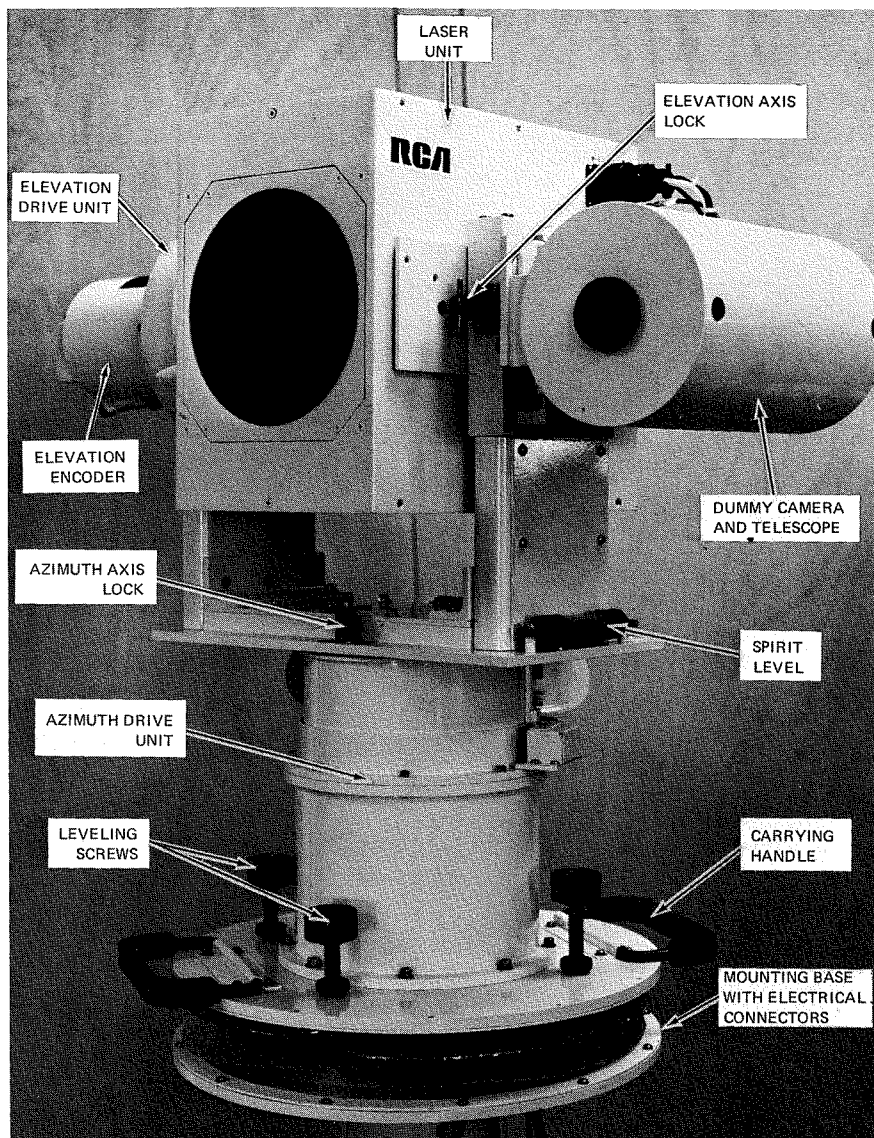


Fig. 7—Tracking pedestal structure.

released, tracking resumes if the target is within the receiver field of view; otherwise acquisition scanning starts after a 10-second delay.

Acquisition control logic

The acquisition control logic provides the control for the acquisition scanning, limit scan, and manual remote positioning. Control of the acquisition scan pattern is determined by the track signal from the range computer. With a track condition, all acquisition logic is held in a reset state which keeps the azimuth and elevation tracking loops closed.

When the track command is lost, the reset condition is terminated and two one-shot multivibrators are triggered in sequence, providing a time delay of 12 seconds. At the end of this time, a scan control flip-flop is triggered and

an output of the azimuth encoder is gated into a divide-by-eight counter. The output of the divide-by-eight counter cycles every $11\frac{1}{4}^\circ$, which is the basic increment of the acquisition scanning pattern.

The acquisition scanning pattern is shown in Fig. 8. The azimuth servo is activated until the retroreflector has been detected or until the system has rotated $11\frac{1}{4}^\circ$. If the $11\frac{1}{4}^\circ$ mark is reached without detecting the retroreflector, the acquisition logic reverses the azimuth servo, and the unit will scan in the opposite direction until the target is detected or the unit has rotated $22\frac{1}{2}^\circ$ past the point of target loss. If the $22\frac{1}{2}^\circ$ of rotation mark is reached without detecting the retroreflector, the unit will again change direction and scan for an angular rota-

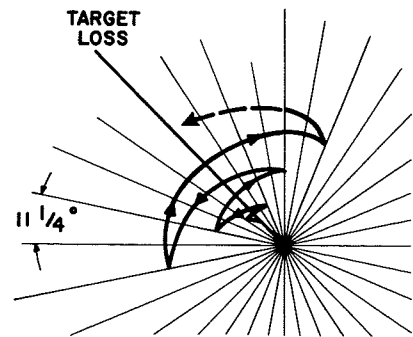


Fig. 8—Acquisition scanning pattern; pattern continues until retroreflector is detected or electrical limit is reached.

tion of $33\frac{3}{4}^\circ$ past the point where the target was lost.

This scan pattern is repeated, each time incrementing the amount of rotation, until the retroreflector is detected or an electrical scan limit is reached. When the scan limit is reached, the limit scan mode is entered.

Data buffering logic

The data buffering logic provides a temporary store of azimuth, elevation, and range data to be sampled by an external data subsystem. Upon receipt of a sample-and-hold signal, azimuth and elevation data are transferred from the encoders into the first 25-bit positions of the buffer. Range data, which is computed continually, is transferred into bit positions 26 to 37 as soon as computed. However, the sample-and-hold signal inhibits the transfer to prevent erroneous range data if sampling were to take place during a range data transfer. Bit position 38 is a status indicator, showing whether or not the range data has been updated since the preceding sample-and-hold pulse. The remaining two positions are status indicators which are made available to the external data subsystem from the acquisition logic—bit 39 indicates the track condition and bit 40 indicates acquisition scanning.

Results and conclusions

The LTRS design approach attained a compact, rugged, lightweight system with high accuracy and low power consumption. Performance met the required specifications. Tracking of the retroreflector target from 12 to 700 m was demonstrated with azimuth and elevation angular accuracies of ± 1 mrad and a range accuracy of ± 1 m. Extension of the range capability to 8000 m with a ranging accuracy of ± 0.5 m is considered possible for a flight instrument.

Effectiveness of IR covert illuminators

F. J. Gardiner

IN MANY APPLICATIONS OF ELECTRO-OPTICS NIGHT-VISION TECHNOLOGY, the available natural illumination is insufficient to provide the desired resolution or image quality. In those cases, it is frequently desired to provide illumination which is covert and cannot be seen by the unaided human eye. In addition to providing illumination, lasers can provide a covert means of measuring range and of designation. The question is "how covert are these devices?" It is hardly surprising that the human eye can see to some degree in the infrared spectrum. Fig. 1 shows the sensitivity of a standard human eye. The lumen unit is devised specifically to express the characteristics of the human eye. By converting any given monochromatic light power from watts to lumens, its effectiveness in providing illumination to the human eye is determined. Whereas the number of lumens/watt in the red spectrum falls steeply, it does not go suddenly to zero. Several investigators have reported the sensitivity of the human eye to IR energy. Walraven and Leebeck give a good summary, which is reproduced as Fig. 2.¹

It has been possible to obtain field test data points (Table I), which provide remarkably close agreement with theoretical estimates. Although additional test points would be welcome, it is to be suspected that the human ability to see infrared radiation varies widely and is effected by race, age, and diet; thus it is not worthwhile to try to achieve a high degree of accuracy based on test data on several human subjects which are probably fairly homogeneous in any event.

Table I—Field test data points.

	A	B
Wavelength (μm)	0.945	0.85
Power output (watts)	1/6	0.85
Beam size (degrees)	16	15
Visibility range (m)	4/5-8	120

This paper provides a practical approximation to the visibility of infra-

Both theoretical and experimental data are presented which lead to a method of estimating the visibility of IR "covert" light sources by human observers. Good agreement is found for a simple formula between its theoretical derivation from standard photopic and scotopic vision data and some field measured data. Means of estimating covertness are presented for GaAs and Nd lasers as well as tungsten and xenon filtered IR/CW sources. These same illuminators are also analyzed for the illumination capability with S-25 photo-emitter receivers and the covert effectiveness of each type of illuminator is assessed. Eye safety for these illuminators is also discussed. It is concluded that near IR sources are, in general, not really covert, but are rather simply less visible than so-called visible sources.



Frank J. Gardiner, Mgr.
Systems Development and Application
Aerospace Systems Division
Burlington, Mass.

received the BS in Aero-Thermodynamics from the Massachusetts Institute of Technology in 1943. After graduation he was commissioned in the U.S. Navy and served with the Pacific Fleet and later with the Bureau of Aeronautics in Washington. In 1947 he became Chief Engineer of Special Products Division, ITE Circuit Breaker, Philadelphia; principal products were microwave antennas and devices for both radar and communication systems. In 1955, he became manager of the division supplying these products. In 1961 he joined RCA, Major Systems Division, and was assigned responsibility for space systems activities. Starting in 1962, he was responsible for RCA's LEM activities as study manager, proposal manager and then program manager at ASD. In 1967, his responsibility was increased to include all tactical and space programs, and in 1969, he was assigned responsibility for Systems Application Engineering.

red sources. An estimate which is correct within a factor of two is quite an acceptable success considering the degree of knowledge and the probable scatter of human eye sensitivity.

Analysis

The ability of a human to detect a point source in relative darkness is given in Fig. 3 as approximately 10^{-7} or 10^{-8} lm/m². This threshold illuminance (I_t) should fit the available test data.

If a source of monochromatic power P (watts) radiates all its energy into a beam whose dimensions are $(\theta \times \theta)$ radians, then the power incident on the recipient at range R (meters)

$$I = \frac{P}{(R\theta)^2} \text{ (watts/m}^2\text{)}$$

Using a K_λ for converting lumens to watts allows the incident power I to be expressed in lumens/m².

Thus the threshold illuminance will be achieved when

$$I_t = \frac{P}{(R\theta)^2} K_\lambda \text{ (lm/m}^2\text{)}$$

As pointed out in Ref. 1, the long K_λ is inversely proportional to λ . This is based on theoretical consideration of the energy in a photon as well as experimental data. The slope of this relation may be found to be

$$\log K_\lambda - \log K_{\lambda'} = \frac{100}{6} \left(\frac{1}{\lambda} - \frac{1}{\lambda'} \right)$$

$$\therefore K_\lambda = K_{\lambda'} \times 10^{\frac{100}{6} \left(\frac{1}{\lambda} - \frac{1}{\lambda'} \right)} \quad (1)$$

Eq. 1 has been patched onto the standard scotopic lumen-watt conversion

Reprint RE-15-5-16
Final manuscript received 25 April 1969

Fig. 1 to extend it into the IR spectrum. The result is shown in Fig. 4.

Now substituting this

$$I_t = \frac{P}{(R\theta)^2} K_\lambda' 10^{\frac{100}{\theta}} \left(\frac{1}{\lambda} - \frac{1}{\lambda'} \right)$$

$$\therefore \frac{I_t}{K_\lambda'} 10^{\frac{100}{\theta}} = \frac{P}{(R\theta)^2} 10^{\frac{100}{\theta}}$$

$$= C \text{ (watts/m}^2\text{)} \quad (2)$$

The value of C , which is a constant for any given human observer, (probably at any one time) can be extrapolated from Figs. 1 and 2 and also can be fitted to test data in the IR spectrum.

By using Eq. 2, data point A from Table I gives a value for C of 6×10^{16} watts/m² and data point B gives a value of 3×10^{16} watts/m². If based on Fig. 3, the value of I_t is taken as 10^{-8} lm/m² representing scotopic eye sensitivity; a point on the scotopic luminosity curve (Fig. 1) is chosen at $K_\lambda = 0.1$ lm/watt at $\lambda = 0.71 \mu\text{m}$; and the computed value of C is 3×10^{16} watts/m², which shows rather good agreement with the experimental points.

If this same calculation is repeated at the edge of photopic vision, then (from Fig. 3) $I_t = 10^{-7}$ lm/m² and (from Fig. 1) $K_\lambda = 0.1$ when $\lambda = 0.745 \mu\text{m}$. Using these values, the constant C is computed at 2.6×10^{16} watts/m². This indicates that the eye condition (scotopic versus photopic adjustment) is not a critical factor. The increased sensitivity ($\lambda\text{m/m}^2$) in the scotopic state is offset by the shift away from red sensitivity.

Thus, a reasonably good and conservative mathematical approximation may be used with $C = 3 \times 10^{16}$ watts/m². These approximations can probably be used from the visible red ($0.65 \mu\text{m}$) to the near infrared ($1.1 \mu\text{m}$).

$$\frac{P}{(R\theta)^2} 10^{100/\theta} = 3 \times 10^{16} \text{ watts/m}^2 \quad (3)$$

The value of C at $0.945 \mu\text{m}$ is somewhat higher than the smoothed proposed value of C shown above. In part, this is due to the appearance of another factor. As shown in Fig. 2, the liquid media in front of the eye's receptor absorbs energy significantly between $0.93 \mu\text{m}$ and $1.03 \mu\text{m}$ having a minimum transmittance of 25% at about $0.96 \mu\text{m}$. Thus, the proposed value of C will give too high a visibility range at this wavelength by about $(1/0.25)^{1/2} = 2$. For simplicity, this is

noted but not taken into account. This absorption is negligible outside the stated wavelength range.

Broad spectrum sources

Whereas monochromatic illuminators can be readily calculated from the above for value, other useful illuminators have broad spectral outputs and must be analyzed by a more tedious

method. Such an analysis has been done for a CW xenon arc lamp and a tungsten filament lamp operating through several IR filters.

Figs. 5 and 6 show typical spectral distributions of xenon arc and tungsten lamps. Fig. 7 shows spectral transmittance of four IR filters. This spectral distribution of the lamps, when multiplied by the filter transmittance and

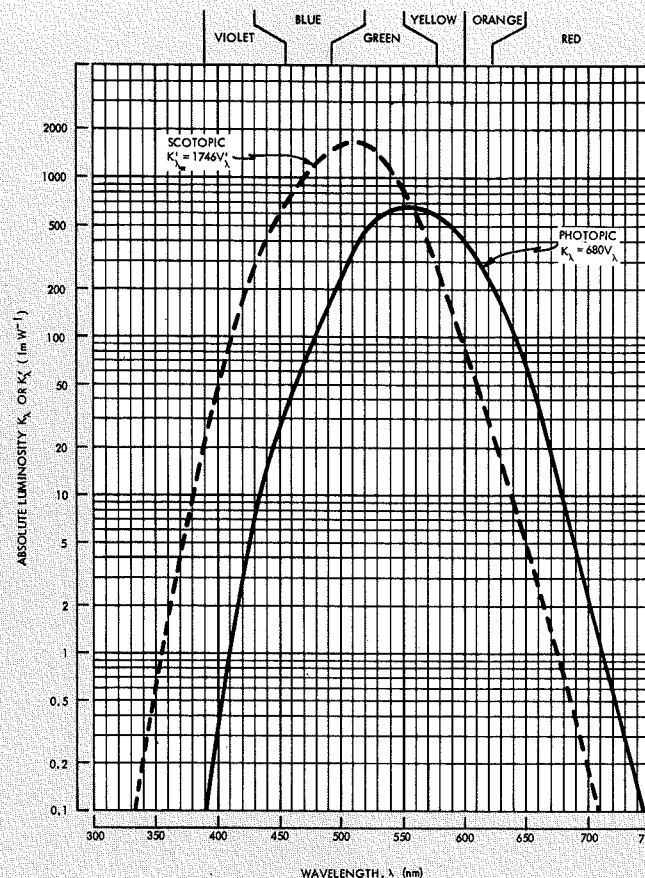


Fig. 1—Absolute luminosity curves K_λ and K_λ' as functions of wavelength (response of the human eye to radiation of a given wavelength).

Table II—Filter attenuation factors for filters A, B, C, D.

Source	Filter	Watts out Watts in	Reduction in lumens due to filter	Reduction in S-25 response	S-25 response (A/W)	Eye response (lm/W)	Covert illum effectiveness (A/lm)	Scene illum at maximum eye detection range (W/m ²)
2854°K black body	None	1.00	1.00	1.00	3.4×10^{-3}	19.00	0.18×10^{-3}	5×10^{-10}
	A	0.78	1.55×10^{-4}	0.216	7.4×10^{-4}	2.9×10^{-3}	0.255	2.6×10^{-6}
	B	0.76	1.21×10^{-5}	0.137	4.7×10^{-4}	2.3×10^{-4}	2.05	3.1×10^{-5}
	C	0.74	1.21×10^{-9}	0.078	2.7×10^{-4}	2.3×10^{-5}	11.7	3.0×10^{-4}
cw xenon (Typical)	None	1.00	1.00	1.00	2.3×10^{-4}	20.00	0.115×10^{-4}	5×10^{-10}
	A	0.8	6.5×10^{-7}	0.152	3.5×10^{-5}	1.3×10^{-5}	2.7	6.3×10^{-4}
	B	0.74	5.6×10^{-8}	0.121	2.8×10^{-5}	1.12×10^{-6}	25.00	6.7×10^{-3}
	C	0.68	1.06×10^{-8}	0.084	2.0×10^{-5}	2.30×10^{-7}	86.5	3.0×10^{-2}
GaAs laser 8500 Å	None				1.0×10^{-5}	3.0×10^{-8}	333.0	2.1×10^{-1}
	D	0.72	1.37×10^{-7}	0.038	1.3×10^{-4}	2.6×10^{-6}	50.00	2.6×10^{-3}
	D	0.64	1.5×10^{-9}	0.042	1.0×10^{-5}	3.0×10^{-8}	333.0	2.1×10^{-1}
	D	0.64	1.5×10^{-9}	0.042	1.0×10^{-5}	3.0×10^{-8}	333.0	2.1×10^{-1}
Nd laser 10600 Å	None				6×10^{-3}	1.3×10^{-5}	300.0	7.7×10^{-4}
Ruby laser 6943 Å	None				$S1 = 6 \times 10^{-4}$	1.6×10^{-9}	230,000	6.2
Ruby laser 6943 Å	None				25×10^{-3}	0.25	0.1	4×10^{-8}

further multiplied by the relative eye IR sensitivity as expressed by the above equation, yields a spectral sensitivity distribution which can be integrated to provide a single value of lumens output per watt of input. Table II summarizes these results. Armed with this datum, the nomograph in Fig. 8 allows rapid estimation of visibility range for several monochromatic and broadband illuminator and filter combinations. It is noted that the "covertness" of several "covert" illuminators is clearly a matter of degree.

Electro-optic imaging devices vs. the eye

It is also possible to multiply and integrate the spectral distribution of these lamps and filters with the spectral sensitivity of a good photoemitter such as the S-25 shown in Fig. 9. This results in a conversion efficiency which can be expressed in amps/watt where the watts are the total power into the illuminator and the "amps" is the resultant photoelectron current, assuming that all the radiated energy which passed through the filter is captured by the photocathode.

This conversion efficiency (amps/watt) is also shown in Table II. The ideal illuminator is one which will be very covert (i.e., produce very few lumens/watt) and at the same time will produce maximum photoelec-

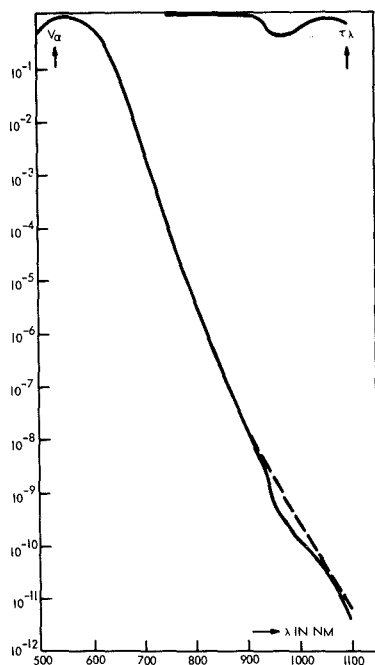


Fig. 2—The transmittance τ_λ of a layer of water of 24 mm (representing the eye media) —the theoretical curve (solid) of the receptor sensitivity, and the eye-sensitivity curve (dashed) in which the transmittance of the eye media is taken into account.

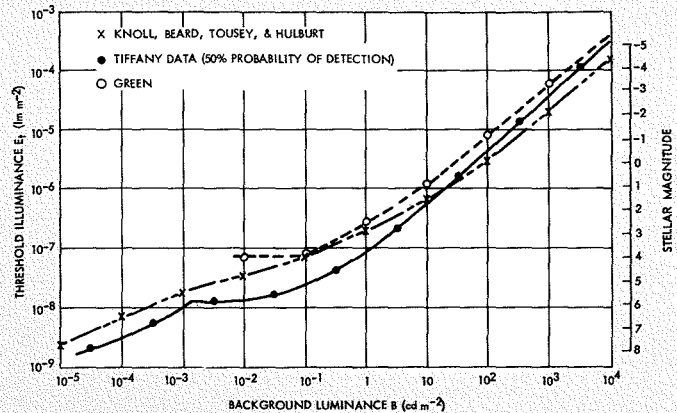


Fig. 3—Threshold illuminance for human eye from a fixed, achromatic point source as a function of background luminance (adapted from Middleton, Ref. 4, with permission).

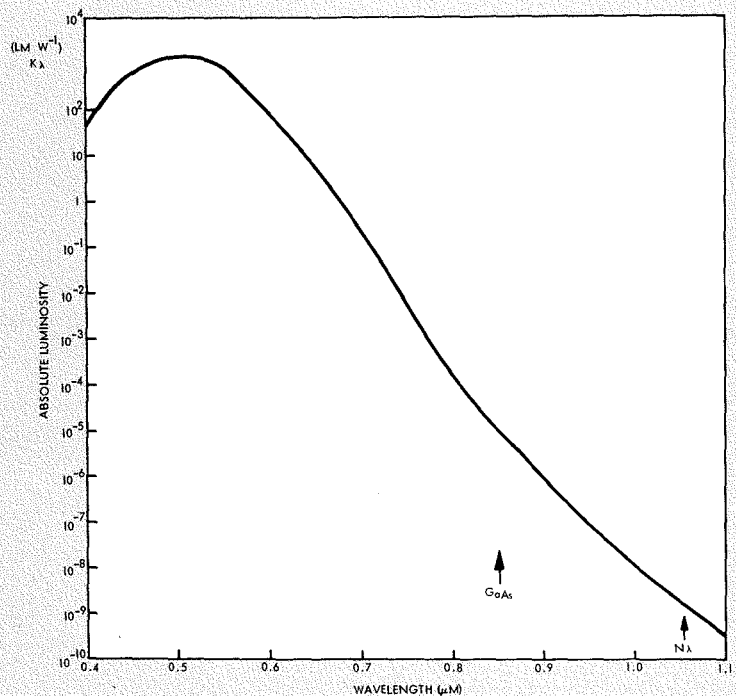


Fig. 4—Standard scotopic lumen-watt conversion.

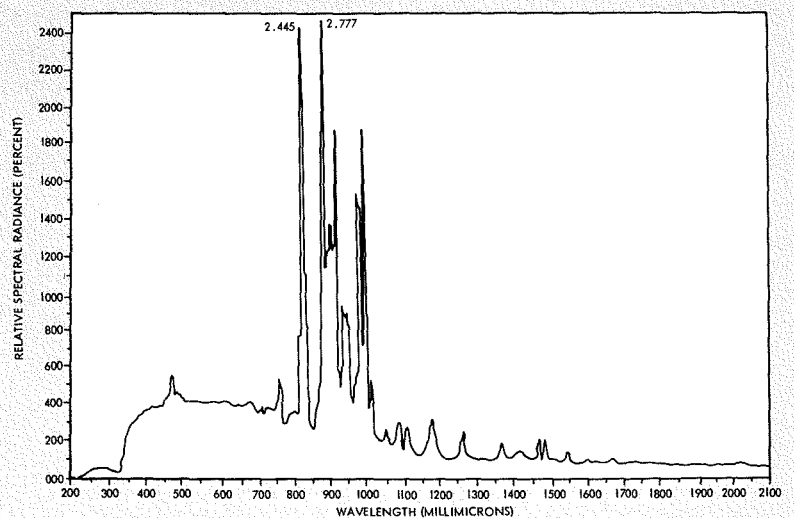


Fig. 5—Spectral radiation distribution—xenon arc.

trons/watt of input. The ratio of these quantities (amps/watt divided by lumens/watt equals amps/lumens) expresses the effectiveness of the illuminator type independently of its power level, beamwidth, etc. This ratio is also

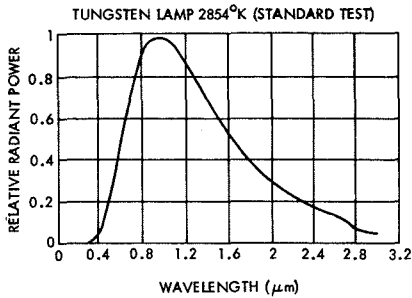


Fig. 6—Relative radiant power vs wavelength (tungsten lamp 2854°K).

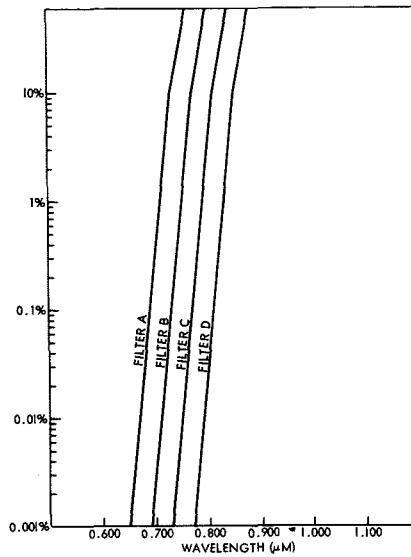


Fig. 7—Special transmittance and four IR filters.

shown in Table II. It is noted that the "darker" filters are preferred to the "pink" filters and that xenon is preferable to tungsten light sources with any given filter, and, further, that GaAs laser illuminators are comparable to the very darkest (best) xenon filtered lights. Ruby lasers, on the other hand, compare to "pink" filtered tungsten lights and, finally, the Nd laser is outstanding in its covert capability.

Eye damage threshold

The power density at the limit of the visibility range is merely the Point Source Threshold Illuminance (I_s) divided by the conversion vector (K_s) $lm/watt$. This power density is also shown in Table II. For cw illuminators, it is clear that this is far below any possible eye damage threshold, when it is recalled that the common and harmless experience of looking at a 100-watt tungsten lamp from a distance of about 10 feet produces about 1 watt/m² of power density.

Since a typical GaAs laser is pulsed at several kHz, the individual pulse energy density at the visibility range is trivial, e.g., for 5 kHz PRF, the pulse energy density will be $7.5 \times 10^{-4} / 5 \times 10^3 = 1.5 \times 10^{-7}$ joules/m², which is many orders of magnitude below a safe limit which is typically set at 10^{-1} joules/m² for Q-switched lasers. Thus, the GaAs laser can be seen long before any possible eye damage can occur both from cw and pulse viewpoint.

A similar exercise with Nd shows that visibility occurs at about 6 watts/m², which may or may not be a safe level. If, for instance, we are considering a Q-switched laser at 10 pps, the limit established by the Office of the Surgeon General of 10^{-3} joules/m² is exceeded, but the current U. S. Air Force limit of about 4 joules/m² is not exceeded. In any event, it seems that "seeing" Nd may not be a really safe experience.

References

1. Kingslake, R. *Applied Optics and Optical Engineering*, Volume I "Light: Its Generation and Modification," (Academic Press, New York and London, 1965).
2. Walraven, P. L. and Leebeck, H. J. "Forced Sensitivity of the Human Eye in the Near Infrared," *J. Optical Soc. of Amer.*, Vol. 53 (June 1963) p. 765.
3. Private Communication from Mr. Attilio Matterna, U.S. Army Night Vision Lab, Fort Belvoir, Va. (Feb. 1969).
4. Middleton, W. E. K. *Vision Through the Atmosphere* (University of Toronto Press, 1958).
5. *Laser Health Hazards Control Air Force Manual* 161-8, (April 1, 1969).

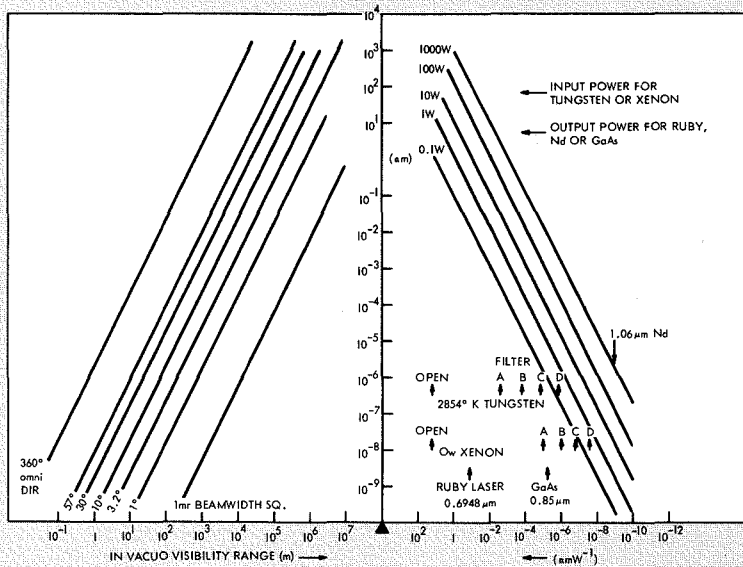


Fig. 8—Nomograph.

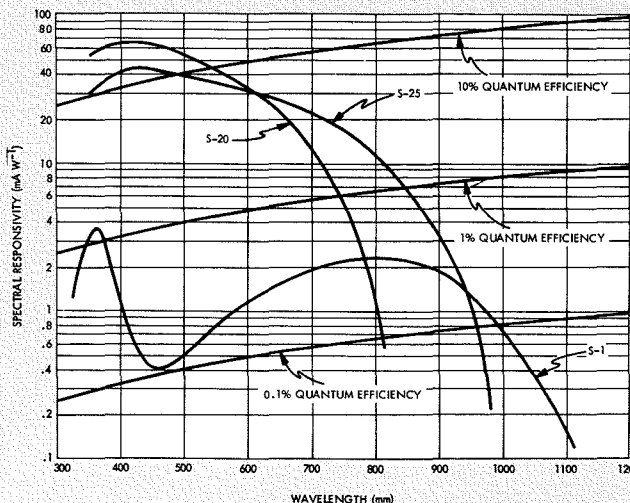


Fig. 9—Visible and near-IR photoemitter characteristics. Absolute spectral responsivity of various photocathode-window combinations useful for the visible and near infrared.

Tradeoff analysis of neodymium and ruby laser rangefinders

E. Kornstein | N. A. Luce

Early pulsed laser rangefinder systems mainly used ruby as the active material. The availability of neodymium-doped materials such as glass, tungstate, yttrium aluminum garnet, fluorapatite, yttrium vanadate, and others has raised the question of suitability of these materials compared with ruby for pulsed laser rangefinders and illuminators. The controlling factors appear to be the properties of the atmosphere along with receiver capability. For practical applications, factors such as efficiency, visibility, safety and other operational parameters must be taken into consideration. The analysis and development of laser range equations has been the subject of previous accounts,^{1,2,3,4} and only the results pertinent to the present application will be presented.

THE MAJOR AREA OF UNCERTAINTY in predicting the performance of rangefinders is the influence of the atmosphere. The atmosphere scatter (and especially backscatter) is difficult to predict, and, in fact, it can be shown that no generally valid relation exists between the atmosphere backscatter properties⁵ and meteorological visibility. The nearest generally valid form is⁵

$$V = \frac{3.9}{\alpha} = C (\alpha_{bs})^{-1.5} \quad (1)$$

where C is a constant of proportionality. However, the constant C and the exponent vary from one case to the next and results reported from the Nevada desert are not valid for coastal^{8,9,10} or varied terrain. Fortunately, the problem of backscatter is not too serious since it can be handled by a time-programmed gain circuit.⁴

A complicating situation arises when the effect of the atmosphere on the transmission of the laser pulse is considered. When specifications for laser rangefinders are given, they are usually expressed in terms of visibility—the requirement being that if one sees the target, one must be able to range to it. One limit occurs when the scattering particles in the atmosphere are random in size and distribution, resulting in a superposition of Mie scattering curves which lead to an attenuation coefficient independent of wavelength. This case is referred to as Mie type scatter-

ing in Figs. 1 and 2. The attenuation coefficient for these curves in Fig. 1 is given by $\alpha = 3.9/V$, so that $\exp(-2\alpha R)$ is always 0.02 for range R (km) equal to visibility (km). The other limiting case is when scattering is by uniform molecular size particles and is referred to as Rayleigh-type scattering. The attenuation coefficient depends upon wavelength and can be expressed by¹¹

$$\alpha_{\lambda} = \frac{3.9}{V} \left(\frac{0.53}{\lambda} \right)^{0.62 V^{1/3}} \quad (2)$$

This expression is used when the wavelengths of interest do not coincide with absorption lines in the atmosphere.

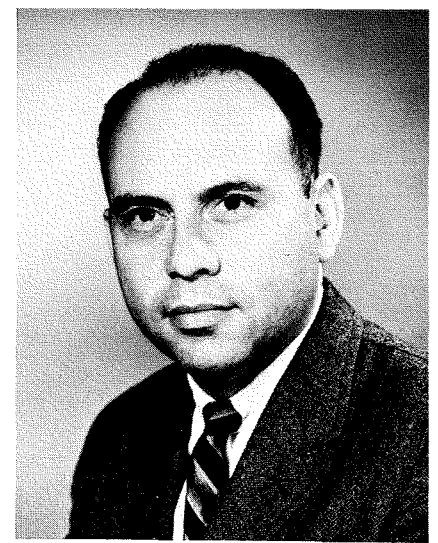
Basic range equation

There are three possible geometric configurations tying together target size, transmitter beamwidth, and receiver beamwidth. These are given in terms of the average number of signal electrons received. For simplicity, the beamwidths are considered uniform and circular in cross section, and the target is also circular. The general expression is

$$n_s = \frac{P_T D_r^2 \rho K_o \exp(-2\alpha R) \tau q}{4R^2 h\nu} N \quad (3)$$

When the receiver field of view is smaller than the target area and the transmitter beamwidth is greater than the receiver angular field of view, $\theta_r > \theta_t$, $\theta_r R < D_t$; then $N = \theta_r^2 / \theta_t^2$.

When the receiver field of view is greater than the target area and the area subtended by the transmitted beam is greater than the target area,



Edward Kornstein, Mgr.
Optical Physics Techniques
Aerospace Systems Division
Burlington, Mass.

received the AB in physics and mathematics from New York University in 1951. He received the MS in Physics from Drexel Institute of Technology in 1954. He attended Boston University on the RCA David Sarnoff research fellowship and completed course requirements for the PhD. Mr. Kornstein joined RCA in Camden in 1951, and for approximately eight years worked in the following areas: development of color TV cameras, TV projectors for theaters, optical-radar rangefinders, infrared detecting and scanning systems, aerial reconnaissance systems, borescopes for medical use and atomic pile monitoring, application of Mie theory to atmospheric scattering, general opto-electronic and opto-mechanical systems, and application of communication and information theory to optical systems. Mr. Kornstein has been with ASD since 1960. His group has developed Q-switching techniques for laser rangefinders; CW optically pumped lasers; undersea second harmonic laser generators for the Navy; 50-MW 10-pps ruby rangefinders for missile trackers; high power lasers for atmospheric research; laser alignment equipment; lightweight, compact, ruby laser rangefinders; and a laser obstacle scanner for the Department of Transportation. Also Mr. Kornstein was responsible for several company-sponsored programs on advanced laser techniques. He is a member of the Optical Society and was Boston regional chairman for the SMPTE. He is the author of several published papers.

$\theta_r R > D_t$, $\theta_t R > D_t$; then $N = D_t^2 / \theta_t^2 R^2$. When the area subtended by the transmitted beam is smaller than the target area and the receiver angular field of view is greater than or equal to the transmitter beam width ($\theta_t R < D_t$, $\theta_r \geq \theta_t$); then $N = 1$.

The background due to solar radiation on the target and atmospheric scatter into the receiver is given by¹

$$n_b = \frac{(Q_s \Delta\lambda + H_s X) K_o \theta_r^2 q \pi D_r^2}{16h\nu} \left[\rho \exp(-\alpha R) + \frac{1 - \exp(-\alpha R)}{4} \right] \quad (4)$$

Receiver characteristics

Two types of detectors are primarily used in rangefinder applications, photomultiplier tubes, S-20 for ruby



Nunzio A. Luce
 Technical Staff
 Aerospace Systems Division
 Burlington, Mass.

received the BSEE from Ohio University in 1962 and the MSEE from Northeastern University in 1968. Mr. Luce is presently working on an advanced isocan low-light-level camera being built for the Air Force. Prior to this assignment, he was the electronics project engineer on a laser obstacle detection system which used various integration techniques to overcome the low peak power output of the transmitter; he was co-winner of RCA's Technical Excellence Award for this work. He has been deeply involved in the development of GaAs laser rangefinders and was project engineer on the electronics for all the green-laser harmonic generators built for the Navy in the past few years and has participated in their test programs. In addition, he was in charge, of the electronics on the development of a sophisticated helicopter rangefinder system. Mr. Luce's initial responsibility on first coming to RCA was for the electronics and the laser development of a laser transmitter to be used in conjunction with a TV system on the semi-active missile-seeker program. Prior to joining ASD, Mr. Luce was with Advanced Technology where he performed logic design on a digital data message generator, experimental studies on GaAs infrared light emitting diode, and assisted on the design and development of an X-band ferro-electric phase shifter. In addition, he assisted in the design, construction, and field test of a high powered laser transmitter for experimental tropospheric backscatter measurements.

and S-1 for neodymium, and silicon reverse-bias P-N diodes. The use of photomultiplier tubes and the validity of the assumption of a Poisson distribution of photoelectrons has been covered in great detail.^{3,12} For the present ruby analysis, we use an S-20 surface (RCA 8645) which has a typical quantum efficiency of 0.035 with an anode dark current of 7×10^{-10} amps at a gain of 10^5 . For the neodymium analysis, we use an S-1 apertured ITT FW-118 which has a typical quantum efficiency of 0.0004 with an anode dark current of 5×10^{-6} amps at a gain of 10^7 .

The analysis of the high quantum efficiency reverse bias P-N diode, such as the SDG-100 (by Edgerton, Gernshausen, and Grier) and Hewlett-Packard 4204, is straightforward and indicates that the system is thermal

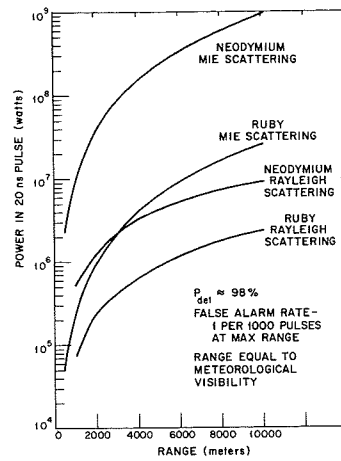


Fig. 1—Power requirements for Neodymium and Ruby using two atmospheric models to range to the limit of visibility.

noise limited. This means that these diodes are very useful under conditions when the background noise predominates as it would in wide-angular field applications. A more complicated detector, not fully analyzed is an avalanche diode. Preliminary results show that the noise spectral density is proportional to the cube of gain, which indicates that the signal-to-noise ratio falls rapidly with increasing gain.¹³ Since the device without gain is thermal noise limited, signal-to-noise ratio increases with gain to the point where

List of symbols

V	visibility as defined by Middleton ⁶
α	atmospheric attenuation coefficient
α_{bs}	backscatter intensity
λ	wavelength (microns)
n_s	average number of signal photoelectrons
P_T	peak power of transmitter after transmitter optics (watts)
D_r	diameter of receiver (0.076 meters)
K_o	optical transmission of receiver at laser wavelength (0.5)
ρ	reflection coefficient of target (0.1 diffuse)
θ_r	receiver angular field of view (10^{-3} radians)
θ_t	transmitter beamwidth (10^{-3} radians)
τ	laser pulse width (20 nanoseconds)
q	quantum efficiency of detector
R	range to target (meters)
D_t	diameter of target (meters)
$h\nu$	energy of photon (2.85×10^{-19} joules for ruby, 1.89×10^{-19} joules for Nd)
n_b	background due to solar irradiance
Q_λ	spectral irradiance ($0.11 \text{ watts m}^{-2} \text{ A}^{-1}$ for ruby, $0.053 \text{ watts m}^{-2} \text{ A}^{-1}$ for Nd)
$\Delta\lambda$	receiver optical filter bandpass (20A for ruby, 100A for Nd)
H_s	total solar irradiance over region of sensitivity of detector (739 watts m^{-2})
X	receiver optical filter transmission outside spectral region $\Delta\lambda$ (-60 dB)

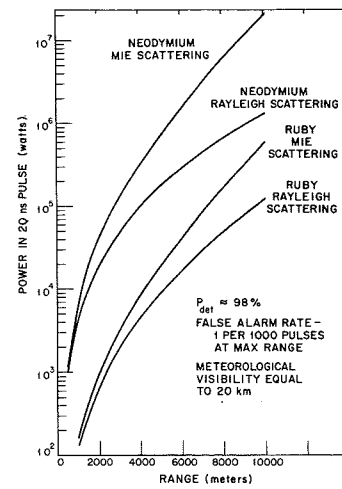


Fig. 2—Power requirements for Neodymium and Ruby using two atmospheric models to range on a clear day.

the noise contribution from the detector shot noise and thermal noise are comparable, then begins to decrease.

Tradeoff curves

As can be seen by the curves in Fig. 1, the laser requirements can vary by a substantial amount when only visibility is specified, depending on the construction of the atmosphere. For a clear day, as shown in Fig. 2 the spread is less, but still significant.

References

1. Flint, G. W., "Analysis and Optimization of Laser Ranging Techniques," *IEEE Trans. on Military Electronics*, Vol. MIL-8 (Jan 1964) pp. 22-28.
2. Goodman, J. W., "Comparative Performance of Optical-Radar Detection Techniques," *IEEE Trans. on Aerospace and Electronic Systems*, Vol. AES-2 (Sept 1966) pp. 526-535.
3. Austin, M.E., et al, "GaAs Laser Radar Components and Techniques," Lincoln Lab. Technical Report 407, NASA Contract NA 59-105 (Oct 1965).
4. Kaplan, R. A. and Daly, R. T., "Performance Limits and Design Procedure for All-Weather Terrestrial Rangefinders," *Lasers and Unconventional Optics Journal*, No. 8, (July 1967; Paris) pp. 137-143.
5. Fenn, R. W., "Correlation Between Atmospheric Backscattering and Meteorological Visual Range," *Applied Optics*, Vol. 5 (Feb 1966) pp. 293-295.
6. Middleton, W. E. K., *Vision Through the Atmosphere* (University of Toronto Press; Canada; 1952).
7. Gibbons, M., et al, "Transmission and Scattering Properties of a Nevada Desert Atmosphere," *JOSA* Vol. 51 (June 1961) pp. 633-640.
8. Curcio, J. A. and Knestrick, G. L., "Correlation of Atmospheric Transmission with Backscattering," *JOSA* Vol. 48 (Oct 1958) pp. 686-689.
9. Gibbons, M., "Experimental Study of the Effect of the Field of View on Transmission Measurements," *JOSA* Vol. 49 (July 1959) pp. 702-709.
10. Barteneva, O. D., *Bulletin of Acad. Sci. USSR*, No. 12, 1 (1960) p. 852.
11. Stewart, H. S., and Hopfield, R. F., "Atmospheric Effects," *Applied Optics and Optical Engineering*, R. Kingslake, Ed., Vol. 1 (Academic Press; N.Y.; 1965), Chapter 4.
12. *RCA Phototubes and Photocells*, Technical Manual PT-60, RCA Corporation, p. 58.
13. McIntyre, R. J., "Multiplication Noise in Uniform Avalanche Diodes," *IEEE Trans. on Electronic Devices*, Vol. ED-13 (Jan 1966) pp. 164-168.

Gated-sensor and pulsed-laser illuminator systems for seeing through fog

Dr. H. J. Wetzstein | E. Kornstein

Visibility in poor weather such as light clouds, fog, and haze is limited by the heavy scattering of light due to the droplets and particles suspended in the atmosphere. This scattering makes it hard for light to penetrate from an illuminator to the scene and then back to the observer. However, when the observer and illuminator are close to each other, such as in a car, the amount of light backscattered from the suspended particles in the immediate vicinity of the observer and light source completely overrides any information coming from a farther distance. This effect of backscatter, called *veiling luminance* is usually most serious and can be overcome only by 1) separating source and receiver and providing illumination from a source as close as possible to the object to be seen (bistatic case of Fig. 1); or 2) "gating" the observing sensor in time synchronized to a pulsed illuminator (monostatic case of Fig. 1). The latter possibility is the subject of this paper.

THE TOOLS NEEDED to achieve visibility enhancement have been developed and used by the Aerospace Systems Division in several related applications: 1) range finders which must operate to the limit of visibility but fortunately not beyond it;² 2) detection of small obstacles on high-speed-train roadbeds;¹⁰ 3) general high-resolution and low-light-level TV reconnaissance systems; and 4) underwater laser propagation in the blue green window.¹ This last application is probably most closely related to seeing through fog because of heavy scattering and attenuation losses.

Range gating

The main parameters involved in range gating are demonstrated in the top part of Fig. 2. The receiver is opened only for a short interval when the illuminating pulse returns from the selected range element. Thus, the depth of the field-of-view is limited unless a synthetic display is computed from several range gates. Because of the high speed of light, there is a requirement to keep pulses very short (in the vicinity of tens to hundreds of nanoseconds) and this introduces the pulsed laser as an essential element for illumination. The complex nature of both forward scatter which results in

some enhancement of object illumination and multiple scattering of the return image energy which results in distortion are also shown in Fig. 2. Detailed solutions are not possible with any rigor for either forward or return scattering. Due to this complexity, an estimate of potential system performance can at best be bracketed with some caution. There is also considerable variation in the actual scattering mechanism underlying *meteorological visibility* or *runway visual range* which will be shown to be important. Approximations showing the effect of forward scattering in water are reported and examined in Ref. 1.

Figs. 3 and 4 show the backscatter from a narrow-beam rangefinder with and without range gating. With gating, it should ideally be possible to eliminate all veiling luminance between the observer and the selected range gate.

Upper limit of range achievable

To estimate the maximum range achievable with a range-gated system, we shall make the following assumptions:

- 1) Wavelength-dependent visibility V_λ is related to the total attenuation coefficient σ_λ at the wavelength λ by the usual relationship:

$$V_\lambda = \frac{3.9}{\sigma_\lambda} = 3.9 \text{ (attenuation lengths)}_\lambda$$

(1)

(this is based on a 50-fold reduction of contrast)



Dr. Hanns J. Wetzstein

Technical Staff
Aerospace Systems Division
Burlington, Mass.

received the BSEE with distinction from the University of Cape Town in 1947 and the MS and SD electrical engineering from Harvard University in 1949 and 1952, respectively. With RCA from 1955 to 1961, Dr. Wetzstein was Leader of a digital computer input/output equipment group and worked as Senior Engineering Scientist on ballistic missile re-entry detection measurement programs and systems. With the Institute of Naval Studies from 1961 to 1965, Dr. Wetzstein had responsibility for a study of power for propulsion of naval vehicles and was principal investigator on a study of science and technology needed for undersea warfare. From 1965 to 1967, Dr. Wetzstein was a Senior Staff Associate at Arthur D. Little. His case work included ASW surveillance, sonar data processing and fire control systems, extra vehicular activity, space mission studies, automatic inspection and test techniques, and hybrid computer evaluation. Dr. Wetzstein rejoined RCA in 1967 as Senior Engineering Scientist and is conducting investigations on advanced electro-optical systems. Dr. Wetzstein is a member of the Institution of Electrical Engineers (London) Sigma Xi, and the Marine Technology Society. He has published several papers in the classified and open literature.

Also, σ_λ will represent the total loss of energy both for outgoing illumination and returning image energy (i.e., no enhancement due to forward scatter or image distortion due to multiple scattering).

- 2) All veiling luminance due to backscatter can be ignored (i.e., a very short range gate approaches this).

- 3) The system is quantum or photon limited (i.e., sensors of adequate sensitivity introducing negligible noise are available).

- 4) Effects due to aircraft and resulting image motion can be neglected as introducing only a small reduction in range.

With these assumption, standard equations for an imaging system without an illuminator can be used:

Reprint RE-15-5-14

Presented at Air Transport Association Symposium on Visibility Enhancement in Poor Weather held on 8 May 1969 in Washington, D.C.



Edward Kornstein, Mgr.
Optical Physics Techniques
Aerospace Systems Division
Burlington, Mass.

received the AB in physics and mathematics from New York University in 1951. He received the MS in Physics from Drexel Institute of Technology in 1954. He attended Boston University on the RCA David Sarnoff research fellowship and completed course requirements for the PhD. Mr. Kornstein joined RCA in Camden in 1951, and for approximately eight years worked in the following areas: development of color TV cameras. TV projectors for theaters, optical-radar rangefinders, infrared detecting and scanning systems, aerial reconnaissance systems, borescopes for medical use and atomic pile monitoring, application of Mie theory to atmospheric scattering, general opto-electronic and opto-mechanical systems, and application of communication and information theory to optical systems. Mr. Kornstein has been with ASD since 1960. His group has developed Q-switching techniques for laser rangefinders; CW optically pumped lasers; undersea second harmonic laser generators for the Navy; 50-MW 10-pps ruby rangefinders for missile trackers; high power lasers for atmospheric research; laser alignment equipment; lightweight, compact, ruby laser rangefinders; and a laser obstacle scanner for the Department of Transportation. Also Mr. Kornstein was responsible for several company-sponsored programs on advanced laser techniques. He is a member of the Optical Society and was Boston regional chairman for the SMPTE. He is the author of several published papers.

$$\frac{\text{angular resolution}}{\text{TV line}} = \frac{1.43 \times 10^{-9}}{C_s} \left[\frac{K}{E\beta T_o D^2} \right]^{1/2} \exp(\sigma R) \quad (2)$$

Illuminator power P is:

$$\frac{E}{K} = \frac{P}{R^2 \theta^2} \quad (3)$$

For a system with illumination:

$$\frac{\text{angular resolution}}{\text{TV line}} = \frac{1.43 \times 10^{-9} R \theta \left[\frac{1}{P\beta D^2 T_o} \right]^{1/2} \exp(\sigma R)}{C_s} \quad (4)$$

Eq. 4 can be used directly to solve for P when R is given as the desired upper

limit of range; σ_λ is then related to the visibility range, V_λ , by Eq. 1. Implicit in Eq. 2 and 4 is an eye integration time of 0.2 seconds and a "Rose picture S/N factor" of about 5.²¹

A baseline high-power system with $\lambda = 0.85 \mu$; $P = 100 W$; and $D = 0.075 m$ achieves 1 meter resolution with an observed area of $100 \times 100 m^2$. This is called system A. System B represents either:

- 1) Power reduction by 10 at the same 1-m resolution, or
- 2) 0.32-m resolution at the same power.

The range is varied between 10 and 10,000 meters and expressed as a multiple of V_λ (Table 1). The factor by which V_λ is multiplied is perhaps the simplest way of assessing the situation. When V_λ is small, this factor saturates slightly above 2 and increases very little with power. Thus it seems unlikely that one can achieve much more than a factor of 2 improvement in very heavy fog. This agrees very well with the 8 to 10 attenuation length estimates presented in other papers and found valid in water (see Ref. 1) in terms of "effective" attenuation lengths. "Effective" in water represents about a two to threefold increase above actual attenuation length in water due to heavy narrow-angle forward scatter.

When V_λ is very large, the factor becomes less than 1 and is more sensitive to power changes. Here the results agree very well with the computer-calculated results presented in Ref. 3 for

Definition of parameters

V_λ	Wavelength-dependent visibility
σ_λ	Total attenuation coefficient
λ	Wavelength
C_s	Contrast factor = $\frac{\rho_t - \rho_b}{\rho_t + \rho_b} = 0.2$ used throughout
ρ_t	Diffuse reflectance of target
ρ_b	Diffuse reflectance of background
K	Source luminosity (lumens/watt)
E	Illuminance on scene (lumens/m ²)
β	Photocathode responsivity (amperes/watt)
T_o	Transmittance of optics = 1.0 used throughout
D	Lens diameter (meters)
R	Range (meters)
σ	Atmospheric attenuation coefficient (meters ⁻¹)
$1/\sigma$	Attenuation length (meters)
$R\theta$	Width and breadth of illuminated area (meters)
θ	Angular dimensions of square field illuminated (radians)
P	Illuminator power (watts)

perfectly gated systems. It is to be noted that in Ref. 3 ungated range was generally about one half the gated range for V between 5000 and 50,000 meters. Under good visibility, in effect the systems become geometry limited.

While the improvements possible look very small, it should be remembered that this is for a monostatic system. The range obtainable without gating is only a probably small fraction of V_λ , as is evident when using car headlights in a fog. Thus gated systems may be worth considering for landing at unlighted and uninstrumented fields.

System alternatives

Table II shows alternatives for systems A and B for four wavelengths at which suitable short-pulse lasers are available. Because the eye integration time of 0.2 seconds was used in the calculations, a single pulse per frame would have to be $1/5$ the average power, P , in joules or could be made up of a number of pulses adding up to this total. Generally, the average powers indicate systems which are just about current state-of-the-art for quite demanding and hence costly military systems. Thus it may be some time before such illuminators can be available in moderate cost and size versions. Gas lasers in the visible and near infrared as well as far infrared may also become available in suitably short-pulse versions.

The ruby and neodymium systems are optically pumped and Q-switched to produce short pulses and this keeps overall efficiency quite low (presently less than one percent) and requires careful cooling. The average power at 0.53 and 0.7 micrometers is low because of the high value of β available at these wavelengths. The systems at 0.85 and 1.06 micrometer will become more reasonable in power demand if greater β becomes available in devices of adequate noise-free sensitivity. Because these systems are outside the visible range, their use becomes attractive from safety considerations, especially if power becomes comparable with that required in the visible.

The gallium arsenide system at 0.85 to 0.905 micrometers is a solid-state injection laser offering higher overall efficiency and greater simplicity. A higher β device at these wavelengths is therefore most desirable to make a

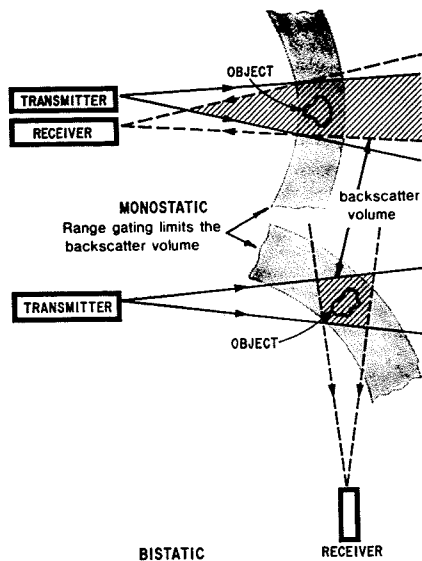


Fig. 1—Gating effectiveness for monostatic and bistatic systems.

practical size and power demand system feasible.

Considering the receiver, the most direct approach is to use a sensitive imaging device which can be gated. Fig. 5 shows the block diagram of such a system. The entire area observed is illuminated at the same time. Such a system will allow examination of only one range gate at a time (unless several receivers are used in parallel and suitably time staggered).

In the presence of heavy forward scattering, image return energy is available over a substantial acceptance angle, as explained in Ref. 1. This can be collected and used if the object scene is illuminated by a scanning raster beam as narrow as the resolution desired. Fig. 6 shows such a system including a doubler and polarizer which may be useful. Due to the need for high resolution and high frame rate leading to very high pulse repetition rates and scanning speeds, such a system will be harder to implement in this application than the underwater case even though it may offer somewhat greater range and allow superposition of several range gates offering depth of field-of-view.

It is evident not only that the system components are demanding in themselves, but that the overall system requires careful timing and coordination. However, with microelectronics techniques this represents no problem in size, weight, and reliability.

Interference from ambient daylight which is not range gated is suppressed

by the very short exposure times. Any further suppression necessary can be accomplished by narrow wavelength filtering at the selected laser wavelength. Thus equal performance is expected in day and night-time operation of such systems.

Visibility range

The *meteorological visibility* or *runway visual range*⁸ is observed as an effective attenuation of the visible spectrum such that $V=3.9/\sigma$ (as in Eq. 1).

In a relatively clear atmosphere, Rayleigh scattering due to molecules is the

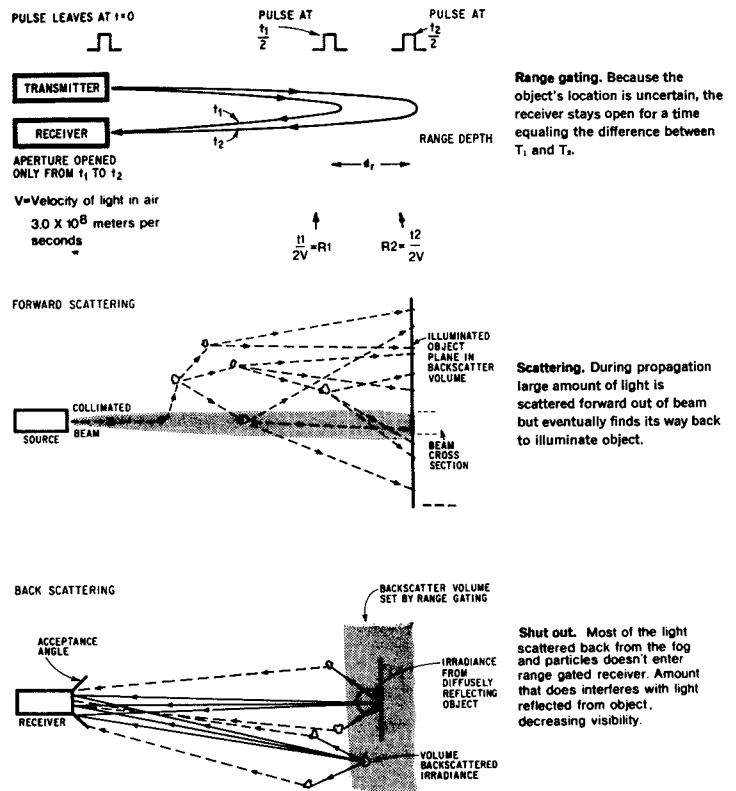


Fig. 2—Details of gating and scattering.

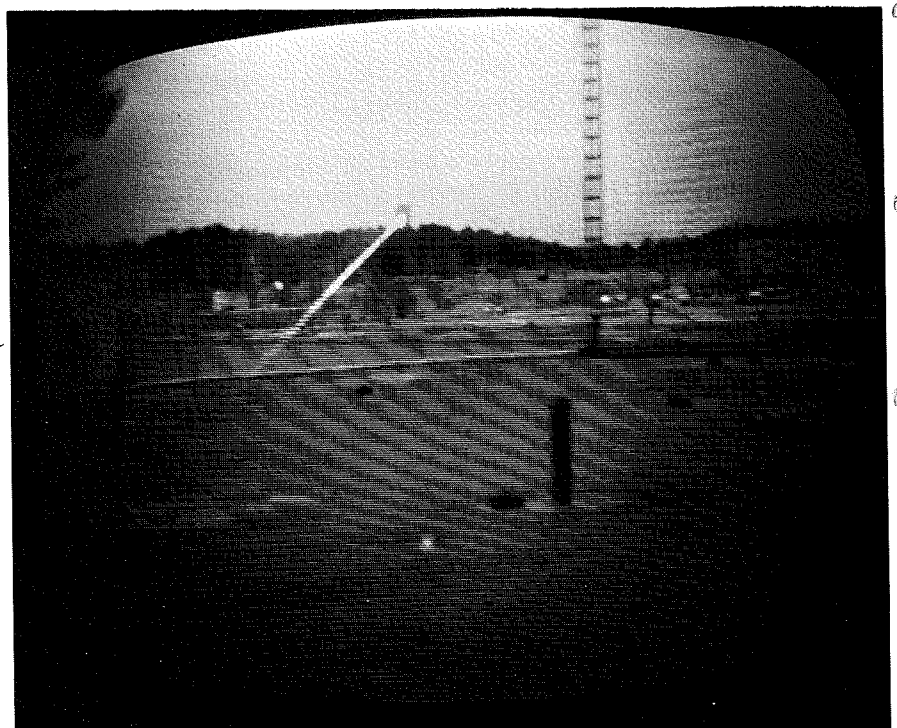


Fig. 3—Atmospheric backscatter from a narrow rangefinder laser beam.

Table I—Upper limit of range achievable without backscatter as a function of visibility range (observed area kept constant at 100×100 m).

System A High-power Low-resolution (1 m)			System B 1/10 power or 0.32-m resolution		
Upper limit of range (m)	= factor	× V _λ (m)	= factor	× V _λ (m)	factor A factor B
10	2.23	4.5	2.00	5	1.115
30	2.00	15			
100	1.66	60	1.42	71	1.17
270	1.42	190			
1000	1.07	930	0.21	48000	1.27
4000	0.75	5320			
10000	0.55	18000	0.84	1200	2.62

Table II—System alternatives at four important wavelengths.

Wavelength (μm)	system A			system B		
	Ave. power (watts)	Resolution (m)	Lens dia. (m)	Ave. power (watts)	Resolution (m)	Lens dia. (cm)
0.53 Nd doubled	16	1	7.5	1.6	1	7.5
β = 84 × 10 ⁻³				16	0.32	7.5
power at fundamental	4	1	15	0.4	1	15
50% conv. ass.				4	0.32	15
0.7 Ruby	32	1	7.5	3.2	1	7.5
β = 21 × 10 ⁻³				32	0.32	7.5
	8	1	15	0.8	1	15
				8	0.32	15
	32	0.5	15	3.2	0.5	15
				32	0.16	15
0.85 GaAs	100	1	7.5	10	1	7.5
β = 7 × 10 ⁻³				100	0.32	7.5
	25	1	15	2.5	1	15
				25	0.32	15
1.06 Nd YAG	2000	1	7.5	200	1	7.5
β = 0.35 × 10 ⁻³				2000	0.32	7.5
	500	1	15	50	1	15
				500	0.32	15

Resolution is proportional to $[1/P\beta D^2]^{1/2}$
 β = detector responsivity (amps/watt)

predominant effect, and for this the wavelength dependence is given by

$$\sigma_{\lambda} = \frac{3.9}{V} \left(\frac{0.53}{\lambda} \right) 0.62 V^{1/2} \quad (5)$$

Thus, for $V=10000$ m, $\sigma=3.9 \times 10^{-4}$; however, due to Rayleigh scattering, $\sigma_{0.7}=2.7 \times 10^{-4}$ for ruby and $\sigma_{1.06}=1.54 \times 10^{-4}$ for neodymium.

When haze or fog introduce particles and droplets in addition to the air molecules, scattering and attenuation become very complex,^{2,6,7} and scattering is referred to as Mie scattering. In the limit when particles and droplets of many sizes are present, Mie scattering predominates and is wavelength independent and thus equal to σ . It is thus important not only to know V , but also the nature of the scattering. For a specific range-finding requirement, Figs. 1 and 2 of Ref. 2 show the change in power required for a given visibility, V , if the scattering mechanism varies between only Rayleigh and only Mie.

When visibility is very low (below 100 m), it is most likely that scattering is predominantly Mie and thus wavelength independent. Figure 6 of Ref. 12 shows that already in light fog, for $V \approx 1000$ m, σ is wavelength independent out to 5 micrometers. The Figure also shows that the substantial gains (due to lower σ) obtainable by going to long-wave infrared at 10 μ when there is haze are already sharply reduced in light fog and will probably be very small in heavy fog. This reduces the attractiveness of going to active systems in this window where efficient CO₂ lasers are available but sensitive imaging detectors are not yet at hand and single cells in mosaics require cooling.

From Ref. 9 and the general trend of much of the literature, the need for visibility enhancement is most pressing when the visibility (or runway visual range) is below a few hundred meters. Under these conditions, the choice of wavelength is not likely to be very strongly influenced by any slight changes between σ and σ_{λ} in the visible and near infrared range indicated by the representative systems in Tables I and II. Actual measurements of σ_{λ} at the various wavelengths and under a full range of visibility conditions and causes (i.e., scattering mechanisms)



Fig. 4—Backscatter shown in Fig. 3 eliminated by gating.

A GaAs transmissometer

Dr. E. J. Fjarlie

A gallium arsenide transmissometer using a silicon photodiode field effect transistor as the detector has been built. This device could possibly find application in air pollution measurements or in determining any type of particulate concentrations in the atmosphere. The special design features of the instrument are described together with the problems encountered in fabrication.

VARIOUS TECHNIQUES have been used to measure the optical transmittance of the atmosphere under a variety of meteorological conditions. Most of the methods suffer either from a lack of dynamic range in the equipment or from using the human eye—a nonquantitative recording process. A transmissometer has been built which has the necessary dynamic range and gives an exact representation of the atmospheric transmittance. It is also possible to give more accurate quantitative data over a greater range due to the increased power of the source available coupled with the noise limit of the detector used.

The instrument was originally developed to correlate microwave communication reception in the GHz frequency range with atmospheric visibility. Accordingly, the transmissometer was designed to measure continuously, and data recording would take place as demanded by the test operator. It was hoped that visibility could be measured over the entire 7-km test path for the microwave link, but it soon was evident that such an arrangement would limit the dynamic range of the measurements.

At the same time as utilizing a transmissometer, the basic components chosen for the instrument were essentially being tested for use in such a device. The source chosen was a gallium arsenide (GaAs) laser diode and the detector was a silicon (Si) diode.

Theory of atmospheric transmittance

Atmospheric transmittance may be separated into two functional components: absorption and scattering. The absorption at 0.9 μm is very small and is mainly due to water vapor. Mie-type scattering is prevalent and is a

very severe function depending on the amount of rainfall or snowfall; dust and micro organisms also are significant scatterers. The empirical model used as the basis for the following calculations holds well for absorption from 0.3 to 15.0 μm and for scattering from 0.4 to 1.5 μm . Bouguer's law states that:

$$\tau = \exp[-\sigma_{\lambda}R]$$

where σ_{λ} is the attenuation coefficient which may be separated into an absorption coefficient, α_{λ} , and a scattering coefficient, β_{λ} ; and R is the range or distance over which the transmittance is measured. Thus,

$$\sigma_{\lambda} = \alpha_{\lambda} + \beta_{\lambda}$$

and the two transmittance functions are exponentials; both the coefficients may be related to the absorbing and scattering number concentrations through the pertinent cross sections. It can be shown that

$$\beta_{\lambda} = \frac{3.91}{V} \left(\frac{\lambda}{0.55} \right)^{-q}$$

and

$$q = 0.585 V^{1/4}$$

where V is the meteorological range in km, and λ is the wavelength used. Temperature and humidity control, α_{λ} , and the absorption may be readily found for various values of these parameters.

The meteorological range assumes a 2% threshold of vision as determined by scattering alone. Note that: $\tau = \tau_a \tau_s$ where τ_a is the transmittance function due to absorption and τ_s is that due to scattering; then,

$$\tau_s = 0.02 = \exp[-\beta_{\lambda}R]$$

and the signal loss may be written as $-17V^{-1}R$ dB for any range and any meteorological range. (See Table I). Fig. 1 shows how τ_s varies with V for given values of R . A range of 200 m was chosen for the experiment to de-



Dr. E. J. Fjarlie
Research Laboratories
RCA Limited
Montreal, Canada

graduated in 1955 with the Engineering Physics degree from the University of British Columbia. He obtained the MSc degree in Electrical Engineering in 1958 from the same university with a thesis on mercury arc discharge switching. The PhD in Physics was received from the University of Saskatchewan for a thesis which was a study of atmospheric emissions in the aurora and air-glow with a Michelson interferometer operated in the spectral region 1.0 to 2.5 microns. He joined RCA Limited in 1965. Dr. Fjarlie's general experience has been in the design, construction, and use of electro-mechanical-optical systems. He has worked on the design of Dewars for liquid-nitrogen and liquid-helium cooled infrared detectors, has been concerned with lens evaluation for micro-photography, Fourier spectroscopy, and atmospheric pollution measurements. Recently he has become more involved with general technical training programs at RCA for engineers from developing countries. Dr. Fjarlie has earlier worked for the Canadian Armament Research and Development Establishment making atmospheric absorption measurements. He is a part-time lecturer in the Physics Department at Sir George Williams University where he has given many different courses in the undergraduate curriculum. Dr. Fjarlie is a member of the Canadian Association of Physicists, the Engineering Institute of Canada, the Optical Society of America, and the American Institute of Physics Teachers.

Table I—Typical meteorological range.

Condition	V (km)
clearer than average	80
average	32
hazier than average	7

fine exactly the attenuation when rain and snow would be prevalent. Table II relates the expected signal losses to V and gives some typical snowfall rates.

System description

The transmissometer consists of a transmitter (T_x) and receiver (R_x) packaged on the same chassis together with a retro-reflector (R_r) placed on a pedestal some distance away; the arrangement is shown in Fig. 2. In order to check on the level of the transmitted signal for calibration purposes, an output monitor is also built into T_x .

Readily available components were used in building the transmissometer

Table II—Meteorological range variation.

Loss (dB)	V (km)	dB/km	Snow rate (mmw) h ⁻¹
0.04	113		
0.05	68	0.25	
0.06	57		
0.08	43		
0.1	34	0.5	0.0455
0.2	17	1.0	0.091
0.5	6.8	2.5	0.227
1	3.4	5	0.455
2	1.7	10	0.91
5	0.68	25	2.27
10	0.34	50	4.55
20	0.17	100	9.10

rather than special parts. No attempt was made to maximize the reliability or carefully engineer the design.

Lens system

The collimator is a double-convex, 3.3-cm-diameter, 5.5-cm-focal-length, quartz lens; the retro-reflector, 6.3 cm in diameter, works on total internal reflection; the quartz collecting lens is 5.4 cm in diameter and has a focal length of 8.8 cm. The beam splitter for the monitor is a piece of microscope-slide glass and in addition there is a long wavelength cut-on filter in front of R_s to limit the background radiation flux to that between the filter "cut-on" and detector "cut-off" which is about 300 Å FWHM (full width at half of maximum amplitude).

Transmitter

The transmitter uses a GaAs laser diode uncooled, thus the output is in

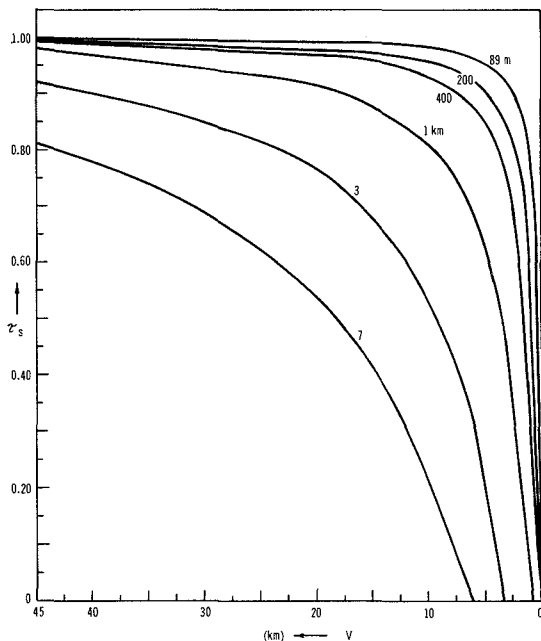
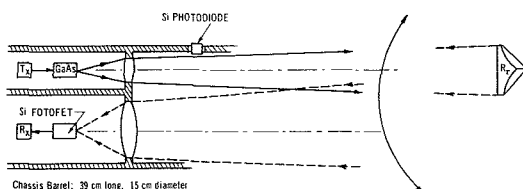


Fig. 1—Meteorological range as a function of scattering.



the near-IR spectral region at a wavelength of about 0.905 μm. The pulser is designed to operate the laser at 10 pulses/second, but is readily adjustable; the output power is continuously variable up to 2 w peak, but the diode was operated at 500 mW at a pulse width of about 100 ns, FWHM. With reference to Fig. 3, the circuit works as follows. The timing unit consists of an FET operating in a relaxation oscillator configuration to give a 5-V-peak pulse to the SCR gate. The transistor, Q_2 , operates as a charging switch for the capacitor C_2 whose charge is controlled by the HV power supply. When the timing pulse is applied, C_2 discharges through D_2 , the SCR, the laser diode, and R_s .

Receiver

The receiver is designed around a Si Fotofet which has a S-14 spectral response characteristic and also it has no difficulty in detecting the very fast pulses which are arriving at the collector. An operational amplifier is used to give a gain of 100 for R_s (Fig. 4). The charge in the pulses is transferred to C_3 which has a 12.6-s charge-leakage time constant so that when the output is recorded, the voltage gives the immediate past history of the atmospheric transmittance.

Monitor

The monitor is a Si photodiode used with no amplifier as shown in Fig. 5. When it is desired to check the size of the transmitted pulse, an oscilloscope is connected to the monitor. There should be no expectation that the transmitted pulse has changed in amplitude; if there has been a change, the high voltage may be adjusted to the original pulse height for the system.

Analysis

The laser emits a pulse with a nominal beam spread of 5° by 15°. The field of view of T_s is determined by this beam spread and the collimator; it was assumed that power is emitted over much wider angles than the beam-spread values given, that these values were in effect e^{-1} for the polar emission of the laser diodes. Thus, a position 5.3 cm behind the collimator was found for the laser which gave the field of view shown in Fig. 6.

Fig. 2—Transmitter receiver monitor

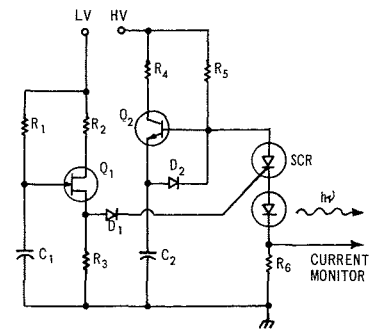


Fig 3—Transmitter circuit.

If the peak emitted flux is P_s , the transmitted radiant intensity J is

$$J = P_s \Omega_s^{-1} \tau_s$$

where the transmitted solid angle is $\Omega_s = 2.25 \times 10^{-5}$ sr, and the transmittance, $\tau_s = 0.92 (0.85) = 0.78$ due to the monitor slide glass and the lens respectively. A fraction of the radiant flux is intercepted by R_s and returned along the T_s axis but is spread out according to the extreme reflection angles established by R_s subtending each radiating point in T_s . Loss at R_s amounts to 0.96 since it only occurs at the front surface. Thus the received power is spread over a 13.6-cm-diameter circle centered on the T_s lens; if the R_s lens was not all within 6.8 cm of this axis, there would have been some vignetting. The radiant flux at R_s is $4J A_{R_s} R^{-2} \tau_{R_s}$ W where A_{R_s} is the R_s area, R is the total range for the atmospheric transmittance, and τ_{R_s} is 0.96. The received power then becomes

$$P_{R_s} = 4J A_{R_s} R^{-2} \tau_{R_s} A_{R_s} \left\{ \frac{\pi}{4} (13.6)^2 \right\}^{-1} \tau_{R_s}$$

where A_{R_s} is the collector area and τ_{R_s} is the R_s transmittance, about 0.7 (0.85) = 0.6 due to the filter and the lens respectively. Substituting, the received power (now taking into account the air attenuation) is given by $3.63 \times 10^4 P_s R^{-2} \tau$ where τ is the atmospheric transmittance. The retro-reflector was placed 10³ m from T_s - R_s . Thus, the nominal received power was 7.26×10^{-4} W since the laser was operated at 0.5 W.

Background radiation flux was calculated to see what the contribution to the total signal at R_s was. At Montreal, the insolation maximum in summer is about $W_B = 10^{-1}$ Wcm⁻². This radiation is scattered from the background in all directions such that R_s can see a part. Thus, the reflected sunlight contributes $W_B (0.1/\pi) A_{R_s} \Omega_{R_s} \tau_{R_s} W$, where 0.1 is the approximate reflectance, π^{-1} is the Lambertian radiator factor, $\Omega_{R_s} =$

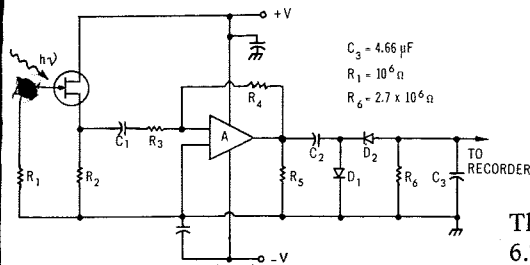


Fig. 4—Receiver circuit.

$\pi(0.32/8.8)^2$ sr, and 0.32 cm is the radius of the Fotofet. Thus, the total isolation maximum is about 1.81×10^{-9} W. But this is for the total spectrum; the filter selects only $0.03 \mu\text{m}$ of the total and is centered at $0.95 \mu\text{m}$ (in the tail of the blackbody curve besides). Taking into account the blackbody factor of 0.15 gives a background radiation flux of 2.7×10^{-7} W.

In addition to reflected sunlight, the direct radiation of the background also must be taken into account. Here the maximum in summer for a temperature of 95°F is about $5.2 \times 10^{-2} \text{ Wcm}^{-2}$, and the background radiation flux seen through the filter is negligible since the blackbody factor is very small.

It is necessary to show that the monitor can detect the expected signal with no difficulty. For the Si photodiode, a typical surface leakage current, I , for a detector 4 mm in diameter is 10^{-10} A at room temperature. The noise limitation is shot noise in this current; that is, $i_n^2 = 2eI\Delta f$; then for a 10^3 -Hz bandwidth, $i_n = 1.79 \times 10^{-10}$ A. The photodiode intercepts about 0.04 (2) $(4/6.9)^2$ (0.85) of P_e . The quantum efficiency of the Si photodiode at $0.9 \mu\text{m}$ is 0.7; hence the number of electrons per second corresponding to the monitored signal is $3.62 \times 10^{10} \text{ s}^{-1}$ and the corresponding current is 5.78×10^{-3} A which is very much greater than the noise. In order to see the fast pulses, the resistor in the monitor circuit is typically 50Ω . Johnson noise in this resistor is given by: $i_n^2 = 4kT\Delta fR^{-1}$ or $i_n = 5.77 \times 10^{-7}$ A which is negligible compared to the large signal.

For the Si Fotofet, the gate leakage is 10^{-9} A at room temperature. The noise limitation here also is shot noise in this current, then for a 10^3 -Hz bandwidth: $i_n = 5.67 \times 10^{-9}$ A. For the separation chosen, 200 m, the nominal minimum signal is $1.97 \times 10^{-5} \text{ W}$ (-20 dB); using the responsivity of $4.34 \times 10^{-2} \text{ AW}^{-1}$ at $0.9 \mu\text{m}$, the minimum expected signal is 8.55×10^{-7} A which is greater than the detector noise. Johnson noise in this resistor is 4.07×10^{-9} A which is still small compared to the signal.

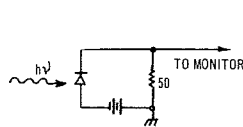


Fig. 5—Monitor circuit.

The total travel time for the pulse is 6.7×10^{-7} s or 670 ns; the pulse width of about 100 ns is the minimum which can be achieved with the laser diode. The group velocity of the pulse has been calculated to be $3 \times 10^8 \text{ ms}^{-1}$.

The pulse which is detected is amplified and then stored. The minimum charge rate due to the pulses is $8.55 \times 10^{-7} (100) (100 \times 10^{-9}) (10) = 8.6 \times 10^{-11} \text{ C s}^{-1}$ when the gain is 100, and the PRF is 10 s^{-1} . The charge leakage time is 12.6 s making a total minimum charge of 1.0×10^{-9} C on the capacitor at any given time. The background signal is in dc and does not pass C_1 in R_x (see Fig. 4). For the minimum visibility condition, the voltage on the capacitor is $V = QC_1^{-1}$ or $2.14 \times 10^{-4} \text{ V}$ which may be sampled by a digital voltmeter.

Noise in the operational amplifier is about 5 mV at the output which appears across R_6 whenever a pulse goes through C_2 . The noise charge is $q_n = 5 \times 10^{-3} R_6^{-1} (100 \times 10^{-9}) C_2$ and the total noise is $1.85 \times 10^{-16} (10) (12.6) = 2.33 \times 10^{-14} \text{ C}$ which is negligible compared to the minimum signal charge stored on the capacitor.

Design problems

No calculations have been presented for the backscattered pulses. No backscattering is seen when the pulses are monitored, but it should be pointed out that T_x and R_x are not concentric and the off-axis backscattering amplitude is expected to be small for Mie scattering. It is only at great distances near R_r that any backscattering would be seen and then it would be hidden by the pulse reflected from R_r .

Initially, it was desired to gate R_x so that the background would not be seen at all. Changes are seen by the present instrument, and any backscatter components do enter the instrument. A synchronizing pulse generator was built to give a gating pulse for the R_x , but it was not possible to find a switch which was fast enough to use the gate pulse and still block effectively any following signal from the amplifier. By choosing an East-West line of sight, the sun's background was reduced.

The safety aspect of using such a transmissometer was investigated. Suppose

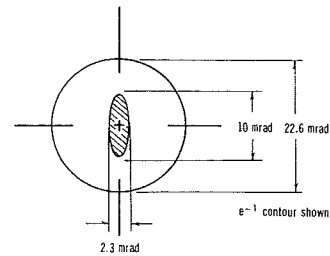


Fig. 6—Field of view of T_x .

someone were to look directly into the transmitter from say 12-in. away. Using the eye iris diameter of 2 mm, and the peak radiant intensity of $J = 8.77 \times 10^{-6} \text{ Wsr}^{-1}$, the peak power admitted to the retina is $8.77 \times 10^{-6} \pi(0.2)^2/4(12 \times 2.54)^2 = 2.97 \times 10^{-10} \text{ W}$. Since the observer would have no bright flash to guide him that the instrument was turned on, he could spend perhaps 2 min examining the aperture. Total energy received would be $2.97 \times 10^{-10} T$ where the total exposure is $T = 2(60)(10)(100 \times 10^{-9}) = 3.3 \times 10^{-4} \text{ s}$. Even if a "hot spot" in the wavefront were present, the total energy would only be $1.57 \times 10^{-13} \text{ J}$.

The transmissometer was extremely sensitive to errors in positioning due to the small field of view. Vibration was a serious problem. If the beam were spread to offset such errors, difficulties would be experienced in achieving the dynamic range.

The GaAs laser diodes were very temperature sensitive with reference to maintaining P_e and λ ; the transmissometer was operated in the laboratory at room temperature looking out through an aperture at R_r .

The laser diodes were unreliable. Catastrophic failure after very short operating times was the rule.

Conclusions

The principle of operation of the instrument lends itself to Lidar for the purpose of air pollution measurements. As higher power GaAs lasers become available, serious consideration will be given to converting the instrument to particulate concentration measurements. Because of the poor reliability of the laser diodes, the instrument has been temporarily abandoned.

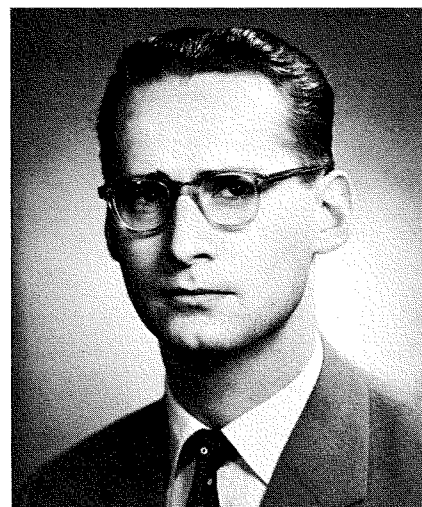
Acknowledgment

Many thanks are due Mr. J. Wood, Mr. R. Bilodeau, and Mr. S. Katz for help during the design and construction of the transmissometer and also due Dr. H. Moody for advice during numerous discussions.

Light scattering with laser sources

Dr. G. Harbeke | Dr. E. F. Steigmeier

The use of the laser as a strong source of highly collimated and very monochromatic light has caused a renaissance of the study of light-scattering spectra in solids. It has now become possible to observe in high-resolution Raman and Brillouin scattering experiments not only lattice vibrations, but also other wavelike excitations as spin waves, collective electron excitations, and polaritons as well as a number of localized excitations. The experimental techniques used in connection with laser sources and a few experimental results are discussed.



Dr. Edgar F. Steigmeier
Laboratories RCA, Ltd.
Zurich, Switzerland

received the Physics Diploma in 1955 and the PhD in Physics in 1960 from the Swiss Federal Institute of Technology (ETH) in Zurich. From 1960 to 1962, he worked at ETH for Brown Boveri Corporation, Baden, Switzerland, engaged in studies of heat conductivity and thermoelectricity. In 1962 he joined the Materials Research Laboratory of RCA Laboratories, Princeton, where he was working on basic properties and applications of thermoelectric materials such as Ge-Si alloys and III-V alloys, which has led to high efficiency materials for power generation. After 2½ years he moved to Laboratories RCA, Zurich, where he worked on problems involving materials with soft lattice vibrations and phase transitions. For two years he has been working in light scattering on these materials as well as on magnetic semiconductors. Dr. Steigmeier has published 20 scientific papers. He is a member of the Swiss and the American Physical Societies.

HUMAN LIFE WOULD BE VERY DULL if light scattering would not exist in nature. It would miss two essentials: the blue sky of a sunny day and the romantic mood of a glowing sunset. These phenomena have occupied the searching mind of man probably for thousands of years. Leonardo da Vinci suggested that the blue sky is caused by scattering of light by air particles. The proof was given in 1899 when Lord Rayleigh discovered the scattering by the air molecules.¹ Rayleigh scattering is an *elastic* process, i.e., the scattered light is of the same frequency as the source.

In 1922 *inelastic* light scattering resulting in the appearance of sidebands in the scattering spectrum, was first considered by Brillouin.² His theory predicted a Doppler shift of the frequency of the incident light due to the existence or generation of sound waves (*acoustical* lattice vibrations—Brillouin scattering). In 1928 Raman succeeded in observing sidebands caused by the interaction of light with *optical* lattice vibrations (Raman scattering).³ Experimental confirmation of Brillouin's theory followed in 1930. These newly discovered effects gave rise to a strong activity in this field, but many physical problems remained unsolved because of the weak light sources available.

With the advent of the laser as a strong source of highly collimated and very monochromatic light, the field of light scattering experienced a real renaissance. Finer details of existing theories could now be tested; new effects could be found; and new materials could be attacked. Moreover, fast

photoelectronic detection techniques could be used for the measurements. In recent years, many different types of lasers have been used depending on the material and the kind of scattering under study.

Basic principles

If an electric field \mathbf{E} is applied to a medium with polarizability α , a polarization \mathbf{P} will be set up according to $\mathbf{P} = \alpha \mathbf{E}$. If the field is associated with electromagnetic radiation of frequency ω , the induced polarization will be oscillating and can thus emit or absorb light. The essential features may easily be understood by considering a diatomic molecule vibrating thermally with frequency ν_1 along the line joining the two atoms. The polarizability for a small displacement, x , can then be written as (assuming harmonic motion)

$$\alpha = \alpha_0 + \frac{d\alpha}{dx} x + \dots = \alpha_0 + \alpha_1 \cos 2\pi \nu_1 t \quad (1)$$

With the electric vector of the incident light $\mathbf{E} = \mathbf{E}_0 \cos 2\pi \nu t$, we obtain for the induced polarization

$$\mathbf{P} = \alpha \mathbf{E} = (\alpha_0 + \alpha_1 \cos 2\pi \nu_1 t) \mathbf{E}_0 \cos 2\pi \nu t = \alpha_0 \mathbf{E}_0 \cos 2\pi \nu t + \frac{1}{2} \alpha_1 \mathbf{E}_0 [\cos 2\pi (\nu + \nu_1) t + \cos 2\pi (\nu - \nu_1) t] \quad (2)$$

where ν_1 is the vibration frequency and ν is the light frequency.

The scattered light now consists of the Rayleigh radiation of frequency ν and the Raman radiation of the frequencies $\nu - \nu_1$ (Stokes line) and $\nu + \nu_1$ (anti-Stokes line). In the general three-dimension case α will be a tensor relating the vectors \mathbf{P} and \mathbf{E} by

$$\begin{bmatrix} P_x \\ P_y \\ P_z \end{bmatrix} = \begin{bmatrix} \alpha_{xx} & \alpha_{xy} & \alpha_{xz} \\ \alpha_{yx} & \alpha_{yy} & \alpha_{yz} \\ \alpha_{zx} & \alpha_{zy} & \alpha_{zz} \end{bmatrix} \begin{bmatrix} E_x \\ E_y \\ E_z \end{bmatrix} \quad (3)$$

and the inelastic scattering may consist of several pairs of Brillouin and Raman lines.

In the quantum-mechanical description of the Stokes scattering process, the incident photon of frequency ν raises the crystal from the ground state into an intermediate state which is reached in a virtual electronic transition. From there, it decays into an excited state of energy $h\nu_1$ above the ground state. The emitted photon lacks this energy $h\nu_1$ and is thus of frequency $\nu - \nu_1$. If the crystal originally is in the excited state, it might give up the energy $h\nu_1$ so that the reverse process takes place. The anti-Stokes photon emitted in this process has the frequency $\nu + \nu_1$. Since the occupation number of the excited state varies according to a Boltzmann factor, the ratio of the intensities of a corresponding pair of anti-Stokes and Stokes lines is governed by the factor $\exp(-h\nu_1/kT)$, and anti-Stokes radiation vanishes at sufficiently low temperatures. Besides the conservation of energy in the overall process, momentum must also be conserved. As shown in Fig. 1,

Reprint RE-15-5-24

Final manuscript received September 12, 1969.



Dr. Günther Harbeke
Laboratories RCA, Ltd.
Zürich, Switzerland

received the Physics Diploma in 1955 and the PhD in Physics in 1958 from the Technical University in Brunswick, Germany. In 1961 he joined the staff of Laboratories RCA, Zurich. Prior to that he has been with the Physikalisch-Technische Bundesanstalt in Brunswick. Dr. Harbeke has been working in research on the basic optical properties of semiconducting and insulating materials. In 1962, he received an RCA Laboratories Achievement Award for team performance in optical studies leading to a better knowledge of the electronic band structure of semiconductors. In 1963, he worked 9 months at the RCA Laboratories in Princeton. He is co-author of the book *Optical Properties and Band Structure of Semiconductors*, with David L. Greenaway. Currently, he is concerned with studies of light scattering in crystals. Dr. Harbeke has published 27 technical papers and has one issued patent. He is a member of the Zurich, Swiss, German and European Physical Societies.

the sum of the momenta of the scattered photon $\hbar\mathbf{k}_s$ and the photon (equivalent description for a normal mode of lattice vibration) $\hbar\mathbf{k}_{ph}$ equals the momentum of the incident photon $\hbar\mathbf{k}_i$. This condition severely limits the number of phonons which can participate in the process. Fig. 2 shows, for example, the dispersion curves of the acoustical and optical phonons of germanium, a lattice with two atoms per unit cell, for only the [111] momentum direction. Since the wave vector of the photon $|\mathbf{k}_i| \approx |\mathbf{k}_s| = 2\pi/\lambda$ for visible light ($\lambda \approx 6000 \text{ \AA}$) is of the order of 10^5 cm^{-1} and since the change in wave vector $|\mathbf{k}_i - \mathbf{k}_s|$ can be no more than $2|\mathbf{k}_i|$, the scattering phonons are located very close to $\mathbf{k}=0$ on the abscissa of Fig. 2 extending to $\mathbf{k}_{max} = 2\pi/a$ (a =lattice constant) which is of the order of 10^8 cm^{-1} . The energy of the scattering optical phonons is practically independent of the scattering geometry since the dispersion is very small. This is not so in Brillouin scattering because of the linear energy-momentum relation for long-wavelength acoustic phonons. The slopes represent the transverse and longitudinal sound velocities which can thus be measured by Brillouin scattering.

In a crystal with N atoms per unit cell there are $3N$, partly degenerate, phonon branches. Group theory predicts the number of branches which are Raman active provided the crystallographic space group of the crystal is known. For each Raman active vibration, those polarizability tensor components which are changing during the vibrational motion inducing the Raman effect can also be calculated. The components of the Raman tensor are measured by arranging different configurations of the polarization of the incoming light, polarization of the scattered light, and the crystallographic axes. This allows us to determine how the atoms move against each other in a certain vibrational motion.

So far, we have discussed the first-order Raman effect where one phonon participates. If we expand the polarizability tensor as in Eq. 1 and keep the next term, it describes the modulation of the polarizability induced by the creation of two phonons. Energy and momentum have to be conserved again which means that only pairs of phonons of opposite and almost equal wave vector \mathbf{k} and $-\mathbf{k}$ adding up to $\mathbf{k}_i - \mathbf{k}_s \approx 0$ fulfill the momentum condition. Phonons throughout the whole Brillouin zone can thus participate provided the symmetry requirements are properly met. This leads to fairly broad second-order bands which are dominated by the contribution from critical points where the dispersion curves are horizontal and the density of phonon states is highest. Such critical points exist preferably at the Brillouin zone edges like at $|\mathbf{k}| \approx 2\pi/a$ in Fig. 2. To illustrate both processes Fig. 3 shows the Stokes side of the Raman spectrum of germanium. There is only one first-order Raman active optical vibration at 300.6 cm^{-1} and the second-order band at 571 cm^{-1} . Note the difference in line-width and amplitude. Although phonons throughout the Brillouin zone can be generated in second order, the process involving two phonons is several orders less probable than in first order so that a much smaller line results.

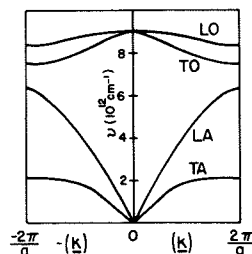
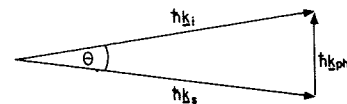


Fig. 2—Frequency versus wave-vector curves of germanium in the [111] momentum direction; T=transverse, L=longitudinal, A=acoustical, O=optical.

Fig. 1—Conservation of momentum in a first-order scattering process.



Enter the laser

Virtually only Raman scattering from phonons was known before the laser entered the scene. This situation has drastically changed since. It has now become possible to observe an impressive series of other excitations in crystals such as magnons or spin waves, plasmons as collective electronic excitations, single electron excitations, polaritons as mixed phononphoton modes. In addition to these also scattering from localized phonons, F -centers, localized magnons and electronic levels was investigated.

Experimental techniques

Figs. 4 and 5 show the experiment for the observation of Raman scattering. The light source is either a 90-mW *He-Ne* laser, emitting red light of wavelength $\lambda=6328 \text{ \AA}$, or an RCA LD 2101 1-W argon-ion laser, emitting several lines in the blue and green, the strongest of them at $\lambda=4880 \text{ \AA}$ and $\lambda=5145 \text{ \AA}$. The linearly polarized laser light passes through a 30 \AA -half-width interference filter to eliminate the spontaneous radiation, and a $\lambda/2$ plate which can be used to turn the plane of polarization and is focussed on the sample to a circular spot of about $50\text{-}\mu$ diameter. The scattered light is collected by a lens, sent through an analyzer, and focussed on the entrance slit of a double-grating spectrometer. This is an arrangement suitable for opaque crystals whereas the scattering from transparent crystals is mostly observed under 90° to the incident beam such that the light path in the crystal is parallel to the entrance slit. The analyzed spectrum emerging from the exit slit is focussed onto the small active central area of the photomultiplier cathode. Each individual pulse from the anode is then amplified and discriminated against the background of pulses arising from the dynodes and other sources of small pulses. The small active area of the cathode serves to reduce the thermal emission of electrons from the cathode considerably. Finally the pulses are counted in a linear and a logarithmic ratemeter, respectively, and the spectra are recorded in analog form. The dark count rate of the photon counting system is about 0.5 count/sec. With a photocathode quantum efficiency of roughly 2%, this dark rate amounts to an energy of 8×10^{-18} Watt which is

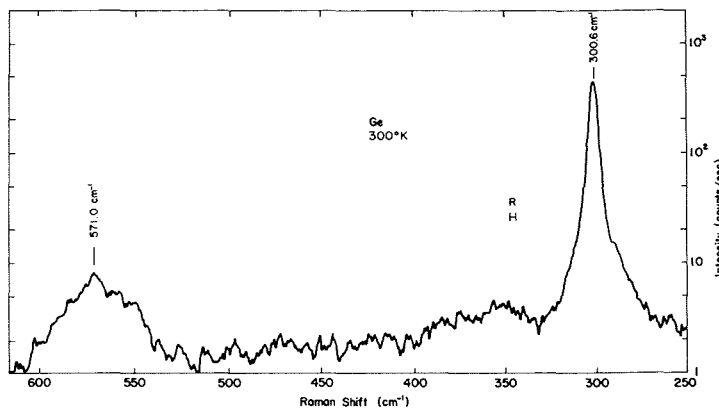


Fig. 3—Raman spectrum of germanium; logarithm of intensity (counts/sec) versus Raman shift (cm^{-1}).

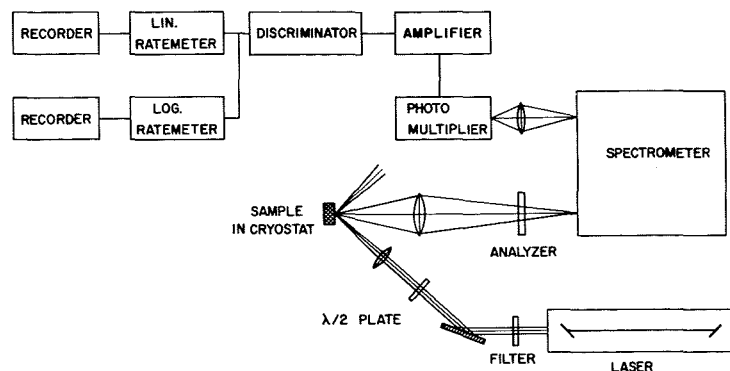


Fig. 4—Experimental arrangement for Raman scattering.

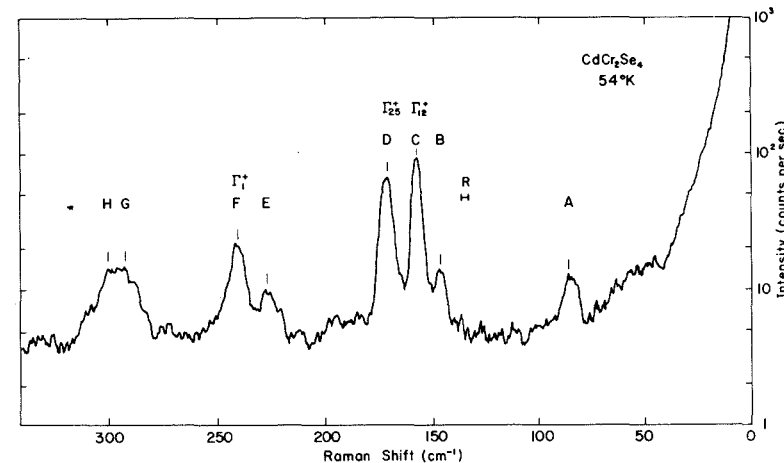
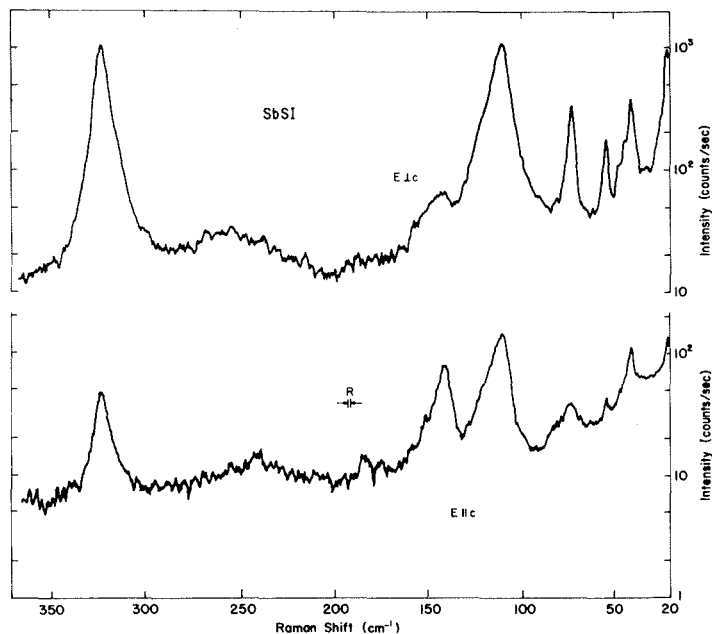


Fig. 7—Raman spectrum of CdCr_2Se_4 at 54°K ; logarithm of intensity (counts/sec) versus Raman shift (cm^{-1}).

Fig. 6—Raman spectrum of SbSI for $E||c$ and $E||c$; logarithm of intensity (counts/sec) versus Raman shift (cm^{-1}).

Table 1—CW lasers useful in Raman spectroscopy. [Note: if operating temperature is not given, room temperature is assumed.]

Laser Type		Power	Wavelength
Gas	CO	20 W	4.65 to 6μ
	CO ₂	10 kW	9.6μ , 10.6μ
	He-Ne	90 mW	6328 Å
	Argon	10 W	4579 to 5145 Å
	Krypton	2 W	4619 to 6764 Å
	Nitrogen	100 mW	3371 Å
Solid state	YAG:Nd ³⁺ (300°K)	270 W	1.06μ
	YAG:Ho ³⁺ (77°K)	15 W	1.33μ
	CaF ₂ :U ³⁺ (77°K)	1 W	2.1μ , 2.6μ
Injection	GaAs (4.2°K)	1 W	8370 Å
	Ga _x In _{1-x} As (4.2°K)	100 mW	
	InAs (4.2°K)	200 mW	3.1μ

more than 15 orders of magnitude below the incident laser energy. The low scattering probabilities of many processes categorically demand such a high ratio. Spectra are recorded with scanning rates between 1 and 5 $\text{cm}^{-1}/\text{min}$. and appropriate time constants of 2 to 35 sec. Normally a resolution of about 3 cm^{-1} is set by the slit width. Table 1 contains a list of various cw laser types which have proven useful in Raman spectroscopy according to Mooradian.⁴

The basic set-up for Brillouin scattering is quite similar with two possible exceptions: 1) the spectrometer is replaced by a high resolution Fabry-Perot interferometer or 2) an optical heterodyne detection technique is used.⁵ The high resolution is required by the position of the acoustical phonon lines which is generally between 0.1 and 1 cm^{-1} and even more by the linewidth which may be again only a fraction of the position. The linewidth is a measure of the lifetime of the phonon (or of any other observable excitation) and is thus a very useful quantity in the study of the in-

teraction of phonons with themselves or other physical entities. These features also necessitate the use of a laser with a linewidth considerably smaller than the Brillouin linewidths. Normal linewidths of gas lasers are of the order of 0.1 cm^{-1} so that for Brillouin scattering experiments a mode-selected, frequency-stabilized laser has to be used. A stability of 10^{-9}cm^{-1} can be reached with a medium effort. On the detection side, it is very useful to store the optical signal from the repetitively scanned interferometer in a multichannel analyzer so that by summing the signal over a sufficient number of

scans, a significant improvement in signal-to-noise is reached. A Brillouin spectrometer with these features is being set up in the Zurich laboratory.

Experimental results

Fig. 6 shows the Stokes side of the Raman spectrum of ferroelectric SbSI ⁶ for two different orientations of the incident polarization relative to the c -axis of the orthorhombic crystal. Here we note several first-order lines since the unit cell contains 12 atoms so that 33 partly degenerate, optical phonon branches exist. We note further that the occurrence and relative

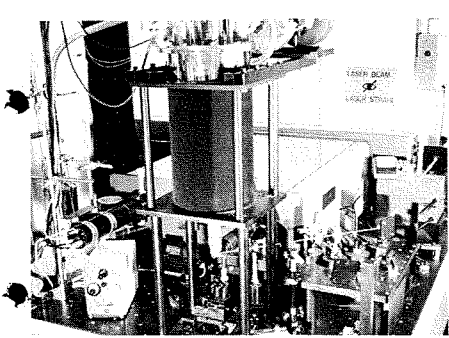


Fig. 5—Experimental setup for Raman scattering.

strength of the lines depend on the orientation according to the differences in the Raman tensor components. These results allowed us to assign a number of symmetry types of vibrations to the lines. *SbSI* represents a very interesting example of a ferroelectric crystal where one or more optical lattice vibrations go "soft," i.e. they decrease strongly in energy by approaching the ferroelectric transition temperature from either side. Although we observe some low energy excitations (compare to *Ge*, Fig. 3) the lowest one with the strongest temperature dependence may be masked by the high Rayleigh intensity below 20 cm^{-1} . A novel optoelectronic subtraction technique⁴ is being developed to eliminate the Rayleigh line from the spectra. This will enable us in connection with Brillouin scattering to study the interesting subject of phase transitions in solids more closely.

An interesting example of interplay between different kinds of excitations is provided by the ferromagnetic semiconductors CdCr_2Se_4 and CdCr_2S_4 . Fig. 7 shows the Stokes side of the Raman spectrum of CdCr_2Se_4 at 54°K . Some lines are found to be pure phonon lines, the frequency and intensity of which vary very little with temperature. The use of different polarizations of the incident and scattered light permits the assignment of lines c and f as first-order lines of symmetry Γ_{12}^+ and Γ_1^+ , respectively. Other lines are interpreted as second-order lines. Line d shows the interesting feature that its intensity is strongly temperature dependent; it is strong only in the magnetically ordered state below the Curie temperature of $T_c=130^\circ\text{K}$. It is a first-order-phonon line of symmetry Γ_{25}^+ the intensity of which is enhanced by the ferromagnetic ordering of the Cr^{3+} spin system. Fig. 8 shows that the temperature dependence of the intensity of this line, normalized to the Γ_{12}^+ phonon line (which for itself is temperature independent), follows exactly that of the ferromagnetic nearest-

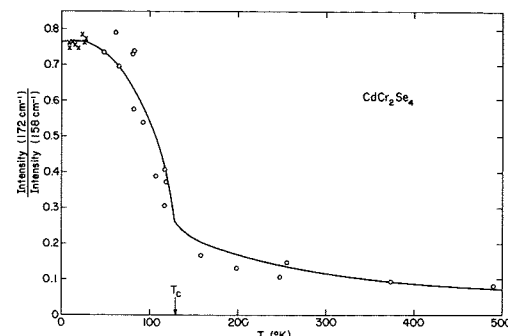


Fig. 8—Intensity of line Γ_{25}^+ (172 cm^{-1}) of CdCr_2Se_4 normalized to line Γ_{12}^+ (158 cm^{-1}) versus temperature; solid line: nearest neighbor spin-correlation function.

neighbor spin-correlation function.

The temperature dependence of the frequency of line d proves, on the other hand, that it is not due to a direct excitation of the spin system alone, i.e., spin wave or magnon. Similar results have been found for CdCr_2S_4 . Fig. 9 shows that the intensity of the Γ_{25}^+ line again is closely related to the ferromagnetic ordering which in this material occurs below $T_c=84^\circ\text{K}$. It is interesting to note that for CdCr_2S_4 a few more lines show this striking behaviour. A comparison of CdCr_2S_4 and CdCr_2Se_4 is given in Fig. 10. It is seen that a great deal of the spectra can be scaled into each other, the replacement of *Se* by *S* causing a stiffening of the lattice. From all the experimental evidence, we have to conclude that the unit cell is gradually distorted with ferromagnetic ordering. This distortion, which may be very small, has not yet been found by X-ray analysis.

Fig. 11 shows an example of Brillouin scattering, the spectrum of *GaP* observed by Fray et al.⁸ Since the momentum configuration was chosen in such a way that phonons in a low-symmetry direction are created or annihilated, three pairs of lines representing two transverse acoustical vibrations and one longitudinal acoustical vibration are found. From these Brillouin shifts, the three corresponding sound velocities could be determined. The central line which can be many orders of magnitude stronger than the Brillouin (or Raman) intensity is the Rayleigh component of the scattered radiation.

Concluding remarks

These briefly discussed examples of experimental work cover only a small section of the modern field of light scattering after its revival. Most of the knowledge about the nature of and interactions among excitations in crystals which we learned from the scattering spectra could only be gained

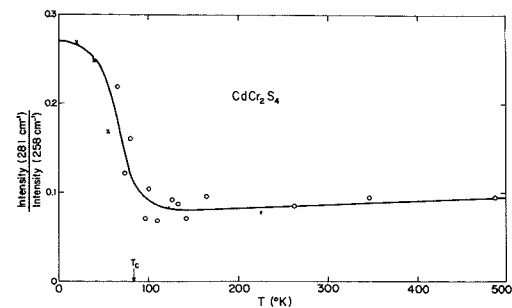


Fig. 9—Intensity of line Γ_{25}^+ (281 cm^{-1}) of CdCr_2S_4 , normalized to line Γ_{12}^+ (258 cm^{-1}) versus temperature.

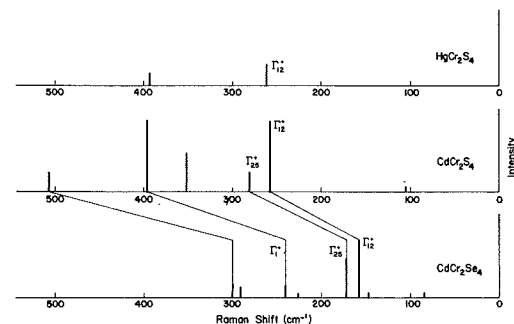


Fig. 10—Comparison of Raman spectra of CdCr_2Se_4 , CdCr_2S_4 and HgCr_2S_4 at 50°K .

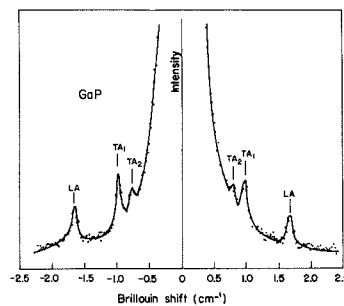


Fig. 11—Brillouin spectrum of *GaP*; intensity in arbitrary units versus Brillouin shift (cm^{-1}); output direction of light $[113]$, input direction $[110]$.

with the help of the laser. In addition to the use of light scattering for materials characterization, this field also offers some prospects for technical applications. Stimulated Raman and Brillouin effect provide the possibility of tunable cw Raman and Brillouin lasers. One can foresee more progress to come from future work.

References

- Lord Rayleigh, *Philadelphia*, Vol. 47, No. 375 (1899).
- Brillouin, L., *Ann. Phys. (Paris)* Vol. 17, No. 88 (1922).
- Raman, C. V., *Indian J. Phys.* Vol. 2, No. 387 (1928).
- Mooradian, A., "Light Scattering in Semiconductors", to be published in *Festkorperprobleme X*, Vieweg, Braunschweig.
- Cummins, H. Z., Knable, N. and Yeh, Y., "Observation of Diffusion Broadening of Rayleigh Scattered Light," *Phys. Rev. Letters*, Vol. 12, No. 150 (1964).
- Fatuzzo, E., Harbecke, G., Merz, W. J., Nitsche, R., Roetschi, H. and Ruppel, W., "Ferroelectricity in *SbSI*," *Phys. Rev. No. 127*, No. 2036 (1962).
- Baltzer, P. K., Lehmann, H. W. and Robbins, M., "Insulating Ferromagnetic Spinels," *Phys. Rev. Letters* Vol. 15, No. 493 (1965).
- Fray, S. Johnson, F. A., Jones, R., Kay, S., Oliver, C. J., Pike, E. R., Russell, V., Sennett, C., O'Shaughnessy, J., and Smith, C., "The Brillouin, Raman and Infra-red Spectra of Gallium Phosphide," *Proc. Int. Conf. Light Scattering Spectra of Solids* (Springer, New York, 1960) p. 139.

Infrared images made visible by laser techniques

Dr. A. H. Firester

Most information enters our brain through our eyes. To extend our sight is one function of instrumentation. Telescopes and microscopes operate upon light to which our eyes respond; x-rays and radar enable us to see where our eyes do not respond. Beyond red, where we cannot see, lies the spectral region called the infrared. This paper presents a new technique for "seeing" in the infrared by upconverting infrared images to visible images.



Dr. Arthur H. Firester
Semiconductor Device Research Laboratory
RCA Laboratories
Princeton, N.J.

graduated with honors in Physics from Brandeis University and received the MA and PhD from Princeton University in 1964 and 1967 respectively. Before joining the staff of RCA's Electronic Research Laboratory, he held the position of Instructor on the faculty of Princeton University. His doctoral dissertation dealt with light modulation by optically-pumped, atomic potassium; however, his recent research is on nonlinear phenomena and their application to image processing. He is a member of the Society of Sigma Xi, the American Physical Society, and the Optical Society of America.

VARIOUS TECHNIQUES NOW EXIST for converting infrared images to visible ones. For example, converters using the *Ag-O-Cs* photoemitter extend sight to about 1.1-micrometer wavelengths. At longer wavelengths, arrays of photoconductive elements must be used. We have researched an entirely different approach to the problem of infrared image conversion. This approach is called image upconversion because each photon from the infrared scene is raised in energy or upconverted to produce a higher-energy, visible photon. These visible photons simulate the original infrared scene.

There are differences between present day image conversion and upconversion. In some photoconductive systems, the resolution depends upon the number of discrete elements in an array. In contrast, the upconversion process takes place within a homogeneous material. Some photoconductors require cooling to 77°K and lower temperatures. The upconverter will not require cryogenic cooling. To use either the photoemissive or the photoconductive image converter, the infrared scene must be focused upon the photosensitive surface by an optical system. However, image upconversion is a truly three-dimensional process. It does not convert infrared intensities as do other image converters; it converts the electric fields themselves. The upconverter can be incorporated within a conventional optical system like a telescope, but it is not necessary to focus the scene upon it. Our interest has been primarily with the imaging properties of upconversion. In the course of our work, we have obtained upconverted images with more than 200x300 resolution elements and resolved more than 750 line pairs/inch.

Theory of image upconversion

Image upconversion has become possible only with the advent of powerful lasers. To upconvert an infrared photon, it must interact and sum with another photon. These other photons must be furnished by a powerful laser because the interaction is quite weak. This interaction does not occur in any medium; it takes place only within nonlinear materials. In such materials, the electric polarization generated by an optical field has a quadratic dependence upon field strength as well as the usual linear dependence. This nonlinearity, measured by a nonlinear susceptibility χ^2 couples two incident waves and generates a nonlinear polarization at their sum frequency. This polarization radiates and produces the upconverted image.

Fig. 1 illustrates how an image upconverter might be implemented. The scattered IR radiation from the laser-illuminated flowerpot and the output of the pump laser are incident upon a nonlinear medium. In the nonlinear material, these two radiations interact and generate their sum frequency which is transmitted by the ν' pass filter. What the eye sees is a flowerpot at the new color. This upconverted image differs in magnification, apparent location and resolution, as well as color, but it does resemble the original flowerpot. We will discuss the physical bases of these differences and their experimental verification.

Consider the interaction of a planar object wave with a planar pump wave in an ideal nonlinear material. As illustrated in Fig. 2, the propagation vector of the object radiation, k_ω , adds vectorially to the propagation vector of the pump wave, k_ν . Their resultant, the vector $k_\nu + k_\omega$, is in the direction of the upconverted wave.

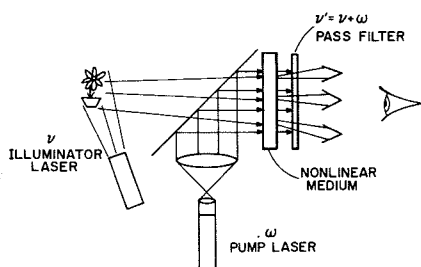


Fig. 1—Typical infrared image upconverter.

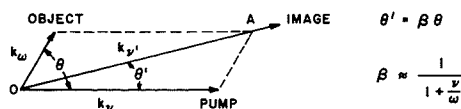


Fig. 2—Interaction of two plane waves in a nonlinear medium.

For small angles, the angle θ , between the object ray and the pump ray, and the angle θ' , which the upconverted image ray makes with the pump ray, are linearly related. Thus the angular relationship of the object waves is preserved by the upconverted image waves.

The nonlinear polarization is driven by a wave whose propagation vector is the vector sum of the object and pump propagation vectors, $k_\nu + k_\omega$, or OA in Fig. 2—a vector from the origin to the upper right apex of the parallelogram. However, the nonlinear polarization radiates a wave with a propagation vector of magnitude $|k_\nu'| = 2\pi \nu'/c$. Only for a collinear object and pump wave are the driving wave vector, $k_\nu + k_\omega$, (OA) and the radiating wave vector k_ν' equal; as the object and pump waves deviate from collinearity, the difference between the driving and radiating wave vectors increases. Thus, the wave driving the polarization and the radiating wave get out of phase, and waves making too large an angle with the pump wave are not efficiently upconverted. Only those rays emanating from a particular object point which make less than a given angle with the pump will be upconverted. The size of this angle depends upon the thickness of the nonlinear material.

To see how these two points determine the imaging process, consider an infinitesimally thick ideal nonlinear material located a distance q from the object and simultaneously illuminated by a planar pump wave as illustrated in Fig. 3. The nonlinear polarization generated in volume dv will radiate an upconverted plane wave which makes an angle θ' with the pump wave. The intersection of all upconverted waves from every volume of the nonlinear material, due to the interaction of pump waves and waves from a particular object point, defines

the location of the corresponding image point.

Under these circumstances, the image undergoes a longitudinal magnification of $1/\beta$ and unity transverse magnification. The image location is not the same as the object location but appears to be further away than the object and of course there is a concomitant depth distortion. The unity transverse magnification implies that the image has the same height and width as the original object. For a finite thickness of nonlinear material, object rays making too large an angle with the pump beam would not be upconverted. This limits the image resolution much the same as a finite-sized lens limits the ultimate resolution of a conventional optical system.

Experiments

We have demonstrated certain features of image upconversion in our laboratory. The apparatus used is illustrated in Fig. 4. It has been convenient to use a single laser both to illuminate the object and to act as the pump source.

Because our object and pump beams have the same frequency, polarizing beamsplitters are used. A 16-millimeter black-and-white film transparency, located in one of the beams, serves as an object while the other orthogonally polarized beam is the pump beam. The nonlinear medium, is a 1.2 cm cube of potassium dihydrogen phosphate (KDP)

Fig. 5 illustrates some of the results. The infrared photograph (Fig. 5a) was made with the camera focused upon the object transparency and the pump beam blocked. The upconverted photograph (Fig. 5b) was made with the camera focused on the virtual upconverted image. This photograph contains at least 300x200 resolution elements and is capable of resolving about 500 line pairs/inch in the object transparency. This resolution is com-

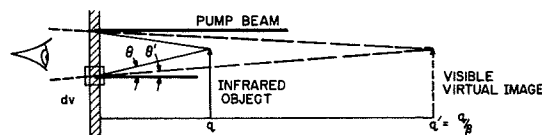


Fig. 3—Imaging of an object point by the upconverter.

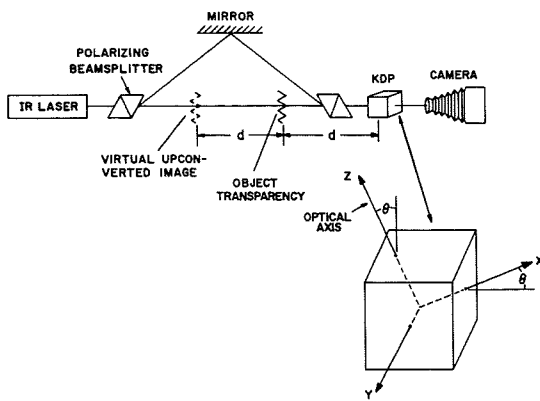


Fig. 4—Experimental apparatus for the demonstration of the imaging properties of upconverters ($\theta=0.527$ radius).

parable with the theoretic maximum determined by the 1.2-cm-thick nonlinear material.

While an image upconverter operating directly on the infrared object's radiation does have an unlimited field of view, it loses resolution because of the finite thickness of the nonlinear material. Field of view can be traded for higher resolution by upconverting not the object radiation but the Fourier transform of this radiation. This upconverted image is *not* resolution-limited by the nonlinear material; however, the field of view is reduced.

These results were demonstrated with a modified version of the apparatus illustrated in Fig. 4. Fig. 6a is an infrared photograph of the original object transparency. The uneven background and the diffraction rings are caused by the laser illumination. Fig. 6b is an enlarged photograph of the upconverted image. The region near the number 400 corresponds to about 750 line pairs/inch. In the original photograph, the resolution is about twice that of the upconversions of Fig. 5.

Present status of image upconversion

Most image upconversion has been done either with or assuming a planar pump beam. However, the image upconverter can operate with point source pump-beams, and can generate good quality upconverted images.¹³ The major effect of the pump-beam divergence is not to degrade the resolution but is to change the transverse and longitudinal magnification of the image upconverter. Furthermore, it has been shown that despite the usual resolution limitations imposed by the thickness of the nonlinear material,

higher resolution might be achieved by the use of a *point* source pump. By lensless Fourier transform holography¹⁴, high resolution objects can be recorded on low resolution film. So too, by using a point source pump, the upconverted image should not be resolution limited by the thickness of the nonlinear material. Indeed the analogy of image upconversion with holography is a correct one.¹⁵ The image from an upconverter is the same as the image from an equivalent hologram.

We have discussed only monochromatic, laser-illuminated objects because only laser illuminated objects have been used in laboratory demonstrations. In principle, the upconversion process is applicable to polychromatic, self-radiant or incoherently illuminated objects. However, a polychromatic object will not generally form a single upconverted image because the upconverter's magnification ($1/\beta$) is wavelength dependent. A number of techniques have been suggested^{10,12} for eliminating this chromatic aberration, but none have yet been tested. The present inefficiency and narrow bandwidth of the upconversion process makes image upconversion of polychromatic objects impractical.

Conclusions

At present, we understand the operation of image upconverters with either planar or nonplanar pump beams, their resolution and their chromatic aberrations. While there is further work to be done to extend the



Fig. 5—Photographs of a) object transparency at 10,640 Å and b) upconverted image at 5320 Å.

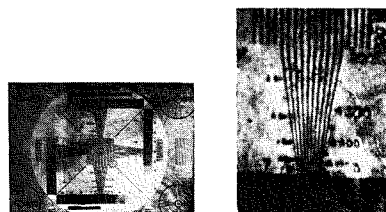


Fig. 6—Photographs of a) object transparency at 10,640 Å and b) upconverted image at 5320 Å using high-resolution upconversion technique.

theory and demonstrate the validity of these extensions, our understanding of the imaging process is sufficiently advanced so that this is not the major impediment to the useful upconversion of images. To transfer the process from the laboratory to the field—to use it rather than to demonstrate it—requires much higher conversion efficiencies. Better nonlinear materials are required. They should be more nonlinear, and perhaps even more important, they must be useful over large acceptance angles and spectral bandwidths. Thus, upconversion offers the possibility of real-time 3D conversion of images of distant objects with the attractive feature that low-noise processing of long-wavelength IR will not require low-temperature cooling.

References

1. Johnson, F., and Duardo, J. A., "Infrared Detection for Parametric Frequency Up-Conversion" *IEEE J. Quant. Elec.*, Vol. QE2, (1966) p. 296.
2. Midwinter, J. E., and Warner, J., "Up-Conversion of Near Infrared to Visible Radiation in Lithium-meta-niobate" *J. Appl. Phys.* Vol. 38 (1967) p. 519.
3. Miller, R. C., and Nordland, W. A., "Conversion of Near Infrared to Visible Light by Optical Mixing" *IEEE J. Quant. Elec.* Vol. QE3 (1967) p. 642.
4. Warner, J., "Photomultiplier Detection of 10.6 μ m Radiation Using Optical Up-Conversion in proustite" *Appl. Phys. Letters* Vol. 12 (1968) p. 222.
5. Boyd, G. D., Bridges, T. J., and Burkhardt, E. G., "Up-Conversion of 10.6 μ Radiation to the Visible and Second Harmonic Generation in HgS " *IEEE J. Quant. Elec.* Vol. QE4 (1968) p. 515.
6. Midwinter, J. E., "Image Conversion from 1.6 μ to the Visible in Lithium-Niobate" *Appl. Phys. Letters* Vol. 12 (1968) p. 68.
7. Midwinter, J. E., "Parametric Infrared Image Converters," *IEEE J. Quant. Elec.* Vol. QE4 (1968) p. 716.
8. Warner, J., "Spatial Resolution Measurements in Up-Conversion from 10.6 μ to the Visible" *Appl. Phys. Letters* Vol. 13 (1968) p. 360.
9. Gampel, K., and Johnson, F. M., "IR Image Detection by CW Parametric Up-Conversion to the Visible" *IEEE J. Quant. Elec.* Vol. QE4 (1968) p. 354.
10. Warner, J., "Infrared to Visible Image Up-Conversion" *IEEE J. Quantum Elec.* Vol. QE5 (1969) p. 354.
11. Andrews, R. A., "IR Image Up-Conversion in KDP" *IEEE J. Quantum Elec.* Vol. QE5 (1969) p. 355.
12. Firester, A. H., "The Imaging Properties of Image Converters Using Optically Nonlinear Material" *IEEE J. Quantum Elec.* Vol. QE5 (1969) p. 355.
13. Firester, A. H., "The Thin Lens Equation for Optical Parametric Image Converters" to be published *Opto-Electronics*, No. 3 (1969).
14. Stroke, G. W., Bruum, D., Funkhouser, A., "Three-dimensional Holography with Lensless Fourier-Transformed Holograms and Coarse P-N Polaroid Film" *J. Opt. Soc. Am.* Vol. 55 (1965) p. 1327.
15. Firester, A. H., "Parametric Image Conversion—Part I" and "Holography Parametric Image Conversion—Part II" *J. Appl. Phys.* (1969).

System tests for the VideoComp 70/830

R. M. Carrell

This paper reviews the technical and aesthetic aspects of typography and shows some test patterns which compare various aspects of the VideoComp Electronic Composition System performance in a way which abnormalities are easily detected by an "eyeball" examination. In a larger sense, this paper provides insight into the methods of establishing system tests for human-oriented systems. A comprehensive test for such systems should be designed so that a quick "eyeball" review of the output will detect any significant abnormalities, which on further review can be numerically evaluated against specifications or indicate further tests required.

A LARGE PART of the electronics industry has its principal reason for being in the satisfaction of a human need. This is most obvious in consumer products, such as television, sound reproduction, and the movies. VideoComp is also in this category, for its output is the photographic image of a page which will be converted to printed copy and distributed to consumer markets of various types.

In all of these systems there is a cost/performance tradeoff which is made in the design and production of equipment. Typically, the ultimate market is stratified into various quality levels—e.g., 70 mm and 8 mm movies; console and miniature TV; and studio and portable radios and phonographs. As these fields have matured, technical criteria have been established which will quantitatively define the performance necessary to satisfy the quality criteria of each part of the market.

Ultimate decisions on the acceptability of such systems frequently combine a typical use with a synthetic system test. In visually oriented systems, this is usually a test pattern. One or more skilled observers classify the subjective quality of the overall result; the appearance of the test pattern through the same system can then be correlated to give thereafter a standard of acceptability. A good test pattern for a system has these basic properties:

- 1) It can be quickly interpreted by a human.
- 2) It is sensitive to all the factors affecting the aesthetic and technical utility of the system.

- 3) It will quickly expose technical abnormalities of the system.
- 4) It can be numerically interpreted in terms of system specification limits.

Television test patterns are familiar examples meeting these criteria. An experienced person need only look at a few patterns in order to accurately assess the performance of a system.

Historical note

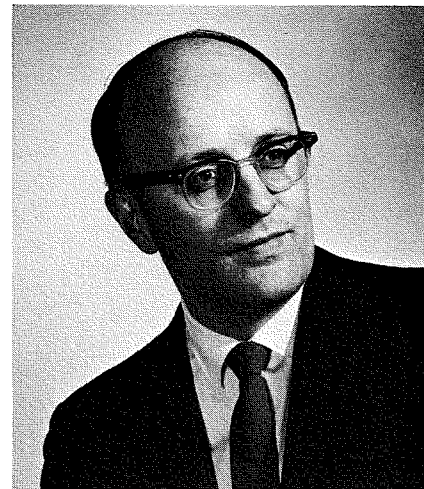
Printing is one of the oldest industries which mass produce an aesthetic product by technical means. The Gutenberg Bible is still a model of aesthetically satisfying typography.

With the invention of typesetting machines, there grew an effort to achieve the mechanical precision necessary to produce a page of aesthetically pleasing type. Even in the earlier days there was a division in application between the Linotype, which is somewhat faster but which imposes constraints on type design, and the slower, more-flexible Monotype.

With the introduction of the VideoComp, the whole question of the system tolerances necessary to achieve an aesthetically pleasing result had to be reexamined. Some problems which are vexing in a Linotype are easy in a VideoComp, such as the vertical alignment of adjacent characters. In a Linotype, getting straight baseline for a set of characters across the page is easy, but in a VideoComp it requires excellent deflection linearity.

Aesthetic and technical aspects of Typography

Typography includes the style, arrangement, and appearance of printed matter, as well as the technique of its



R. Michael Carrell
Systems Engineering
Graphic Systems Division
Dayton, N.J.

received a BSEE from Iowa State University in 1949 and joined RCA Engineering Products the same year. He has been active in development of acoustical transducers, magnetic recording, and military keyboards and printers, and has participated in system studies of electromagnetic interference. He joined GSD in 1965 as a member of the Product Planning staff, and is now in Systems Engineering. He holds several patents and is author or co-author of a number of technical papers. He is a member of IEEE.

production. Fig. 1 shows a schematic relationship between typographical and technical factors as they relate to the VideoComp System.

The aesthetic aspects of typography resolve into character form and char-

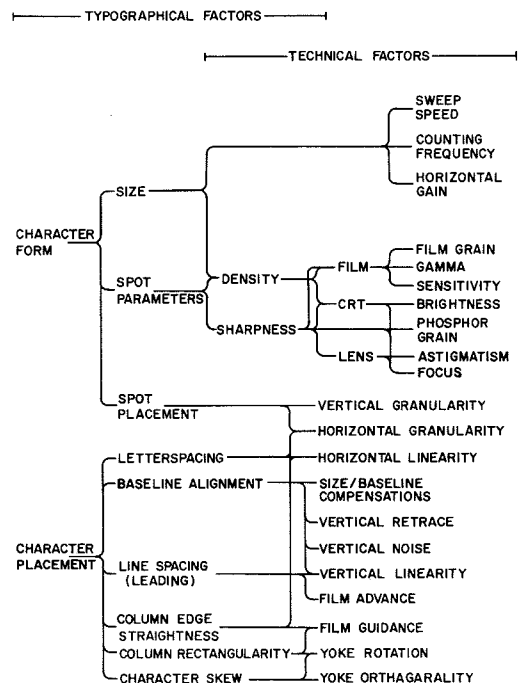


Fig. 1—Relationship of typographical factors and technical factors in VideoComp 70/830.

acter placement. An artist creates a set of letter forms, called a *font*, which are mutually compatible and convey a distinctive style and feeling. The mutual placement of these characters, called *letterspacing*, is critical in achieving an overall even appearance to a page, which contributes to legibility and ease of reading.

In the VideoComp, the reproduction of an original character form is constrained by the digital techniques used and limitations of the CRT, lens and film. Character placement is constrained by the digital and analog electronics and the film advance mechanism. In general, the VideoComp 70/800-series embodies a very successful series of tradeoffs which are able to meet high standards of typographic quality. In some respects, VideoComps excel all machine methods of typesetting, except the basic foundry-type methods which are hand set.

VideoComp electronic composition system

The VideoComp Electronic Composition System is primarily a text-setting machine. Steps in the preparation of text are:

- 1) Typefonts, each containing a set of 80 or more characters, are stored in a large processor such as a Spectra 70/45.
- 2) Text containing alphanumeric characters and format instructions is fed into the processor.
- 3) A composition program, such as RCA PAGE-1, combines the text instructions and font data into a VideoComp control tape.
- 4) The VideoComp control program is loaded into the control processor (RCA 1600).
- 5) The composed tape is played on the VideoComp which produces text-bearing film or paper.

VideoComp test patterns

There are two basic parts to the tests; text simulation and technical performance.

Text simulation

In the text simulation tests, a font consisting of special characters is used. Fig. 2 shows this character, which is placed at each of 80 character addresses in the font tape. The text consists of a repeated sequence of all 80 characters, broken up into regular

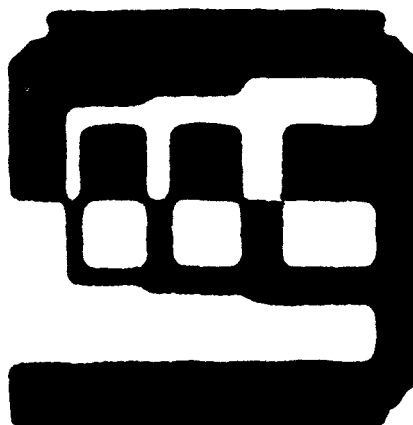


Fig. 2—VideoComp test character.

word groups. When the resulting composed tape is played on a VideoComp, the result is a regular array of the same repeated character, as shown in Fig. 3.

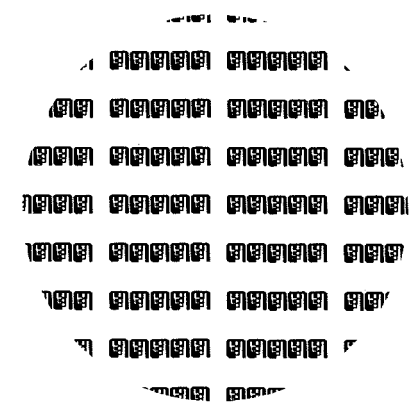
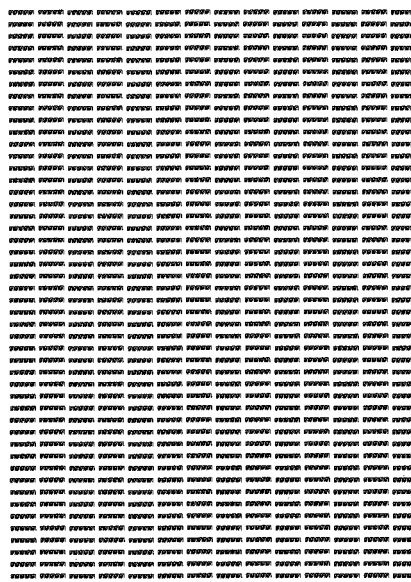


Fig. 3—Test character array (the circle shows a portion of the test pattern in full size).

The features of test character (Fig. 2) include:

- 1) The digital parameters (number of strokes, number of elements per stroke, number of bytes of storage required) are the same as a typical character used in standard English.
- 2) Top and sides are straight, making it easy to check alignment of rows and columns.
- 3) Horizontal and vertical, black and white lines are provided as a test of spot size, shape and exposure.
- 4) Steps are provided in the corners as a check on astigmatism along the $\pm 45^\circ$ axes.

The completed array (Fig. 3) comprises a test of the following items:

- 1) Font loading and addressing functions,
- 2) VideoComp control program functions,
- 3) System writing speed,
- 4) Column rectangularity,
- 5) Baseline alignment,
- 6) Spot size and shape, and
- 7) Exposure.

Items 1 and 2 are proven by correct appearance of the completed text pattern. Item 3 is a stopwatch test of the time required to set a large number of characters. Because the digital characteristics are the same as the average English characters used in a speed formula, the actual speed can be checked against a specification model. Items 4 and 5 can be checked against a straightedge. Items 6 and 7 affect the appearance of the thin lines within the character. Fig. 4 shows the appearance of the character for several conditions of focus, astigmatism, and exposure.

The first level of evaluation is an overall visual impression of the evenness of the text and the impression of blackness. Next, the rows and columns are checked against a straightedge. Next, the characters are examined through a 10x magnifier and compared with a standard. Finally, microdensitometer and microscope measurements are used to give quantitative results.

Since the character is digitally similar to a normal text character, it can be printed as a routine part of every text sample as a check on the machine focus and exposure.

Technical performance

Technical performance tests supplement the text simulation tests by providing patterns which are directly

related to key technical factors. Important characteristics of these tests are:

- 1) A quick visual inspection will reveal an abnormal condition.
- 2) The tests can be numerically interpreted with simple aids (magnifying comparator, reference standards).

Density tests

Proper exposure is basic in phototype-setting. The VideoComp has the capability of varying character size by changing the spacing and length of the writing strokes in eight steps over a 2:1 range. Since a constant density must be maintained over this range, the beam current must be compensated for variation in spot size and writing velocity. In some cases, the height of a character is changed by varying the sweep velocity; in other cases, the velocity is constant, and the vertical timebase clock frequency is changed. Four quality modes are provided, with different numbers of strokes/character and elements/stroke. Proper operation of each of the compensation circuits is checked by writing a square patch in each of 8 sizes in the four quality modes, as shown in Fig. 5. Every possible stroke is written, producing a density representative of the maximum density in a written character. A large patch is made for convenience in use of an area densitometer in checking density against a numerical specification standard. Normally the patches are too dense for eyeball judgement.

Visual judgement of density is possible by writing in every third stroke position, which reduces the average density to the point where the patches appear gray. Density of the gray patches is directly related to that of the solid black patches, so that operation of the intensity-compensating circuits, and overall density, can be seen immediately. The density of the gray patches fall within the range of some simple densitometers used for checking halftone screen densities. Such devices can be used with the gray

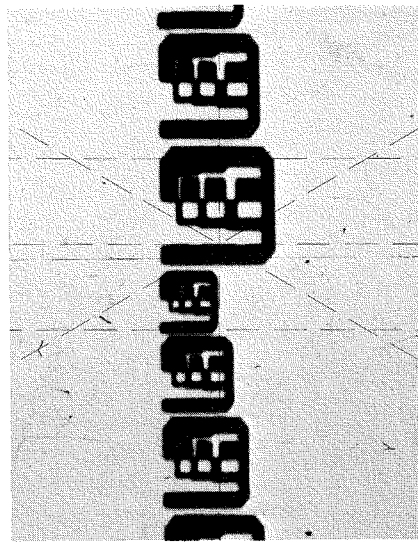


Fig. 4a—Test character near edge of film at 20X magnification.

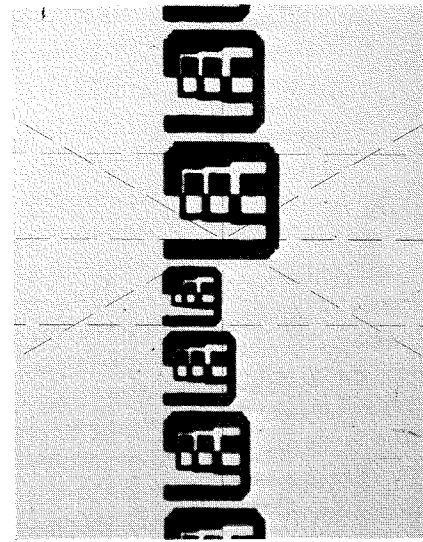


Fig. 4b—Test character near center of film, at 20X magnification.

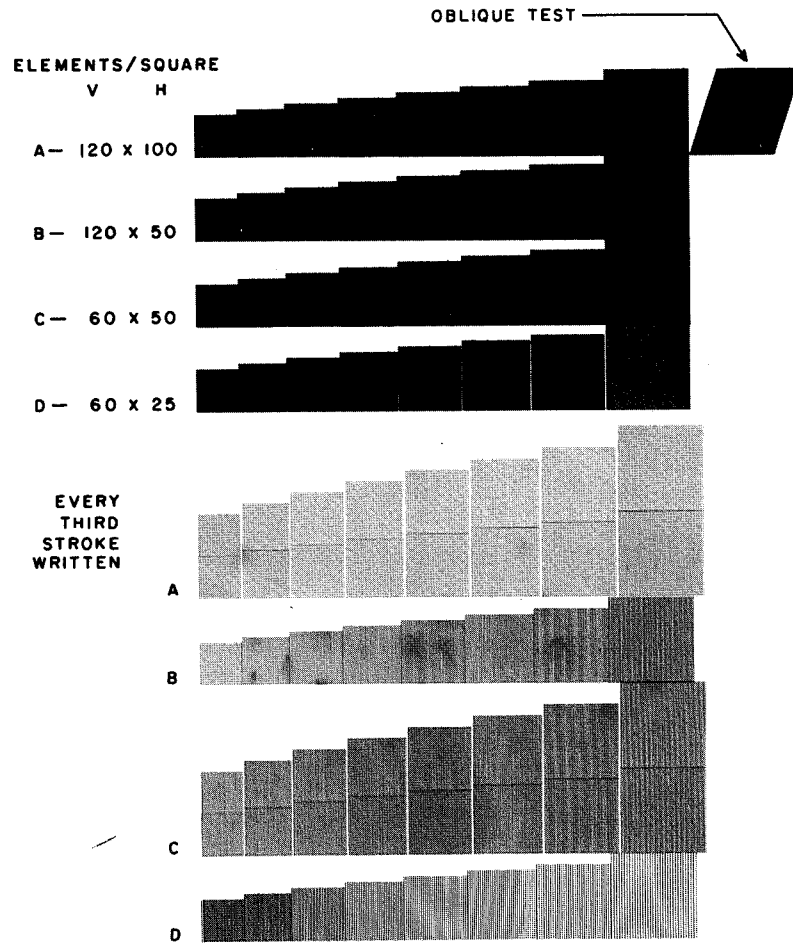


Fig. 5—Density and size test.

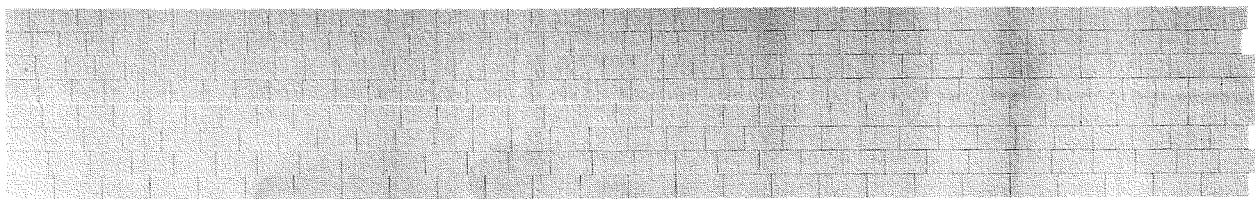
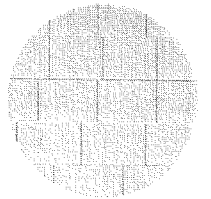


Fig. 6—Density-uniformity and width test (circle at right shows a portion of the test pattern in full size).



patches to maintain a close control on film density during an operating run.

Additional information on density is given by the pattern of Fig. 6. Here, patches are written contiguously to form bands spanning the entire writing area. Eight bands of constant patch height but varying width are written. The eight bands should be of equal density if the compensation for stroke spacing is working properly. Each band should be of uniform density across the page. Horizontal amplifier noise and errors in the D/A converter will produce striations. Processing nonuniformities and lens vignetting will produce broad bands of differing density.

Deflection-system tests

Horizontal deflection is controlled by a 16-bit D/A converter and a geometry correction network which rectifies the inherent CRT pincushion distortion.

Vertical deflection is controlled by

- 1) A vertical sweep generator for character writing,
- 2) Two vertical D/A converters for character positioning, and
- 3) The geometry correction networks.

Alignment and operation of these systems are checked by the following tests.

Vertical-sweep height

Character height is determined by sweep velocity and the clock which measures units of distance. Proper adjustment of velocity and clock frequency are measured by writing a square of known height, then writing above it an equal square displaced upward by the character height, as in Fig. 5.

In writing the second square, the sweep starting point is displaced by use of the vertical D/A converter. The height of the squares is measured in points (one point equals 1/72 inch). The vertical D/A converter least increment is 1/32 point. If both character height and D/A calibration are correct, there will be no gap or overlap between the upper and lower squares.

Small gaps or overlaps are highly visible and indicate an abnormal condition. Note that this does not indicate what function is in error; this must be

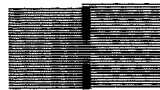


Fig. 7—Vertical-sweep test pattern.

determined by careful measurement or by further, more specialized, tests.

Vertical-sweep linearity

Vertical-sweep linearity is checked by coding a character consisting of thin horizontal lines and partially overlapping this with a similar set of lines spaced by the vertical D/A converter. This is shown at the top of Fig. 7. Unequal line spacing produces an alternating black/white band pattern where the two sets of lines overlap. This may be due to a) vertical sweep nonlinearity, b) incorrect character size, c) vertical deflection nonlinearity, or d) malfunctioning vertical D/A converter.

Vertical-settling time

The vertical sweep must be allowed to fully recover between strokes. Otherwise, the start point for long sweeps will differ from that for short sweeps, resulting in irregularities in the bottom of characters such as the *L*, and differences in the baseline alignment of characters of different sizes. Sweep recovery is checked using the character shown in Fig. 8, consisting of alternating long and short sweeps. The bottom edge of this character should be straight under 10x magnification.

Horizontal-settling time

Horizontal settling is checked by the scheme of Fig. 9. A single vertical line is written after a horizontal jump. Two more are then written on either side of the first. The digital addresses are such that the lines should be equally spaced. Small displacements of the first (center) lines are easily visible. Such displacements may be due to yoke hysteresis or insufficient settling time.

Geometry correction

Magnetic CRT deflection produces inherent pincushion distortion which must be electronically corrected. In the VideoComp, this is done by nonlinear networks which must be carefully

Fig. 8—Vertical-settling-time test.



trimmed to give the best overall results.

A comprehensive test of the geometry correction is provided by the pattern of Fig. 10. The cruciform area is that used for normal writing. The area is filled by contiguous squares, 18 points on a side. Each square itself consists of a grid pattern. This pattern consists of lines which are 0.005-inch wide, spaced 100 lines to the inch, horizontally, and 96 lines to the inch, vertically. The specific numbers were chosen for compatibility with the basic D/A converter increments in the system. A regular array 100 x 96 lines to the inch results from the contiguous squares.

Geometrical errors are made visible by superimposing a standard grid consisting of 0.005-inch lines, 100x96 to the inch, generated by the precision Gerber coordinatograph at the David Sarnoff Research Center.

Moiré patterns resulting from superposition of the VideoComp output and the reference grid are shown in Fig. 11 and 12. In Fig. 11, the patterns are crossed so that 96 and 100 lines per inch are found on each axis. A 4-line/inch beat pattern is seen, which is normal. These lines are effectively a 25X enlargement of the lines in the grid. Irregularities in this pattern are directly related to errors in the VideoComp output, with about 25x magnification. Fig. 12 shows the result with the patterns aligned for the best "zero beat".

Film Advance

VideoComps have a mechanical film advance which drives sprocketed film in increments of approximately one point. The advance is not exact because of the numerical incompatibility of

- 1) The integral number of teeth on the advance ratchet wheel,
- 2) The standard sprocket spacing,
- 3) The integral number of teeth on the drive sprocket, and
- 4) the traditional value of the point.

Because of instabilities when the mechanical film advance is less than five-

Fig. 9—Horizontal-settling-time test.

point increments, advance commands of less than five points are executed by the vertical D/A converter. Advances of five points or more are executed by a combination of mechanical advance and the D/A converter.

Operation of the film advance is checked by writing a column of bars one-half-point wide separated by one-point advance commands. Every fifth bar is displaced to indicate where the mechanical advance occurs.

There are 216 teeth on the advance ratchet wheel. To assure that every tooth is tested, with the mechanical advance moving is five teeth at a time, it is necessary to provide enough advances for five revolutions of the wheel. Every 96 points of advance, an overlapping column of lines is written using the vertical D/A converter. The resultant pattern looks like Fig. 13. Because the close spacing of the lines, irregularities of advance show up as striations or bands.

Overlapping of the lines spaced by mechanical advance and the D/A converter exposes relative errors, which appear as dark bands. The appearance and width of these bands can be quantitatively interpreted.

Spot size and astigmatism

The quality of the writing spot affects the test character of Fig. 2 and the density of the grid of Fig. 9. Density variations over the writing area of Fig. 9 can be due to phosphor nonuniformity, to geometrical error, or to spot focus and astigmatism.

Summary

The tests described provide a quick, comprehensive overview of the system operation. They can be used as part of system checkout, as an acceptance test upon installation, and as a check on system performance during preventive maintenance calls. Because it exercises all parts of the system, it can also be used for life tests.

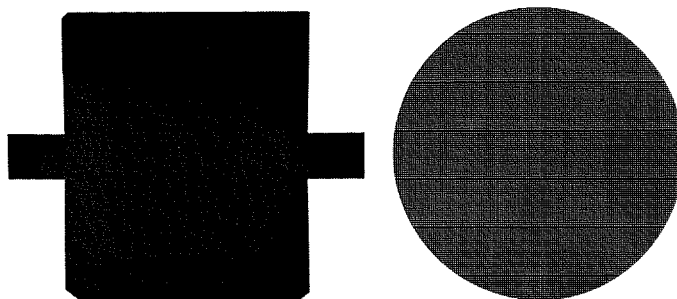


Fig. 10—Deflection-geometry test pattern (circle at right shows a portion of the test pattern in full size).

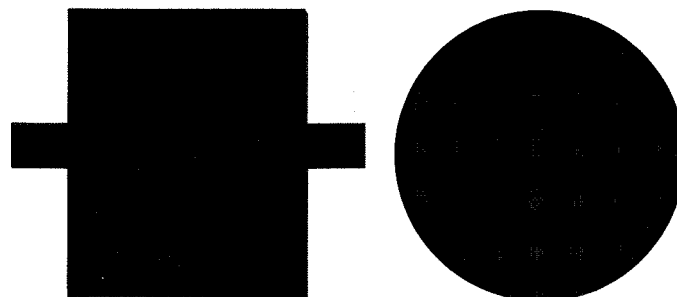


Fig. 11a—Moire pattern with good linearity, crossed mode (circle at right shows a portion of the test pattern in full size).

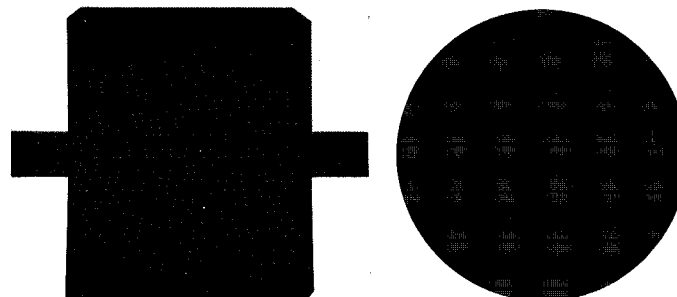


Fig. 11b—Moire pattern with poor linearity, crossed mode (circle at right shows a portion of the test pattern in full size).

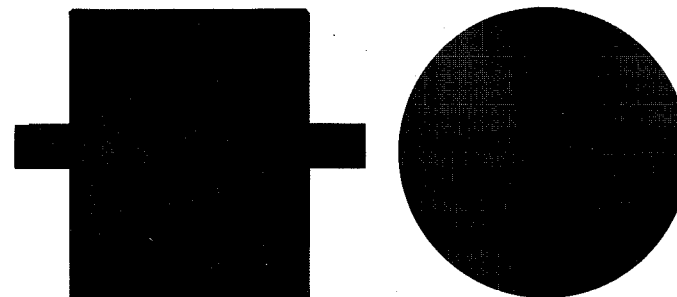


Fig. 12a—Moire pattern with good linearity, parallel mode (circle at right shows a portion of the test pattern in full size).

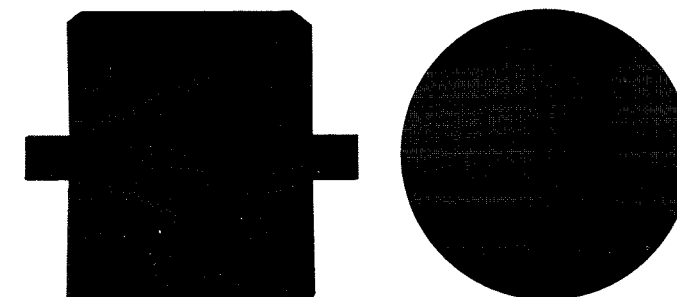


Fig. 12b—Moire pattern with poor linearity, parallel mode (circle at right shows a portion of the test pattern in full size).

Mechanical advance increment

Vertical D/A converter test

Fig. 13—Advance-uniformity test pattern.

New developments in controlled solder plating of printed-wire boards

E. E. Gilbert

The phenomenon of tin-lead co-deposition plating of printed-wire boards has been explored and the limitations of a tin-lead fluoborate system are given. Innovations in test and alloy evaluation procedures have led to the discovery that the concentration of boric acid in the tin-lead fluoborate bath is extremely critical. The results indicate that the homogeneity of deposits can be optimized by boric acid additions, used to stabilize the lead and fluoboric acid complexes. However even under the most ideal conditions, the fluoborate solution deposits a wide range of tin-lead combinations because of chemical equilibrium changes that occur during electrolysis.

Editor's Note: Although the new techniques described in this paper have been applied with success in several RCA divisions (including the author's), these methods have not yet been adopted Corporate wide.

THE REQUIREMENTS IMPOSED upon printed-wire boards, electrolytically coated with tin-lead, have been difficult to meet because of the limited state-of-the-art of co-deposition plating. The problems may be summarized as follows:

- 1) Inconsistency in the composition of tin-lead deposits in the various current-density areas of a plated board;
- 2) Inconsistency in the composition of tin-lead deposits in similar current-density areas of boards plated at the same time and under the same conditions;
- 3) Lack of correlation in the results of analyses reported by the two laboratories testing the plating solutions and tin-lead deposits;
- 4) Lack of correlation between Betascope and chemical analyses [Betascope is a trade name of Twin City Testing Corp., North Tonawanda, N.Y.];
- 5) Inconsistency in the reflow or fusing properties of deposits plated in the various current-density areas of a board;
- 6) Abrupt changes in the composition of the deposit following the addition of lead-fluoborate concentrate; and
- 7) The formation of small nodules of tin-lead upon the photo-resist.

Production time lost during any problem-solving or trouble-shooting investigation always poses a problem to the production engineer. The tendency of relying upon the results of chemical analysis, which is extremely time con-

suming in the case of tin-lead, proved to be a duration factor in shut-down. The lack of correlation in results reported by laboratories involved in the analyses and the inability to reproduce results reported by a given laboratory made a review of the state-of-the-art, in its entirety, imperative. This review led to the development of new methods for testing, for the interpretation of test data, and for the subsequent solutions of several of the problems cited above.

Sampling control

Proper sampling proved to be of extreme importance during the investigation of inconsistencies in the composition of tin-lead electro-deposits on the printed-wire boards. The sampling procedure in use at the time involved submitting samples from the top and bottom edges of plated panels. These areas were supposedly indicative of the printed-wire board patterns contained within the panels. However, neither the top nor the bottom edge were acceptable, because the top edge was masked during plating by the plating rack (clamp-type) and the bottom edge was plated at a higher current density than either the top edge or the contained circuitry.

This condition was eliminated by changing the artwork to include, within the functional-circuitry portion of the panel, representative test coupons which could be removed readily for analysis. The test coupons were selectively placed above, below, and between the circuit patterns on the panels (see Fig. 1). This change in



Ernest E. Gilbert
Technical Operations
Printed Circuit Manufacturing Operations
Information Systems Division
Camden, N.J.

received the BS in Chemistry from Hampton Institute and has 14 years of diversified experience in metal finishing and plating. He joined the RCA as a Senior Staff Production Engineer in September of 1967 and is presently engaged in the manufacturing and development of complex printed-wire boards. His responsibilities include directing the control plating laboratory solving production problems, and coordinating plating automation. He is coordinator for IPC Process Effects Committee in Philadelphia area and is a member of American Electroplaters Society, New York Branch. He was elected to the Beta Kappa Chi Honorary Society in 1953.

sampling technique was found to be very significant; the results of composition analyses were now reproducible. Additional control was obtained by plating similar patterns together. Plating boards of dissimilar patterns at the same time proved undesirable.

Chemical analysis procedures—their uses and limitations

The second area of control brought under close scrutiny was the analytical procedures used to determine 1) the composition of the alloy deposited and 2) the composition of the plating solution. Three analytical techniques were in use by the manufacturing shop's laboratory and by the consulting laboratory monitoring the operation. They are commonly referred to as:

- 1) Lead-by-difference method
- 2) Electrolytic method
- 3) Lead sulfate method.

All three methods utilize the precipitation of tin as meta-stannic acid. The *lead-by-difference* method has an advantage over the other two in that sufficient tin-lead may be obtained by

scraping the deposit off of the large area of the sample, weighing the sample, and having a known total weight. However, this method became obsolete when the new sampling technique was introduced because of the smaller size of the samples submitted; thus new methods were adopted.

The alternative methods selected by the two laboratories doing the analysis were different; the shop laboratory used the *lead-sulfate* method and the independent laboratory adopted the *electrolytic* method. Both techniques had the disadvantage of having no "known" reference point. In the previously used method, once the tin content had been determined, the lead content could be calculated by difference. However, using the new methods, the lead content had to be chemically derived, since the tin-lead had to be dissolved from the test coupon using a dilute solution of nitric acid (the solution is boiled to precipitate the tin as meta-stannic acid). Thus, it became necessary to rely solely on the accuracy of the particular method used for the analysis. Because of the considerable differences in results obtained by the two laboratories, both analytical methods became suspect and were investigated.

The shop's laboratory felt that the electrolytic method was not sufficiently accurate to serve as a primary standard where no known weight was involved. The consulting laboratory considered the sulfate precipitation method limited because of the solubility product of lead sulfate. The shop laboratory decided to continue the use of the sulfate precipitation method because the method has been known, historically, as the "classical" method for the determination of lead, and any error in results due to the solubility product of lead sulfate could be reduced by the addition of sulfuric acid in excess to a point that the error would be negligible.

On investigation, the electrolytic method was found to contain the following weaknesses:

- 1) The solution was not sufficiently acidic to dissolve the copper deposited at the cathode, thereby creating the possible deposition of lead, both cathodically and anodically.
- 2) The deposition of lead oxide, the essence of the method, resulted in reliance upon the measurement of a de-

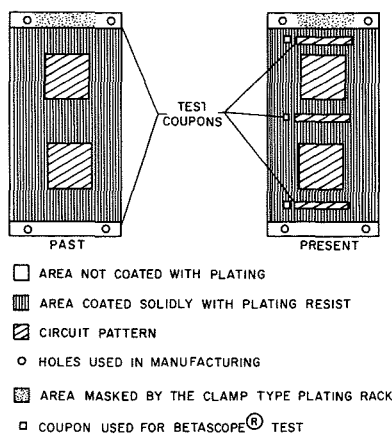


Fig. 1—The previously used method of collecting test coupons (left) was found to be unacceptable because of plating inconsistencies at the edges of the panel; this method was replaced by that shown at the right.

posit which is poor in both adhesion and cohesion. Where the quantity is sufficiently large, some of the lead oxide is lost during the electrolyzing and drying stages.

3) Literature advised against the use of the electrolytic method when the alloy being tested contains more than 5% lead, or the sample contains more than 5 milligrams of lead.¹

The nonelectrolytic method, adopted by the shop's laboratory, involves the precipitation of lead as a sulfate. The lead sulfate is filtered through a Gooch crucible, washed with dilute sulfuric acid, dried at a temperature of less than 500°C, cooled to constant weight in a desiccator, and weighed. The result is multiplied by a factor to give the amount of lead.

It was discovered later that the variation in the results of the two laboratories was reduced with the introduction of the new sampling coupons. The total weight of the tin-lead dissolved from the coupons was less than 0.100 gram, and the expected lead did not exceed 0.05 gram. At this point in the investigation, the two laboratories reported results which were comparable to each other. A modified version of the proposed electrolytic method was introduced in the shop's laboratory once it had been shown that the method was suitable to serve as an alternate for the precipitation method, if used within the proper limits of sample size and acidity.

Alloy variations with respect to time

The results obtained by chemically analyzing the tin-lead composition was indicative of the *average* composition

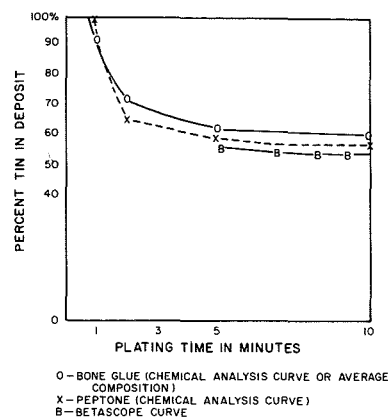


Fig. 2—Alloy variations with respect to time.

of the various laminae rather than the composition of any one deposit. One of the limitations of the solution from which two metals are deposited simultaneously is the variation in the ratio of the two metals being deposited as a function of time.

Indications of this gradual change in the composition became apparent when variations were reported for the same board tested at three different stages of the operation. The three stages involved were:

- 1) Immediately after plating,
- 2) After the tin-lead had been fused in hot oil, and
- 3) After the excess solder was removed in a solder leveling machine, which leaves a film of tin-lead, approximately 50×10^{-6} in.

A summary of the results is given in Table I.

Table I—Variation in tin contents as a function of time.

Board	As plated (% tin)	After fusing (% tin)	After leveling (% tin)
1	52.65	54.36	70.27
2	67.21	69.37	79.23
3	59.26	65.42	67.76
4	56.20	—	74.26
5	63.08	—	78.71

Table I shows that the tin deposits at a much faster rate during the first few minutes of deposition than it does during the final period. Once this became known, the results obtained with the use of a Betascope (an instrument that uses Beta back-scatter rays to determine the thickness of a coating) which did not appear valid, initially, became of primary importance in understanding the solution capabilities and limitations. A comparison of the results of chemical analyses and Betascope readings is given in Table II.

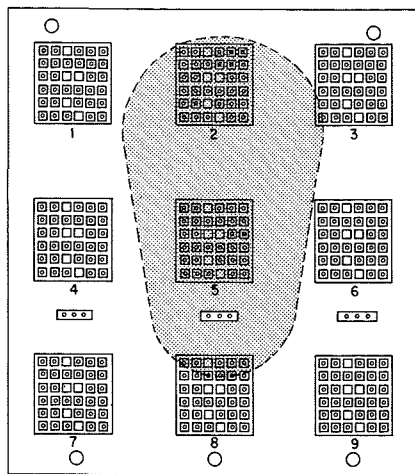


Fig. 3—Variation in tin-lead plating due to macro-current-density variation; this typical platter contains nine circuit boards and is 18 x 19 inches.

Table II—Comparison of various methods for determining tin content.

Coupon number	Betascope (% tin)	Shop lab (% tin)	Second lab (% tin)
1/2	57	61.9	60.8
3/4	57	63.2	59.6
5/6	58	63.1	58.8
19/20	42	51.2	50.5
21/22	42	52.1	49.7
23/24	41	50.7	51.2
37/38	48	56.4	54.1
39/40	48	56.7	53.8
41/42	49	57.3	54.8
49/50	48	52.0	49.4
51/52	43	52.4	49.2
53/54	43	52.0	48.5
55/56	43	54.0	51.8

Note that the results of the Betascope are much lower than those reported by the two laboratories; however, these results are as consistent as those of the chemical analyses. The Betascope results are more indicative of the percentage of tin in the final laminae deposited during the last few minutes of deposition; while the chemical analysis results (after solder leveling) are more indicative of the percentage of tin deposited during the first few minutes of deposition. Chemical analysis prior to solder leveling gives the average.

Additional data was obtained using Hull Cell panels [Hull Cell is a trade name of R. O. Hull & Co., Cleveland, Ohio]. The panels were plated for 1, 5, and 10 minutes and were marked so that that portion of the panels which represented the 24 to 30 Amp/ft² areas could be cut out of each panel and chemically analyzed for tin-lead. The results are illustrated in Fig. 2.

Samples of the solution were taken from the cathode region to determine if there was a change in the concentration of tin and lead as a result of electrolysis. There was no appreciable change. The gradual change in the ratio of one metal to the other appears to be due to any one, or all, of the following:

- 1) Chemical equilibrium shifting during electrolysis.
- 2) Pressure created at the anode and cathode as gases are generated.
- 3) A change in the surface with which the solution is in contact.

These aspects are treated in more detail later in this paper.

Effects of macro-current-density variations

The effects of macro-current-density variations upon the tin-lead composition deposited on a given part can be observed immediately after the "reflowing" or fusing operation. This operation involves immersing the tin-lead plated part in hot oil (495°F) from six to twenty seconds. The degree of fusing depends upon the percents of tin and lead plated in a given area of the part. The effects of macro-current-density variation are more evident on large parts than on small ones.

One program involved the tin-lead plating of boards approximately 18x19 inches in size. The size of the boards caused the tin-lead composition to vary greatly as shown in Fig. 3. The low-current-density areas contained a high percentage of lead and exhibited poor reflow properties. A test method was devised to determine the extent of the tin-lead variations in the deposit.

The test involved plating a large panel at the prescribed current density and reflowing in hot oil. The dimensions of the panel were 9x18 inches, and the time required to fuse the tin lead varied between 12 and 20 seconds. The edges of the panel flowed better than the center, forming a parabola as shown in Fig. 4.

An analysis was made of the tin-lead in different current-density areas. The lead content within the parabola of Fig. 4 was found to be as much as 14% higher than that along the edge of the panel. Other tests (discussed later) indicated that the higher the lead content, the longer the reflow time. Thus, the time required for the

room temperature panel to reach the reflow temperature of various tin-lead combinations was found to be a good indication of the composition.

Importance of boric acid

Chemical analyses had shown that the bath components were maintained within the limits recommended by the vendor during production. The problem of obtaining uniform reflow became so acute at times that it was necessary to "shutdown" the operation. Although representatives of vendors' Technical Service Staffs were cooperative, no recommendations were offered which gave the desired reflow results. The inability to solve the reflow problem indicated a void in the state of the art. Therefore, attempts were made to correct the reflow problem by varying the concentration of the components in the solution above and below recommended limits. Variations in the tin and lead fluoroborates and fluoboric acid did not affect the plating characteristic of the plating solution to the extent of removing the parabolic pattern obtained subsequent to reflow. The results may be summarized as follows:

- 1) Changing the tin concentration above and below the recommended limits reduced the tin content in the deposit—all the other components being kept constant. This may be explained in terms of the reduction of the ionization of tin and the lack of available tin ions at high and low tin concentrations, respectively.
- 2) Increasing the lead concentration increased the rate at which it was plated. Decreasing the lead content in the bath had a corresponding effect with respect to the deposit, but not to the extent of affecting the composition distribution pattern previously described.
- 3) Increasing the free fluoboric acid had little, if any, effect above recommended minimum.
- 4) The increasing of the bone glue or Peptone concentration when one or the other was used, did not change the composition pattern. However, as the concentration of Peptone was increased, the average tin in the deposit increased until an undetermined point was reached and the reverse effect was obtained.

The presence and concentration of boric acid in a fluoboric acid bath is usually taken for granted by most platers. Its presence in the concentrates of tin and lead fluoroborates and fluoboric acid, added periodically to maintain the bath, causes one to as-

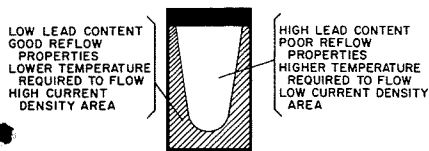


Fig. 4—9 x 18-inch test panel showing the parabolic inconsistencies in the tin-lead content for different current-density areas.

sume, wrongly, that boric acid is being adequately replenished. Boric acid, at this point in the study, was the only component used in the original make-up which had not been purposely varied.

The role of boric acid in a fluoboric acid solution is not clearly explained in the technical literature commonly referred to by most platers, nor is it emphasized by most suppliers in their brochures. Some vendor brochures simply state that boric acid is used, initially, to prevent the formation of free hydrofluoric acid.

Experience with several acid-nickel-plating solutions, in which boric acid must be controlled if the desired quality of the deposit is to be obtained, led to an investigation of boric acid as a means of controlling the plating characteristic to the tin-lead bath.

Impurities more noble than nickel (such as copper and lead) tend to build-up in a nickel plating solution during normal operation when copper and white metals are being plated; therefore, it seemed reasonable that boric acid might decrease the rate at which lead was being deposited from the tin-lead solution. In order of increasing nobility (requiring the least amount of electrical energy to deposit at the cathode of a cell) the elements are listed as follows (the electrode potential for Hydrogen is arbitrarily selected as zero):²

Element	Ion electrode reaction	Electrode potential
Nickel	$Ni \rightarrow Ni + 2e$	+0.250
Molybdenum	$Mo \rightarrow Mo + 3e$	+0.20
Tin	$Sn \rightarrow Sn + 2e$	+0.136
Lead	$Pb \rightarrow Pb + 2e$	+0.126
Deuterium	$1/2D_2 \rightarrow D + e$	+0.003
Hydrogen	$1/2H_2 \rightarrow H + e$	0.000
Copper	$Cu \rightarrow Cu + 2e$	-0.337

Copper and lead are more noble than nickel and should plate out preferentially to, or co-deposit with, nickel making "dummying" unnecessary. Hydrogen should be liberated at the

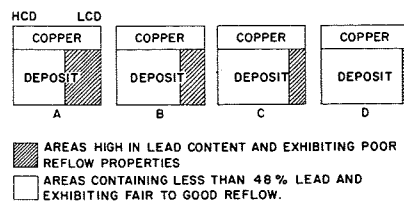


Fig. 5—Tin-lead plated Hull Cell panels.

cathode in preference to the deposition of nickel. However, the presence of boric acid retards these electrode reactions, allowing nickel to deposit when the thermodynamic concentration of these elements are below a certain level. A slight change in the deposition potential of lead in the tin-lead fluoborate solution could, seemingly, bring it sufficiently close to that of tin to prevent the preferential plating of lead in the low-current-density areas.

Several Hull Cell panels were run using the solution as it existed on the production floor and with additions of boric acid to obtain tangible evidence of the effects of the additions (Fig. 5). The dark areas, which appeared within the plating-current-density range (recommended in the process) receded to lower ranges as the boric-acid additions were increased. Whereas, it had been impossible to obtain the required reflow properties within the 25-to-30 Amp/ft² range prescribed, previously, it became possible to obtain good reflow over the entire range of the panel.

It should be noted that the solution in use on the production floor was several years old, and boric acid had never been added except for the initial charge and for that which was contained in the tin, lead, and fluoboric-acid concentrates. The difficulties involved in trying to determine the concentration of boric acid, chemically, when in the presence of fluoboric acid, left a void in the accumulation of data. However, having determined that boric acid was needed, it was added to all of the tin-lead solutions on the plating floor. The criteria for the addition were the Hull Cell and the panel reflow test (discussed earlier). There was not complete agreement between the two tests: removing the parabolic area of high lead on the test panel required 1 to 2 oz/gal more acid than the Hull Cell test indicated.

Results of boric acid adjustment

With the establishment of these controls, boric acid is added regularly to the production baths, and sometimes in preference to fluoboric acid. These control tests proved equal in importance to, but did not replace, the required chemical analysis. They proved valuable in controlling the solder leveling operation as well.

During the six months following the initial boric acid adjustment, several observations were made with respect to the overall performance of the plating baths. These observations may be summarized as follows:

- 1) Little or no additions of lead were required, whereas before, lead was added at a rate of 1 oz/gal/week.
- 2) The quantity of white precipitate, previously thought to be stannic tin but could have been lead fluoride or a mixture of the two, decreased.
- 3) Deviating from the recommended current density of 25 or 30 Amp/ft² did not appreciably affect the composition of the deposit. It was possible to plate between 15 and 40 Amp/ft².
- 4) The tin concentration in the deposit, which previously averaged 48 to 57%, was being reported in the range of 58 to 70%, consistently.
- 5) Recrystallization occurred occasionally as the solution level and/or temperature dropped indicating that the bath was saturated with one of the components, perhaps boric acid.
- 6) Whereas the process allows 15 to 20 seconds for reflow, it was found that 6 to 10 seconds was sufficient for the tin-lead combination being deposited.
- 7) The throwing power of the solution had been increased, especially in the low-current-density areas, thereby reducing the ratio of deposit on the surface to that in the holes.
- 8) Observation of micro-sections became the basis for concluding that greater uniformity in the dispersement of lead had occurred.

Theoretical aspects of co-deposition

To co-deposit two metals, such as tin (*Sn*) and Lead (*Pb*), their deposition potential, *E*, must be equal or nearly so, as represented by the following:

$$E(Sn) = E(Pb) \quad (1)$$

$$E_o(Sn) + \frac{RT}{n(Sn)F} \ln[a(Sn) - p(Sn)] =$$

$$E_o(Pb) + \frac{RT}{n(Pb)F} \ln[a(Pb) - p(Pb)]$$

where *E_o* is the electromotive force of the element with respect to hydrogen (the value for hydrogen arbitrarily selected as 0.00); *T* is the absolute

temperature; R is the gas constant; n is the valence of the element; a is the activity of the ions, or thermodynamic concentration of the element; and p is the anionic back pressure or voltage.¹¹ When the deposition potentials are not equal $E(Sn) \neq E(Pb)$, $a(Pb)$ and $a(Sn)$ or $p(Pb)$ and $p(Sn)$ must be adjusted. It is easier to adjust $a(Pb)$ and $a(Sn)$ because they can be controlled by varying the concentration of the element-containing-electrolyte or by complexing the element and reducing the degree of ionization, as discussed later.

The deposition potential of lead and tin in an electrochemical reaction are:

$$\begin{aligned} E_o(Pb) &= 0.126 \\ E_o(Sn) &= 0.136 \end{aligned} \quad (3)$$

It can be seen that these are sufficiently close to allow co-deposition, if the anionic media selected is compatible with the two metals. It is obvious that the sulfate anionic media used in nickel plating is not satisfactory because the solubility product and ionization constant of lead sulfate are so low that only tin would plate out to any great extent. The tin and lead salts of fluoboric acid, in an excess of the acid, have proven satisfactory.

The deposition potentials of lead and tin (Eq. 3) also indicate that the energy level required to deposit lead is less than that required to deposit tin. To compensate for the difference in energy-level requirements, lead is reduced in concentration to one half that of tin, thereby lowering the activity of lead in the bath:³

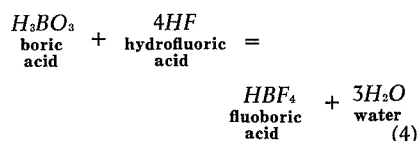
"In order to pass a current through a solution, a certain voltage is required. The solution itself will have an ohmic resistance proportional to the length of the path between the electrodes and inversely proportional to the effective area. In addition, there will be a potential drop across the thin film surrounding each electrode due to the evolution of gas or a sharp concentration gradient. This may be reduced to some extent by efficient agitation. Finally, there will be the potential necessary to deposit the material which would be present at equilibrium even though no current were flowing. This is the minimum for deposition. Of course, if the solution is very dilute, and the ions comparatively scarce, the required potential will be very high [one of the causes for the build-up of impurities in a bath], and at high concentration the reverse will be true. By Nernst's law,

$$E = \frac{0.05915}{n} (\log C) - E_o$$

where E = the electrode voltage drop
 C = the ion concentration in moles per liter
 n = the number of charges on the ion".

Boric Acid in a fluoborate system

Fluoboric acid may be prepared in accordance with the following reaction:⁴



Once formed, fluoboric acid, to a limited extent, undergoes hydrolysis:



adding the two equations, we obtain:



From Eq. 6, it can be seen that one molecule less of hydrofluoric acid is required to react with boric acid to form the product of hydrolysis than was used in Eq. 4 to form fluoboric acid. This means that, depending upon the degree of hydrolyzation, hydrofluoric acid is always present in the solution when the ratio of molecules of boric acid to that of hydrofluoric acid is 1 : 4, as can be seen by the left side of Eq. 4 and the right side of Eq. 5. This tendency is accelerated by electrolysis (explained later) because of the volatile nature of hydrogen which is generated at the cathode and oxygen generated at the anode. (It is doubtful that fluorine can be generated at the anode during electrolysis because of its high negativity.) The state of chemical equilibrium is expressed as follows:

$$\frac{[HBF_4]}{[H_3BO_3] \times [HF]^4} = K \quad (4a)$$

where K is the equilibrium constant.

According to LeChatelier's Principle:

"Increasing the concentration of any component of a system in equilibrium will promote the action which tends to consume some of the added substance."

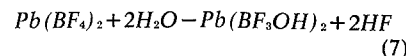
Therefore, increasing the boric-acid concentration tends to bring about the condition shown in the right side of Eq. 6, which shows no free hydrofluoric acid, as the ratio of boric acid to hydrofluoric acid approaches 1 : 3, shown on the left side of Eq. 6. The

chemical equilibrium is expressed as follows:

$$\frac{[HBF_3OH]}{[H_3BO_3] \times [HF]^3} = K \quad (6a)$$

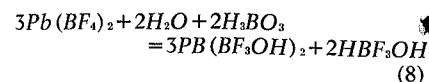
It can be seen through the comparison of the equilibrium constants in Eqs. 4a and 6a that K in Eq. 6a is higher in value because of the differences in exponential concentrations of hydrofluoric acid (HF). The larger the value of K , the greater the tendency to move toward completion.

Lead fluoborate, which behaves similarly to fluoboric acid, forms complexes when undergoing hydrolysis. It releases twice as much free hydrofluoric acid per mole as can be seen in Eq. 7:



The greater the dilution, the more complete the release. This accounts for the so-called "shock which occurs when adding lead fluoborate concentrate to the plating solution."

Multiplying Eq. 7 by a factor of 3 and adding two moles of boric acid to the left side of the equation, we have:



By substituting molecular weights, we can compute the weight relationship of the left side of the equation, thus:

$$\begin{aligned} 3(380.85) + 2(18.02) + 2(83.46) \\ = 1,142.55 + 36.04 + 166.92 \end{aligned}$$

If we assume that the reaction goes to completion, we find that for every 6.85 ounces of lead fluoborate added to the plating bath, the bath should contain 1 ounce of free boric acid. Further calculations show that for every ounce of lead (as metal in lead fluoborate) added, 0.27 ounce of free boric acid is needed, which represents a ratio of 3.7 : 1. The equilibrium constant, when expressed in molar concentration, for Eq. 7 is:

$$\frac{[Pb(BF_3OH)_2] \times [HF]^2}{[PB(BF_4)_2]} = K \quad (7a)$$

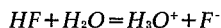
showing a greater tendency for the reaction to move toward the right and a high concentration of the products on the right side. On the other hand, the equilibrium constant for Eq. 8, where the mole of reactant equals the number of moles produced, lead fluoborate

is more stable and the effects of hydrolysis is off-set

$$\frac{[Pb(BF_3OH)_2]^3 \times [HBF_3OH]^2}{[Pb(BF_4)_2]^3 \times [H_3BO_3]^2} = K \quad (8a)$$

indicating that boric acid stabilizes lead fluoborate and buffers fluoboric acid's decomposition products.

When free hydrogen fluoride (HF), referred to as hydrofluoric acid earlier because of the presence of water, is allowed to exist, it ionizes as follows:



Electrolysis causes the reduction of the hydronium ion (H_3O^+) at the cathode, liberating hydrogen, and the migration of fluoride ions to the anode, dissolving tin-lead. The deposition potential for hydrogen has been given as $E_o(H) = 0.0$.

The stress created by electrolysis tends to keep the reaction moving in the direction which favors the migration of the gases to the electrodes. Boric acid, in retarding the release of hydrofluoric acid, increases the amount of energy required to liberate hydrogen, which may be expressed as follows:

$$E(H) = \frac{RT}{n(H)F} \ln[a(H) - p(H)]$$

The same being true for the lead fluoborate molecule causes an increase in the energy requirements to deposit lead. The net result is the deposition of more tin, which must occur to fulfill Faraday's Law as shown below.

$$\sum_{n=0}^{\infty} n(aH_2 + bPb + cSn) = (96,500 \text{ coulombs})n$$

where a , b , and c are fractions of a gram-equivalent, and n is the number of equivalents ($a + b + c = 1$).

Empirical verification

In attempting to prove the applicability of the theories referred to above, additions of hydrofluoric acid were made to the Hull Cell containing a sample of the corrected solution. As the free boric acid in the solution was consumed by the hydrofluoric acid, the effects caused by the boric-acid additions discussed previously, were reversed and the condition of the initial solution was reproduced.

Other observations made may be summarized as follows:

1) As the hydrofluoric acid additions were increased, the conductivity of the solution increased, whereas, boric acid additions lowered the conductivity.

2) With increased conductivity, more gas was generated at the cathode.

It appears that the stabilization of the fluoborate radical accounted for the increase in the anode efficiency, previously mentioned. The formation of lead fluoride in the bath seemed to have been a factor in that lead fluoride is only slightly soluble in water. This slight solubility is increased by acid; however, the formation at the anode would tend to polarize the anode, decreasing its efficiency.

The tendency toward depletion of the tin can be more readily explained. The percentage of tin deposited is greater than that in the anode. This can be overcome by either using an anode with a higher tin content or using pure tin anodes in conjunction with the tin lead anodes.

Concluding remarks

The limited advancement in the state of the art of tin-lead plating is due to the inadequacies of test and control procedures and to the manner in which test data are interpreted. For example: chemical analysis procedures have been relied upon too heavily without recognizing their individual limitations. The method to be used must be selected with care and samples submitted for test must be truly representative of the circuitry plated when alloy composition is being determined. The same is true for plating bath analysis. Poor sampling can precipitate needless and costly activity within the operation and the rejection of components that should meet specifications.

Samples for deposit composition determination should have a configuration similar to the circuitry of the board being evaluated. They should be designed into the "artwork" and be selectively placed, so that the current density, at which they plate, is similar to that at which the circuit board is being plated.

So-called "dewetting" could, in fact, be delamination of the lower melting point layers/laminae of the deposit from the higher melting point layers.

The difference in the solderability properties of a board which has been solder leveled and one that is still in the "as-plated" condition is a result of the former surface being much higher in tin content.

The role of boric acid in the fluoborate bath has been greatly underestimated, and it is recognized that the acid should be added to the solution during initial make-up to prevent the existence of free hydrofluoric acid. The concentration of boric acid, subsequent to make-up, is difficult to determine by chemical analysis. Vendors frequently state in their brochures, that it can be maintained by adding tin, lead, and fluoboric-acid concentrates. However, dependence upon the addition of concentrates for boric acid replenishment can lead to difficulties in the "reflow" operation because the composition of the deposit varies drastically between the high and low current density areas of the part. One way of determining boric acid addition requirements, empirically, is to plate a panel in a Hull cell and to "reflow" the deposit in hot oil at 480°F.

The broad limits recommended by vendors for component concentrations should be narrowed by the user. With imagination, new methods can be developed which will give consistent results in tin-lead plating, reduce operational cost, and lead to furthering the state-of-the-art.

References

1. Hamilton and Simpson, *Quantitative Chemical Analysis* (The MacMillan Co., 1954).
2. Hodgman, Weast, & Selby, *Handbook of Chemistry and Physics* (Chemical Rubber Publishing Company, 38th Edition, 1956).
3. Eshbach, Ovid W., *Handbook of Engineering Fundamentals* (John Wiley & Sons, Inc., 1952).
4. Stecher, Finkel, Siegmund, Szafranski, *The Merck Index of Chemicals and Drugs* (Merck and Company, Inc., 1960).
5. Graham, A. Kenneth, *Electroplating Engineering Handbook* (Reinhold Publishing Corp., 1962).
6. Brenner, Abner, *Electrodeposition of Alloys*, Vol. 1 & 2, (Academic Press, 1963).
7. Glasstone, Samuel, and Lewis, David, *Elements of Physical Chemistry* (D. Van Nostrand Company, Inc., 1960).
8. MacInnes, Duncan A., *The Principles of Electrochemistry* (Reinhold Publishing Corporation, 1939).
9. Willard and Furman, *Elementary Quantitative Analysis* (D. Van Nostrand Co., Inc., 3rd edition, 1940).
10. Daniels, Farrington, *Outline of Physical Chemistry* (John Wiley and Sons, Inc., 1952).
11. Clauser, H. R. (Editor) *Encyclopedia of Engineering Materials and Processes* (Reinhardt, 4th Ed., New York).

Three RCA men elected IEEE Fellows

The three RCA men cited herein have been honored for their professional achievements by being elected Fellows of the Institute of Electrical and Electronics Engineers. This recognition is extended each year by the IEEE to those who have made outstanding contributions to the field of electronics.

Dr. J. Guy Woodward
Data Processing Applied Research Lab.
RCA Laboratories
Princeton, New Jersey



... for contributions in magnetic tape and disk recording.

Dr. Woodward received the BA from North Central College in 1936, the MS in Physics from Michigan State College in 1938, and the PhD in Physics from the Ohio State in 1942. In 1942 he joined the RCA Laboratories. His research has covered vehicular radio noise, underwater sound, ferroelectricity, electromechanical feedback devices, rheological measurements at audio frequencies, musical acoustics, sound-reinforcement systems, stereophonic sound reproduction, magnetic-tape recording and disk-phonograph recording. He served as Head of the Recording and Electromechanical Research at the Laboratories. Currently he is engaged in the development of an advanced digital, magnetic-recorded disk file for computers. Dr. Woodward is a member of Sigma Xi and a Fellow of the Acoustical Society of America, of the Audio Engineering Society and of the American Association for the Advancement of Science. In 1963 he received the AES Emile Berliner Award for outstanding developments in audio engineering. He has served on the Administrative Committee of the IEEE Group on Audio and Electroacoustics and on the Board of Governors of the AES; he was Eastern Regional Vice-President of the latter organization in 1967-1968. He was a joint recipient of RCA Laboratories Achievement Awards in 1940, 1953 and 1964, and shared in a "David Sarnoff Birthday" Award in 1956. Dr. Woodward has had seven patents issued.

Dr. Arthur S. Robinson, Manager
Systems and Advanced Technology
Missile and Surface Radar Division
Moorestown, New Jersey



... for leadership in digital and analog computing and control systems, solid-state radar, coherent electro-optical systems, and medical electronics instrumentation.

Dr. Arthur S. Robinson received the BSEE from Columbia University the MSEE from New York University, and the Doctor of Engineering Science degree from Columbia University. As Technical Director of RCA's Missile and Surface Radar Division, Dr. Robinson is responsible for the synthesis of both present and future systems, and for developing advanced technology consistent with these system goals. RCA's Missile and Surface Radar Division is active in the areas of air defense systems, surveillance, warning and control systems, range and reentry instrumentation, and tactical sensors. Before joining RCA, Dr. Robinson was Assistant Chief Engineer of the Bendix Eclipse-Pioneer Division and then Director of Kollsman Instrument Corporation's Research Division. He is a member of the Tau Beta Pi and has received 42 U.S. and foreign patents covering electronic sensing, signal processing, computing, and control systems.

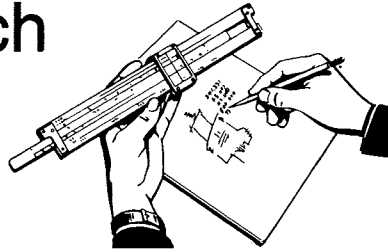
Paul Rappaport, Director
Process and Materials Applied Research Lab.
RCA Laboratories
Princeton, New Jersey



... for contributions to energy-conversion devices, and for leadership in the professional organization of this field.

Mr. Rappaport received the BS and MS in Physics from Carnegie Institute of Technology in 1948 and 1949. In that year, he joined RCA Laboratories, and from 1949 to 1951, he worked on secondary emission of electrons from solids and received an RCA Achievement Award for outstanding work in this area. His work in energy conversion started in 1952 and resulted in his invention of the atomic battery. Mr. Rappaport received a second RCA Achievement Award for this work in 1955. During the period up to 1960 his work contributed to the following: the first demonstration that minority carrier lifetime was the most sensitive indicator of radiation damage in semiconductors, the first accurate measurement of the threshold for radiation damage in germanium and silicon, the development of the first gallium arsenide and cadmium telluride solar cell, the measurement of the effect of Van Allen type radiation on solar cells, the use of lithium in silicon to remove the effects of radiation damage. This latter work resulted in a third RCA Achievement Award for 1966. His work has resulted in over 40 publications, three book articles and 15 patents. In 1960 he was appointed head of the Energy Conversion Research Group. In 1966, he was appointed Associate Laboratory Director, and in 1968 he was appointed Director of the Process and Materials Applied Research Lab. He is a member of Pi Mu Epsilon, Sigma Xi, APS (Fellow), IEEE and AIAA (Assoc. Fellow). He is listed in *American Men of Science*, *Who's Who in Atoms*, *Leaders in American Science* and *Who's Who in the East*.

Engineering and Research Notes



Brief Technical Papers
of Current Interest

Inventions and obviousness

A. Russinoff

Staff Patent Counsel
Patent Operations
Princeton, N.J.



Reprint RE-15-5-25 | Final manuscript received December 8, 1969.

A patent is granted by the Government and provides the patent owner with the right to exclude others from making use of his invention for the term of the patent. In the United States, this term is 17 years.

The purpose of granting patents is to stimulate invention and disclosure of the inventions to the public, for otherwise there might be no incentive to invent or to tell others about an invention once it is made.

For an invention to be patentable, it must satisfy three statutory requirements: it must be *new*, *useful* and *not obvious*.

New, means that the invention was not earlier published or patented or, in other words, generally available to the public. If the invention had already been public knowledge, there would be no advantage flowing to the public in return for the Government's granting a patent.

The requirement of *usefulness* means pretty much what it says and need not be explained further.

The last hurdle which an invention must clear to be patentable—*non-obviousness*—is more difficult. One way of looking at it is that, if an invention would have been a routine matter to anyone with normal experience in the field of invention, then it is not patentable. For example, it was obvious to make a doorknob from ceramic material instead of iron, even though it had not been done before.

The "doorknob" case, which established the obviousness test for patentability, was decided by the Supreme Court more than a century ago. But it has not been an easy test to apply, and the Courts have evolved some "sub-tests" or secondary considerations to which they can resort in doubtful cases.

One of these secondary considerations is that if there has been a "long felt need" for a device to do a particular job and none was forthcoming, then the inventor who filled the bill may well have made an unobvious invention. Another is to the effect that, if an invention has enjoyed great "commercial success," that may tip the scale in favor of its patentability. And, of course, the fact that one man succeeded in making a thing work notwithstanding the "failure of others" who had tried before him, tends to establish that what he did was not obvious.

This does not rule out inventions merely because they seem simple to understand in retrospect. It is not necessary, to be patentable, for an invention to be complicated or understandable only by a PhD. If there is a problem and the solution to it wouldn't have occurred immediately to any mechanic presented with the problem, then the solution may well pass the test of non-obviousness and be patentable.

It is well, therefore, to advise RCA's patent attorneys of anything which seems to be new and useful and out of the humdrum category. RCA Patent Operations, which is located at the David Sarnoff Research Center in Princeton, will provide helpful forms on which to describe inventions and will advise on their patentability and the company's interest in them.

Mini-skirts, micro-skirts, and mini-microwave couplers

R. E. Bridge

Microwave Device Operations
Electronic Components
Harrison, N.J.



Reprint RE-15-5-25 | Final manuscript received July 2, 1969.

The general trend toward reduction in size of everything from dresses to microwave components has led to a new generation of traveling-wave tubes. Although these tubes are not really miniature, they are tiny in size compared to their predecessors of a decade ago. This "miniaturization" creates a problem in providing suitable coupling systems to transfer power into and out of the tubes with good bandwidth and fine-grain gain structure. As a result, the question arises as to how small a device can become without reduction of quality and performance. After much research and "cut-and-try," the answer seems to be "as small as desired." This concept may sound impossible, but the following discussion indicates that it is not.

A helical coupler system designed to cover a bandwidth of a full octave or more at s, c, and x band presents four basic areas of design: 1) the connector-to-cable match, 2) the helical-coupler-to-tube match, 3) the connector-cable-to-helical-coupler match, and 4) the termination match. Because of the frequency range desired, considerable refinement was necessary in the connector-to-cable connection. The major work effort centered on craftsmanship and reproducibility. Eventually a vswr of 1.1 to 1 or better was obtained over the complete s-, c-, and x-band range for two connectors joined by a short piece of suitable cable. This connection also provided a maximum insertion loss of 1 dB at 12.4 GHz.

The second phase of the work involved the coupler-to-tube match. One parameter was established as fixed, and all others were varied until the desired results were obtained. The coupler ratio (i.e., the ratio of helical-coupler mean diameter to tube-helix mean diameter) was assumed to be 1.75, and equations were developed for an initial coupler design. Because the resulting coupler was slightly oversized for the desired application, the coupler wire size and ground-plane distance were reduced, while the proper impedance relationship was maintained, to produce a miniature version. When this first miniaturized coupler was mated to a connector-cable assembly, it produced a rather poor match with large periodicities (of the order of 2 to 1); but it had good bandwidth. Additional units of the same design produced similar results. Inspection on a time-domain reflectometer system indicated that the problem was in the transition between the helical coupler and the connector-cable assembly. Various approaches were tried to solve this problem until one technique reduced the coupler match to less than 1.22 to 1 over a full octave and less than 1.5 to 1 over an octave and a half. Further refinement in assembly techniques and craftsmanship did not appreciably improve the system.

The first test of the miniaturized coupler with a complete traveling-wave tube, however, produced unacceptable fine-grain gain. Proper termination appeared to be the only solution to this problem, but existing methods were bulky, unreliable, and not easily reproducible. A wire-wound system was designed to provide 50-ohm DC and RF paths to ground with a return match to the coupler of 1.5 to 1 maximum for any given operating band. Tests with this system produced satisfactory results. Again, further refinements in assembly technique served only to improve reproducibility to a mass-production level.

At this point, temperature testing of a complete traveling-wave-tube package showed a catastrophic weakness in the miniaturized coupler design. Many tests and ideas later, a completely temperature-stable reproducible coupler emerged. This new coupler has such impressive inherent characteristics as compared to its predecessor that it still appears as a minor miracle.

The results of this miniaturization effort can be illustrated by comparison of "old" and "new" c-band couplers. Insertion loss at 8 GHz averages 2 dB for the conventional type, but less than 1 dB for the new design. Conventional couplers have a bandwidth of 4 to 8 GHz with a vswr of less than 1.5 to 1; the new design has a bandwidth of 3 to 9 GHz with a vswr of less than 1.25 to 1 (less than 2 to 1 for a double octave). Periodicity has been drastically reduced, and temperature reliability is now reliably stable. The only disadvantage of this new coupler is that it requires a little more care in manufacture. However, this extra care makes it possible to produce traveling-wave tubes as small as desired without sacrifice of quality and performance.

Method of producing a photographic-type transparency with a CO₂ laser beam

Dr. Daniel L. Ross
Materials Research Laboratory
RCA Laboratories
Princeton, New Jersey



As part of the research conducted by the Graphic Systems Applied Research Laboratory, various means of preparing printing plates or their immediate precursors by laser irradiation of appropriate substrates were investigated.

One of the substrates examined was "Cronapress Conversion Film." [A product of E. I. DuPont de Nemours & Co.] This material consists of a Mylar base coated with a thin layer of a polymer permeated with numerous densely-packed voids of about 1 micron or less in diameter. On treatment with a developing solution containing a dye, the voids become filled, and the dye can be fixed in place by subsequent processing. When the film is laid over a chase of type and pressure is applied, the voids in regions corresponding to raised areas of type are collapsed, and these regions are thus rendered non-dyeable. A "negative" image of the chase produced in this way can then be used to produce a printing plate by photographic contact printing on an appropriate sensitized plate.

It was observed that heat or exposure to a beam of 10.6-micron wavelength radiation from a CO₂ gas laser would also render Cronapress film non-dyeable. A pulse of milliseconds (or less) duration from the focussed beam brought from a 2-watt CO₂ laser, produced a non-dyeable spot on the film whose area depended on the amount of energy delivered.

As an application of this finding, a half-tone negative transparency could be produced by scanning a film of Cronapress with a suitably deflected and modulated CO₂ laser beam, causing each spot produced to correspond spatially to a dark area on a photograph (or half-tone image) (Fig. 1). Upon processing the film, the resulting half-tone transparency (Fig. 2), which permits light to pass through each spot where it has been exposed, can then be used to prepare a printing plate as described above.

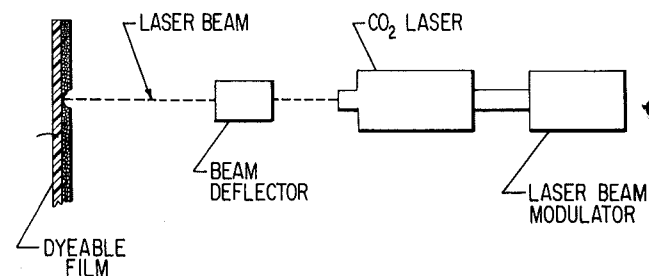


Fig. 1—Schematic diagram showing an apparatus for producing a photographic-type transparency.

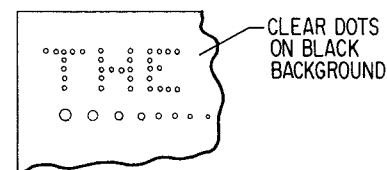
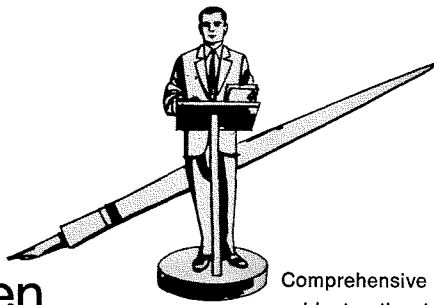


Fig. 2—Drawing of a transparency obtained using the apparatus shown in Fig. 1, followed by dyeing and fixing of the film. The size of the dots produced is controlled by the amount of energy delivered to the film.



Pen and Podium

Comprehensive subject-author index to Recent RCA technical papers

Both published papers and verbal presentations are indexed. To obtain a published paper, borrow the journal in which it appears from your library, or write or call the author for a reprint. For information on unpublished verbal presentations, write or call the author. (The author's RCA Division appears parenthetically after his name in the subject-index entry.) For additional assistance in locating RCA technical literature, contact: RCA Staff Technical Publications, Bldg. 2-8, RCA, Camden, N.J. (Ext. PC-4018).

This index is prepared from listings provided bimonthly by RCA Division Technical Publications Administrators and Editorial Representatives—who should be contacted concerning errors or omissions (see inside back cover)

Subject index categories are based upon the *Thesaurus of Engineering Terms*, Engineers Joint Council, N.Y., 1st Ed., May 1964.

Subject Index

Titles of papers are permuted where necessary to bring significant keyword(s) to the left for easier scanning. Authors' division appears parenthetically after his name.

ACOUSTICS

ACOUSTIC PHONONS in Crystals—C. H. Anderson (Labs., Pr) Physics Colloquium, University of Delaware, Newark, Delaware; 12/3/69

ACOUSTIC PHONONS in Crystals and Liquid Helium Films—C. H. Anderson (Labs., Pr) University of Washington, Seattle, Washington; 11/11/69

ACOUSTIC PHONONS in Crystals and Liquid Helium Films—C. H. Anderson (Labs., Pr) University of Oregon, Eugene, Oregon; 11/6/69

ACOUSTIC PHONONS in Crystals and Liquid Helium Films—C. H. Anderson (Labs., Pr) UCLA, Los Angeles, Calif.; 10/29/69

RIBBON VELOCITY MICROPHONE—H. J. Olson (Labs., Pr) Acoustical Society of America, San Diego, Calif.; 11/4/69

SONIC PEN—a Digital Stylus System—P. deBruyne (ASD, Burl) *IEEE Computer Group News*; 11/69

ULTRASONIC ATTENUATION due to Phonon-Phonon Interactions—R. Klein, R. K. Wehner (Labs., Pr) Swiss Physical Society Meeting, St. Gallen; 10/3-5/69

AMPLIFICATION

AVALANCHE DIODE, Power Amplification Using an—J. F. Dienst, R. V. D'Aiello, E. E. Thomas (Labs., Pr) *Electronics Letters*, Vol 5, No. 4; 7/10/69

POWER AMPLIFIER, All-Transistor, UHF, 1-kW, High-Gain—R. L. Bailey, W. P. Bennett, L. F. Heckman, I. E. Martin (EC, Lanc) *IEEE Trans. on Microwave Theory and Techniques*; 12/69

POWER AMPLIFIERS, UHF Integrated—W. E. Poole (EC, Som) *IEEE J. of Solid-State Circuits*; 12/69

THIN-LAYER GaAs AMPLIFIERS, Optimum Design of—R. H. Dean (Labs., Pr) *Proc. of the IEEE*, Vol. 57, No. 7; 7/69

TRANSFERRED-ELECTRON AMPLIFIERS—F. Sterzer (EC, Pr) *IEEE J. of Solid-State Circuits*; 12/69

TRANSFERRED-ELECTRON AMPLIFIERS, Stabilized Supercritical—B. S. Perlman, T. E. Walsh, R. E. Enstrom (EC, Pr) *IEEE J. of Solid-State Circuits*; 12/69

ANTENNAS

PHASED ARRAYS—V. Mikenas (MSR, Mrstn) Symp. on Advances in Sciences, Midway House Hotel, Chicago, Ill; 11/27-30/69

PHASED ARRAY RADARS, Future Trends in—A. S. Robinson (MSR, Mrstn) NEREM 69, Hotel Sheraton, Boston, Mass.; 11/5-7/69

PHASED ARRAY RADAR Systems—A. S. Robinson (MSR, Mrstn) N.J. Coast Chapter of the Aerospace & Electronic System Group, IEEE, Little Silver, N.J.; 11/19/69

SIDELobe PHASED ARRAY, a Low-Loss N-Way Optical Power Divider for a Ku-Band Low—C. Profera (MSR, Mrstn) *Microwave Journal*; 11/69

CHECKOUT

APTE—Automatic Production Test Equipment—N. A. Teixeira (ASD, Burl) 1969 Automatic Support Systems Symposium, Chase-Park Plaza Hotel, St. Louis, Mo.; 11/3-5/69; *Symp. Proc.*

CIRCUIT ANALYSIS

OTA OBSOLETEs OP AMP—C. F. Wheatley, H. A. Wittlinger (EC, Som) National Electronics Conf., Chicago, Ill.; 12/10/69; 1969 *N.E.C. Proc.*

TRIANGULAR CONNECTION NETWORKS, Rearrangeability of—M. C. Paull (Labs., Pr) 10th Annual Symposium on Switching and Automata Theory, Waterloo, Canada; 10/15-17/69

CIRCUITS, INTEGRATED

COS/MOS MSI COUNTER and register design and applications—R. Heuner, J. Litus, A. Havasy, J. Harmon (EC, Som) National Electronics Conf., Chicago, Ill.; 12/10/69; 1969 *N.E.C. Proc.*

COMPLEMENTARY SYMMETRY MOS TRANSISTOR Integrated Circuits, TREE Effects in—W. J. Dennehy (AED, Pr) 1969 GOMAC Conf., Washington, D.C.; 9/16/69

DIFFUSED RESISTORS, Designing High-Frequency—R. E. Kleppinger (EC, Som) *RCA Review*; 12/69

LAMINAR FLOW CLEAN ROOMS, are they necessary?—W. A. Bosenberg (Labs., Pr) *Contamination Control Magazine*; 6/69

LAYERED SEMICONDUCTOR-METAL TRANSFERRED-ELECTRON OSCILLATOR Geometry, Pulsed Heat Conduction in a—B. S. Perlman, T. E. Walsh (EC, Pr) *RCA Review*; 12/69

MICROWAVE INTEGRATED CIRCUITS—H. Sobol (EC, Som) Naval Research Laboratories, Washington, D.C.; 12/9/69

MICROWAVE INTEGRATED CIRCUIT Reliability, Design for—V. J. Lukach, R. E. Kleppinger (EC, Som) *IEEE Group on Reliability*, Phila., Pa.; 11/20/69

MICROWAVE INTEGRATED CIRCUITS, Lumped-Element—H. Sobol (EC, Som) *IEEE Group on Microwave Theory and Techniques*, Washington, D.C. Chapter Meeting; 11/11/69

MICROWAVE INTEGRATED CIRCUITS, Current Applications of—W. C. Curtis, H. Honda (ASD, Burl) NEREM, Sheraton-Boston Hotel; 11/5-7/69; *NEREM Record*

POWER AMPLIFIER, All Transistor, UHF, 1-kW, High-Gain—R. L. Bailey, W. P. Bennett, L. F. Heckman, I. E. Martin (EC, Lanc) *IEEE Trans. on Microwave Theory and Techniques*; 12/69

10-Watt CW BROADBAND POWER SOURCE at S-Band, Hybrid Integrated—E. Belohoubek, A. Rosen, D. Stevenson, A. Presser (EC, Pr) *IEEE J. of Solid-State Circuits*; 12/69

THICK FILM HYBRID CIRCUITS, Computer Design for the Resistor Component for—M. Wolf (AED, Pr) 1969 International Society for Hybrid Micro Electronics Conf., Dallas, Texas; 9/29/69

CIRCUITS, PACKAGED

COMPUTER DESIGNED ARTWORK for P.C. Boards—J. A. Bauer (MSR, Mrstn) *Electronics World*; 10/69

HYBRID CIRCUITS, System Partitioning for—F. Gargione, H. Fenster (AED, Pr) International Society for Hybrid Microelectronics Conf., Dallas, Texas; 9/29/69

LARGE SCALE INTEGRATED and Computer Architecture—S. Y. Levy (Labs., Pr) Machines of Great Power, Paris, France; 9/6/69

COMMUNICATIONS COMPONENTS

DEMODULATOR, A Universal Threshold Extending FMFB—M. M. Gerber (DCSD, Cam) International Conference on Communications, Boulder, Colorado; 6/6/69; *Record of the Conference*; 1969 *IEEE Proc. on the International Conference on Communications*

MICROWAVE OSCILLATORS, Avalanche Diode—L. S. Napoli (Labs., Pr) Electron Devices IEEE Section, Pittsburgh, Pa.; 10/9/69

MICROWAVE OSCILLATORS, Stacked Kilowatt Avalanche-Diode—S. G. Liu, J. J. Risko (Labs., Pr) IEEE International Electron Devices Meeting, Washington, D.C.; 10/29-31/69

POWER AMPLIFIER, All-Transistor, UHF, 1-kW, High-Gain—R. L. Bailey, W. P. Bennett, L. F. Heckman, I. E. Martin (EC, Lanc) *IEEE Trans. on Microwave Theory and Techniques*; 12/69

POWER AMPLIFIERS, UHF Integrated—W. E. Poole (EC, Som) *IEEE J. of Solid-State Circuits*; 12/69

COMMUNICATIONS SYSTEMS

REMOTE VIEW SYSTEMS Applications—R. J. Gildea (ASD, Burl) Second Annual Armed Forces Audio-Visual Communications Conference, Sheraton-Park Hotel, Washington, D.C.; 11/3-7/69

COMPUTER APPLICATIONS

AUTOMATED INTERFACE DESIGN for ATE—J. Fay (ASD, Burl) 1969 Automatic Support Systems Symposium, Chase-Park Plaza Hotel, St. Louis, Mo.; 11/3-5/69; *Symp. Proc.*

COMPUTER DESIGNED ARTWORK for P.C. Boards—J. A. Bauer (MSR, Mrstn) *Electronics World*; 10/69

MOS MODELS, Large-Signal—A. Feller (ATL, Cam) Transistor & Integrated Circuit Modeling for Computer-Aided Design, New York, N.Y.; 10/15/69

COMPUTERS, PROGRAMMING

DIAGNOSTIC PROGRAMS for Video-Comp Phototypesetting Systems—G. W. Maymon (GSD, Dayton) *Information Display Journal*; 12/69

SCIENTIFIC SUBROUTINE LIBRARY Construction—R. L. Crane (Labs., Pr) Worcester Polytechnic Institute, Worcester, Mass.; 12/9/69

COMPUTER STORAGE

COMPUTER MEMORIES and the Impact of Semiconductor Technology—J. A. Rajchman (Labs., Pr) IEEE International Electron Devices Meeting, Washington, D.C.; 10/29-31/69

HIGH-SPEED ASSOCIATIVE MEMORY, Silicon-on-Sapphire Complementary MOS Circuits for—J. R. Burns, J. H. Scott (Labs., Pr) Fall Joint Computer Conference, Las Vegas, Nevada; 11/18-20/69

OPTICAL MEMORIES, A Photosensitive Readout Array for—J. M. Adour, R. D. Lohman (Labs., Pr) IEEE International Electron Devices Meeting, Washington, D.C.; 10/29-31/69

OPTICAL MEMORIES, The Promise of—J. A. Rajchman (Labs., Pr) 15th Annual Conference on Magnetism and Magnetic Materials, Phila., Pa.; 11/18-21/69

COMPUTER SYSTEMS

LARGE SCALE INTEGRATED and Computer Architecture—S. Y. Levy (Labs., Pr) Machines of Great Power, Paris, France; 9/6/69

PHYSICAL REALIZATION of Computers—J. A. Rajchman (Labs., Pr) Livingston College, Rutgers University, Livingston, N.J.; 10/21/69

RCA 215 MULTIPROCESSOR—E. J. Dieterich, L. C. Kay (ASD, Burl) Fall Joint Computer Conference, Las Vegas, Nev.; 11/17-20/69; 1969 *FJCC Record*

CONTROL SYSTEMS

FEEDFORWARD STABILIZATION, Effectiveness of—P. Tokareff, C. V. Hatley (MTP, Cocoa Beach) Instrument Society of America Conf., Houston, Texas; 10/69

TRIANGULAR CONNECTION NETWORKS, Rearrangeability of—M. C. Paull (Labs., Pr) 10th Annual Symposium on Switching and Automata Theory, Waterloo, Canada; 10/15-17/69

DISPLAYS

ELECTROSTATIC IMAGES, Developing—D. A. Ross (Labs., Pr) The Royal Photographic Society Symposium, Oxford, England; 10/1-3/69

SONIC PEN—a Digital Stylus System—P. deBruyne (ASD, Burl) *IEEE Computer Group News*; 11/69

SURFACE ILLUMINATION of Semiconductor Panels—B. J. Levin, R. Mavaddat (ATL, Cam) *J. Appl. Phys.*, Vol. 40; 12/69

DOCUMENTATION

MEDIUM for the Message—R. S. Mezrich (Labs., Pr) Metropolitan Chapter of the National Microfilm Assoc., New York, N.Y.; 11/19/69

NEW PRODUCT RELEASE, A Neglected Form of Technical Communication—H. K. Mintz (ASD, Burl) *IEEE Trans. on Engineering Writing and Speech*, Vol. EWS 12, No. 3; 10/69

ELECTROMAGNETIC WARFARE

MAGNETOPLASMA LOADED WAVEGUIDE at Room Temperature, Field Distribution in a—R. Hirota, K. Suzuki (Labs., Pr) Conference of the Physical Society of Japan, Kagawa University, Japan; 11/15-18/69

MICROWAVE OSCILLATION in $Al_xGa_{1-x}As$ Avalanche Diodes—C. Yeh, S. G. Liu, F. Z. Hawrylo (Labs., Pr) *Proc. of the IEEE*, Vol. 57, No. 10; 10/69

RADIO WAVES, Ionospheric Phase Distortion & Faraday Rotation of—T. Murakami, G. Wickizer (MSR, Mrstn) *RCA Review*; 9/69

SIDELobe PHASED ARRAY, A Low-Loss N-Way Optical Power Divider for a Ku-Band Low—C. Profera (MSR, Mrstn) *Microwave Journal*; 11/69

SURFACE CHARGE WAVES in the n-InSb MOS Structure in a Magnetic Field, Propagation of—M. Toda (Labs., Pr) *J. of the Physical Society of Japan*, Vol. 27, No. 2; 8/69

ELECTRO-OPTICS

OPTICAL FILTERS Utilizing Nematic Liquid Crystals, Electronically-Tuned—J. A. Castellano, E. E. Pasierb (Labs., Pr) IEEE International Electron Devices Meeting, Washington, D.C.; 10/29-31/69

OPTICAL MEMORIES, A Photosensitive Readout Array for—J. M. Assour, R. D. Lohman (Labs., Pr) IEEE International Electron Devices Meeting, Washington, D.C.; 10/29-31/69

SURFACE ILLUMINATION of Semiconductor Panels—B. J. Levin, R. Mavaddat (ATL, Cam) *J. Appl. Phys.*, Vol. 40; 12/69

ENERGY CONVERSION

HEAT PIPE—A progress report—G. Y. Eastman (EC, Lanc) ASME Mtg., Poughkeepsie, N.Y.; 11/18/69

MICROWAVE ENERGY in the Freeze-Drying Process, A Technical and Economic Appraisal of the Use of—A. C. Grimm (EC, Lanc) *RCA Review*; 12/69

SPACECRAFT PROPULSION SYSTEM Employing Surface Tension Feed, Modeling of a—Y. Brill, R. Lynch, J. Scussel (AED, Pr) 11th Liquid Propulsion Meeting, Miami, Fla.; 9/17/69; to be published in Chemical Propulsion Information Agency Bulletin.

10-WATT CW BROADBAND POWER SOURCE at S-Band, Hybrid Integrated—E. Belohoubek, A. Rosen, D. Stevenson, A. Presser (EC, Pr) IEEE J. of Solid-State Circuits; 12/69

THERMIONIC ENERGY CONVERSION, Editorial for special issue of the Transactions on Electron Devices dealing with—J. D. Levine (Labs., Pr) *Trans. on Electron Devices*, Vol. ED-16, No. 8; 8/69

THERMOELECTRIC AIR-CONDITIONER Applications—B. Shelpuk (ATL, Cam) Tri-State Power Club, New York, N.Y.; 12/1/69

THERMOELECTRIC REFRIGERATION Applications—B. Shelpuk (ATL, Cam) ASME Winter Annual Meeting, Los Angeles, Calif.; 11/19/69

WICK PROPERTIES, Experimental Determination of—W. E. Harbaugh (EC, Lanc) ASME Mtg., Poughkeepsie, N.Y.; 11/18/69

ENVIRONMENTAL ENGINEERING

LAMINAR FLOW CLEAN ROOMS, Are They Necessary?—W. A. Bosenberg (Labs., Pr) *Contamination Control Magazine*; 6/69

MICROWAVE ENERGY in the Freeze-Drying Process, A Technical and Economic Appraisal of the Use of—A. C. Grimm (EC, Lanc) *RCA Review*; 12/69

RANDOM VIBRATION TESTING and Analysis—A. S. Baran (AED, Pr) Institute of Environmental Sciences Practical Lecture Series, Phila., Pa.; 10/6/69; *IES Mid-Atlantic Chapter Lecture Notes*

SHOCK ANALYSIS and Testing—J. R. Fagan (AED, Pr) Institute of Environmental Sciences Practical Lecture Series, Phila., Pa.; 10/13/69; *Mid-Atlantic Chapter Lecture Notes*

THERMOELECTRIC AIR-CONDITIONER Applications—B. Shelpuk (ATL, Cam) Tri-State Power Club, New York, N.Y.; 12/1/69

THERMOELECTRIC REFRIGERATION Applications—B. Shelpuk (ATL, Cam) ASME Winter Annual Meeting, Los Angeles, Calif.; 11/19/69

FILTERS, ELECTRIC

DIGITAL FILTERS, Improving the Accuracy and Speed of—M. S. Corrington (ATL, Cam) *Proc. of the Second Biennial Cornell Electrical Engineering Conf. on Computerized Electronics*; 8/69

GEOPHYSICS

BROADCAST SATELLITE and Conservation of a Natural Resource—K. H. Powers (Lab., Pr) Preparatory Policy Conf., Canada; 11/21-23/69

REMOTE SENSING OF THE SEA CONDITIONS with Microwave Radiometer Systems—R. Groshans, J. C. Aukland, P. J. Caruso, W. H. Conway (AED, Pr) Sixth International Symp. on Remote Sensing of Environment, Ann Arbor, Mich.; 10/69

GRAPHIC ARTS

MEDIUM for the Message—R. S. Mezrich (Labs., Pr) Metropolitan Chapter of the National Microfilm Assoc., New York, N.Y.; 11/19/69

HOLOGRAPHY

HOLOGRAMS in Thin Bismuth Films—J. J. Amodi, R. S. Mezrich (Labs., Pr) *Applied Physics Letters*, Vol. 15, No. 2; 7/15/69

INFORMATION THEORY

DETERMINISTIC CONTEXT-SENSITIVE Languages—D. A. Walters (Labs., Pr) 10th Annual Symposium on Switching and Automata Theory, Waterloo, Ontario, Canada; 10/15-17/69

PARSING PROCEDURES, A Representation System for—D. A. Walters (Labs., Pr) 3rd International Symposium on Computer and Information Science, Bal Harbour, Florida; 12/18-20/69

LABORATORY TECHNIQUES

ACOUSTIC-PHONON SPECTROSCOPY—E. S. Sabisky (Labs., Pr) Johns Hopkins University, Baltimore, Maryland; 11/19/69

ACOUSTIC-PHONON SPECTROSCOPY—E. S. Sabisky (Labs., Pr) Pennsylvania State University, University Park, Penn.; 11/4/69

ELECTRON MICROSCOPY in Ceramics—M. D. Coutts (Labs., Pr) English Department, Rutgers University, New Brunswick, N.J.; 10/4/69

HIGH-TEMPERATURE MICROSCOPY—T. F. Barry (EC, Hr) American Ceramic Society Mtg., Phila., Pa.; 11/18/69

NEW SENSITIVE SPECTROMETER for Acoustic Phonons—C. H. Anderson (Labs., Pr) Acoustical Society of America, San Diego, Calif.; 11/4/69

PULSED GALLIUM ARSENIDE AVALANCHE DIODE OSCILLATORS, Measurement of AM Noise in—P. A. Levine (Labs., Pr) IEEE International Electron Devices Meeting, Washington, D.C.; 10/29-31/69

SCANNING ELECTRON MICROSCOPY—M. D. Coutts (Labs., Pr) American Chemical Society Meeting of South Jersey, Woodbury, N.J.; 11/11/69

SPARK SOURCE MASS SPECTROSCOPY, Impurity Analysis by—W. L. Harrington, J. R. Woolston (Labs., Pr) American Society of Metals Congress and Exposition, Phila., Pa.; 10/14/69

SPECTROSCOPIC ANALYSIS, Cathode-Ray-Excited—S. Larach (Labs., Pr) Hebrew University, Jerusalem, Israel; 12/69

TRANSITION SPEED OF JOSEPHSON JUNCTIONS, Measurement of—W. C. Stewart (Labs., Pr) *Applied Physics Letters*, Vol. 14, No. 12; 6/15/69

LASERS

$Al_xGa_{1-x}As$ INJECTION LASERS near the Direct-Indirect Transition, Properties of—H. Kressel, H. Nelson, H. Lockwood (Labs., Pr) IEEE Semiconductor Laser Conference, Mexico City, Mexico; 12/1-3/69

$Al_xGa_{1-x}As$ LASER Diodes Using the Close-Confinement Structure, Improved Red and Infrared Light-Emitting—H. Kressel, H. Nelson (Labs., Pr) *Applied Physics Letters*, Vol. 15, No. 1; 7/1/69

CLOSE-CONFINED GaAs LASER STRUCTURES, Field Distribution in—N. E. Byer, J. K. Butler (Labs., Pr) IEEE Semiconductor Laser Conference, Mexico City, Mexico; 12/1-3/69

CLOSE-CONFINEMENT EPITAXIAL P/N JUNCTION LASERS: Theory and Experiment, Optical Losses in—H. Kressel, F. Z. Hawrylo, H. Nelson (Labs., Pr) IEEE Semiconductor Laser Conference, Mexico City, Mexico; 12/1-3/69

FLUORESCENCE OF $SrTiO_3:Cr^{3+}$, Anomalous Stress Effects on the—W. J. Burke, R. J. Pressley (Labs., Pr) *Solid State Communications*, Vol. 7; 1969

GaAs INJECTION LASERS Prepared by Liquid-Phase Epitaxy, Effect of Substrate Imperfections on—H. Kressel, H. Nelson, S. H. McFarlane, M. S. Abrahams, Pr. LeFue, C. J. Buiochi (Labs., Pr) *Journal of Applied Physics*, Vol. 40, No. 9; 8/69

HETEROEPITAXIAL LAYERS: GaAs-P on GaAs, Stresses in—M. S. Abrahams, L. R. Weisberg, J. J. Tietjen (Labs., Pr) *J. of Applied Physics*, Vol. 40, No. 9; 8/69

HIGH-GAIN FLOWING-GAS CARBON DIOXIDE LASER, Diffraction Gating Timing of a—T. R. Schein (ASD, Burl) Laser Industries Association 1969 Laser Conf., Los Angeles, Calif.; 10/20-22/69; *Conf. Proc.*

INFRARED IMAGE UPCONVERTERS, The Imaging Properties of—A. H. Firester (Labs., Pr) IEEE International Electron Devices Meeting, Washington, D.C.; 10/29-31/69

LASER AND LASER Applications—D. Herzog (ATL, Cam) Northeastern University, Boston, Mass.; 10/21/69

LASER FUNDAMENTALS & Applications—Dr. J. Vollmer (ATL, Cam) Princeton University; 10/28/69

LASER WRITING—R. S. Braudy (ATL, Cam) *Proceedings of the IEEE*; 10/69

NONLINEAR IMAGE UNCONVERTERS with Nonplanar Pump Beams—A. H. Firester (Labs., Pr) Annual Meeting of the Optical Society of America, Chicago, Illinois; 10/21-24/69

PULSED GALLIUM ARSENIDE AVALANCHE DIODE OSCILLATORS, Measurement of AM Noise in—P. A. Levine (Labs., Pr) IEEE International Electron Devices Meeting, Washington, D.C.; 10/29-31/69

SEMICONDUCTORS WITH POPULATION INVERSION, Index of Refraction Changes in—J. K. Butler (Labs., Pr) IEEE Semiconductor Laser Conference, Mexico City, Mexico; 12/1-3/69

SOLID STATE Lasers—W. S. Byk (ASD, Burl) U. of Michigan IEEE Student Chapter; 1/23/69

LOGIC THEORY

THRESHOLD LOGIC in LSI—R. O. Winder (Labs., Pr) Fall Joint Computer Conf., Las Vegas, Nevada; 11/18-20/69

LOGIC ELEMENTS

THRESHOLD GATE Building Blocks—S. Cohen, R. O. Winder (Labs., Pr) *IEEE Trans. on Computer*, Vol. C-18, No. 9; 9/69

LOGISTICS

OPTIMAL SPARES SELECTION, Availability Assurance by—E. J. Westcott, H. R. Barton (DCSD, Cam) October Meeting of Philadelphia Section IEEE Group on Reliability, Phila., Pa.; 10/21/69

MANAGEMENT

MANAGEMENT of the Computer Complex, Security and Catastrophe Prevention—F. P. Congdon (ASD, Burl) Chairman, AMA National Briefing Session; Americana Hotel, New York, N.Y.; 11/17-19/69

MANAGING AND CONTROLLING A Project—I. Brown (AED, Pr) Philadelphia Section of IEEE, General Electric, Valley Forge, Pa.; 12/2/69

PROGRAM PREPARATION on ATE Supported Systems, Allocation of Responsibility for—A. Greenspan, E. Schmuhi (ASD, Burl) 1969 Automatic Support Systems Symposium, Chase-Park Plaza Hotel, St. Louis, Mo.; 11/3-5/69; *Symp. Proc.*

MANUFACTURING

AUTOMATED PLATING for Printed Circuits—H. F. Schellack (DCSD, Cam) *Solid State Technology*, Vol. 12, No. 11; 11/69

ELECTROLESS PLATING TECHNIQUES Survey of Selective—N. Feldstein (Labs., Pr) Allentown-Reading Branch of the American Electroplaters' Society, Allentown, Pa.; 11/20/69

ELECTROLESS PLATING, Anionic Inhibition in—N. Feldstein, P. R. Amodio (Labs., Pr) Symposium on Dielectrics in Device Technology, Electro-chemical Society Meeting, Detroit, Michigan; 10/5-10/69

LAMINAR FLOW CLEAN ROOMS, Are They Necessary?—W. A. Bosenberg (Labs., Pr) *Contamination Control Magazine*; 6/69

MASERS

ELECTRON-HOLE PLASMA, Coherent Microwave Emission from an—B. B. Robinson, G. A. Swartz (Labs., Pr) *IBM Journal of Research and Development*, Vol. 13, No. 5; 9/69

MICROWAVE EMISSION FROM InSb: Gross Features and Possible Explanations, Summary of—M. Glicksman (Labs., Pr) *IBM Journal of Research and Development*, Vol. 13, No. 5; 9/69

MATHEMATICS

CALCULATIONS OF FATIGUE DAMAGE, Analysis of Random Response for—C. C. Osgood (AED, Pr) 40th Shock and Vibration Symposium, Langley, Va.; S&V Bulletin (DoD)

- CRITICAL POINT PHENOMENA OF YIG, The Use of the Kink-Point Locus to Study the**—K. Miyatani, K. Yoshikawa (Labs., Pr) 15th Annual Conf. on Magnetism and Magnetic Materials, Phila., Pa.; 11/18-21/69
- MODELING SEMICONDUCTOR DEVICES, Approximate Methods for**—R.B. Schilling (EC, Som) Symp. on Models for Solid-State Devices, University of Wisconsin; 11/69
- MOTION OF OBJECTS EJECTED from an Orbiting Body, Bounds on the**—S. A. Musa (MSR, Mrstn) *AIAA Journal*; 10/69
- MECHANICAL DEVICES**
- CALCULATIONS OF FATIGUE DAMAGE, Analysis of Random Response for**—C. C. Osgood (AED, Pr) 40th Shock and Vibration Symposium, Langley, Va.; S&V Bulletin (DoD)
- HEAT PIPE—A Progress Report**—G. Y. Eastman (EC, Lanc) ASME Mtg., Poughkeepsie, N.Y.; 11/18/69
- WICK PROPERTIES, Experimental Determination of**—W. E. Harbaugh (EC, Lanc) ASME Mtg., Poughkeepsie, N.Y.; 11/19/69
- OPTICS**
- DISCHARGE OF ELECTROPHOTOGRAPHIC MATERIAL by Light, Note on the**—H. Kiess (Labs., Pr) *J. of Applied Physics*, Vol. 40, No. 10; 9/69
- OPTICAL MEMORIES, The Promise of**—J. A. Rajchman (Labs., Pr) 15th Annual Conf. on Magnetism and Magnetic Materials, Phila., Pa.; 11/18-21/69
- PROPERTIES, ATOMIC**
- ACOUSTIC PHONONS in Crystals**—C. H. Anderson (Labs., Pr) Physics Colloquium, University of Delaware, Newark, Delaware; 12/3/69
- ACOUSTIC PHONONS in Crystals and Liquid Helium Films**—C. H. Anderson (Labs., Pr) University of Washington, Seattle, Washington; 11/11/69
- ACOUSTIC PHONONS in Crystals and Liquid Helium Films**—C. H. Anderson (Labs., Pr) University of Oregon, Eugene, Oregon; 11/6/69
- ACOUSTIC PHONONS in Crystals and Liquid Helium Films**—C. H. Anderson (Labs., Pr) UCLA, Los Angeles, Calif.; 10/29/69
- COLLECTIVE THOMSON SCATTERING, Effect of Charged Particle-Neutral Collisions on**—I. Gorog (Labs., Pr) *The Physics of Fluids*, Vol. 12, No. 8; 8/69
- ULTRASONIC ATTENUATION due to Phonon-Phonon Interactions**—R. Klein, R. K. Wehner (Labs., Pr) Swiss Physical Society meeting, St. Gallen; 10/3-5/69
- PROPERTIES MOLECULAR**
- CdCr₂Se₄, Review of the Crystal Growth of**—F. Okamoto, T. Oka (Labs., Pr) Institute of Scientific and Industrial Research, Osaka University, Osaka, Japan; 11/10-11/69
- Cu_{1-x}M_xCr₂X₄ (M=Fe, Al, Ga and In; X=S, Se), Crystal Growth of**—K. Kato (Labs., Pr) Institute of Scientific and Industrial Research, Osaka University, Osaka, Japan; 11/10-11/69
- CuCr₂Se_{4-2x}Br_{2x} (x=0 to 1), Crystal Growth of**—K. Kato, Y. Wada, K. Miyatani (Labs., Pr) Institute of Scientific and Industrial Research, Osaka University, Osaka, Japan; 11/10-11/69
- CHALCOGENIDE SPINELS, Chemical Analysis of**—K. Ametani, F. Okamoto (Labs., Pr) Institute of Scientific and Industrial Research, Osaka University, Osaka, Japan; 11/10-11/69
- CHROMIUM CHALCOGENIDE SPINELS, The Crystal Growth and Thermal Analysis of**—Y. Wada, K. Ametani, S. Harada (Labs., Pr) Institute of Scientific and Industrial Research, Osaka University, Osaka, Japan; 11/10-11/69
- CHROMIUM CHALCOGENIDE SPINELS, On the Origin of Anomalous Absorption Edge Shifts in**—S. B. Berger (Labs., Pr) 15th Annual Conf. on Magnetism and Magnetic Materials, Phila., Pa.; 11/18-21/69
- CRYSTAL GROWTH and Growth Rates of CdS by Sublimation and Chemical Transport**—E. Kaldis (Labs., Pr) *J. of Crystal Growth*, Vol. 5; 1969
- FERROMAGNETIC HgCr₂Se₄, Crystal Growth, Semiconducting and Optical Properties of**—H. W. Lehmann, F. P. Emenegger (Labs., Pr) *Solid State Communications*, Vol. 7, No. 4; 1969
- HgCr₂Se₄ Single Crystals, Growth of**—T. Takahashi (Labs., Pr) Institute of Scientific and Industrial Research, Osaka University, Osaka, Japan; 11/10-11/69
- LIQUID CRYSTALS, Guest-Host Interactions in Nematic**—G. H. Hellmeier, J. A. Castellano, L. A. Zanoni (Labs., Pr) *Molecular Crystals and Liquid Crystals*, Vol. 8; 1969
- LIQUID CRYSTALS, Capillary Flow of Cholesteric and Smectic**—W. Helfrich (Labs., Pr) *Physical Review Letters*, Vol. 23, No. 7; 8/18/69
- NEMATIC LIQUID CRYSTALS, Electronically-Tuned Optical Filters Utilizing**—J. A. Castellano, E. F. Pasierb (Labs., Pr) IEEE International Electron Devices Meeting, Washington, D.C.; 10/29-31/69
- NEMATIC p-AZOXYANISOLE, Orientation Pattern of Domains in**—W. Helfrich (Labs., Pr) *J. of Chemical Physics*, Vol. 51, No. 6; 9/15/69
- SILICON ON ALUMINA-RICH SINGLE-CRYSTAL SPINEL, Epitaxial Growth and Properties of**—G. W. Cullen, G. E. Gottlieb, C. C. Wang, K. H. Zaininger (Labs., Pr) *J. of the Electrochemical Society*, Vol. 116, No. 10; 10/69
- SINGLE CRYSTAL SPINEL as Dielectric Substrate Material for Epitaxial Silicon Devices, The Use of**—C. C. Wang (Labs., Pr) Symp. on Dielectrics in Device Technology, Electrochemical Society Meeting, Detroit, Michigan; 10/5-10/69
- SPINEL SINGLE CRYSTALS for Substrate Use in Integrated Electronics, Growth and Characterization of**—C. C. Wang (Labs., Pr) *J. of Applied Physics*, Vol. 40, No. 9; 8/69
- SYSTEM HgCr₂Se₄-ZnCr₂Se₄ and its Crystal Growth**—T. Takahashi, K. Miyatani (Labs., Pr) Institute of Scientific and Industrial Research, Osaka University, Osaka, Japan; 11/10-11/69
- SYSTEM HgCr_{2-x}In_xSe₄; x<0.45, Single Crystal Growth of the**—T. Takahashi, T. Oka (Labs., Pr) Institute of Scientific and Industrial Research, Osaka University, Osaka, Japan; 11/10-11/69
- PROPERTIES, SURFACE**
- CdSe/Se HETEROJUNCTION DIODES, Evaporated Thin-Film**—R. M. Moore, C. J. Busanovich (Labs., Pr) IEEE International Electron Devices Meeting, Washington, D.C.; 10/29-31/69
- FLUCTUATIONS OF THE SUPERCONDUCTING ORDER PARAMETER, Anisotropy of the Surface Impedance in the Surface-Sheath Regime as Evidence for**—K. Maki, G. Fischer (Labs., Pr) *The Physical Review*, Vol. 184, No. 2; 8/10/69
- HOLOGRAMS in Thin Bismuth Films**—J. G. Amodei, R. S. Mezrich (Labs., Pr) *Applied Physics Letters*, Vol. 15, No. 2; 7/15/69
- LIQUID CRYSTALS, Electric-Field-Induced Cholesteric-Nematic Phase Change in**—G. H. Hellmeier, J. E. Goldmacher (Labs., Pr) *J. of Chemical Physics*, Vol. 51, No. 3; 8/1/69
- Pb₃Sn_{1-2x}Te EPITAXIAL FILMS, Preparation and Properties of**—T. O. Farinre (Labs., Pr) Symp. on Semiconductor Alloys, American Vacuum Society, Seattle, Washington; 10/28-31/69
- SURFACE-STATE THEORIES, Evaluation of**—J. D. Levine, P. Mark (Labs., Pr) *The Physical Review*, Vol. 192, No. 2; 6/10/69
- THIN FILM DEVICES on Dielectric Substrates**—C. W. Mueller (Labs., Pr) Meeting of the Thin-Film Division of the American Vacuum Society, Seattle, Washington; 10/28-31/69
- THIN-FILM DIELECTRIC MATERIALS for Microelectronics**—K. H. Zaininger, C. C. Wang (Labs., Pr) *Proc. of the IEEE*, Vol. 57, No. 9; 9/69
- THIN-FILM SILICON: Preparation, Properties, and Device Applications**—J. F. Allison, D. J. Dumin, F. P. Heiman, C. W. Mueller, P. H. Robinson (Labs., Pr) *Proc. of the IEEE*, Vol. 57, No. 9; 9/69
- THIN-FILM SILICON: Preparation, Properties, and Devices Applications**—D. J. Dumin (Labs., Pr) IEEE Student Branch, University of Virginia, Charlottesville, Virginia; 11/8/69
- THIN GERMANIUM FILMS, Acceptor States Due to Defects in**—D. J. Dumin (Labs., Pr) *J. of Vacuum Science and Technology*, Vol. 6, No. 4; 7-8/69
- THIN-LAYER GaAs AMPLIFIERS, Optimum Design of**—R. H. Dean (Labs., Pr) *Proc. of the IEEE*, Vol. 57, No. 7; 7/69
- III-V and II-VI SEMICONDUCTORS, The Nature of Surface States on**—J. D. Levine (Labs., Pr) *J. of Vacuum Science and Technology*, Vol. 6, No. 4; 7-8/69
- PROPERTIES, CHEMICAL**
- FLUORINATED ACRYLIC POLYMERS, NMR Studies of**—W. M. Lee (Labs., Pr) *J. of Polymer Science, Part C*, No. 22; 1969
- GaAs_{1-x}P_x Alloys, Stacking Faults in**—M. S. Abrahams, J. J. Tietjen (Labs., Pr) *J. of the Physics and Chemistry of Solids*, Vol. 30, No. 9; 10/69
- GROUP II-VI COMPOUNDS, Chemistry and Photoelectronic Applications of**—S. Larach (Labs., Pr) Institute of Chemistry, Hebrew University, Jerusalem, Israel; 11/69
- PROPERTIES, ELECTRICAL**
- Cd_{1-x}In_xCr₂Se₄, Two-Band Model of Charge Transport in**—L. R. Friedman, A. Amith (Labs., Pr) Symp. on Magnetic Semiconductors, IBM Research Center, Yorktown Heights, N.Y. 11/13-14/69
- CuCr₂Se_{4-2x}Br_{2x} SYSTEM, Magnetic and Electrical Properties of the**—K. Miyatani, K. Minematsu, F. Okamoto, P. K. Baltzer (Labs., Pr) 15th Annual Conf. on Magnetism and Magnetic Materials, Phila., Pa.; 11/18-21/69
- IMPURITY DOPED HgCr₂Se₄, Electrical and Magnetic Properties of**—K. Minematsu, K. Miyatani, T. Takahashi (Labs., Pr) 15th Annual Conf. on Magnetism and Magnetic Materials, Phila., Pa.; 11/18-21/69
- MAGNETIC SEMICONDUCTOR, FMR Controlled Electrical Properties in a**—M. Toda (Labs., Pr) Conference of the Physical Society of Japan, Kagawa University, Japan; 11/15-18/69
- N-TYPE SI-DOPED GaAs Prepared by Liquid-Phase Epitaxy, Electrical and Optical Properties of**—H. Kressel, H. Nelson (Labs., Pr) *J. of Applied Physics*, Vol. 40, No. 9; 8/69
- NEODYMIUM ETHYL-SULFATE, Effect of Hyperfine Interactions on Electron Spin Spin Relaxation in**—R. B. Clover (Labs., Pr) 15th Conf. on Magnetism and Magnetic Materials, Phila., Pa.; 11/18-21/69
- SEMICONDUCTOR BAND TAIL STATES from Transient Measurements, Properties of**—D. Redfield, J. P. Wittke, J. I. Pankove (Labs., Pr) Electronic Density of States Symposium, Gaithersburg, Maryland; 11/3/69
- PROPERTIES, MAGNETIC**
- COPPER, PHTHALOCYANINE, Magneto-photoconductive Effects in**—S. E. Harrison (Labs., Pr) *J. of Chemical Physics*, Vol. 51, No. 1; 7/1/69
- CRITICAL POINT PHENOMENA OF YIG, The Use of the Kink-Point Locus to Study the**—K. Miyatani, K. Yoshikawa (Labs., Pr) 15th Annual Conf. on Magnetism and Magnetic Materials, Phila., Pa.; 11/18-21/69
- CuCr₂Se_{4-2x}Br_{2x} SYSTEM, Magnetic and Electrical Properties of the**—K. Miyatani, K. Minematsu, F. Okamoto, P. K. Baltzer (Labs., Pr) 15th Annual Conf. on Magnetism and Magnetic Materials, Phila., Pa.; 11/18-21/69
- HEISENBERG FERROMAGNET CdCr₂Se₄, Critical Point Phenomena of the**—K. Miyatani (Labs., Pr) 15th Annual Conf. on Magnetism and Magnetic Materials, Phila., Pa.; 11/18-21/69
- IMPURITY DOPED HgCr₂Se₄, Electrical and Magnetic Properties of**—K. Minematsu, K. Miyatani, T. Takahashi (Labs., Pr) 15th Annual Conf. on Magnetism and Magnetic Materials, Phila., Pa.; 11/18-21/69
- NEODYMIUM ETHYL-SULFATE, Effect of Hyperfine Interactions on Electron Spin Spin Relaxation in**—R. B. Clover (Labs., Pr) 15th Conf. on Magnetism and Magnetic Materials, Phila., Pa.; 11/18-21/69
- SURFACE CHARGE WAVES in the n-InSb MOS Structure in a Magnetic Field, Propagation of**—M. Toda (Labs., Pr) *J. of the Physical Society of Japan*, Vol. 27, No. 2; 8/69
- PROPERTIES, MECHANICAL**
- HETERODE PRESSURE TRANSDUCER, The Feasibility of a**—R. M. Moore, C. J. Busanovich (Labs., Pr) *Proc. of the IEEE*, Vol. 57, No. 8; 8/69
- STRESS RELAXATION and the Activation Energy for Plastic Flow in Solids: Commercially-Pure Aluminum**—R. B. Clough (Labs., Pr) *Physica Status Solidi*, Vol. 36; 1969
- PROPERTIES, OPTICAL**
- CATHODOCHROMISM—A State of the Art Review**—W. Phillips (Labs., Pr) IEEE-PPGD Meeting, Boston, Mass.; 11/20/69
- CLOSE-CONFINEMENT EPITAXIAL P/N JUNCTION LASERS: Theory and Experiment, Optical Losses in**—H. Kressel, F. Z. Hawrylo, H. Nelson (Labs., Pr) IEEE Semiconductor Laser Conf., Mexico City, Mexico; 12/1-3/69
- COPPER PHTHALOCYANINE, Magneto-photoconductive Effects in**—S. E. Harrison (Labs., Pr) *J. of Chemical Physics*, Vol. 51, No. 1; 7/1/69
- FERROMAGNETIC HgCr₂Se₄, Crystal Growth, Semiconducting and Optical Properties of**—H. W. Lehmann, F. P. Emenegger (Labs., Pr) *Solid State Communications*, Vol. 7, No. 4; 1969
- FIELD EFFECT ELECTROLUMINESCENCE in Silicon**—A. M. Goodman (Labs., Pr) IEEE International Electron Devices Mtg., Washington, D.C.; 10/29-31/69

FLUORESCENCE OF SrTiO₃:Cr³⁺, Anomalous Stress Effects on the—W. J. Burke, R. J. Pressley (Labs., Pr) *Solid State Communications*, Vol. 7; 1969

GROUP II-IV COMPOUNDS, Chemistry and Photoelectronic Applications of—S. Larach (Labs., Pr) Institute of Chemistry, Hebrew University, Jerusalem, Israel; 11/69

LOG-NORMAL OR RAYLEIGH DISTRIBUTED? Are Strong Irradiance Fluctuations—D. A. DeWolf (Labs., Pr) Annual Meeting of the Optical Society of America, Chicago, Illinois; 10/21-24/69

LOG-NORMAL OR RAYLEIGH-DISTRIBUTED? Are Strong Irradiance Fluctuations—D. A. DeWolf (Labs., Pr) *J. of the Optical Society of America*, Vol. 59, No. 11; 11/69

MAGNETIC SEMICONDUCTORS, Optical Properties of—S. B. Berger (Labs., Pr) Drexel Institute, Phila., Pa.; 12/3/69

MAGNETIC SEMICONDUCTORS, Optical Effects in—G. Harbeke (Labs., Pr) Meeting on Magnetic Semiconductors, Nottingham, England; 10/14/69

N-TYPE GaAs, Generation and Detection of 10¹² Hz Phonons in—R. S. Crandall (Labs., Pr) *Solid State Communications*, Vol. 7; 1969

N-TYPE SI-DOPED GaAs Prepared by Liquid-Phase Epitaxy, Electrical and Optical Properties of—H. Kressel, H. Nelson (Labs., Pr) *J. of Applied Physics*, Vol. 40, 9; 8/69

OPTICAL ABSORPTION Spectra of Cu:Te—R. Dalven (EC, Pr) American Physical Society Meeting, Los Angeles, Calif.; 12/29-31/69

ZEEMAN EFFECT of Cr³⁺ Fluorescence in SrTiO₃—W. J. Burke, R. J. Pressley (Labs., Pr) *The Physical Review*, Vol. 182, No. 2; 6/10/69

RADAR

ANGLE ESTIMATION TECHNIQUES in the Presence of Multipath—R. Ottinger, J. T. Nessmith (MSR, Mrstn) Tripartite Symp.—NRL; 11/13-14/69

BISTATIC CLUTTER in a Moving Receiver System—E. G. McCall (MSR, Mrstn) *RCA Review*; 9/69

COMPARISON OF SIMULATED OUTPUT WITH THEORY AND EXPERIMENTAL RESULTS (Secret), An OTH Simulation II—C. Brindley, R. Roop (MSR, Mrstn) OHD Technical Review Meeting (ARPA) IDA, Arlington, Va.; 12/11-12/69

LM RENDEZVOUS RADAR Characteristics—N. L. Naschever (ASD, Burl) Patriots Roost Chapter Meeting, Old Crows Association, L. G. Hanscom Field, Mass.; 11/10/69

LM RENDEZVOUS RADAR/Transmitter—J. D. Johnson (ASD, Burl) IEEE Student Chapters: Iowa State Univ.; 9/23/69; Manhattan College; 10/10/69; Vanderbilt Univ.; 11/5/69

PHASED ARRAY RADAR Systems—A. S. Robinson (MSR, Mrstn); N.J. Coast Chapter of the Aerospace & Electronic System Group, IEEE, Little Silver, N.J.; 11/19/69

PROPAGATION, TARGET, AND RADAR MODELS, An OTH Simulation I: C. Brindley, R. Roop (MSR, Mrstn) OHD Technical Review Meeting (ARPS) IDA, Arlington, Va.; 12/11-12/69

RADAR REFLECTIVITY of Metallic Bodies of Revolution—D. A. DeWolf (Labs., Pr) *IEEE Trans. on Antennas and Propagation*, Vol. AP-17, No. 5; 9/69

RECORDING

DYNAMIC RECORDING CORRELATOR, The Second Generation—M. Pradervand (REC, Indpls) AES Convention, New York; 11/69

RECORDING, AUDIO

AUDIO TAPE KEYS—G. D. Hanchett (EC, Som) *RCA Ham Tips*; 12/69

RECORDING, IMAGE

ELECTROSTATIC IMAGES, Developing—D. A. Ross (Labs., Pr) The Royal Photographic Society Symposium, Oxford, England; 10/1-3/69

IMAGING SENSORS, Frame Type—G. Barna (AED, Pr) Princeton University Conference "Aerospace Methods for Revealing and Evaluating Earth's Resources," Princeton, N.J.; 9/25/69

RELIABILITY

MICROWAVE INTEGRATED CIRCUIT Reliability, Design for—V. J. Lukach, R. E. Kleppinger (EC, Som) IEEE Group on Reliability, Phila., Pa.; 11/20/69

QUALITY VS. QUANTITY—T. I. Arnold (ASD, Burl) Hexagon Electric Seminar during NEREM, Sheraton-Boston Hotel; 11/5-7/69

SOLID-STATE DEVICES

Al₂O₃-CdSe THIN-FILM TRANSISTORS, Improved Stability in—A. Waxman, G. Mark (Labs., Pr) *Solid State Electronics*, Vol. 12; 1969

Al₂Ga_{1-x}As AVALANCHE DIODES, Microwave Oscillation in—C. Yeh, S. G. Liu, F. Z. Hawrylo (Labs., Pr) *Proc. of the IEEE*, Vol. 57, No. 10; 10/69

AVALANCHE DIODE, A Qualitative Model of the—B. B. Robinson (Labs., Pr) *Proc. of the IEEE*, Vol. 57, No. 10; 10/69

AVALANCHE-DIODE Microwave Oscillators, Stacked Kilowatt—S. G. Liu, J. J. Risko (Labs., Pr) IEEE International Electron Devices Meeting, Washington, D. C.; 10/29-31/69

AVALANCHE DIODE Microwave Oscillators—L. S. Napoli (Labs., Pr) Electron Devices IEEE Section, Pittsburgh, Pa.; 10/9/69

AVALANCHE DIODE, Amplification Using an—J. F. Dienst, R. V. D'Aiello, E. E. Thomas (Labs, Pr) *Electronics Letters* Vol. 5, No. 14; 7/10/69

COS/MOS MSI COUNTER and Register Design and Applications—R. Heuner, J. Litus, A. Havasy, J. Harmon (EC, Som) National Electronics Conf., Chicago, Ill.; 12/10/69; 1969 *N.E.C. Proc.*

COMPLEMENTARY SYMMETRY MOS TRANSISTOR Integrated Circuits, TREE Effects in—W. J. Dennehy (AED, Pr) 1969 GOMAC Conf., Washington, D.C.; 9/16/69

DIFFUSED RESISTORS, Designing High-Frequency—R. E. Kleppinger (EC, Som) *RCA Review*; 12/69

HETEROEPITAXIAL LAYERS: GaAs_{1-x}P_x on GaAs, Stresses in—M. S. Abrahams, L. R. Weisberg, J. J. Tietjen (Labs, Pr) *J. of Applied Physics*, Vol. 40, No. 9; 8/69

HIGH-SPEED ASSOCIATIVE MEMORY, Silicon-on-Sapphire Complementary MOS Circuits for—J. R. Burns, J. H. Scott (Labs., Pr) Fall Joint Computer Conference, Las Vegas, Nevada; 11/18-20/69

LAYERED SEMICONDUCTOR-METAL TRANSFERRED-ELECTRON OSCILLATOR Geometry, Pulsed Heat Conduction in a—B. S. Perlman, T. E. Walsh (EC, Pr) *RCA Review*; 12/69

MICROWAVE INTEGRATED CIRCUITS, Current Applications of—W. C. Curtis, H. Honda (ASD, Burl) NEREM, Sheraton-Boston Hotel; 11/5-7/69; *NEREM Record*

MOS APPLICATIONS, Improved Insulators for—K. H. Zaininger (Labs., Pr) Moore School of Electrical Engineering, University of Pennsylvania, Phila., Pa.; 10/10/69

MNOS DEVICE PERFORMANCE, Optimization of—E. C. Ross, M. T. Duffy, A. M. Goodman (Labs, Pr) IEEE Electron Devices Meeting, Washington, D.C.; 10/29-31/69

MOS DUAL-GATE TRANSISTOR for UHF Applications—R. H. Dawson, J. O. Preisig (EC, Som) NEREM, Boston, Mass.; 11/5-7/69; 1969 *NEREM Record*

MODELING SEMICONDUCTOR DEVICES, Approximate Methods for—R. B. Schilling (EC, Som) Symp. on Models for Solid-State Devices, University of Wisconsin; 11/69

PIEZO-FERROELECTRIC TRANSFORMER, An adaptive—A Solid State Analog Storage Device—S. S. Perlman, J. H. McCusker (Labs., Pr) IEEE International Electron Devices Meeting, Washington, D.C.; 10/29-31/69

POWER AMPLIFIER, UHF Integrated—W. E. Poole (EC, Som) *IEEE J. of Solid-State Circuits*; 12/69

THIN-LAYER GaAs AMPLIFIERS, Optimum Design of—R. H. Dean (Labs., Pr) *Proc. of the IEEE*, Vol. 57, No. 7; 7/69

III-V AND II-VI SEMICONDUCTORS, The Nature of Surface States on—J. D. Levine (Labs., Pr) *J. of Vacuum Science and Technology*, Vol. 6, No. 4; 7-8/69

TRANSFERRED-ELECTRON AMPLIFIERS—F. Sterzer (EC, Pr) *IEEE J. of Solid-State Circuits*; 12/69

TRANSFERRED-ELECTRON AMPLIFIERS, Stabilized Supercritical—B. S. Perlman, T. E. Walsh, R. E. Enstrom (EC, Pr) *IEEE J. of Solid-State Circuits*; 12/69

SPACE COMMUNICATION

BROADCAST SATELLITE and Conservation of a Natural Resource—K. H. Powers (Labs., Pr) Preparatory Policy Conf., Canada; 11/21-23/69

MANNED SPACE STATION, Communications for a—A. J. Lynch, F. A. Hartshorne (DCSD, Cam) AIAA Sixth Annual Meeting and Technical Display, Anaheim, Calif.; 10/21/69

SHF TACTICAL SATELLITE COMMUNICATION Ground Terminals, A Family of—R. S. Lawton, V. C. Chewey (DCSD, Cam) EASCON 1969, Washington, D.C.; 10/28/69

SPACE NAVIGATION

APOLLO VHF RANGING—E. J. Nossen (DCSD, Cam) IEEE Boston Chapter Communication Technology Group Mtg., Waltham Mass.; 10/8/69

MOTION OF OBJECTS EJECTED from an Orbiting Body, Bounds on the—S. A. Musa (MSR, Mrstn) AIAA Journal; 10/69

SPACECRAFT

LM RENDEZVOUS RADAR Characteristics—N. L. Laschever (ASD, Burl) Patriots Roost Chapter Meeting, Old Crows Association, L. G. Hanscom Field, Mass.; 11/10/69

MEDIUM ALTITUDE SATELLITE, A Study of the Prediction Accuracies of Several Atmosphere Models Used on a—J. A. Ward (MTP, Cocoa Beach) National Meeting of the America Astronautical Society, Las Cruces, New Mexico; 10/69

REMOTE SENSING OF THE SEA CONDITIONS with Microwave Radiometer Systems—R. Groshans, J. C. Aukland, P. J. Caruso, W. H. Conway (AED, Pr) Sixth International Symp. on Remote Sensing of Environment, Ann Arbor, Mich.; 10/15/69

SATELLITE SURVEILLANCE, Space Science and—C. Brindley (MSR, Mrstn) Michigan State University; 11/18/69

SPACECRAFT PROPULSION SYSTEM Employing Surface Tension Feed, Modeling of—Y. Brill, R. Lynch, J. Scussel (AED, Pr) 11th Liquid Propulsion Meeting, Miami, Fla.; 9/17/69; to be published in Chemical Propulsion Information Agency Bulletin

SUPERCONDUCTIVITY

ANISOTROPIC Superconducting Energy Gap of Nb₃Sn—V. Hoffstein, R. W. Cohen (Labs., Pr) *Physics Letters*, Vol. 29A, No. 6; 8/11/69

FERROMAGNETIC HgCr₂Se₄, Crystal Growth, Semiconducting and Optical Properties of—H. W. Lehmann, F. P. Emmenegger (Labs., Pr) *Solid State Communications*, Vol. 7, No. 4; 1969

FLUCTUATIONS OF THE SUPERCONDUCTING ORDER PARAMETER, Anisotropy of the Surface Impedance in the Surface-Sheath Regime as Evidence for—K. Maki, G. Fischer (Labs., Pr) *The Physical Review*, Vol. 184, No. 2; 8/10/69

INTRABAND AND INTERBAND SCATTERING in the Resistivity of High T_c Superconductors—R. W. Cohen, G. Cody (Labs., Pr) *Solid State Communications*, Vol. 7; 1969

ISOTOPE EFFECT in Superconductors—A. Rothwarf (Labs., Pr) *Physics Letters*, Vol. 29A, No. 9; 7/28/69

MAGNETIC SEMICONDUCTORS, Optical Effects in—G. Harbeke (Labs., Pr) Meeting on Magnetic Semiconductors, Nottingham, England; 10/14/69

SUPERCONDUCTIVITY and the Density of States Model for Beta-Tungsten Compounds—R. W. Cohen, G. D. Cody, L. J. Vieland (Labs., Pr) Electronic Density of States Conf, Washington, D.C.; 11/3-6/69

TUNNELING DENSITY OF STATES, Effect of Fluctuations in Superconducting Order Parameter on the—R. W. Cohen, B. Abeles, C. F. Fuselier (Labs., Pr) *Physical Review Letters*, Vol. 23, No. 7; 8/18/69

VAPOR DEPOSITED TUNGSTEN as a Metallization and Interconnection Material for Semiconductor Devices—J. A. Amick, J. M. Shaw (Labs., Pr) Symposium on Dielectrics in Device Technology, Electrochemical Society Meeting, Detroit, Michigan; 10/5-10/69

TELEVISION BROADCASTING

ONE TUBE COLOR CAMERA—H. Ball (CESD, Burbank) NAEB Convention, Washington, D.C.; 11/10/69

TELEVISION EQUIPMENT

LOW LIGHT LEVEL Television—R. J. Gildea (ASD, Burl) Altoona, Pa. Engineering Society; 12/9/69

SLOW-SCAN TELEVISION—B. M. Soltoff (AED, Pr) Student Branch of IEEE, Rutgers University, New Brunswick, N.J.; 12/17/69

TRANSMISSION LINES

COPLANAR WAVEGUIDE, A Surface Strip Transmission Line Suitable for Nonreciprocal Gyromagnetic Device Application—C. P. Wen (Labs., Pr) Seminar at the City University of New York; 10/27/69

HELICON DISPERSION RELATION for a Square Plasma Guide—R. Hirota (Lab, Pr) *J. of the Physical Society of Japan*, Vol. 27, No. 3; 9/69

MAGNETOPLASMA LOADED WAVEGUIDE at Room Temperature, Field Distribution in a—R. Hirota, K. Suzuki (Labs., Pr) Conf. of the Physical Society of Japan, Kagawa University, Japan; 11/15-18/69

GENERAL TECHNOLOGY

APPLIED SCIENCE, Technology & Curricula—Dr. J. Vollmer (ATL, Cam) Polytechnic Institute of Brooklyn Graduate Center, Brooklyn, N.Y.; 10/16/69

CONSUMER ELECTRONICS—What Lies Ahead?—D. S. McCoy (Labs., Pr) Howard University, Washington, D.C.; 12/8/69

Author Index

Subject listed opposite each author's name indicates where complete citation to his paper may be found in the subject index. An author may have more than one paper for each subject category.

ASTRO-ELECTRONICS DIVISION

Aukland, J. C. geophysics
Aukland, J. C. spacecraft
Baran, A. S. environmental engineering
Barna, G. recording, image
Brill, Y. energy conversion
Brill, Y. spacecraft
Brown, I. management
Caruso, P. J. geophysics
Caruso, P. J. spacecraft
Conway, W. H. geophysics
Conway, W. H. spacecraft
Dennehy, W. J. circuit, integrated
Dennehy, W. J. solid-state devices
Fagan, J. R. environmental engineering
Fenster, H. circuits, packaged
Gargione, F. circuits, packaged
Groshans, R. geophysics
Groshans, R. spacecraft
Lynch, R. energy conversion
Lynch, R. spacecraft
Osgood, C. C. mathematics
Osgood, C. C. mechanical devices
Scussel, J. energy conversion
Scussel, J. spacecraft
Soltoff, B. M. television equipment
Wolf, M. circuits, integrated

AEROSPACE SYSTEMS DIVISION

Arnold, T. I. reliability
Byk, W. S. lasers
Congdon, F. P. management
Curtis, W. C. circuits, integrated
Curtis, W. C. solid-state devices
DeBruyne, P. acoustics
DeBruyne, P. displays
Dieterich, E. J. computer systems
Fay, J. computer applications
Gildea, R. J. communications systems
Gildea, R. J. television equipment
Greenspan, A. management
Honda, H. circuits, integrated
Honda, H. solid-state devices
Johnson, J. D. radar
Kaye, L. C. computer systems
Laschever, N. L. radar
Laschever, N. L. spacecraft
Mintz, H. K. documentation
Schein, T. R. lasers
Schmuhl, E. management
Teixeira, N. A. checkout

ADVANCED TECHNOLOGY LABORATORIES

Braudy, R. S. lasers
Corrington, M. S. filters, electric
Feller, A. computer applications
Herzog, D. G. lasers
Levin, B. J. displays
Levin, B. J. electro-optics
Mavaddat, R. displays
Mavaddat, R. electro-optics
Shelpuk, B. energy conversion
Shelpuk, B. environmental engineering
Vollmer, Dr. J. general technology
Vollmer, Dr. J. lasers

COMMERCIAL ELECTRONIC SYSTEMS DIVISION

Ball, H. television broadcasting

DEFENSE COMMUNICATION SYSTEMS DIVISION

Barton, H. R. manufacturing
Chewey, V. C. space communication
Gerber, M. M. communications components
Hartshorne, F. A. space communication
Lawton, R. S. space communication
Lynch, A. J. space communication
Nossen, E. J. space navigation
Schellack, H. F. manufacturing
Westcott, E. J. manufacturing

ELECTRONIC COMPONENTS

Bailey, R. L. amplification
Bailey, R. L. circuits, integrated
Bailey, R. L. communications components
Belohoubek, E. circuits, integrated
Belohoubek, E. energy conversion
Bennett, W. P. amplification
Bennett, W. P. circuits, integrated
Bennett, W. P. communications components
Daivan, R. properties, optical
Dawson, R. H. solid-state devices
Eastman, G. Y. energy conversion
Eastman, G. Y. mechanical devices
Enstrom, R. E. amplification
Enstrom, R. E. solid-state devices
Grimm, A. C. energy conversion
Grimm, A. C. environmental engineering
Hanchett, G. D. recording, audio
Harbaugh, W. E. energy conversion
Harbaugh, W. E. mechanical devices
Harmon, J. circuits, integrated
Harmon, J. solid-state devices
Havasy, A. circuits, integrated
Havasy, A. solid-state devices
Heckman, L. F. amplification
Heckman, L. F. circuits, integrated
Heckman, L. F. communications components
Heuner, R. circuits, integrated
Heuner, R. solid-state devices
Kleppinger, R. E. circuits, integrated
Kleppinger, R. E. reliability
Litus, J. circuits, integrated
Litus, J. solid-state devices
Lukach, V. J. circuits, integrated
Lukach, V. J. reliability
Martin, I. E. amplification
Martin, I. E. circuits, integrated
Martin, I. E. communications components
Perlman, B. S. amplification
Perlman, B. S. solid-state devices
Perlman, B. S. circuits, integrated
Poole, W. E. amplification
Poole, W. E. communications components
Poole, W. E. solid-state devices
Preisig, J. O. solid-state devices
Presser, A. circuits, integrated
Presser, A. energy conversion
Rosen, A. circuits, integrated
Rosen, A. energy conversion
Schilling, R. B. mathematics
Schilling, R. B. solid-state devices
Sobol, H. circuits, integrated
Sterzer, F. amplification
Sterzer, F. solid-state devices
Stevenson, D. circuits, integrated
Stevenson, D. energy conversion
Walsh, T. E. circuits, integrated
Walsh, T. E. solid-state devices
Walsh, T. E. amplification
Wheatley, C. F. circuit analysis
Wittlinger, H. A. circuit analysis

GRAPHIC SYSTEMS DIVISION

Maymon, G. W. computers, programming

LABORATORIES

Abeles, B. superconductivity
Abrahams, M. S. lasers
Abrahams, M. S. solid-state devices
Abrahams, M. S. properties, chemical
Allison, J. F. properties, surface
Amatani, K. properties, molecular
Amick, J. A. superconductivity
Amith, A. properties, electrical
Amodei, J. J. holography
Amodei, J. J. properties, surface
Amodio, P. R. manufacturing
Assour, J. M. computer storage
Assour, J. M. electro-optics
Anderson, C. H. laboratory techniques
Anderson, C. H. acoustics
Anderson, C. H. properties, atomic
Baltzer, P. K. properties, electrical
Baltzer, P. K. properties, magnetic
Barry, T. G. laboratory techniques
Berger, S. B. properties, optical
Berger, S. B. properties, molecular
Bosenberg, W. A. circuits, integrated
Bosenberg, W. A. environmental engineering
Bosenberg, W. A. manufacturing

Buicocchi, C. J. lasers
Burke, W. J. lasers
Burke, W. J. properties, optical
Burns, J. R. computer storage
Burns, J. R. solid-state devices
Busanovich, C. J. properties, mechanical
Busanovich, C. J. properties, surface
Butler, J. K. lasers
Byer, N. E. lasers
Castellano, J. A. electro-optics
Castellano, J. A. properties, molecular
Clough, R. B. properties, mechanical
Clover, R. B. properties, electrical
Clover, R. B. properties, magnetic
Cody, G. D. superconductivity
Cohen, R. W. superconductivity
Cohen, S. logic elements
Coutts, M. D. laboratory techniques
Crandall, R. S. properties, optical
Crane, R. L. computers, programming
Cullen, G. W. properties, molecular
D'Aiello, R. V. amplification
D'Aiello, R. W. solid-state devices
Dean, R. H. amplification
Dean, R. H. properties, surface
Dean, R. H. solid-state devices
DeWolf, D. A. radar
DeWolf, D. A. properties, optical
Dienst, J. F. amplification
Dienst, J. F. solid-state devices
Duffy, M. T. solid-state devices
Dumin, D. J. properties, surface
Emmenegger, F. P. properties, molecular
Emmenegger, F. P. properties, optical
Emmenegger, F. P. superconductivity
Farinre, T. O. properties, surface
Faldstein, N. manufacturing
Firester, A. H. lasers
Fischer, G. properties, surface
Fischer, G. superconductivity
Friedman, L. R. properties, electrical
Fuselier, C. R. superconductivity
Glicksman, M. masers
Goldmacher, J. E. properties, surface
Goodman, A. M. solid-state devices
Goodman, A. M. properties, optical
Gorog, I. properties, atomic
Gottlieb, G. E. properties, molecular
Harada, S. properties, molecular
Harbeke, G. properties, optical
Harbeke, G. superconductivity
Harrington, W. L. laboratory techniques
Harrison, S. E. properties, magnetic
Harrison, S. E. properties, optical
Hawrylo, F. Z. electromagnetic waves
Hawrylo, F. Z. solid-state devices
Hawrylo, F. Z. lasers
Hawrylo, F. Z. properties, optical
Heilmeler, G. H. properties, molecular
Heiman, F. P. properties, surface
Helfrich, W. properties, molecular
Hirota, R. electromagnetic waves
Hirota, R. transmission lines
Hoffstein, V. superconductivity
Kaldis, E. properties, molecular
Kato, K. properties, molecular
Kiess, H. optics
Klein, R. acoustics
Klein, R. properties, atomic
Kressel, H. lasers
Kressel, H. properties, optical
Kressel, H. properties, electrical
Larach, S. laboratory techniques
Larach, S. properties, chemical
Larach, S. properties, optical
Lee, W. M. properties, chemical
LeFur, P. lasers
Lehmann, H. W. properties, molecular
Lehmann, H. W. properties, optical
Lehmann, H. W. superconductivity
Levine, J. D. properties, surface
Levine, J. D. energy conversion
Levine, J. D. solid-state devices
Levine, P. A. laboratory techniques
Levine, P. A. lasers
Levy, S. Y. circuits, packaged
Levy, S. Y. computer systems
Liu, S. G. electromagnetic waves
Liu, S. G. solid-state devices
Liu, S. G. communication components
Lockwood, H. lasers
Lohman, R. D. computer storage
Lohman, R. D. electro-optics
Maki, K. properties, surface
Maki, K. superconductivity
Mark, P. properties, surface
Mark, G. solid-state devices
McCoy, D. S. general technology
McCusker, J. H. solid-state devices
McFarlane, S. H. lasers

Mezrich, R. S. holography
Mezrich, R. S. properties, surface
Mezrich, R. S. documentation
Mezrich, R. S. graphic arts
Minematsu, K. properties, electrical
Minematsu, K. properties, magnetic
Miyatani, K. properties, electrical
Miyatani, K. properties, magnetic
Miyatani, K. properties, molecular
Miyatani, K. mathematics
Moore, R. M. properties, surface
Moore, R. M. properties, mechanical
Mueller, C. W. properties, surface
Napoli, L. S. communication components
Napoli, L. S. solid-state devices
Nelson, H. lasers
Nelson, H. properties, electrical
Nelson, H. properties, optical
Oka, T. properties, molecular
Okamoto, F. properties, electrical
Okamoto, F. properties, magnetic
Okamoto, F. properties, molecular
Olson, H. F. acoustics
Pankove, J. I. properties, electrical
Pasierb, E. F. electro-optics
Pasierb, E. F. properties, molecular
Pauli, M. C. circuit analysis
Pauli, M. C. control systems
Perlman, B. S. solid-state devices
Phillips, W. properties, optical
Powers, K. H. geophysics
Powers, K. H. space communication
Pressley, R. J. properties, optical
Pressley, R. J. lasers
Pressley, R. J. properties, optical
Rajchman, J. A. computer storage
Rajchman, J. A. optics
Rajchman, J. A. computer systems
Redfield, D. properties, electrical
Robinson, B. B. solid-state devices
Robinson, B. B. masers
Robinson, P. H. properties, surface
Ross, E. C. solid-state devices
Ross, D. A. displays
Ross, D. A. recording, image
Rothwarf, A. S. superconductivity
Sabisky, E. S. laboratory techniques
Scott, J. H. computer storage
Scott, J. H. solid-state devices
Shaw, J. M. superconductivity
Stewart, W. C. laboratory techniques
Suzuki, K. electromagnetic waves
Suzuki, K. transmission lines
Swartz, G. A. masers
Takahashi, T. properties, molecular
Takahashi, T. properties, electrical
Takahashi, T. properties, magnetic
Thomas, E. E. amplification
Thomas, E. E. solid-state devices
Tietjen, J. J. properties, chemical
Tietjen, J. J. lasers
Tietjen, J. J. solid-state devices
Toda, M. properties, electrical
Toda, M. properties, magnetic
Toda, M. electromagnetic waves
Vieland, L. J. superconductivity
Wada, Y. properties, molecular
Walters, D. A. information theory
Wang, C. C. properties, surface
Wang, C. C. properties, molecular
Waxman, A. solid-state devices
Wehner, R. K. acoustics
Wehner, R. K. properties, atomic
Weisberg, L. R. lasers
Weisberg, L. R. solid-state devices
Wen, C. P. transmission lines
Winder, R. O. logic theory
Winder, R. O. logic elements
Wittke, J. P. properties, electrical
Woolston, J. R. laboratory techniques
Yeh, C. electromagnetic waves
Yeh, C. solid-state devices
Yoshikawa, K. mathematics
Yoshikawa, K. properties, magnetic
Zaininger, K. H. properties, molecular
Zaininger, K. H. properties, surface
Zaininger, K. H. solid-state devices
Zanoni, L. A. properties, molecular

MISSILE AND SURFACE RADAR DIVISION

Bauer, J. A. circuits, packaged
Bauer, J. A. computer applications
Brindley, C. spacecraft
Brindley, C. radar
McCall, E. G. radar
Mikenas, V. antennas
Musa, S. A. mathematics

Musa, S. A. space navigation
Murakami, T. electromagnetic waves
Nessmith, J. T. radar
Ottinger, R. radar
Profera, C. antennas

Profera, C. electromagnetic waves
Robinson, A. S. antennas
Robinson, A. S. radar
Roop, R. radar
Wickizer, G. electromagnetic waves

MISSILE TEST PROJECT

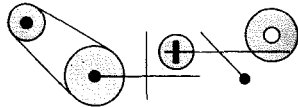
Hatley, C. V. control systems
Tokareff, P. control systems
Ward, J. A. spacecraft

RECORD DIVISION

Bradervand, M. recording

Patents Granted

to RCA Engineers



As reported by RCA Domestic Patents,
Princeton

Aerospace Systems Division

Electronic Shutter Employing Two Normally Non-Conducting SCR's in which Second SCR is Self-Extinguishing by RC Timer and is Triggered on When First SCR Turns off—H. Chin, J. Salvato (ASD, Burl) U.S. Pat. 54,162; Assigned to U.S. Government; September 9, 1969

Missile and Surface Radar Division

Self-Synchronizing Tunnel Diode and Circuit—M. J. Campanella (MSR, Mrstn) U.S. Pat. 53,357; July 1, 1969; Assigned to U.S. Government

Analog Pulse Variation Digital-to-Analog Converter—I. Brown (MSR, Mrstn) U.S. Pat. 44,295; July 8, 1969; Assigned to U.S. Government

Integral Multiple Hybrid Comparator—G. Hyde, B. W. Watson (MSR, Mrstn) U.S. Pat. 51,612; August 5, 1969; Assigned to U.S. Government

Consumer Electronics Division

Detent System—W. F. Speer, J. M. Simons (CED, Indpls) U.S. Pat. 3,477,299; November 11, 1969

Spindle Adapter—P. E. O'Connell (CED, Indpls) U.S. Pat. 3,477,727; November 11, 1969

Shield—N. W. Hursh, R. R. Mooreland (CED, Indpls) U.S. Pat. 3,479,566; November 18, 1969

Gain Control Biasing Circuits for Field-Effect Transistors—G. W. Carter (CED, Indpls) U.S. Pat. 3,480,873; November 25, 1969

Asynchronous Drive System—H. R. Warren (CED, Indpls) U.S. Pat. 3,481,214; December 2, 1969

Wide Band Recording and Reproducing System—H. R. Warren (CED, Indpls) U.S. Pat. 3,482,038; December 2, 1969

Video Peaking Control Network—G. E. Anderson, D. H. Willis (CED, Indpls) U.S. Pat. 3,487,165; December 30, 1969

Intermediate Frequency Coupling Network Having a Sharply Tuned Sound Carrier Cancellation Trap Inductively Coupled to the Input Circuit—D. F. Griepentrog (CED, Indpls) U.S. Pat. 3,487,339; December 30, 1969

Geodesic Electromagnetic Deflection Yoke—R. L. Barbin (CED, Indpls) U.S. Pat. 3,488,541; January 6, 1970

Deflection Control—J. A. McDonald, T. J. Christopher (CED, Indpls) U.S. Pat. 3,488,553; January 6, 1970

Electronic Components

Method of Cleaning Stem Leads for Electron Devices—F. W. Brill, M. R. Weongarten (EC, Lanc) U.S. Pat. 3,477,835; November 11, 1969

Strip-Line Power Transistor Package—D. R. Carley (EC, Som) U.S. Pat. 3,478,161; November 11, 1969

Photomultiplier or Image Amplifier with Secondary Emission Transmission Type Dynodes made of Semiconductive Material with Low Work Function Material Deposited Thereon—R. E. Simon, B. F. Williams, R. Wasserman (EC, Pr) U.S. Pat. 3,478,213; November 11, 1969

Penetration Color Displays—W. H. Barlow (EC, Pr) U.S. Pat. 3,478,245; November 11, 1969

Bonding Graphite with Fused Silver Chloride—R. D. Faulkner (EC, Lanc) U.S. Pat. 52,249; July 1, 1969; Assigned to U.S. Government

Encapsulation and Connection Structure for High Power and High Frequency Semiconductor Devices—G. J. Gilbert (EC, Som) U.S. Pat. No. 3,479,570; November 18, 1969

Method of Providing Contact Leads for Semiconductors—M. J. Grimes, D. F. Henrikson, H. R. Meisel (EC, Som) U.S. Pat. 3,478,420; November 18, 1969

Thermoelectric Device with Embossed Graphite Member—A. G. F. Dingwall (EC, Hr) U.S. Pat. 3,485,679; December 23, 1969

Cathode Ray Tube Manufacture—G. L. Fassett, M. Van Renssen (EC, Lanc) U.S. Pat. 3,482,286; December 9, 1969

Balanced Matrix Driver Arrangement—R. A. Gange, E. M. Nagle (EC, Pr) U.S. Pat. 3,483,517; December 9, 1969

Automatic Gain Control System Employing Multiple Insulated Gate Field Effect Transistor—L. A. Kaplan, O. P. Hart (EC, Som), U.S. Pat. 3,482,167; December 2, 1969

Magnetostrictive Delay Line Having a Flat, Thin Sheet of Magnetostrictive Material—T. N. Chin (EC, Pr) U.S. Pat. 3,482,191; December 2, 1969

Commercial Electronic Systems

Coaxial Circuit for Vacuum Tubes—R. N. Clark, M. W. Duris, L. L. Koros (CESD, Gibbs) U.S. Pat. 49,529; September 9, 1969; Assigned to U.S. Government

Apparatus for Comparison and Correction of Successive Recorded Pulses—M. Rosenblatt (CESD, Gibbs) U.S. Pat. 3,488,663; January 6, 1970

Laboratories

Method of Depositing Refractory Metals—J. A. Amick (Labs., Pr) U.S. Pat. 3,477,872; November 11, 1969

Ferroelectric Control Circuits—B. J. Lechner (Labs., Pr) U.S. Pat. 3,478,224; November 11, 1969

Testing for the Presence of a Contaminant in an Insulating or Semiconducting Medium—L. Pensak (Labs., Pr) U.S. Pat. 3,478,260; November 11, 1969

System for Automatic Correction of Burst-Errors—C. Srinivason (Labs., Pr) U.S. Pat. 3,478,313; November 11, 1969

Converter for VHF-Omnirange (VOR) Receiver—C. J. Hirsch (Labs., Pr) U.S. Pat. 3,478,360; November 11, 1969

Magnetic Heads—J. J. Hanak (Labs., Pr) U.S. Pat. 3,479,738; November 25, 1969

Superconductors—R. E. Enstrom, J. R. Appert (Labs., Pr) U.S. Pat. 3,484,208; December 16, 1969

Self-Propelling Hose—A. V. Bedford (Labs., Pr) U.S. Pat. 3,485,237; December 23, 1969

Sputter Resistive Cold Cathode for Low Pressure Gas Discharge Device—K. G. Hernqvist (Labs., Pr) U.S. Pat. 3,486,058; December 23, 1969

Silicate Glass Coating of Semiconductor Devices—W. Kern (Labs., Pr) U.S. Pat. 3,481,781; December 2, 1969

Cryoelectric Memories—L. S. Cosentino, W. C. Stewart (Labs., Pr) U.S. Pat. 3,482,220; December 2, 1969

Threshold Gates and Circuits—R. O. Winder (Labs., Pr) U.S. Pat. 3,487,316; December 30, 1969

Laser Color Control—C. P. Wen (Labs., Pr) U.S. Pat. 3,487,329; December 30, 1969

Three Terminal Semiconductor Device for Converting Amplitude Modulated Signals into Frequency Modulated Signals—A. Matzelle, A. E. Hahn (Labs., Pr) U.S. Pat. 3,487,338; December 30, 1969

Superconductors having a Flexible Substrate and a Coating Substantially of NbSn—J. J. Hanak, J. L. Cooper (Labs., Pr) U.S. Pat. 3,488,165; January 6, 1970

Solid State Image Sensor Panel—P. K. Weimer (Labs., Pr) U.S. Pat. 3,488,508; January 6, 1970

Electromagnetic and Aviation Systems Division

Method of Spacing a Plurality of Magnetic Heads from the Surface of a magnetic Drum—D. A. Vigil (EASD, Van Nuys) U.S. Pat. 3,478,262; November 11, 1969

Data Storage Apparatus Including Laminated Annuli Transducer Supports Concentric with the Data Storage Means—A. Lichowsky (EASD, Van Nuys) U.S. Pat. 3,478,339; November 11, 1969

Record Division

Transducer with Curved Surface for Cartridge Tape Player—H. E. Roys (REC, Indpls) U.S. Pat. 3,485,959; December 23, 1969

Defense Communication Systems Division

Linear Frequency Modulation System Including an Oscillating Transistor, An Internal Capacity of White is Varied in Accordance with a Modulating Signal—L. A. Harwood (DCSD, Cam) U.S. Pat. RE26,715; November 18, 1969

Condition Indicator for Appliance—Z. Lieser (DCSD, N.Y.) U.S. Pat. 3,480,940; November 25, 1969

Printed Circuit Boards—W. A. Cottfried (DCSD, Cam) U.S. Pat. 3,483,615; December 16, 1969

Integrated Array of Thin-Film Photovoltaic Cells and Method of Making Same—W. L. C. Hui, G. R. Auth (DCSD, Pr) U.S. Pat. 3,483,038; December 9, 1969

Protective System—W. H. Buchsbaum (DCSD, N.Y.) U.S. Pat. 3,482,243; December 2, 1969

Astro-Electronics Division

Circuits for Thermistor Bolometer with Increased Responsivity—J. J. Horan, A. C. Rudomanski (AED, Pr) U.S. Pat. 3,487,213; December 30, 1969

Corporate Staff

Method for Preparing Color Separation Printing Negatives—T. A. Smith (CS, Cam) U.S. Pat. 3,488,190; January 6, 1970

RCA Service Company

Hybrid Circuit Arrangement—O. T. Rhyne (Cocoa Beach, Fla) U.S. Pat. 3,479,617; November 18, 1969

Graphic Systems Division

Photocomposing Apparatus Support Structure—J. F. Delany, G. O. Walter (GSD, Dayton) U.S. Pat. 3,479,934; November 25, 1969

Advanced Technology Laboratories

Method of Spicing a Magnetic Tape Having Diagonal Record Tracks Thereon—F. E. Shashoua, F. D. Kell (ATL, Cam) U.S. Pat. 3,488,455; January 6, 1970

Industrial and Automation Products Department

Article Handling Apparatus—R. G. Walz (IAP, Plymouth) U.S. Pat. 3,487,909; January 6, 1970

Random House

Game Board or Similar Article—R. Price (RH, N.Y.) U.S. Pat. D216,402; December 30, 1969

Information Systems

Memory Driver Monitoring Circuit—D. H. Montgomery (IS, Cam) U.S. Pat. 3,479,650; November 18, 1969

Timing Arrangement for Document Processor—N. A. Del Vecchio (IS, W. Palm) U.S. Pat. 3,489,762; November 25, 1969

Multiple State Logic Circuits—A. Turecki, J. A. Vallee (IS, W. Palm) U.S. Pat. 3,482,172; December 2, 1969

Printer Feed Speed Control—E. L. Neilson, R. C. Peyton (IS, W. Palm) U.S. Pat. 3,487,986; January 6, 1970

Binary Magnetic Recording with Information-Determined Compensation for Crowding Effect—J. A. Vallee (IS, W. Palm) U.S. Pat. 3,488,662; January 6, 1970

* Dates and Deadlines

Be sure deadlines are met—consult your Technical Publications Administrator or your Editorial Representative for the lead time necessary to obtain RCA approvals (and government approvals, if applicable). Remember, abstracts and manuscripts must be so approved BEFORE sending them to the meeting committee.

Calls for papers

MAY 7-8, 1970: **Midwest Symposium on Circuit Theory**, Pick Nicollet Hotel, Minneapolis, Minn., G-CT, Minneapolis Section. **Deadline info (sum) 2/5/70 to:** B. A. Shenoi, EE Dept., Univ. of Minn., Minneapolis, Minn. 55455.

JUNE 2-5, 1970: **Conference on Precision Electromagnetic Measurements**, Nat'l Bureau of Standards, Boulder, Colorado, G-1M, NBS, URSl. **Deadline info (abst & sum) 2/6/70 to:** G. M. R. Winkler, U. S. Naval Observatory, Washington, D.C. 20390.

JULY 12-17, 1970: **Summer Power Meeting & EHV Conference**, Biltmore Hotel, Los Angeles, Calif., G-P. **Deadline info (papers) 2/15/70 to:** Tech. Conf. Svcs., 345 E. 47th St., New York, N.Y. 10017.

JULY 21-23, 1970: **Conf. on Nuclear & Space Radiation Effects**, San Diego Campus Univ. of Calif., San Diego, Calif., G-NS. **Deadline info (sum) 2/16/70 to:** Richard Thatcher, Battelle Mem. Inst., 505 King Ave., Columbus, Ohio 43201.

AUG. 18-21, 1970: **Int'l Conference on Microelectronics, Circuits & Systems Theory**, Univ. of New South Wales, Kensington, Sydney, Australia, G-CT, G-ED, Univ. of New South Wales, IRE. **Deadline info (syn) 3/23/70 to:** Jt. Conf. Secretariat, IREE, Australia, Box 3120, GPO, Sydney, 2001 Australia.

AUG. 25-28, 1970: **Western Electronic Show & Convention (WESCON)**, Biltmore Hotel, Sports Arena, Los Angeles, Calif., Region 6, WEMA. **Deadline info (abst) 3/15/70 (papers) 6/25/70 to:** WESCON Office, 3600 Wilshire Blvd., Los Angeles, Calif. 90005.

AUG. 31-SEPT. 2, 1970: **8th Electric Propulsion Conference**, Stanford University, Stanford, Calif., AIAA Technical Committee on Electric Propulsion. **Deadline info (abst) 3/16/70 (ms) 7/20/70 to:** General Chairman, Howard S. Seifert, Professor, Aeronautics and Astronautics, Stanford University, Room 265, Durand Space Engineering Building, Stanford, Calif. 94305.

SEPT. 2-4, 1970: **Seoul Int'l Electrical & Electronics Engineering Conference**, Korean Inst. of Sc. & Tech., Seoul, Korea, IREE, Korean Inst. of EE, Korean Inst. of Sci. & Tech., KIEE. **Deadline info (papers) 3/1/70 to:** S. K. Chung, c/o KIST, POB 131, Cheong Ryang, Seoul, Rep. of Korea.

SEPT. 14-16, 1970: **ASTM/AIAA/IES 5th Space Simulation Conference**, Gaithersburg, Md., National Bureau of Standards. **Deadline info (abst) 3/2/70 (ms) 5/30/70 to:** Eugene N. Borson, 120/2431, The Aerospace Corp. Box 95085, Los Angeles, Calif. 90045.

SEPT. 20-25, 1970: **Intersociety Energy Conversion Engineering Conference**, Frontier Hotel, Las Vegas, Nev., G-ED, G-AES, AIAA, ASME, AICHE et al. **Deadline info (abst) 2/1/70 (ms) 4/1/70 to:** ENERGY-70, Box 9123, Albuquerque, New Mexico 87119. General Chairman, A. J. Smith III, Air Force Weapons Lab., Albuquerque, New Mexico and Technical Program Chairman, G. S. Leighton, Sundstrand, Washington, D.C.

SEPT. 21-23, 1970: **AIAA Aerodynamic Deceleration Conference**, Dayton, Ohio, Technical Committee on Aerodynamic Deceleration Systems. **Deadline info (first draft) 4/20/70:** Solomon R. Metres, USAF Flight Dynamics Lab., Recovery and Crew Station Branch, (FDFR) Wright-Patterson Air Force Base, Ohio 45433.

SEPT. 21-24, 1970: **Int'l Conf. on Engineering in the Ocean Environment**, City Marina Aud., Panama City, Fla., Panama City Sec., TAB coordinating Comm. on Ocean Engrg., (14 IEEE Groups). **Deadline info (abst & sum) 3/3/70 to:** C. B. Koesty Code P 750, Naval Ship R & D Lab., Panama City, Florida 32401.

SEPT. 21-25, 1970: **5th Intersociety Energy Conversion Engineering Conference—ENERGY 70**, Las Vegas, Nev., ACS AIAA, AICE, ANS, APC, ASME, IREE, MTS, SAE. **Deadline info (abst) 2/1/70 (ms) 4/1/70 to:** ENERGY-70, Box 9123, Albuquerque, N. Mex. 87119.

OCT. 14-16, 1970: **Systems Science & Cybernetics Conference**, Webster Hall Hotel, Pittsburgh, Penna., G-SSC. **Deadline info (abst) 4/15/70 to:** A. Lavi, Carnegie-Mellon Univ., Pittsburgh, Penna. 15213.

NOV. 1970: **G-MTT Transactions is planning a special issue on Microwave Circuit Aspects of Avalanche Diode and Transferred Electron Devices**, IEEE. **Deadline info (complete ms) three copies of each 4/15/70 to:** Guest Editor, Mr. A. H. Solomon, Sylvania Electric Products, Inc., 100 Sylvan Road, Woburn, Mass. 01801.

NOV. 4-6, 1970: **Northeast Electronics Research & Engineering Meeting (NEREM)**, Sheraton Boston Hotel & War Mem. Aud., Boston, Mass., New England Sections. **Deadline info: (abst) 5/29/70 (papers) 7/3/70 to:** IEEE Boston Office, 31 Channing St., Newton, Mass. 02158.

NOV. 15-19, 1970: **Engineering in Medicine & Biology Conference**, Washington Hilton Hotel, Washington, D.C., AEMB, G-EMB. **Deadline info (abst) 6/1/70 to:** Richard Johns, 522 Traylor Bldg., Johns Hopkins School of Med., Baltimore, Md. 21205.

NOV. 29-DEC. 3, 1970: **Vibrations in Heat Exchangers—1970 Winter Annual Meeting**, New York Hilton Hotel, New York, New York, Heat Transfer Division & FED. **Deadline info (sum) three copies (ms) four copies 3/20/70 to:** D. D. Reiff, Division of Reactor Development & Technology, U. S. Atomic Energy Commission, Washington, D.C. 20545.

JAN. 31-FEB. 5, 1971: **Winter Power Meeting**, Statler Hilton Hotel, New York, N.Y., G-P. **Deadline info (papers) 9/15/70 to:** IEEE Hdqs., Tech. Conf. Svcs., 345 E. 47th St., New York, N.Y. 10017.

Meetings

FEB. 18-20, 1970: **Int'l Solid State Circuits Conference**, Sheraton Hotel, Univ. of Penna., Phila., Penna., SSC Council, Univ. of Penna., Phila. **Prog info:** T. Bray, Gen'l Elec. Co., Bldg. 3, Rm. 261, Elec. Pk., Syracuse, N.Y. 13201.

MARCH 11-13, 1970: **Scintillation & Semiconductor Counter Symposium**, Shoreham Hotel, Washington, D.C., G-NS, USAEC, NBS. **Prog info:** R. L. Chase, Brookhaven Nat'l Lab., Upton, N.Y. 11973.

MARCH 11-13, 1970: **Int'l Seminar on Digital Processing of Analog Signals**, Swiss Federal Inst. of Tech., Zurich, Swit., Switzerland Sect., G-AE, VDE, GALF, SEV, DAS. **Prog info:** E. H. Rothaus, IBM Res. Lab., Zurich, Switzerland.

MARCH 17-19, 1970: **Conference on Field Effect Transistors**, Freiburg, F. R. Germany, German Section IEEE, NTG. **Prog info:** H. H. Burghoff, Stresemann Allee 21, 6 Frankfurt/Main 70 (F. R. Germany)

MARCH 17-20, 1970: **Symposium on Management & Economics in the Electronics Industry**, Univ. of Edinburg, Edinburg, Scotland, IEE, IERE, IME, IEEE, UKRI Sect., et al. **Prog info:** IEE, Savoy Place, London W. C. 2 England.

MARCH 23-26, 1970: **IEEE International Convention & Exhibition**, Coliseum & N.Y. Hilton Hotel, New York, N.Y., IEEE. **Prog info:** IEEE Hdqs., 345 E. 47th St., New York, N.Y. 10017.

MARCH 31-APRIL 2, 1970: **Int'l Symposium on Submillimeter Waves**, Commodore Hotel, New York, N.Y., G-MTT, PIB, et al. **Prog info:** Jerome Fox, Microwave Res. Inst., PIB, 333 Jay St., Bklyn., N.Y. 11201.

APRIL 5-9, 1970: **Cybernetics Congress**, Berlin, German Section IEEE, the *Nachrichtentechnische Gesellschaft im VDE richtentechnische Verein* (NTG) and the *Elektrotechnischer Verein* (ETV). **Prog info:** *Elektrotechnischer Verein Berlin im VDE, Bismarckstrabe 33, D-1 Berlin 12* (F. R. Germany).

APRIL 6-7, 1970: **Rubber and Plastics Industries Tech. Conf.**, Holiday Inn, Akron, Ohio, G-IGA, Akron Section. **Prog info:** Chet Blumenauer, Uniroyal Inc., 154 Grove St.

APRIL 6-7-8, 1970: **Third Annual National Symposium on Zero Defects**, Disneyland Hotel, Anaheim, California, American Society for Zero Defects. **Prog info:** Bill Bailey, Manager, Special Projects, 1600 W. 135th Street, Gardena, California 90249.

APRIL 7-8, 1970: **Joint Railroad Tech. Conference**, Sheraton Hotel, Phila., Penna., G-IGA, ASME. **Prog info:** J. J. Foster, Reading Co., Reading Terminal, Phila., Penna. 19107.

APRIL 7-9, 1970: **Reliability Physics Symposium**, Stardust Hotel, Las Vegas, Nev., G-ED, G-R. **Prog info:** K. H. Zaininger, RCA Labs., Princeton, N.J. 08540.

APRIL 14-16, 1970: **Computer Graphics Int'l Symposium**, Brunel Univ., Uxbridge, Middlesex, England, IEE, IERE, IEEE, UKRI Section. **Prog info:** IEE Office, Savoy Place, London W. C. 2 England.

APRIL 14-16, 1970: **Conference on Automatic Test Systems**, Univ. of Birmingham, Birmingham, Warwickshire, Eng., IERE, IEE, IEEE, UKRI Section. **Prog info:** IERE, 8/9 Bedford Sq., London W. C. 1 England.

APRIL 14-17, 1970: **Int'l Geoscience Electronics Symposium**, Marriott Twin Bridges Motor Hotel, Washington, D.C., G-GE. **Prog info:** Ralph Bernstein, IBM Corp., 18100 Frederick Pike, Gaithersburg, Md. 20760.

APRIL 16-19, 1970: **USNC/URSI-IEEE Spring Meeting**, Statler Hilton Hotel,

Washington, D.C., USNC/URSI, 6 co-operating groups. **Prog info:** F. S. Johnson, Nat'l Acad. of Sci., NRS, 2101 Constitution Ave., Washington, D.C. 20418.

APRIL 20-21, 1970: **Aerospace Power Conditioning Specialists Conference**, Royal Pines Motel NASA, Greenbelt, Maryland, G-AES. **Prog info:** T. G. Wilson, Duke Univ., Durham, N. Carolina 27706.

APRIL 21-24, 1970: **International Magnetics Conference (INTERMAG)**, Statler Hilton Hotel, Washington, D.C., G-MAG. **Prog info:** D. S. Shull, Bell Telephone Labs., 3300 Lexington Ave., Winston-Salem, N.C. 27102.

APRIL 22-24, 1970: **Southwestern IEEE Conference & Exhibition (SWIEECCO)**, Memorial Audit., Dallas, Texas, Region 5, Dallas Section. **Prog info:** A. P. Sage, Inst. of Tech., SMU, Dallas, Texas 75222.

APRIL 22-24, 1970: **Offshore Technology Conference**, Albert Thomas Convention Ctr., Houston, Texas, G-AES, G-Com Tech., G-GE et al. **Prog info:** D. K. Adams, 6200 N. Central Expressway, Dallas, Tx. 75206.

APRIL 26-MAY 1, 1970: **107th SMPTE Technical Conference and Equipment Exhibit**, Drake Hotel, Chicago, Ill. **Prog info:** Leonard F. Coleman, Eastman Kodak Co., Southwest Region, Motion Picture and Education Markets Div., 6300 Cedar Springs Rd., Dallas, Tx. 75235.

APRIL 27-30, 1970: **National Telemetering Conference**, Statler Hilton Hotel, Los Angeles, Calif., G-AES, G-Com Tech. **Prog info:** A. V. Balakrishnan, UCLA, Rm. 3531, 405 Hilgard Ave., Los Angeles, Calif. 90024.

MAY 4-5, 1970: **Transducer Conference**, Governor's House, NBS, Gaithersburg, Maryland, G-IECI. **Prog info:** H. P. Kalmus, Harry Diamond Labs., Dept. of the Army, Wash., D.C. 20438.

MAY 4-7, 1970: **Ind. & Comm. Power Sys. & Elec. Space Heating & Air Conditioning Jt. Technical Conference**, Jack Tar Hotel, San Francisco, Calif., G-IGA San Francisco Section. **Prog info:** D. B. Carson, Gen'l Elec. Co., 212 N. Vignes, L. A. Calif. 90012.

MAY 2-7, 1970: **72nd Annual Meeting & Exposition**, Philadelphia Civic Center and Sheraton Hotel, Philadelphia, Pa., The American Ceramic Society, Inc. **Prog info:** ACS, 4055 North High Street, Columbus, Ohio 43214.

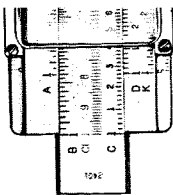
MAY 5-6, 1970: **Appliance Technical Conference**, Leland Motor Hotel, Mansfield, Ohio, G-IGA, North Central Ohio Section. **Prog info:** J. G. Idle, Westinghouse Elec. Corp., 246 E. 4th St., Mansfield, Ohio 44902.

MAY 5-7, 1970: **Spring Joint Computer Conference**, Convention Hall, Atlantic City, New Jersey, G-C, AFIPS. **Prog info:** AFIPS Hdqs., 210 Summit Ave., Montvale, New Jersey 07645.

MAY 11-13, 1970: **Conference on Television Measuring Techniques**, Middlesex Hosp, Medical School, London, England, IERE, RTS, IEE, IEEE UKRI Sect. **Prog info:** IERE Office, 8/9 Bedford Sq., London W. C. 1, England.

MAY 11-14, 1970: **International Microwave Symposium**, Newporter Inn, Newport Beach, Calif., G-MTT. **Prog info:** R. H. DuHamel, Granger Assoc., 1601 Calif. Ave., Palo Alto, Calif. 94304.

MAY 13-15, 1970: **Electronic Components Technical Conference**, Statler Hilton Hotel, Washington, D.C., G-PMP, EIA. **Prog info:** Darnall Burks, Sprague Elec. Co., Marshall St., N. Adams, Mass. 01247.



Butler named Director, Engineering Planning and Equipment Development for NBC

Mr. Robert J. Butler was appointed Director, Engineering Planning and Equipment Development in the NBC Engineering Department.

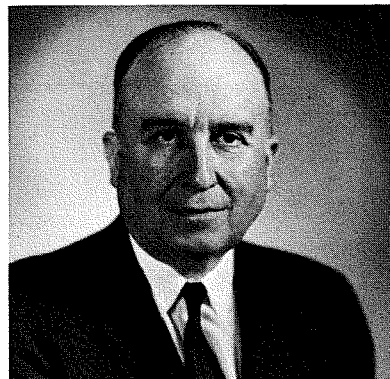
Mr. Butler studied Electrical Engineering at New York University and joined the RCA Service Company in February, 1947. He was transferred to the National Broadcasting Company in March, 1952, and has worked in all phases of color studio development. Mr. Butler was appointed Project Engineer in the NBC Engineering Planning and Equipment Development Group at NBC in October, 1966. He is a member of the Society of Motion Picture and Television Engineers. He has contributed several articles to the RCA ENGINEER in the last few years.

Instructional Systems joins CSD

RCA's Instructional Systems group—a pioneer in bringing computers to the classroom—joined the Computer Systems Division. Established in Palo Alto, Calif. three years ago, the group has concentrated on applying RCA Spectra 70 computer systems to a range of instructional, administrative and educational needs and was part of the Company's Services organization. The Palo Alto facility will become the nucleus of a major RCA West Coast systems programming center. **Norman N. Alperin** was named to direct the Palo Alto programming center, reporting to **Arthur W. Carroll**, Division Vice President, Systems Programming. **Gerald R. Jensen**, former Instructional Systems Marketing Manager, will head an educational marketing support group. He will report to **Joseph W. Rooney**, Division Vice President, Marketing, for CSD. Presently, RCA has computer-assisted instructional (CAI) systems in New York City, Cincinnati and Waterford township, Mich., which provide individualized instruction daily to several thousand students.

Degrees Granted

J. C. Graebner, AED, MSEE from Princeton University, November 1969. **A. Fandozzi**, CES, Meadow Lands, MSEE from University of Pittsburgh, August 1, 1969.



Dr. Olson receives two IEEE awards

Dr. Harry F. Olson, RCA Laboratories, Princeton, N.J., recently received the 1969 Consumer Electronics Award of the IEEE and the IEEE Lamme Medal.

The Consumer Electronics Award presentation, which was made at the National Electronics Conference, cited Dr. Olson's many contributions toward the improvement of consumer electronic home instruments. The Lamme Medal cited Dr. Olson "for his pioneering and continuing leadership in the field of electroacoustics, notably the invention and development of the velocity microphone."

Presently a consultant to RCA Laboratories, Dr. Olson, until his retirement two years ago, had been a Staff Vice-President and Director of the Acoustical and Electromechanical Research Laboratory at the David Sarnoff Research Center, in Princeton, N.J.

Contents: December 1969 *RCA Review*
Volume 30 Number 4

A Photodetector Array for Holographic Optical Memories	J. M. Assour and R. D. Lohman
A Reflex Electro-Optic Light Valve Television DisplayD. H. Pritchard
A Technical and Economic Appraisal of the Use of Microwave Energy in the Freeze-Drying ProcessA. C. Grimm
Designing High-Frequency Diffused Resistors	R. E. Kleppinger
Pulsed Heat Conduction in a Layered Semiconductor-Metal Transferred-Electron Oscillator GeometryB. S. Perlman
Digital Logic for Radiation Environments: A Comparison of Metal-Oxide-Semiconductor and Bipolar TechnologiesC. P. Wen
.....W. J. Dennehy, A. G. Holmes-Seidle, and K. H. Zaininger	
Parallel Processing for Phased-Array Radars	J. E. Courtney and H. M. Halpern
Integrated-Circuit Metalized Plastic Symmetrical Millimeter Trough Waveguide System with Nonreciprocal ElementsC. P. Wen
Prediction of the Dielectric Behavior of Titanate DispersionsJ. M. Guiot

The *RCA Review* is published quarterly. Copies are available in all RCA libraries. Subscription rates are as follows (rates are discounted 20% for RCA employees):

	DOMESTIC	FOREIGN
1-year	\$4.00	\$4.40
2-year	7.00	7.80
3-year	9.00	10.20

1970-1971 David Sarnoff Fellowship Program

Applications for the 1970-1971 David Sarnoff Fellowship Program are now being accepted.

The Fellowships, established in 1956 in honor of the Honorary Chairman of the Board of RCA and to commemorate his fifty years in the radio-television-electronics business, have been significantly revised beginning with the 1970-1971 academic year, and are the top educational awards available to RCA employees.

David Sarnoff Fellows will now be compensated at full base salary—up to maximum policy limits—during the period of their attendance at school. In addition, RCA will pay full tuition and make a \$1000 contribution to the university in which the Fellow is enrolled.

Eleven Fellowships will be available to RCA employees for study toward either technical or non-technical graduate degrees at approved universities. They will be granted for one academic year, and upon application, may be renewed for one additional year.

Recipients will be selected by the RCA Educational Aid Committee on the basis of:

- 1) Outstanding job performance,
- 2) Character,
- 3) Prior academic performance,
- 4) Promise of professional and/or business achievement,
- 5) Actual or tentative acceptance for graduate study at an approved university, and
- 6) Relevance of intended graduate study to future RCA employment.

For technical applicants, preference will be given to those who have indicated by successful completion of courses at the graduate level, their ability to proceed on a doctoral or equivalent program. In the case on non-technical applicants, the end degree need not necessarily be the Doctorate.

To be eligible for a David Sarnoff Fellowship award, an applicant must be a full time permanent RCA employee with at least three years continuous service as of August 31, 1970. Also, the Fellow will be required to sign a written agreement to continue in the employ of RCA or its subsidiaries for a minimum of three years after expiration of the Fellowship.

The head of the employee's division or subsidiary will nominate outstanding candidates to the RCA Educational Aid Committee.

Employees interested in applying for these prized awards for the 1970-1971 academic year may obtain application forms and additional information from the Organization Development Representative in Personnel.

Awards

Electronic Components

Three engineers were recently presented the EC "Man of the Year" awards for their technical performances in 1969. The trio were **Anthony Ameo** of Microwave Operations in Harrison, N.J., **John Krynock** of the Findlay, Ohio, plant, and **Brandice LeMay** of the Marion, Indiana, facility.

Astro-Electronics Division

K. R. Johnson received the Engineering Excellence award for the month of November. **J. Barletta**, **J. Board**, **H. Rouland**, and **J. Swale** received the award for the month of December.

Aerospace Systems Division

Richard H. Holder of Systems Support Engineering was selected as Engineer of the Month for August, 1969, for his performance on the Walt Disney World Project.

The team of **E. E. Corey**, **R. F. Dearborn**, **M. E. DeFlumere**, **F. J. Kudirka**, **C. E. LaCount**, **N. Meliones**, **N. L. Roberts**, **J. F. Salemme**, **R. P. Seversen**, and **G. A. Tromblee** from Electro-Optics and Controls Engineering received the Technical Excellence Team Award for August, 1969. The award recognized excellent team performance in the design, construction, test and delivery of the Integrated Observation Device.

R. A. Welter of Systems Support Engineering, was selected as Engineer of the Month for September, 1969, for his performance on the TRIM Special Support Equipment Program.

The team of **T. E. Kupfrian**, **R. B. Mark**, **D. J. Morand**, **M. Z. Neiman**, **H. J. Porter**, and **S. Waldstein** has received the Technical Excellence Team Award from Electro-Optics and Controls Engineering for September, 1969. The award recognizes the outstanding work of the team on the temperature-controlled filter for a narrow-band, high-sensitivity detector.

Professional Activities

Astro-Electronics Division

Members of the AED Environmental Simulation and Test Engineering Activity will chair two sessions of the Institute of Environmental Sciences Meeting at Boston, Massachusetts, April 13 to 16, 1970. **F. J. Yannotti**, Manager of the Environmental Simulation and Test Engineering Activity, will be the Chairman of the session entitled "Laboratory Management" and **J. E. Herrmann**, will be the Co-Chairman. **J. McClanahan** and **T. Baran**, will be Chairman and Co-Chairman of the session entitled "Digital Control of Shock and Vibration Testing." Mr. Yannotti is the DEP Member on the Aerospace Industry Association Environmental Testing Committee.

Plans and Systems Development

J. C. Bry of the Communication/Navigation Systems activity served as Financial Chairman for the 1969 IEEE Systems Science and Cybernetics Conference, held at the Warwick Hotel in Philadelphia, October 22-24, 1969.

W. E. Rapp of the Systems Evaluation and Simulation activity was a panelist at a meeting of the Philadelphia Chapter of the Society of Logistics Engineers at the Naval Aviation Supply Office in Philadelphia.

Aerospace Systems Division

J. W. Vickroy, Manager of System Projects, has been elected to the Administrative Committee for the IEEE Group on Engineering Management.

M. M. Miller, Senior Member, Technical Staff, was among those listed in the 1970-71 edition of *Who's Who in the East*. This is the second consecutive year for Mr. Miller.

Defense Engineering

H. S. Ingraham, Jr., Defense Engineering Staff, was elected to the post of Vice-Chairman of the National Conference of Standards Laboratories, in its annual election of officers, completed September 30,

1969. Mr. Ingraham has been an RCA delegate to the NCSL since 1962, was first elected to the Board of Directors in 1968, and is currently Chairman of the NCSL Measurement Comparison and Statistical Procedures Committee.

T. B. Martin of Advanced Technology Laboratories has been selected as Chairman of the IEEE Subcommittee on Speech Processing.

Electromagnetic and Aviation Systems Division

G. F. Fairhurst, Manager, Engineering Support and Logistics, was recently elected the National President of the Society of Logistics Engineers (SOLE) for the year 1969/1970. Previously, Mr. Fairhurst has served as Chairman of the 1968 national convention and as National Membership Chairman for 1968/1969. He holds Charter and Fellow membership and has been on the Board of Directors since September 1968.

J. Valtos, Manager, Design Drafting, was elected President of the California Council of the American Institute for Design and Drafting (AIDD) for the year 1969/1970. Mr. Valtos previously served as the Program Chairman for the California Council of AIDD.

Electronic Components

W. E. Harbaugh, Industrial Tube Division, Lancaster, Pa., was Chairman of a session on Heat Pipe Technology at the 4th Inter-Society Energy Conversion Engineering Conference held September 22 to September 26, 1969 in Washington, D.C.

Dr. Harold Sobol, Manager, Microwave Microelectronics, Solid State Division, Somerville, N.J., has been elected National Lecturer for the IEEE Group on Microwave Theory and Techniques for 1970. Dr. Sobol's topic will be microwave integrated circuits and devices. The G-MTT National Lectureship was instituted in 1967 to make available to chapters a prominent speaker on one of the current microwave technologies. The National Lecturer receives \$2000 subsidy from IEEE for expenses during his one-year tenure.

G. F. Fairhurst (center), Manager Engineering Support and Logistics, at Electromagnetic and Aviation Systems Division, and recently elected national president of the Society of Logistics Engineers, admires gavel and desk plaque presented by Dr. Werner von Braun (left) to John C. Goodrum (right), past president of the Society, in recognition of outstanding performance during his term of office.

Denton Clark, Division Vice President, RCA Range Projects (right), accepts congratulations from Dr. Thomas Paine, NASA Administrator (left), and Dr. Kurt Debus, Director, NASA Kennedy Space Center after receiving NASA's coveted Public Service Award. Mr. Clark was cited for "outstanding contributions as a key leader of the government industry team which made possible the exceptional success of the Apollo program."



Staff Announcements

Commercial Electronic Systems

A. F. Inglis, Division Vice President, has announced the Commercial Electronic Systems organization as follows: **N. R. Amberg**, Manager, Industrial and Automation Systems Dept.; **T. J. Barlow**, Manager, Production Department; **G. W. Bricker**, Manager, Professional Electronic Systems Dept.; **E. J. Hart**, Division Vice President, Commercial Communications Systems Department; **A. F. Inglis**, Acting, Broadcast Systems Department; **A. L. Hammerschmidt**, Division Vice President, Broadcast Engineering and Product Management; **E. C. Tracy**, Division Vice President, Broadcast Sales; **A. Mason**, Chief Engineer; **A. M. Miller**, Division Vice President, Systems Program; **J. P. Taylor**, Division Vice President, Marketing Programs.

Defense and Commercial Systems

I. K. Kessler, Executive Vice President, Defense and Commercial Systems has appointed **W. V. Goodwin** as Division Vice President, AEGIS Program.

I. K. Kessler, Executive Vice President, Defense and Commercial Systems has appointed **J. H. Sidebottom** as Division Vice President, Special Projects.

AEGIS Program

W. V. Goodwin, Division Vice President, has announced the organization of the AEGIS Program as follows: **F. G. Adams**, Manager, Management Operations; **R. M. Fritz**, Manager, System Requirements; **W. V. Goodwin**, Acting Manager, Engineering; **D. Lesser**, Manager, Quality Assurance and Value Engineering; **H. A. Magnus**, Manager, Project Management; **P. C. Westhead**, Manager, Contract Management.

Aerospace Systems Division

J. R. McAllister, Division Vice President and General Manager, has appointed **E. F. Lockwood** as Manager, Command and Control Programs.

Missile and Surface Radar Division

P. A. Piro, Division Vice President and General Manager, has appointed **J. C. Volpe**, Manager, MFAR Program.

Operations Staff

R. C. Bitting, Program Director, Video Playback Systems, has announced the organization as follows: **D. F. Miller**, Manager, Marketing; **H. Ball**, Manager, System Development; **F. X. Conaty**, Manager, Administration and Controls; **R. C. Bitting**, Acting Executive Producer, Program Albums; **R. C. Bitting**, Acting, Business Development.

Research and Engineering

J. Hillier, Executive Vice President, has appointed **B. A. Jacoby** as Operations Director of the new Integrated Circuit Technology Center.

Global Communications, Inc.

H. R. Hawkins, President, has announced the organization of RCA Global Communications, Inc. as follows: **E. D. Becken**, Executive Vice President, Operations; **E. W. Peterson**, Executive Vice President, Finance and Business Development; **P. Schneider**, Vice President, Engineering and Leased Systems; **R. J. Angliss**, Vice President, Marketing and Traffic; **L. W. Tuft**, Vice President, Washington, D.C.; **E. F. Murphy**, Vice President and General Attorney; **H. Polish**, Vice President, Personnel; **F. D. Chiei, Jr.**, Executive Vice President, RCA Alaska Communications, Inc.; **G. A. Shawy**, Director, Public Affairs.

Services

D. M. Knight, Division Vice President, Educational Development, has announced the organization of Educational Development as follows: **D. T. Bobbitt, Jr.**, Director, Educational Sales Development; **D. M. Cook**, Director, Educational Development Planning; **R. E. Dickerson**, Manager, Educational Project Development; **A. L. Hardwick**, Manager, Educational Sales; **L. F. Jones**, Director, Educational Development; **D. M. Knight**, Acting Director, Educational Development Administration; **C. D. Sullivan**, Manager, Educational Project Development; **J. W. Wentworth**, Director, Educational Development Engineering; **G. Wyckoff**, Director, Audio-Visual Programs.

Consumer Electronics Division

D. L. Mills, Senior Executive Vice President, Consumer Products and Components has appointed **B. I. French** as Manager, News and Information.

Information Systems

J. R. Bradburn, Executive Vice President, has announced the organization of Information Systems as follows: **L. E. Donegan, Jr.**, Division Vice President and General Manager of the newly named Computer Systems Division, formerly called Information Systems Division; **S. P. Marcy**, Division Vice President and General Manager, Memory Products Division; **N. R. Miller**, Division Vice President and General Manager, Graphic Systems Division; **J. Stefan**, Division Vice President and General Manager, Magnetic Products Division; **S. W. Cochran**, Division Vice President, Business and Economic Planning; **H. H. Jones**, Controller, Finance; **E. S. McCollister**, Division Vice President, Marketing Staff; **M. J. Shuman**, Manager, Personnel.

Computer Systems Division

L. E. Donegan, Jr., Division Vice President and General Manager has announced the organization of the Computer Systems Division as follows: **A. W. Carroll**, Division Vice President, Systems Programming; **M. E. Heisley**, Administrator, Computer Systems Programs; **H. W. Johnson**, Division Vice President, Field



Andrews



Stellman

Andrews and Stellman are new Ed Reps

Mr. Raymond N. Andrews has been appointed Editorial Representative for the Record Division in New York. **Mr. W. D. Stellman** has been appointed Editorial Representative for the Computer Systems Division in Marlboro, Mass. Editorial Representatives are responsible for planning and processing articles for the RCA ENGINEER, and for supporting the activities of the TPA's in their respective divisions (see listing on inside back cover).

Mr. Andrews joined the RCA Record Engineering Labs at Indianapolis as a technician. After receiving the BSEE from Purdue University in 1968, he returned to Record Engineering as a member of the Engineering staff. In April of 1969, he was appointed Manager of Recording Engineering Liaison, responsible for new equipment for the RCA Recording Studios at New York, Chicago, Nashville, and Hollywood. He is a Member of the IEEE groups on Audio and Magnetics and the AES.

Mr. Stellman received the BA in Economics from Muskingum College, New Concord, Ohio in 1947 and the MBA from Drexel University (evening division) in 1955. He joined RCA in 1953 as Budget Analyst in Bizmac Engineering, and then progressed to Leader, Office Services—to Leader, Financial Control and Office Services—to Manager, Financial Control and Office Services—to Manager, Engineering Administration. He transferred to Palm Beach Gardens operation in 1962, and was promoted to Manager, Engineering Accounting in 1963. In December 1967, he joined the Computer Peripheral activity of the Computer Systems Division (now at Marlboro, Mass.) as Manager, Stores. In September 1969, he was promoted to Manager, Engineering Services.

Engineering; **J. R. Lenox**, Division Vice President, Manufacturing and Engineering; **J. W. Rooney**, Division Vice President, Marketing; **D. L. Stevens**, Manager, Product and Programming Planning; **J. J. Worthington**, Manager, Product Assurance; **D. H. Campbell**, Manager, Financial Controls; **L. E. Donegan, Jr.**, Acting Manager, Personnel.

H. N. Morris, Manager, Engineering—Palm Beach, has appointed **J. K. Mulligan** as head of the new consolidated Communications Engineering function for the Computer Systems Division in Palm Beach Gardens, Florida.

Editorial Representatives

The Editorial Representative in your group is the one you should contact in scheduling technical papers and announcements of your professional activities.

Defense and Commercial Systems

Defense Electronic Products

Aerospace Systems Division

Electromagnetic and Aviation Systems Division

Astro-Electronics Division

Missile & Surface Radar Division

Defense Communications Systems Division

Defense Engineering

Commercial Electronics Systems

Industrial and Automation Systems

Information Systems

Computer Systems Division

Magnetic Products Division

Memory Products Division

Graphic Systems Division

Research and Engineering

Laboratories

Consumer Products and Components

Electronic Components

Solid State Division

Receiving Tube Division

Television Picture Tube Division

Industrial Tube Division

Technical Programs

Consumer Electronics Division

Services

RCA Service Company

RCA Global Communications, Inc.

National Broadcasting Company, Inc.

Record Division

RCA International Division

RCA Ltd.

D. B. DOBSON* Engineering, Burlington, Mass.

R. J. ELLIS* Engineering, Van Nuys, Calif.

J. McDONOUGH Engineering, West Los Angeles, Calif.

I. M. SEIDEMAN* Engineering, Princeton, N.J.

S. WEISBERGER Advanced Development and Research, Princeton, N.J.

T. G. GREENE* Engineering, Moorestown, N.J.

A. LIGUORI* Engineering, Camden, N.J.

M. G. PIETZ* Advanced Technology Laboratories, Camden, N.J.

M. R. SHERMAN Defense Microelectronics, Somerville, N.J.

E. J. PODELL Plans and Systems Development, Moorestown, N.J.

J. E. FRIEDMAN Advanced Technology Laboratories, Camden, N.J.

J. L. KRAGER Central Engineering, Camden, N.J.

D. R. PRATT* Chairman, Editorial Board, Camden, N.J.

N. C. COLBY Mobile Communications Engineering, Meadow Lands, Pa.

C. E. HITTLE Professional Electronic Systems, Burbank, Calif.

R. N. HURST Studio, Recording, & Scientific Equip. Engineering, Camden, N.J.

R. E. WINN Broadcast Transmitter & Antenna Eng., Gibbsboro, N.J.

H. COLESTOCK Engineering, Plymouth, Mich.

A. D. BEARD (acting)* Engineering, Camden, N.J.

M. MOFFA Engineering, Camden, N.J.

S. B. PONDER Palm Beach Engineering, West Palm Beach, Fla.

W. D. STELLMAN Engineering, Marlboro, Mass.

E. M. MORTENSON* Instructional Systems Engineering, Palo Alto, Cal.

A. G. EVANS Development, Indianapolis, Ind.

L. A. WOOD Engineering, Needham, Mass.

J. GOLD* Engineering, Dayton, N.J.

C. W. SALL* Research, Princeton, N.J.

C. A. MEYER* Chairman, Editorial Board, Harrison, N.J.

M. B. ALEXANDER Solid State Power Device Engrg., Somerville, N.J.

T. J. REILLY Semiconductor and Conversion Tube Operations, Mountaintop, Pa.

J. D. YOUNG Semiconductor Operations, Findlay, Ohio

I. H. KALISH Solid State Signal Device Engrg., Somerville, N.J.

R. W. MAY Commercial Receiving Tube and Semiconductor Engineering, Somerville, N.J.

J. KOFF Receiving Tube Operations, Woodbridge, N.J.

R. J. MASON Receiving Tube Operations, Cincinnati, Ohio

J. H. LIPSCOMBE Television Picture Tube Operations, Marion, Ind.

E. K. MADENFORD Television Picture Tube Operations, Lancaster, Pa.

J. M. FORMAN Industrial Tube Operations, Lancaster, Pa.

H. J. WOLKSTEIN Microwave Tube Operations, Harrison, N.J.

D. H. WAMSLEY Engineering, Harrison, N.J.

C. HOYT* Chairman, Editorial Board, Indianapolis, Ind.

D. J. CARLSON Advanced Devel., Indianapolis, Ind.

R. C. GRAHAM Procured Products Eng., Indianapolis, Ind.

P. G. McCABE TV Product Eng., Indianapolis, Ind.

J. OSMAN Electromech. Product Eng., Indianapolis, Ind.

L. R. WOLTER TV Product Eng., Indianapolis, Ind.

R. F. SHELTON Resident Eng., Bloomington, Ind.

B. AARONT EDP Service Dept., Cherry Hill, N.J.

W. W. COOK Consumer Products Service Dept., Cherry Hill, N.J.

M. G. GANDER* Consumer Product Administration, Cherry Hill, N.J.

K. HAYWOOD Tech. Products, Adm. & Tech. Support, Cherry Hill, N.J.

W. R. MACK Missile Test Project, Cape Kennedy, Fla.

W. S. LEIS* RCA Global Communications, Inc., New York, N.Y.

W. A. HOWARD* Staff Eng., New York, N.Y.

M. L. WHITEHURST* Record Eng., Indianapolis, Ind.

R. ANDREWS Record Eng. New York, N.Y.

C. A. PASSAVANT* New York, N.Y.

W. A. CHISHOLM* Research & Eng., Montreal, Canada

* Technical Publication Administrators listed above are responsible for review and approval of papers and presentations.